TFAWS Short Course Session

Non-Intrusive Measurement Techniques for Flow Characterization of Hypersonic Wind Tunnels

Paul Danehy, Josh Weisberger, Daniel Reese

NASA Langley Research Center, VA

Craig Johansen

The University of Calgary, Calgary, Canada

Timothy Fahringer

National Institute of Aerospace, Hampton VA

Nicholas Parziale

Stevens Institute of Technology, Hoboken NJ

Chloe Dedic

University of Virginia, Charlottesville, VA

Jordi Estevadeordal

North Dakota State University, Fargo, ND

Brett Cruden

AMA Inc., NASA Ames Research Center, Moffett Field, CA

Thermal & Fluids Analysis Workshop TFAWS 2019 August 26-30, 2019

NASA Langley Research Center Hampton, VA

Non-Intrusive Measurement Techniques for Flow Characterization of Hypersonic Wind Tunnels

***Paul Danehy, Josh Weisberger**, NASA Langley Research Center, VA, USA*
***Craig Johansen**, The University of Calgary, Calgary, Canada*
***Daniel Reese, Timothy Fahringer**, National Institute of Aerospace, Hampton VA, USA*
***Nicholas Parziale**, Stevens Institute of Technology, Hoboken NJ USA*
***Chloe Dedic**, University of Virginia, Charlottesville, VA, USA*
***Jordi Estevadeordal**, North Dakota State University, Fargo, ND, USA*
***Brett Cruden**, AMA Inc. at NASA Ames Research Center, Moffett Field, CA, USA*

Von Karman Institute Lecture Series on:
Flow Characterization and Modeling of Hypersonic Wind Tunnels
STO-AVT-325
Brussels Belgium Dec 3-5, 2018.

Trade names and trademarks are used in this report for identification only. Their usage does not constitute an official endorsement, either expressed or implied, by the National Aeronautics and Space Administration

Context of the current manuscript

- Previous review manuscripts:
  - VKI lecture manuscript (May 2014)
    - *"Spectroscopy and measurements techniques for aerospace flows"*
    - Was expanded to AIAA book chapter.
  - AIAA Progress Series Book (May 2015)
    - Fluids TC Working group led by E. Josyula
    - Chapter: *"Molecular-Based Optical Diagnostics for Hypersonic Nonequilibrium Flows"*
    - *http://hdl.handle.net/2060/20150010961*
- Purposes:
  - Educate those new to field of laser based measurements (students)
    - Develop and explain theory for each technique
  - Let collaborators from other fields know what is possible to measure
  - Provide updates / ideas for those working in measurement technology

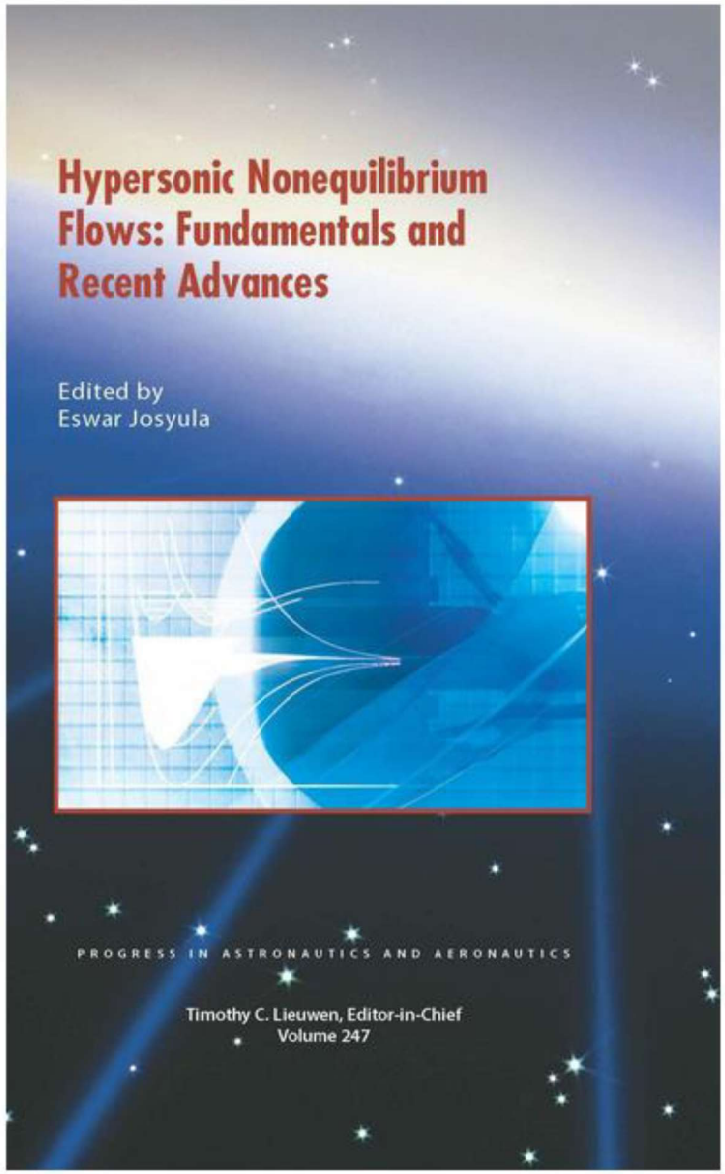

Current AVT-325 Manuscript

Non-Intrusive Measurement Techniques for Flow Characterization of Hypersonic Wind Tunnels

- 140 pages, 395 references
- http://hdl.handle.net/2060/20190029251 (also on my web page)
- Almost entirely new content (few of same figures).
- Focuses on *promising non-intrusive methods* for studying hypersonic freestream flows
  - Examples where possible from hypersonic freestream flows
- Manuscript avoids lengthy derivations, explanations
  - Referenced to earlier works and/or AIAA book chapter
- Ignores conventional instrumentation for characterization of wind tunnels (out of scope)
- Not an exhaustive review: but a good start…
- Several charts are recycled from prior presentations.

Outline for Today's talks

1. Introduction
2. Absorption Spectroscopy
3. Planar Laser-Induced Fluorescence (PLIF)
4. Molecular Tagging Velocimetry (MTV)
5. Focused Laser Differential Interferometry (FLDI)
6. Laser Scattering Techniques
7. Coherent anti-Stokes Raman Scattering (CARS)
8. Particle Image Velocimetry (PIV)
9. Emission Spectroscopy
10. Conclusions

Break around 10!

Time permitting…

Introduction and Application Considerations

- Hypersonic facilities and operating conditions
- Characteristics of hypersonic freestream flows
  - What needs measuring?
- Advantages of spectroscopic measurement
- Aspects of a good measurement technique
- Choosing which measurement technique to use

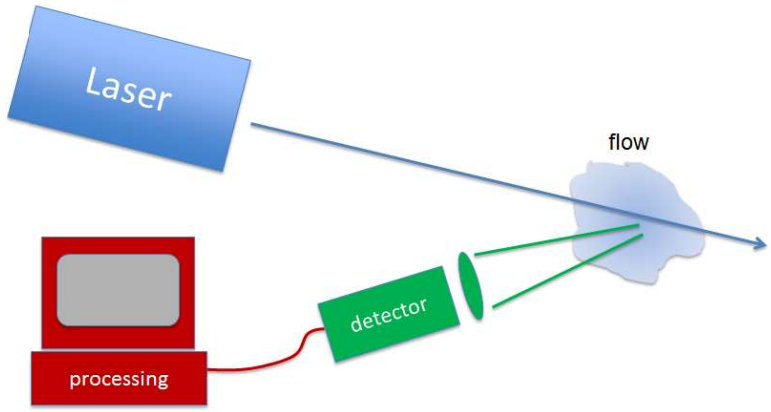

Hypersonic Flight

- Hypersonic vehicles fly at high altitude (low P) and high speed ($M > 5$) resulting in gas and vehicle heating (high T)

- Characteristics of hypersonic flow:
  - Steep gradients (shocks, expansions)
  - Chemical reaction / "real gas" effects
    - Dissociation, ionization, recombination
    - Vibrational, electronic excitation ($\gamma \neq$ constant)
    - Low collision rate ($\sim P/\sqrt{T}$) causes <u>nonequilibrium</u>

  Flowfield

  Complicated! Modelled! Limited data!

  - Oxidation, ablation, spallation of materials
  - Catalycity, radiative heat transfer, etc.

  Material Response
- Plus phenomena occurring in lower speed flow:
  - Laminar-to-turbulent BL transition, turbulence, compressibility, flow separation and combustion

No one hypersonic facility can simulate all of these phenomena

Hypersonic Facilities

- Wide range of hypersonic facilities[1,2] developed to study subsets of hypersonic flow phenomena:
  - Blowdown air tunnels
  - Blowdown nitrogen tunnels
  - Ludwieg tubes
  - Shock tubes
  - Shock tunnels
  - Expansion tubes and tunnels
  - Combustion heated tunnels
  - Arc-Jets / Plasmatrons

Short duration <<1 sec

Low enthalpy
(aerodynamic performance, aeroheating, Reynolds number effects, etc.)

High enthalpy
(real gas effects, aeroheating, nonequilibrium, chemistry, etc.)

Material Response

- Often short duration (msec-sec), few runs / day, large scale, expensive, optical access an afterthought.

[1] Lu, F. K., and Marren, D. E., eds. Advanced hypersonic test facilities. Vol. 198. AIAA, 2002.
[2] Chazot, O. and Panerai, F., 2014. High-enthalpy facilities and plasma wind tunnels for aerothermodynamics ground testing. Hypersonic Nonequilibrium Flows: Fundamentals and Recent Advances, p.329.

Characterizing Hypersonic Facilities

- Many conventional measurement techniques exist, are used in these facilities and are compared with computational fluid dynamics (CFD) codes.
  - Force, moment, surface pressure, heating, etc.
  - When they disagree… is CFD wrong?
    Or did CFD compute the wrong problem?
  - **Critical need for establishing inflow and boundary conditions required for CFD simulations**.
- Need detailed experimental data for inflow:
  - Distributions of flowfield properties (P, T, ρ, u, v, w, χ_i)
  - Time variation of inflow properties desirable (u', $u'T'$, spectra)
  - Will help validate CFD codes and gain confidence in their use for predicting flight
- Focus of this manuscript: <u>freestream measurement</u>

Energy Modes

- Translation

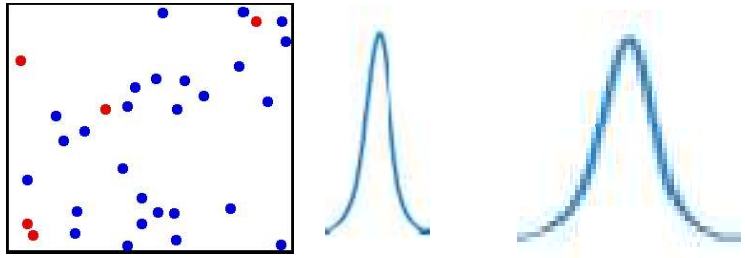

- Rotation

- Vibration

- Electronic

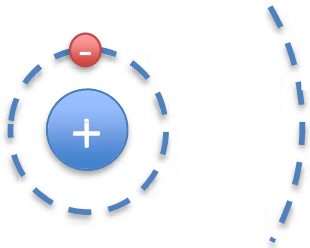

All these states are quantized! 1, 2, 3, …

- These can all be described by a temperature:
  - T_{trans}, T_{rot}, T_{vib}, T_{elec}
  - Thermal equilibrium: these T's are all equal

Nonequilibrium

- Thermal Nonequilibrium:
  - Different energy modes described by different *T*'s
    - e.g.: $T_{rot} \neq T_{vib}$
  - Or, the distribution of population can't be described by Maxwell-Boltzmann statistics ("non-thermal" distribution)
- Chemical Nonequilibrium:
  - Products and reactants are in a state of change
  - If held at those conditions (*P, T*) the composition <u>will</u> change.
- Equilibrium occurs via *collisions*

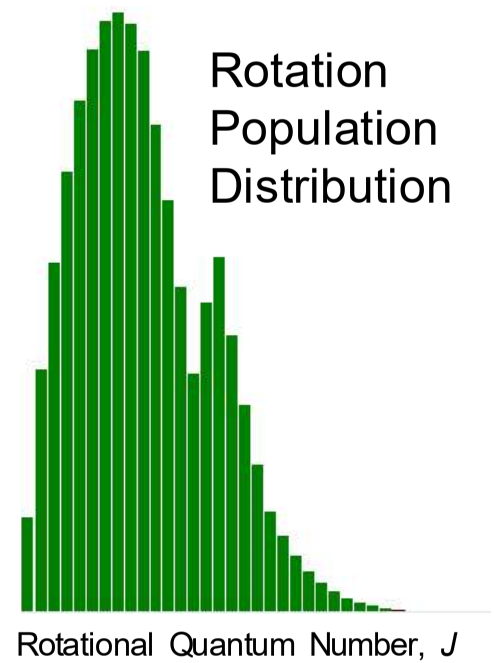

Computed using LIFBASE
(J. Luque, SRI International)

Typical Hypersonic Freestream Flow

- To achieve M>4, air flows must be heated.
  - High enthalpy flow leads to non-equilibrium
- Nozzle Expansion:

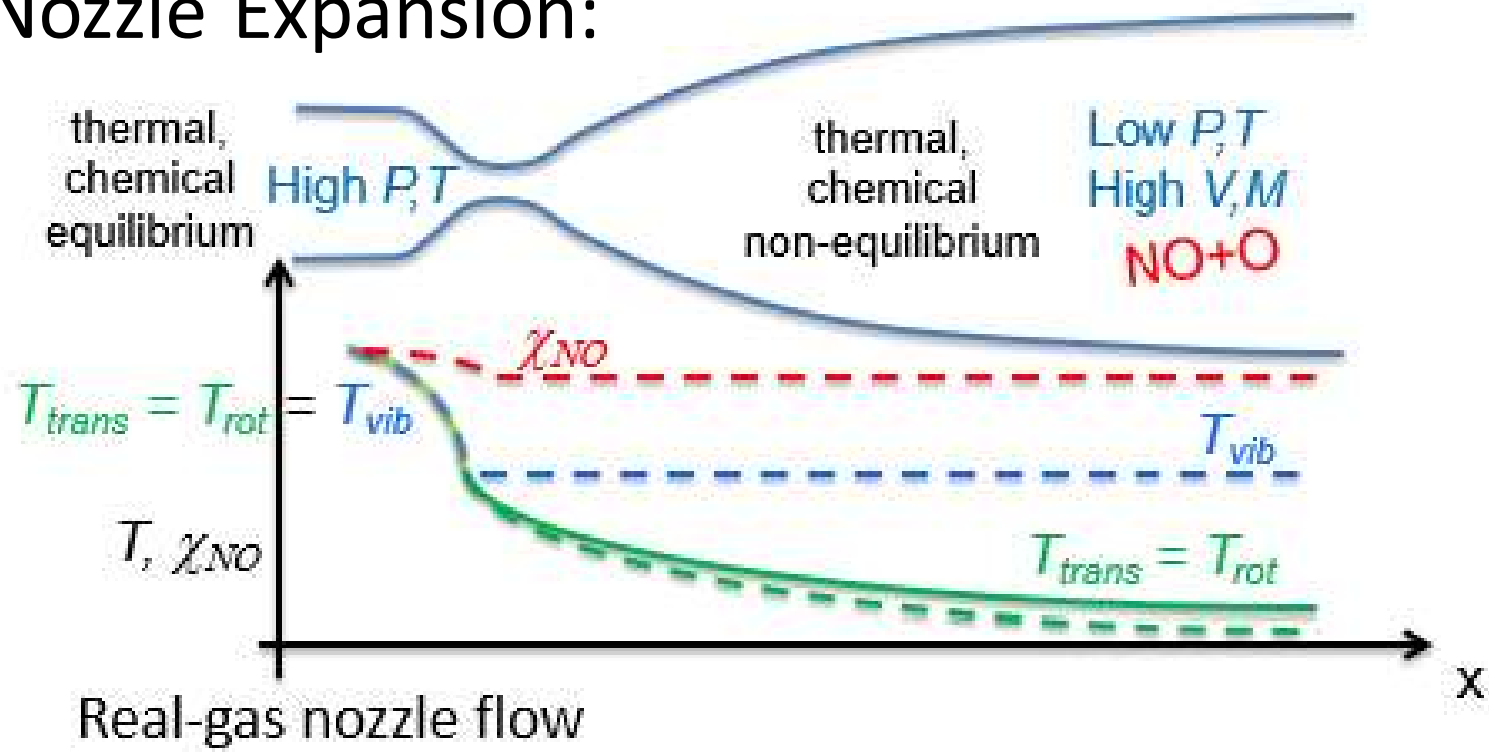

- We can measure, quantify these effects!

Parameters to measure

- Typical parameters of interest in Hypersonic Freestream Flows:
  - Velocity, Pressure, Density, Temperature**s**, Species
    - *And non-thermal population distributions*
  - *How is energy in flow partitioned in terms of:*
    - *thermal energy (T)*
    - *chemical energy (species) and*
    - *kinetic energy (V)?*

Typical Freestream Conditions

Facility	Type	Mach Number	Enthalpy (MJ/kg)	Velocity (m/s)	P_{static} (kPa)	T_{static} (K)	Density (kg/m3)
VKI Mach 6 H3	Blowdown Air	6	--	939	1.28	61.0	0.073
AEDC Tunnel 9	Blowdown N2	13.2	1.9	1920	0.5	51	0.003
Purdue Boeing Mach 6 Quiet Tunnel	Ludwig Tube	5.93	--	872.7	0.37	53.9	0.024
EAST	Shock Tube	4	94	9400	30	10000	0.005
T5	Free Piston Shock Tunnel	5.1	11.9	4320	34	1800	0.062
Lens XX	Expansion Tunnel	7.3	20.7	6086	3.68	1881	0.0068
NASA Ames IHF	Arc Jet	4	20	4000	3	1500	0.004

- Wide range of conditions! (50 K < Temperature < 10,000 K) Low ρ.
- Many measurement techniques only work in a certain range of conditions
- Need many different measurement techniques.
- Only 1 typical condition per facility shown here, but they can often study a range.

Fluctuating Quantities

Facility	Type	U'/U	T'/T	m'/m (rho'/rho)	P'/P
VKI Mach 6 H3	Blowdown Air	0.6%	0.8%	5.2%	1.0%
Purdue Boeing Mach 6 Quiet Tunnel	Ludwig Tube	--	--	0.2%	0.01%
T5	Free Piston Shock Tunnel	--	--	<1% @ high frequency	--

- Values shown for a very limited set of facilities
- Measurements should be 5x more precise than parameter being measured to resolve
- Measurement precisions <1% needed.
- For quiet tunnels, <<1% needed!

Some advantages of Spectroscopic Measurement Techniques

- Non-intrusive
  - No probes, particles perturb the flow
- Remote detection
  - Can be used in hostile environments
- Can measure multiple parameters, states:

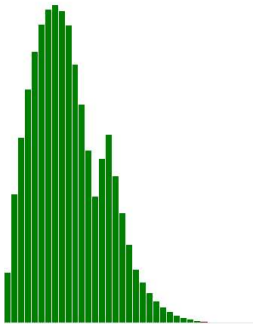

  - Sometimes simultaneously
  - Can be instantaneous (<10 ns) and high freq. (MHz)
  - Can be precise, accurate, high spatial res. (2D, 3D)
- *But…*

No one measurement technique can meet all requirements

  - Can have more complicated theory, expensive and complex equipment, more difficult data analysis
  - May require seeding of (sometimes toxic) gases, more expertise, slower data acquisition, analysis

What makes a good measurement technique?

- A reliable measurement system matched with well-understood physics to make a quantified measurement that meets a customer's requirements.

Explore each of these…

Typical Measurement System

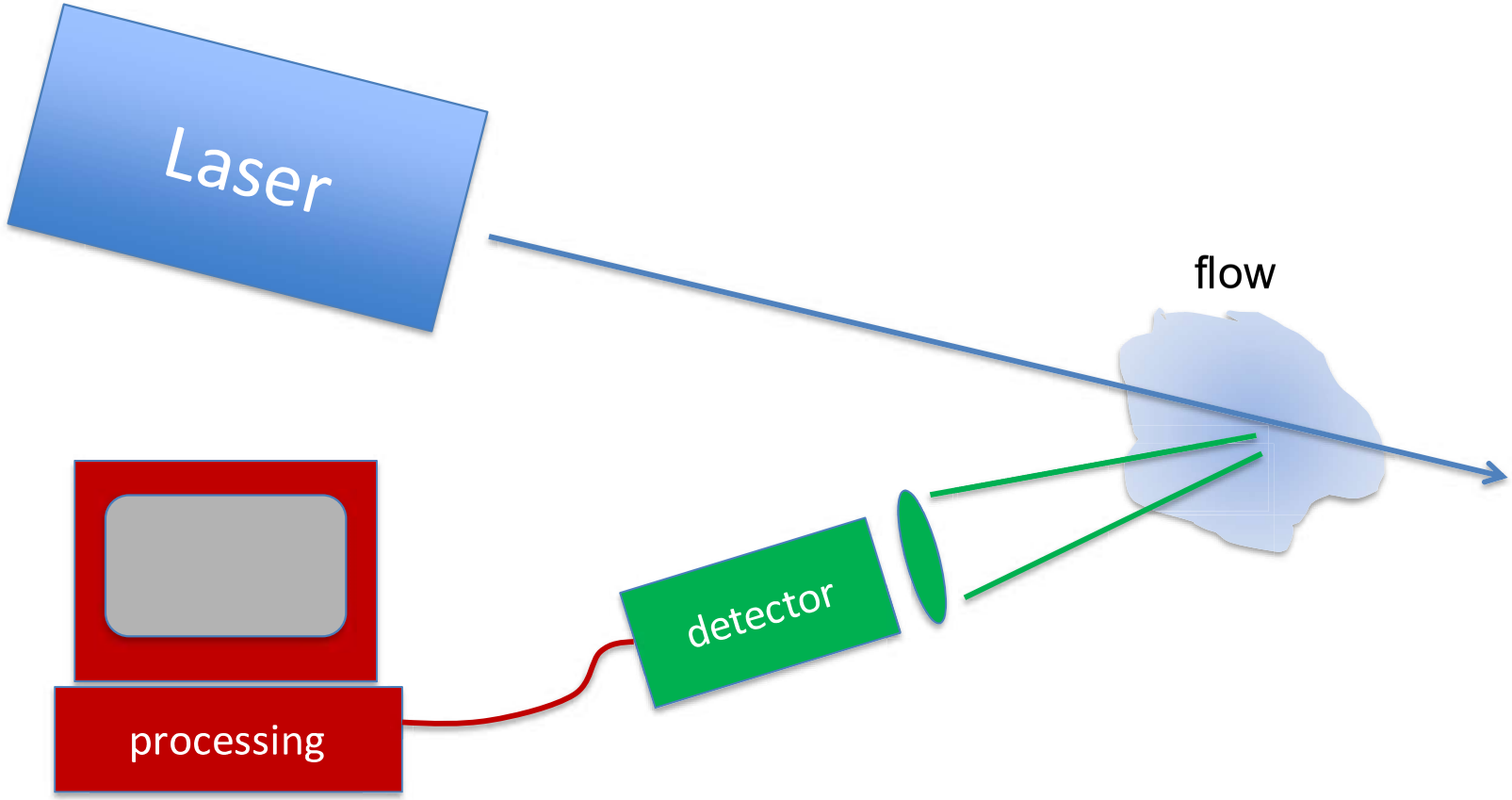

- Need to understand equipment and physics of process to make a measurement
  - Absorption, LIF, Rayleigh, Raman, CARS, etc.

Measurement System: Lasers

- Lasers: pulsed vs. continuous wave (cw)
  - Continuous wave: lower power (mW to Watt)
  - Pulsed: higher power
    - 10 ns, picosecond, femtosecond all commercially available
    - 'Freeze' the flow
    - Much higher power vs cw (MWatt-GWatt, even TWatt)
    - Frequency conversion (useful in linear techniques such as Raman, Rayleigh, LIF)
    - Provide high powers for nonlinear techniques (CARS)
    - Repetition rate: 10-100 Hz, 16 kHz, 1 MHz, 80 MHz…
- What colors of laser light do we need?

Colors of Light: Spectroscopy

Molecular response: vibrational electronic rotational

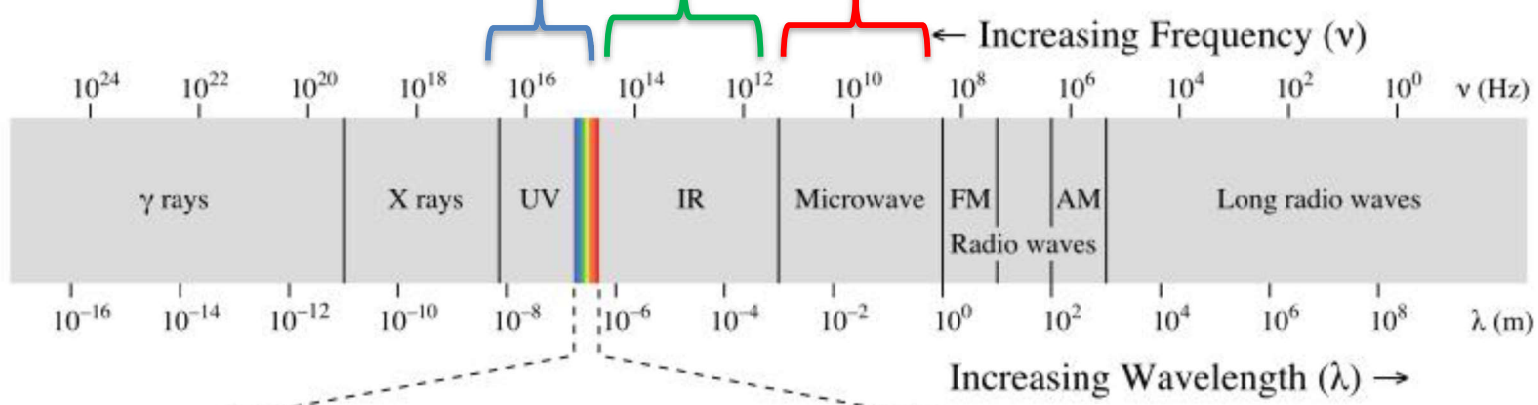

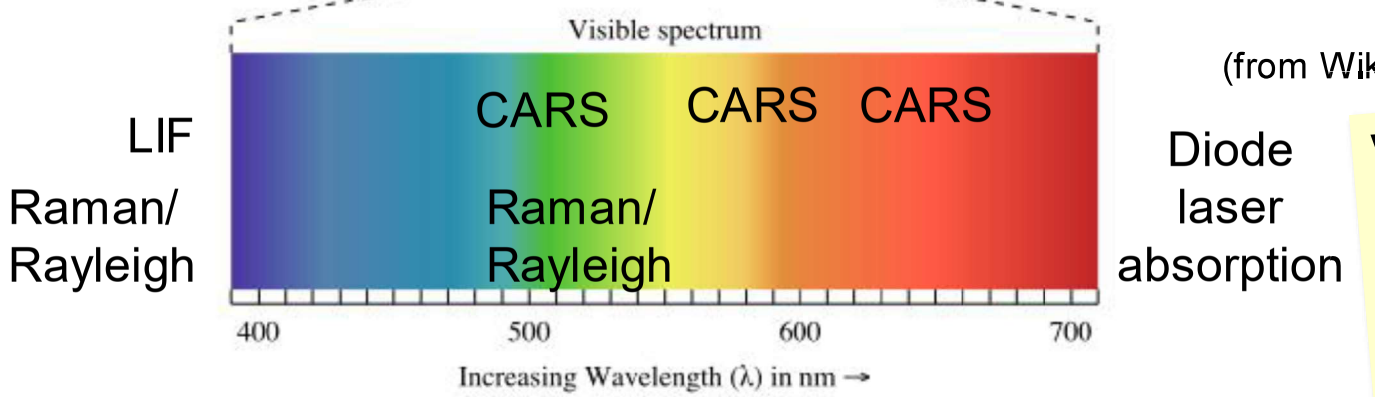

(from Wikipedia, "frequency")

Wavelength →
←Frequency
←Energy
←Wavenumbers
= 1/Wavelength

- Many different colors can be useful for spectroscopy
- As energy increases, more modes can be excited
  - LIF: can see electronic, vibrational and rotational structure

Measurement System 2

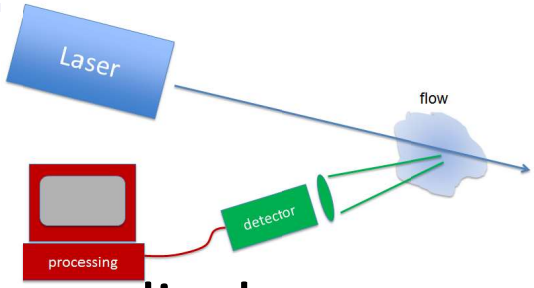

- Detectors:
  - Single point detectors: Photomultipler tubes (PMT) and photodiodes
  - Camera technology is rapidly evolving:
    - CCDs provide 'scientific grade' (low noise, linear, etc.)
    - CMOS cameras are faster
    - Commercially available cameras at up to 10's, 100's of kHz steady streaming or MHz for short bursts or few pix
  - Fiber optics and fiber-optic bundles often used for either transmitting laser or collecting signal
- Processing:
  - Some data processing codes are available (CARSFT, LIFBASE) but many are proprietary.

What makes a good measurement technique?

- A reliable measurement system matched with well-understood physics to make a quantified measurement that meets a customer's requirements.

SKIP

Explore each of these…

Quantified Measurements

- Accuracy and precision of a measurement must be quantified to be useful, for example when comparing to a code
  - Qualitative measurements (flow vis) can be useful

- Quantified measurement:
  - Accuracy and precision are well characterized

Accurate but not precise

Precise but not accurate

(from Wikipedia, "accuracy and precision")

  - <u>Accuracy</u>: compared to a 'standard' or 'accepted'
  - <u>Precision</u>: 1σ of large sample of measurements
    - Averaging reduces precision's contribution to uncertainty
    - High precision required to quantify fluctuations (turbulence)

Customer Requirements

Interview the customer… (sometime the customer is you!)

- What do you want to measure?
- Simultaneous measurements to obtain correlations: $T'u'$, $\rho u'v'$
- Time resolution (< μsec), and frequency response (> MHz)
- Spatial resolution: near walls; smallest scales in shear layer
- Where are the measurement to be made?
  - Inflow to establish B.C., exit, near walls?
  - Point, line, plane, volume?
- Accuracy and precision requirement?
- What quantity of data is required? Uncertainty required?
- When is the data needed? Is "real-time" data required?
- What type of optical access is available?
- Can (toxic) seed gases be introduced? Will they influence the properties being measured? Can particles be used?
- What is the ordered priority of the above requirements?

What makes a good measurement technique?

- A reliable measurement system matched with well-understood physics to make a quantified measurement that meets a customer's requirements.

- Now the lecture will focus on different measurement systems, introducing the physics.
  - How's the basic physics of the method work?
  - Can the measurements be made instantaneously (aka. single-shot) at high frequencies?
  - What accuracy and precision can be obtained?

Outline for Today's talks

1. Introduction
2. Absorption Spectroscopy
3. Planar Laser-Induced Fluorescence (PLIF)
4. Molecular Tagging Velocimetry (MTV)
5. Focused Laser Differential Interferometry (FLDI)
6. Laser Scattering Techniques
7. Coherent anti-Stokes Raman Scattering (CARS)
8. Particle Image Velocimetry (PIV)
9. Emission Spectroscopy
10. Conclusions

Absorption Spectroscopy

Josh Weisberger, NASA Langley Research Center

Craig Johansen, The University of Calgary, Canada

Sean O'Byrne, University of New South Wales, Canberra, Australia

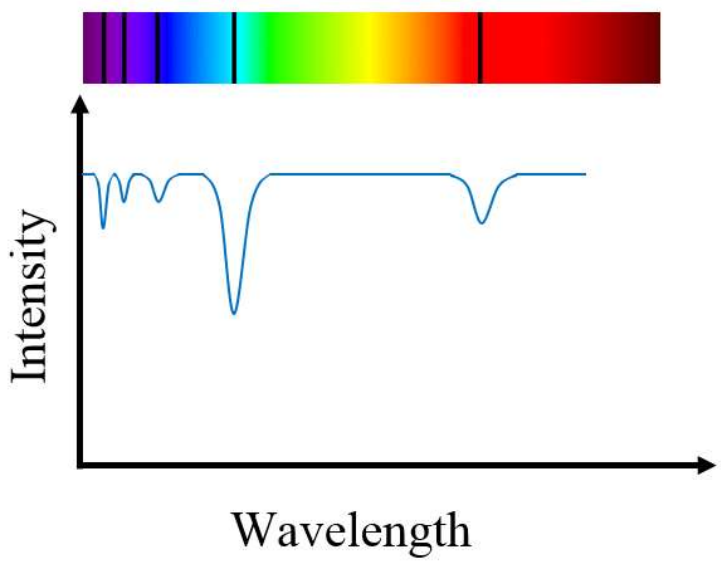

Absorption Spectroscopy

- Light of specific wavelength can be absorbed by a gas of interest
  - Size and shape of absorption features used to obtain properties of gas (T, P, X, V, etc.)
- Spectrum of CO_2 and H_2O transitions shown in plot on right

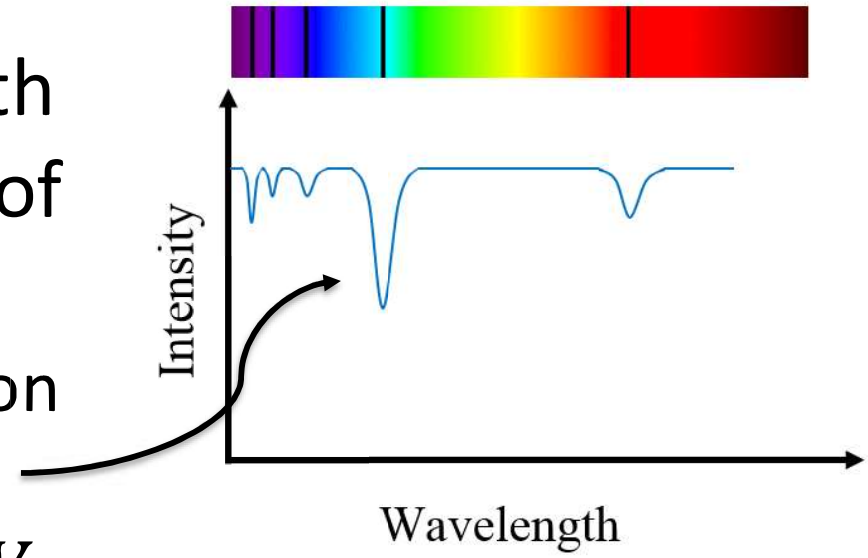

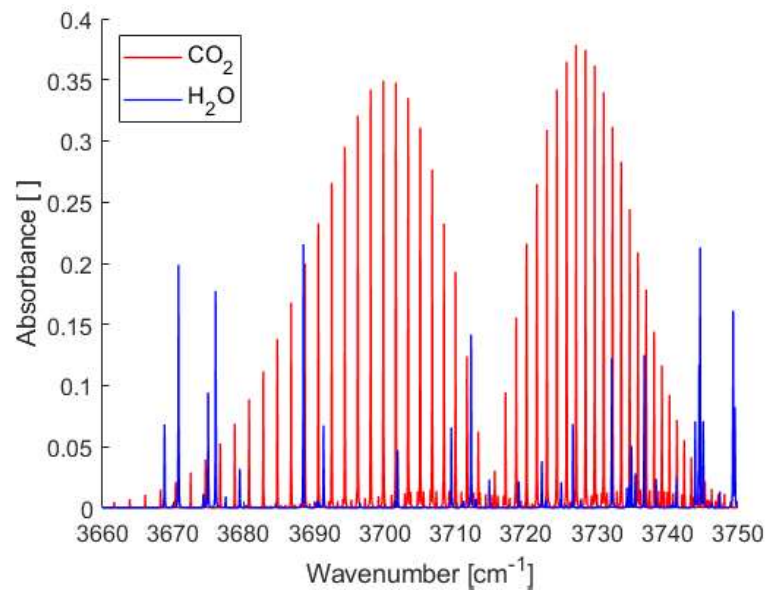

Absorption Experiment Setup

- Laser (L) shines through a gas and onto a detector (D)
- Wavelength reference (WR) is used to convert from time to wavelength

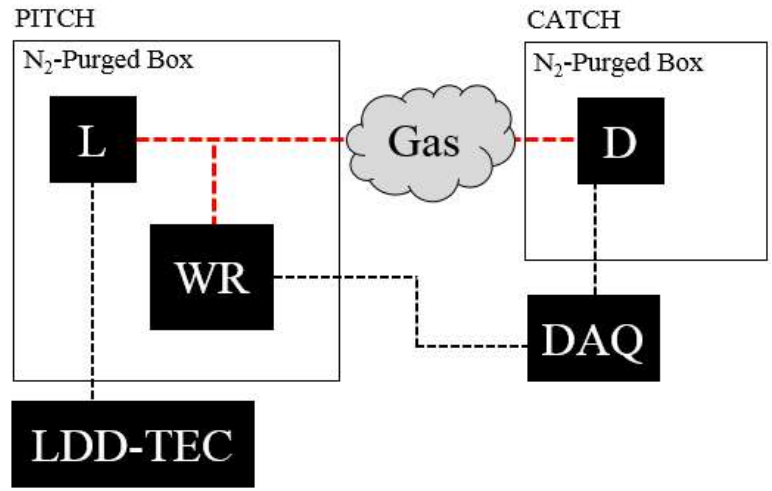

- Typical raw data ramp with absorption feature shown in black
- Divide transmitted signal (black) by baseline (blue) to get absorption

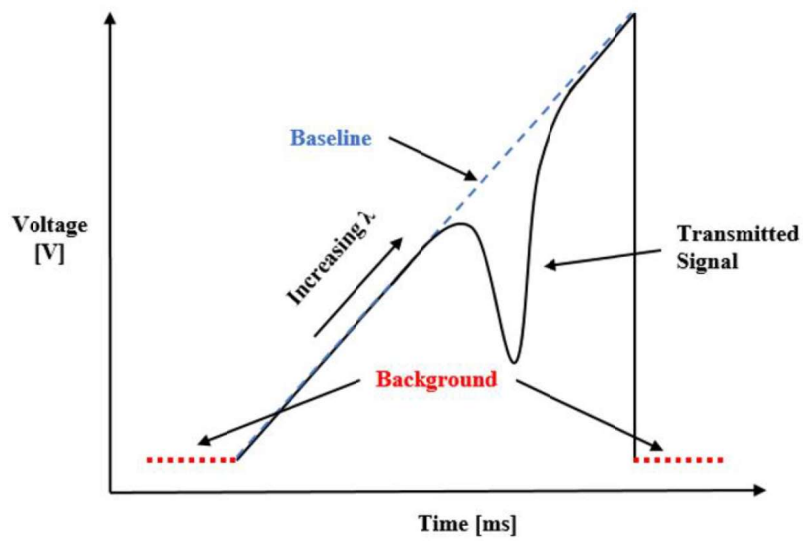

Absorption Spectroscopy Theory

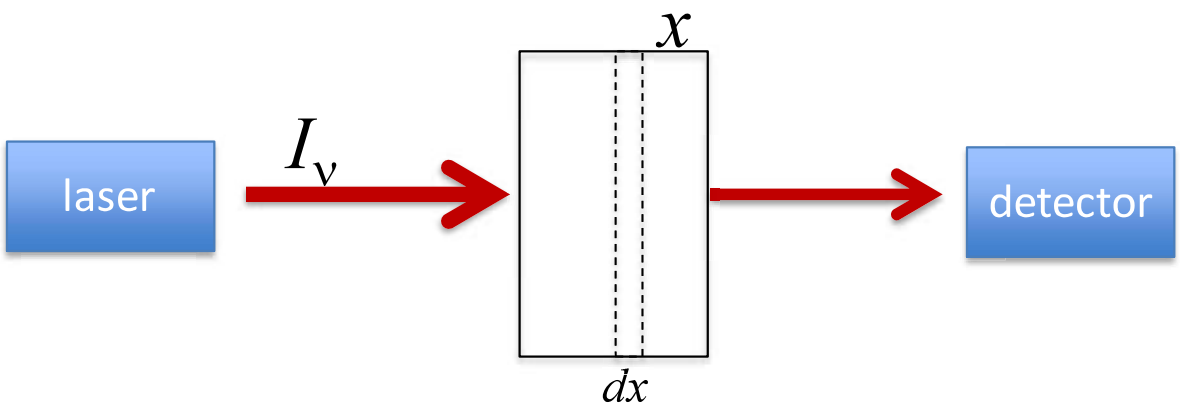

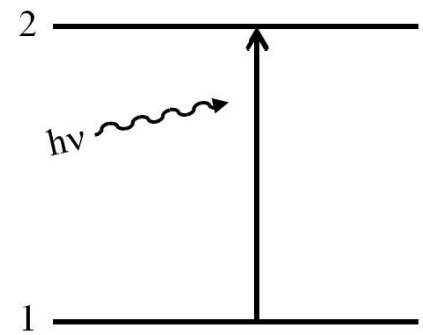

- Absorption is described by the Beer-Lambert Law:

$$\boxed{-dI_\nu = I_\nu k_s(\nu)\,dx}$$

where $k_s(\nu)$ is the spectral absorption coefficient

- This leads to exponential decay of laser intensity:

$$\boxed{I_{\nu,x} = I_{\nu,0} e^{-k_s(\nu)x}}$$

- Measure I_ν, know x, directly measure $k_s(\nu)$
- $k_s(\nu)$ contains information about temperature, concentration, velocity of gas

Broadening Mechanisms

- Spectral shape of $k_s(\nu)$ is from "broadening"
- Pressure (homogeneous) broadening

$$g_H = \frac{\Delta\nu_H}{2\pi} \frac{1}{(\nu - \nu_0)^2 + (\Delta\nu_H/2)^2}$$

  - Caused by collisions with other atoms/molecules, a high-pressure effect causing a Lorentzian shape
  - Generates a broadening

$$\Delta\nu_c = P \sum_i (\chi_i \gamma_i)$$

and a shift in the transition

$$\Delta\nu_s = P \sum_i (\chi_i \delta_i)$$

P is the pressure
χ_i is the mole fraction
γ_i is width per unit pressure
δ_i is shift per unit pressure
i is the index over all species

  - If temperature can be independently determined, pressure can be measured from these quantities

Broadening Mechanisms

- Doppler (inhomogeneous) broadening
  - Due to thermal motion of absorbing particles towards or away from laser

$$g_D = \frac{2\sqrt{\ln 2}}{\pi^{1/2}\Delta\nu_D} \exp\left[\frac{-4\,(\ln 2)\,(\nu - \nu_0)}{\Delta\nu_D^2}\right]$$

  - $\Delta\nu_D$ is the full-width at half-maximum of the measured peak, and is given by

$$\Delta\nu_D = 2\nu_0\sqrt{\frac{2kT_{\text{trans}}}{(\text{MW})\,c^2}\ln 2}$$

ν_0 is the transition center
k is the Boltzmann constant

Voigt Profile

- The Voigt profile is a convolution of the two previous broadening effects

$$V(a,x) = \frac{a}{\pi}\int_{-\infty}^{\infty}\frac{e^{-y^2}}{a^2+(x-y)^2}dy$$

$$a = \sqrt{\ln 2}\frac{\Delta\nu_H}{\Delta\nu_D}$$

$$x = 2\sqrt{\ln 2}\frac{(\nu-\nu_0)}{\Delta\nu_D}$$

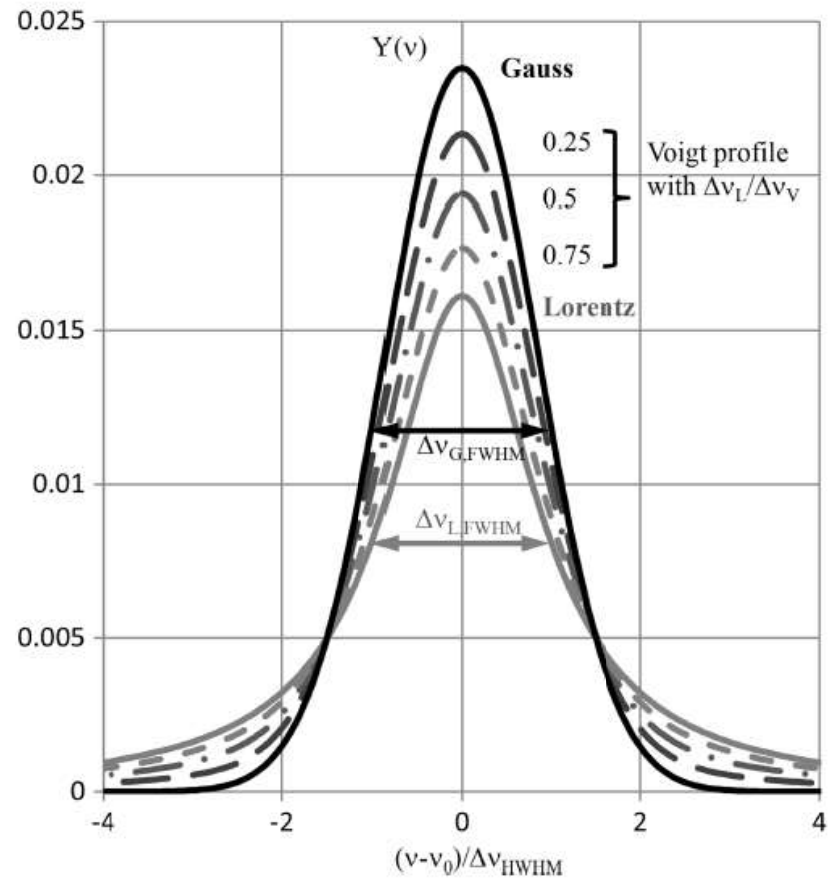

Laser Sources

- In 1970s, dye lasers were often used in visible and NIR absorption studies, and Pb salt for IR
- Now mostly replaced with diode laser sources
  - **Distributed feedback (DFB) lasers**
    - Tune over $\sim 0.1\ nm$
    - Robust and well tested in telecoms
    - Very spectrally narrow (1 - $30\ MHz$)
  - **Vertical cavity surface-emitting lasers (VCSELs)**
    - Tune over $1\ nm$
    - Tune very rapidly
    - Spectrally narrow ($< 30\ MHz$)
  - **Quantum cascade lasers (QC)**
    - High-power pulsed source operating in the IR

Detection Schemes

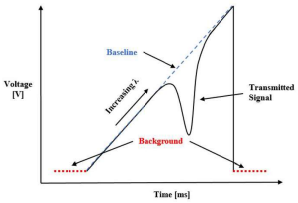

- **Direct absorption**
  - Simple, direct measurements, but poor use of dynamic range
- **Difference amplification**
  - Removes intensity modulation, but only when perfectly balanced
- **Log-ratio detection**
  - Simple circuit, and cancels common-mode electronic and laser noise very efficiently
- **Wavelength modulation**
  - Removes DC offset from signal, reduced $1/f$ noise
  - Signal proportional to the *derivative* of the input intensity
  - Ratio of second-harmonic ($2f$) and first-harmonic ($1f$) signals to account for the laser intensity (self calibrating)
    - GB Rieker *et al. Appl. Opt.* 48.29 (2009): 5546-5560.
- **Cavity-based methods**
  - Useful for measurements of trace quantities, but practical challenges in hostile environments.

Velocity Measurements

- Simplest quantity to measure in high-speed flow
  - Measured through Doppler shift between beams with velocity components in two different directions relative to the flow

$$\Delta\nu_{Doppler\ shift} = \frac{U}{c}\nu_{laser} \qquad U = \frac{c\ \Delta\nu_{Doppler\ shift}}{\nu_{laser}}$$

  - Shift in the peak position relatively insensitive to amplitude noise
  - Shift typically calibrated to etalon measurements

Velocity Measurements

- *E.g. Lyle et al.,* mass flux sensor based on measurements of density and velocity using oxygen *A*-band near $760\ nm$
- Measured speed with time-averaged precision of $0.25\ m/s$

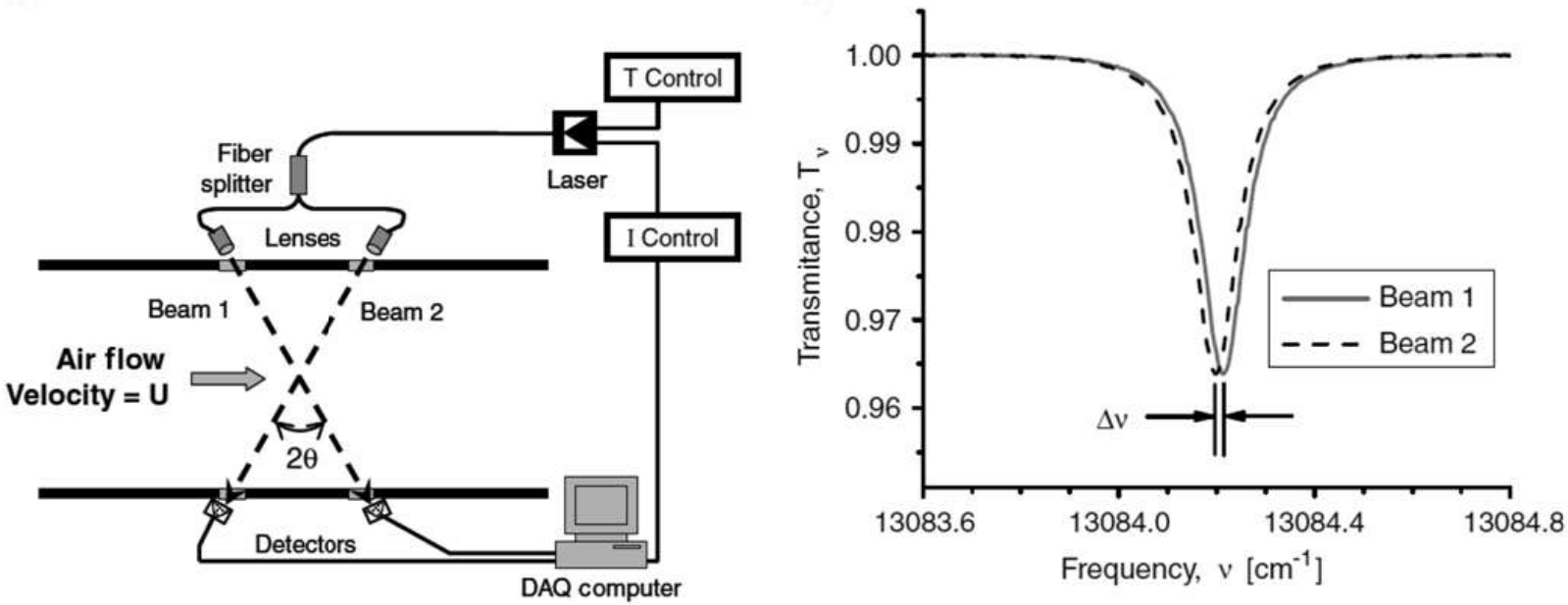

K. H. Lyle, J. B. Jeffries and R. K. Hanson "Diode-laser Sensor for Air-Mass Flux 1: Design and Wind Tunnel Validation," AIAA Journal, 45 (9), 2204–2212, 2007.

Translational Temperature

- Can be determined through the Doppler width, but as $T_{trans} \propto \left(\frac{\Delta\nu_D}{\nu_0}\right)^2$, small errors in Doppler width have a significant effect on *T*

$$\frac{\Delta T}{T} = \frac{2\Delta\left(\Delta\nu_D\right)}{\Delta\nu_D}$$

  - *E.g.* An uncertainty in width measurement of 1.5% for a Doppler-broadened transition in the oxygen *A*-band will cause an uncertainty of 3% in temperature
  - Uncertainty further increased in the presence of pressure broadening
  - Measuring T through linewidth has the advantage of only requiring 1 transition for a measurement

Translational Temperature

- *E.g.* Measurements of temperature in an arcjet facility using an Ar I line at $811.531\ nm$
- 12% uncertainty in width translated to 30% uncertainty in T_{trans} over $2000 - 10{,}000\ K$

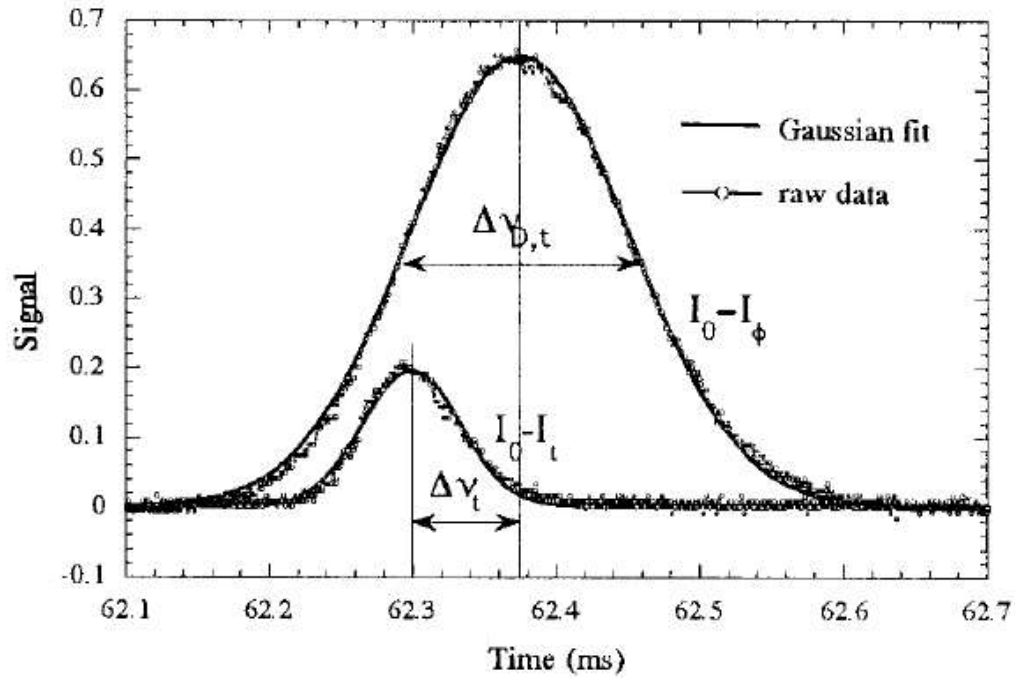

F-Y Zhang, K Komurasaki, T Iida, and T Fujiwara, "Diagnostics of an Argon Arcjet Plume with a Diode Laser," Applied Optics, 38 (9), pp. 1814–1822, 1999.

- This method has recently been used to measure temperature/pressure in a shock tube at up to $1.6\ MHz$ rate!

B. Kaebe, N. Robins, T. Boyson, H. Kleine, and S. O'Byrne, "1.6 MHz scanning rate direct absorption temperature measurements using a single vertical-cavity surface-emitting laser diode," Appl. Opt. 57, 5680-5687 (2018).

T_{trans}: NASA Ames IHF

- Measured uniformity of nozzle inlet temperature
  - Probed electronically excited oxygen (O*)
- Modified upstream plenum to increase mixing before nozzle inlet

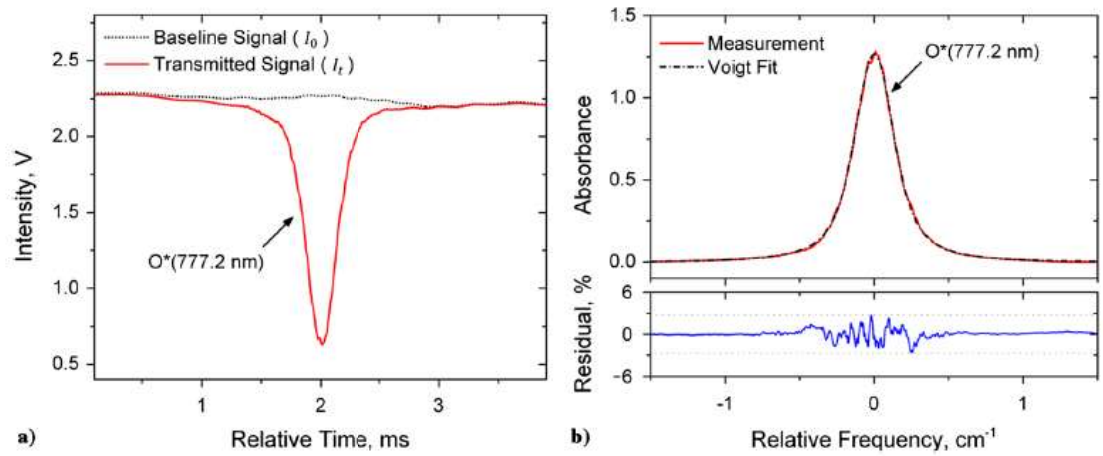

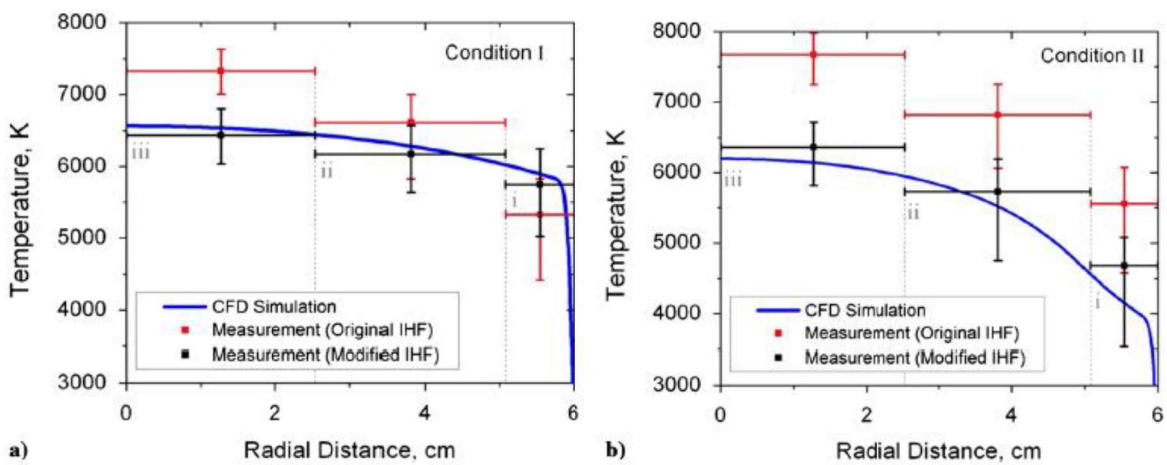

- Compared measured and CFD results
  - Modified plenum design (black) shows better agreement with ideal CFD predictions (blue)

Nations, M., Chang, L. S., Jeffries, J. B., Hanson, R. K., MacDonald, M. E., Nawaz, A., Taunk, J. S. T., Gökçen, T., and Raiche, G., "Characterization of a Large-Scale Arcjet Facility Using Tunable Diode Laser Absorption Spectroscopy," *AIAA Journal*, Vol. 55, No. 11, 2017, pp. 3757-3766.

Rotational Temperature

- Typically measured using the ratio of integrated absorbance *a over* two lines with different linestrength variations with T

$$a_j = P\chi_i L S_j$$

  - for transition j of an absorbing species i
  - L is the path length and S_j is the linestrength of the transition
- All quantities other than S_j are common to the two lines and divide out

$$\frac{a_1}{a_2} = \frac{S_1}{S_2} = \frac{S_1\left(T_0\right)}{S_2\left(T_0\right)} \exp\left[-\frac{hc\Delta E_{\mathrm{rot}}}{k}\left(\frac{1}{T_{\mathrm{rot}}} - \frac{1}{T_0}\right)\right]$$

Rotational Temperature

- *E.g. Wehe et al.* measured H_2O rotational and translational temperature in the 10 MJ/kg Calspan 96-inch hypersonic shock tunnel freestream
- $\nu_1 + \nu_3$ band near $1396\ nm$ (λ_2) and $1400\ nm$ (λ_1)
- $8\ kHz$ scan rate
- T_{rot} uncertainty of $\pm 2.3\ \%$ compared with T_{trans} uncertainty of $\pm 2.7\ \%$ and $\pm 6.4\ \%$ for the T_{trans} measurements on the two lines

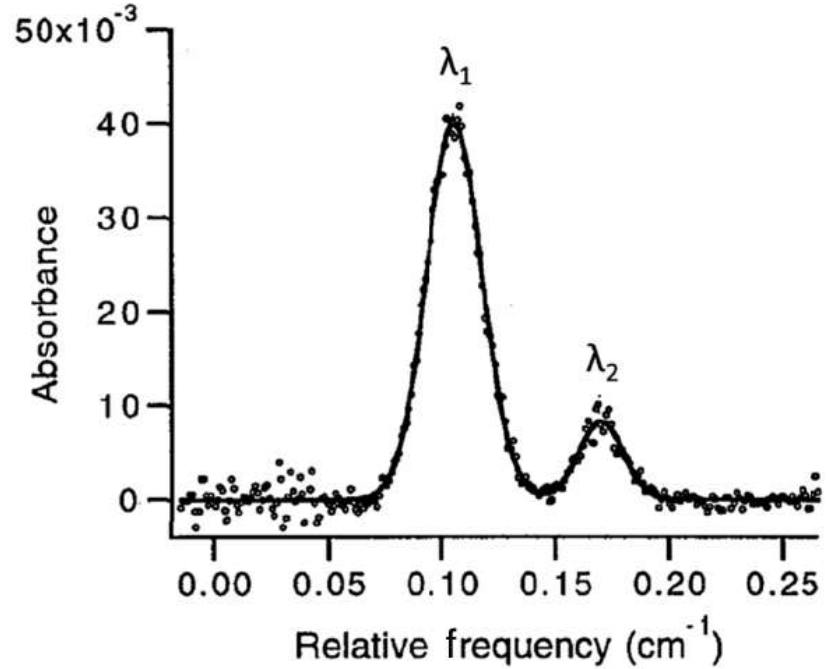

S. Wehe, D. S. Baer, and R. K. Hanson "Tunable Diode-laser Absorption Measurements of Temperature, Velocity, and H_2O in Hypervelocity Flows," 33rd Joint Propulsion Conference and Exhibit, Seattle, WA, AIAA Paper 97-3267, 1997.

Vibrational Temperature

- *E.g. Brandt and Roth* measured T_{vib} and T_{trans} in CO in a reflected shock tube, using a lead salt laser operating at 2100-2200 cm^{-1}, at 20 kHz scan rate.

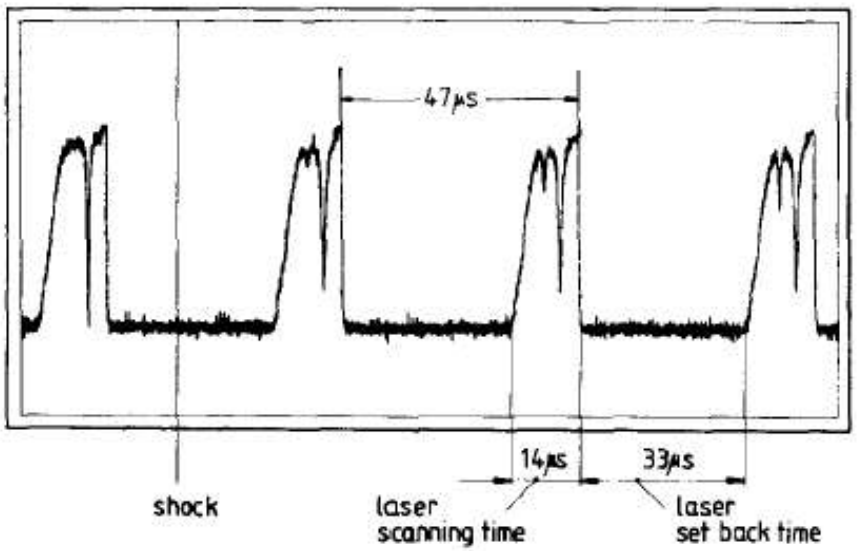

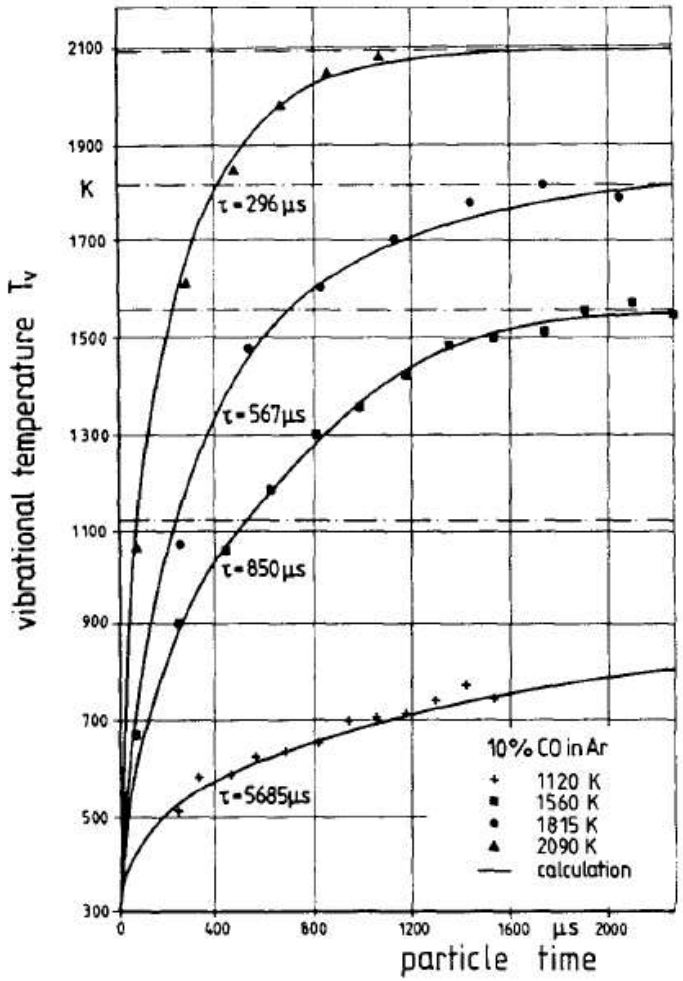

O. Brandt, and P. Roth, "Temperature Measurements behind Shock Waves using a Rapid Scanning IR-diode Laser," Physics of Fluids, Vol. 30, No. 5, pp. 1294–1298., 1987.

Multi Parameter: VKI Longshot

- Measure freestream T, P, and V using CO_2 transition at $1.6\ \mu m$
  - Separation of two Doppler-shifted peaks results in velocity
- T and P harder to fit in harsh conditions
- V uncertainty $\sim 6.5\%$ in flow of $1500\ m/s$

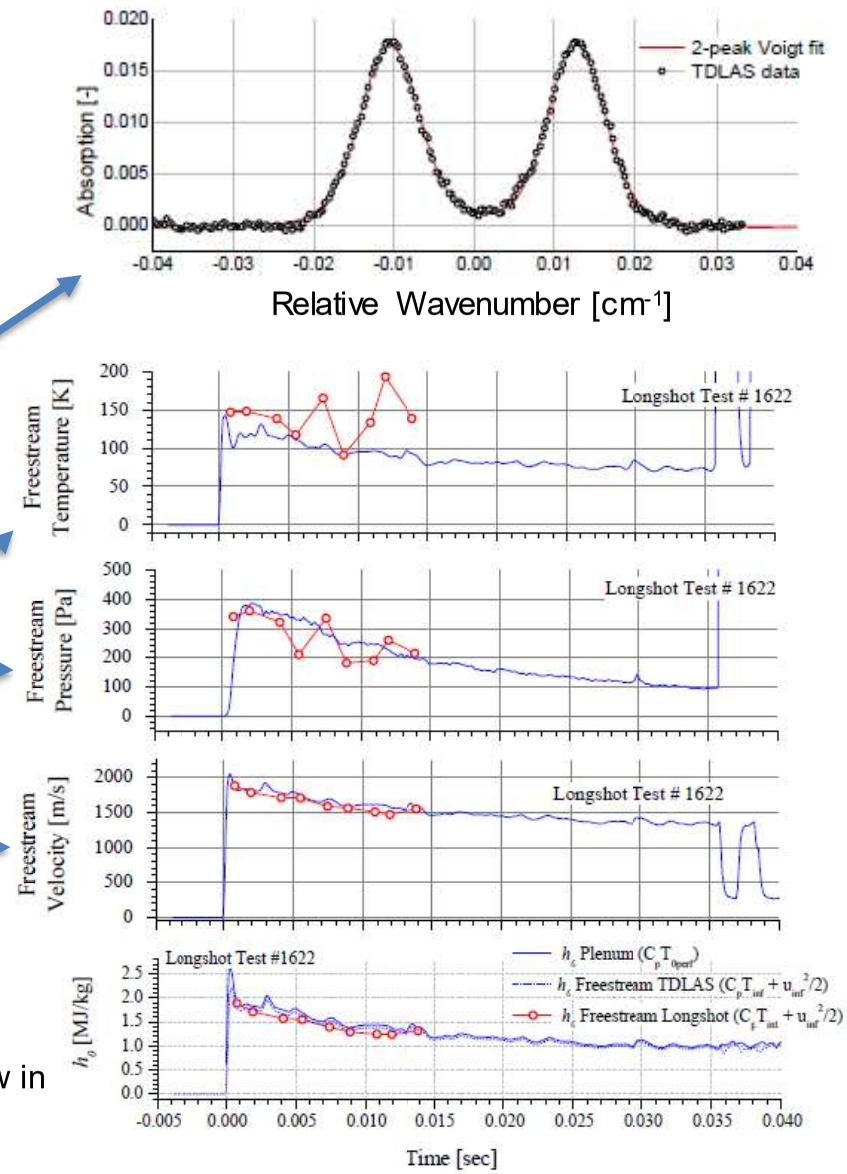

Meyers, J. M., Paris, S., and Fletcher, D. G., "Characterization of CO_2 flow in a hypersonic impulse facility using DLAS," *Experiments in Fluids*, 57:25, February 2016.

TDLAS Tomography

- Major limitation of TDLAS: path-averaged
  - Can do tomography

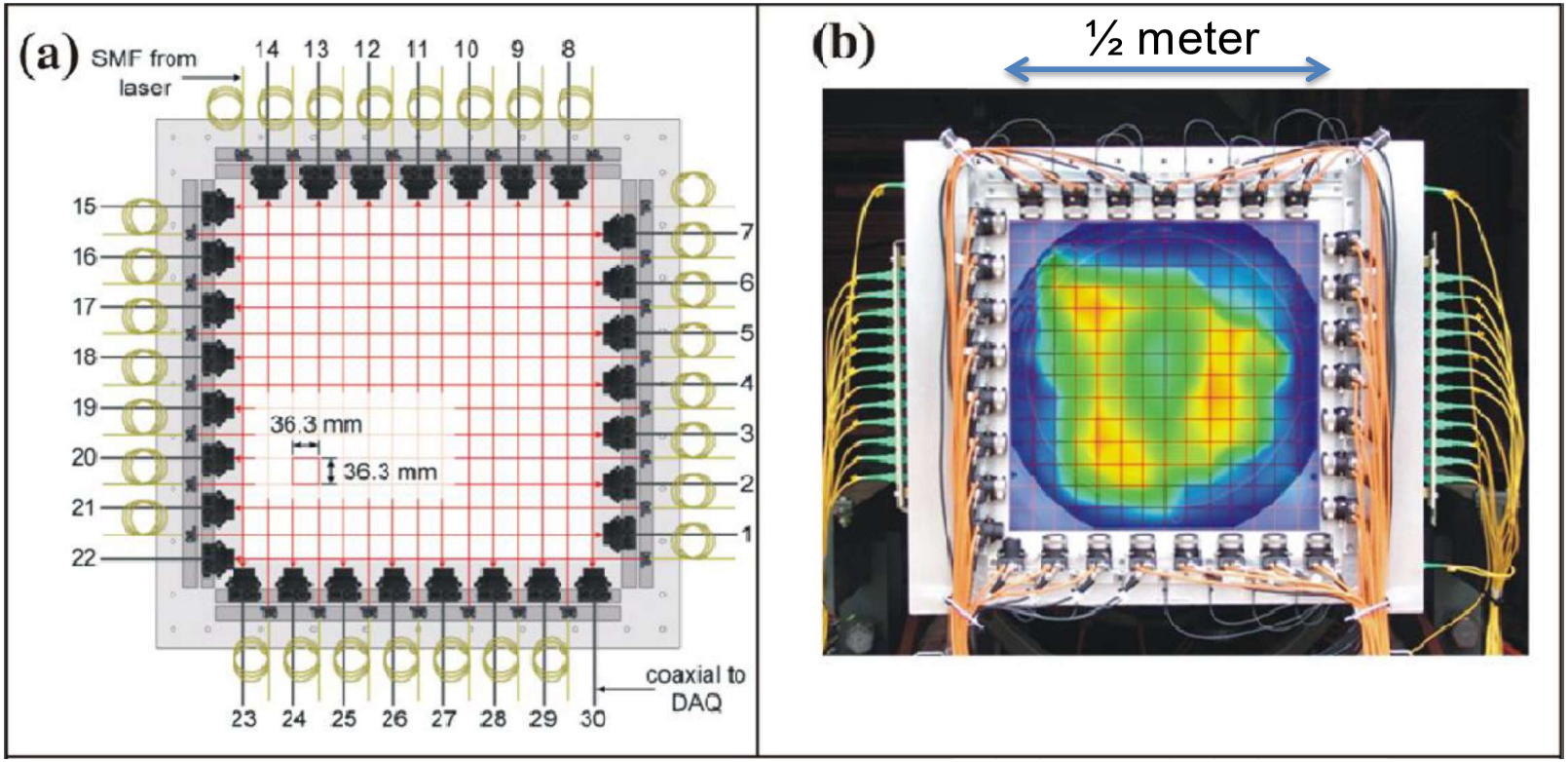

  - 15×15 grid provides data at 225 points ($36\ mm$ grid)

L. Ma, X. Li, S. T. Sanders, A. W. Caswell, S. Roy, D. H. Plemmons, and J. R. Gord, "50-kHz-rate 2D imaging of temperature and H_2O concentration at the exhaust plane of a J85 engine using hyperspectral tomography," Optics Express, Vol. 21, Issue 1, pp. 1152-1162, 2013

TDLAS Tomography

- General Electric J85 gas turbine engine
  - University of Tennessee Space Institute (UTSI)

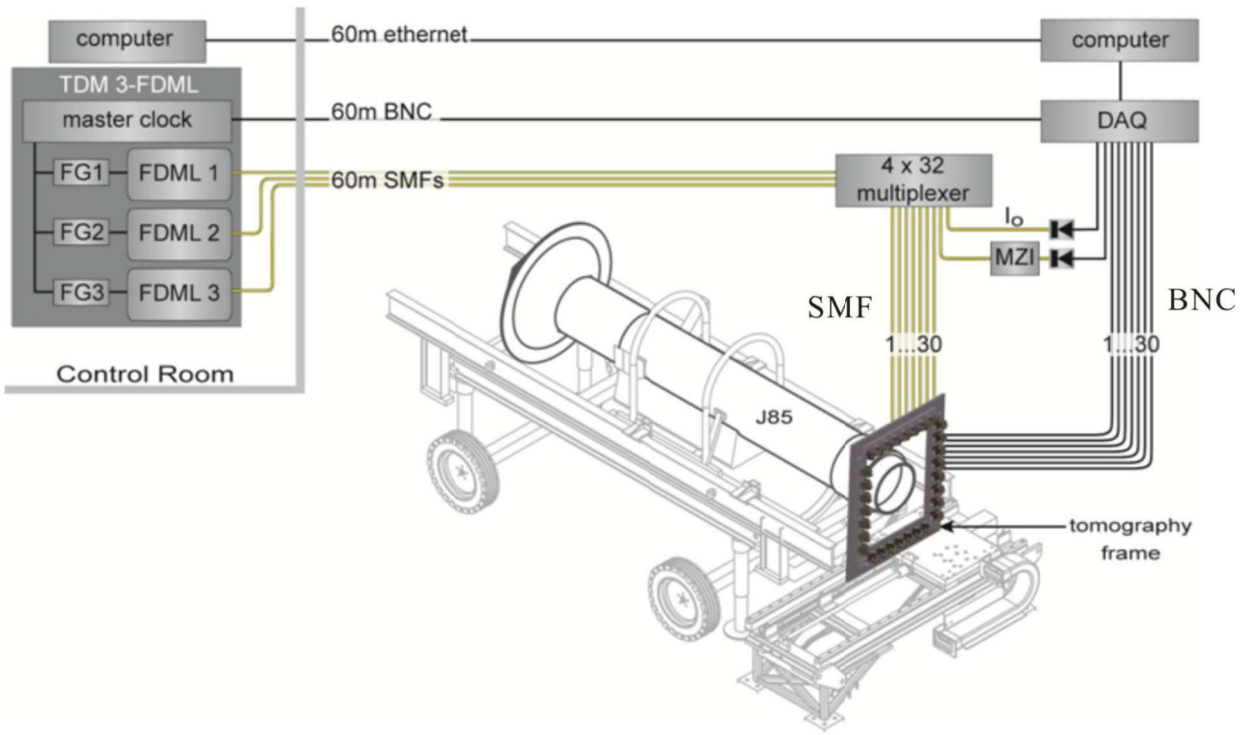

- Measure water and temperature at 50 kHz rate

L. Ma, X. Li, S. T. Sanders, A. W. Caswell, S. Roy, D. H. Plemmons, and J. R. Gord, "50-kHz-rate 2D imaging of temperature and H_2O concentration at the exhaust plane of a J85 engine using hyperspectral tomography," Optics Express, Vol. 21, Issue 1, pp. 1152-1162, 2013

TDLAS Tomography Results

Temperature

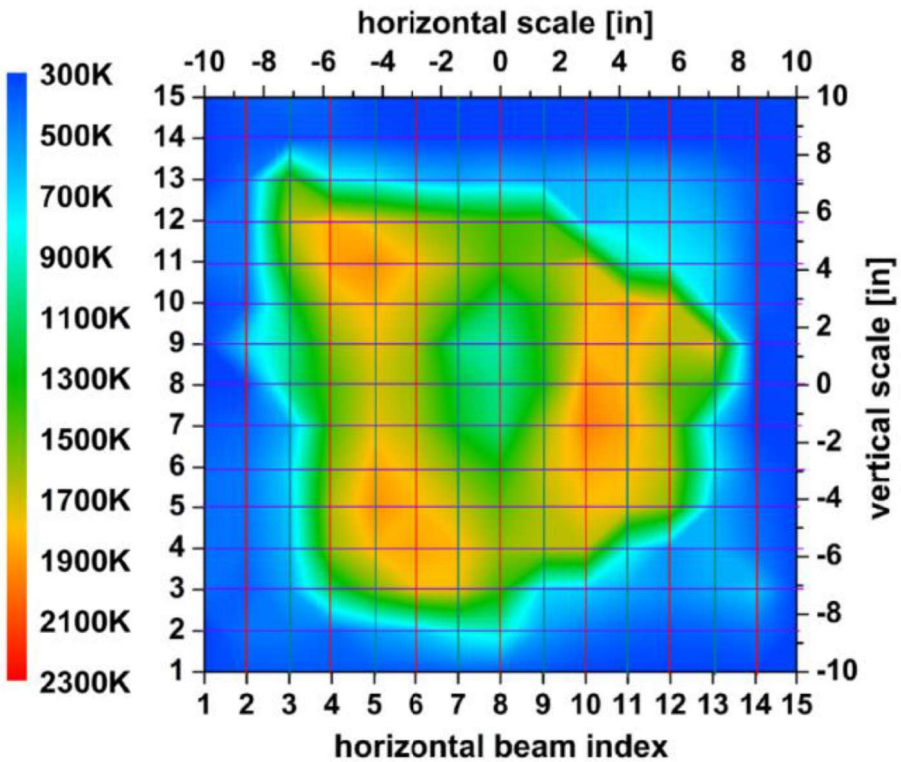

Water Vapor

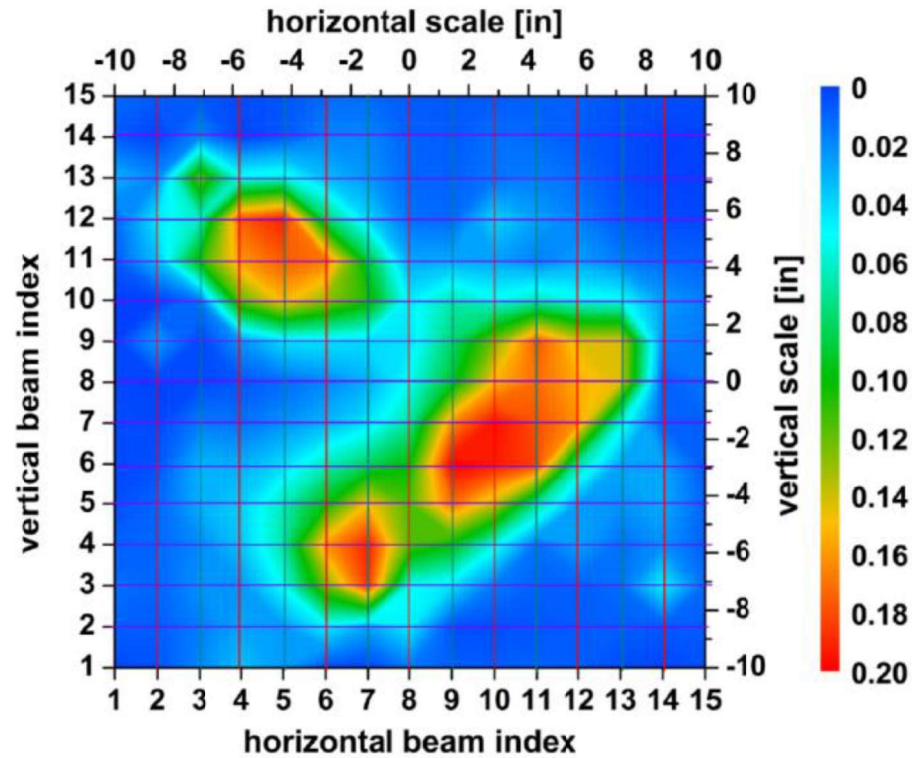

- Measurement is over ~ 0.5 meter square
  - Time resolution is $20\ \mu s$ $(50\ kHz)$
  - Spatial resolution is $\sim 36\ mm$

L. Ma, X. Li, S. T. Sanders, A. W. Caswell, S. Roy, D. H. Plemmons, and J. R. Gord, "50-kHz-rate 2D imaging of temperature and H_2O concentration at the exhaust plane of a J85 engine using hyperspectral tomography," Optics Express, Vol. 21, Issue 1, pp. 1152-1162, 2013

TDLAS: Strengths and Weaknesses

Strengths

- Can probe non-luminous flows and ground-state populations
- Simple, rugged optical arrangements with no moving parts
- Comparatively inexpensive
- Fast wavelength scanning capability (wavelength agile)
- Can provide quantitative multi-parameter measurement with a single instrument
  - No systematic errors due to quenching

Weaknesses

- Path-integrated technique
  - Distributions can be determined tomographically, but time consuming and analysis can be complex
- Spatial and temporal flow nonuniformity can produce bias errors in measurements unless the freestream is well characterized
- Some important diatomics (e.g. N_2) do not have a dipole moment and do not have a direct absorption spectrum

Conclusions

- TDLAS is a reliable and well established nonintrusive measurement technique, capable of precise path-averaged measurements of velocity, density and trans/rot/vib temperatures
- Availability of telecoms lasers and detectors makes it comparatively economical
- Path-averaging disadvantages can be mitigated using tomography or additional spectral information
- Particularly valuable for flight-test applications and time-resolved online facility monitoring
- Rapid development in mid-IR sources and detectors will significantly expand applications

Planar Laser-Induced Fluorescence (PLIF)

Craig Johansen, The University of Calgary, Canada
Paul Danehy, NASA Langley Research Center, Virginia, USA
Brett Bathel, NASA Langley Research Center, Virginia, USA

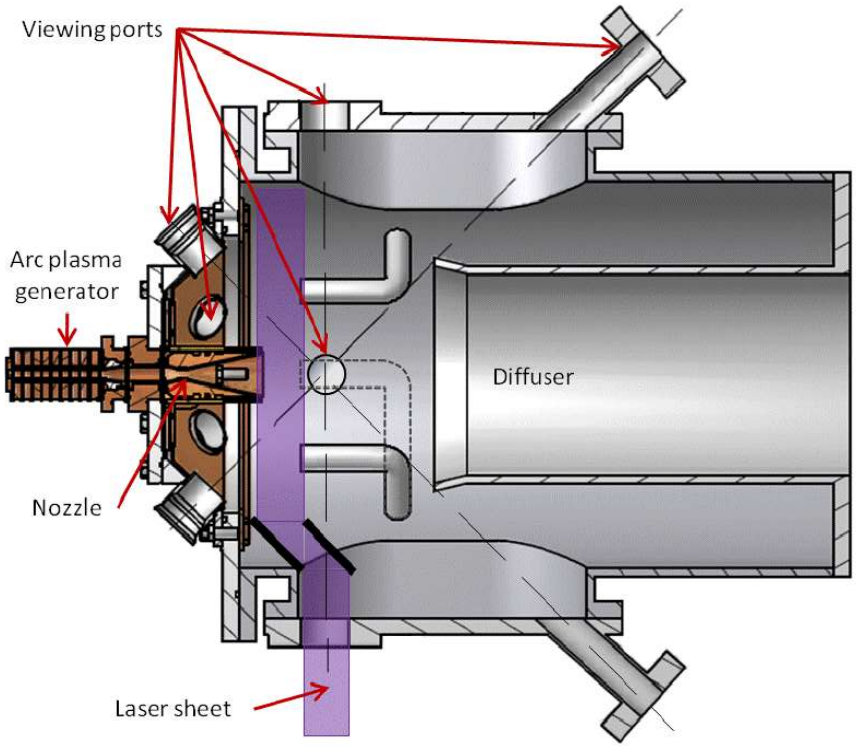

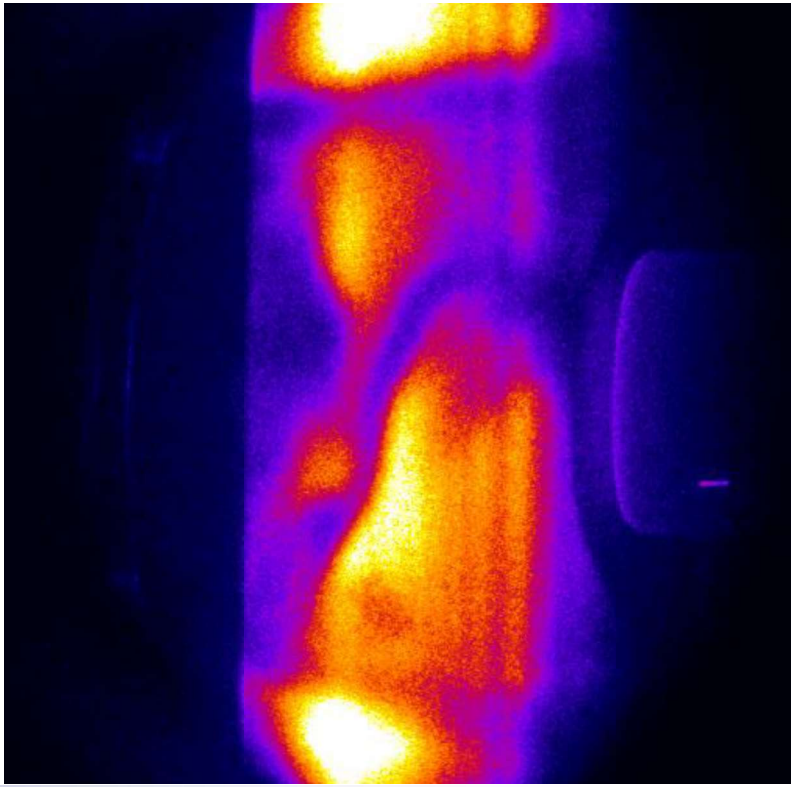

Figures from Inman, J., Bathel, B., Johansen, C., Danehy, P., Jones, S., Gragg, J., and Splinter, S., (2013) "Nitric oxide planar laser-induced fluorescence measurements in the Hypersonic Materials Environment Test System," *AIAA Journal,* Vol. 51, No. 10, pp. 2365-2379

Planar Laser-Induced Fluorescence (PLIF)

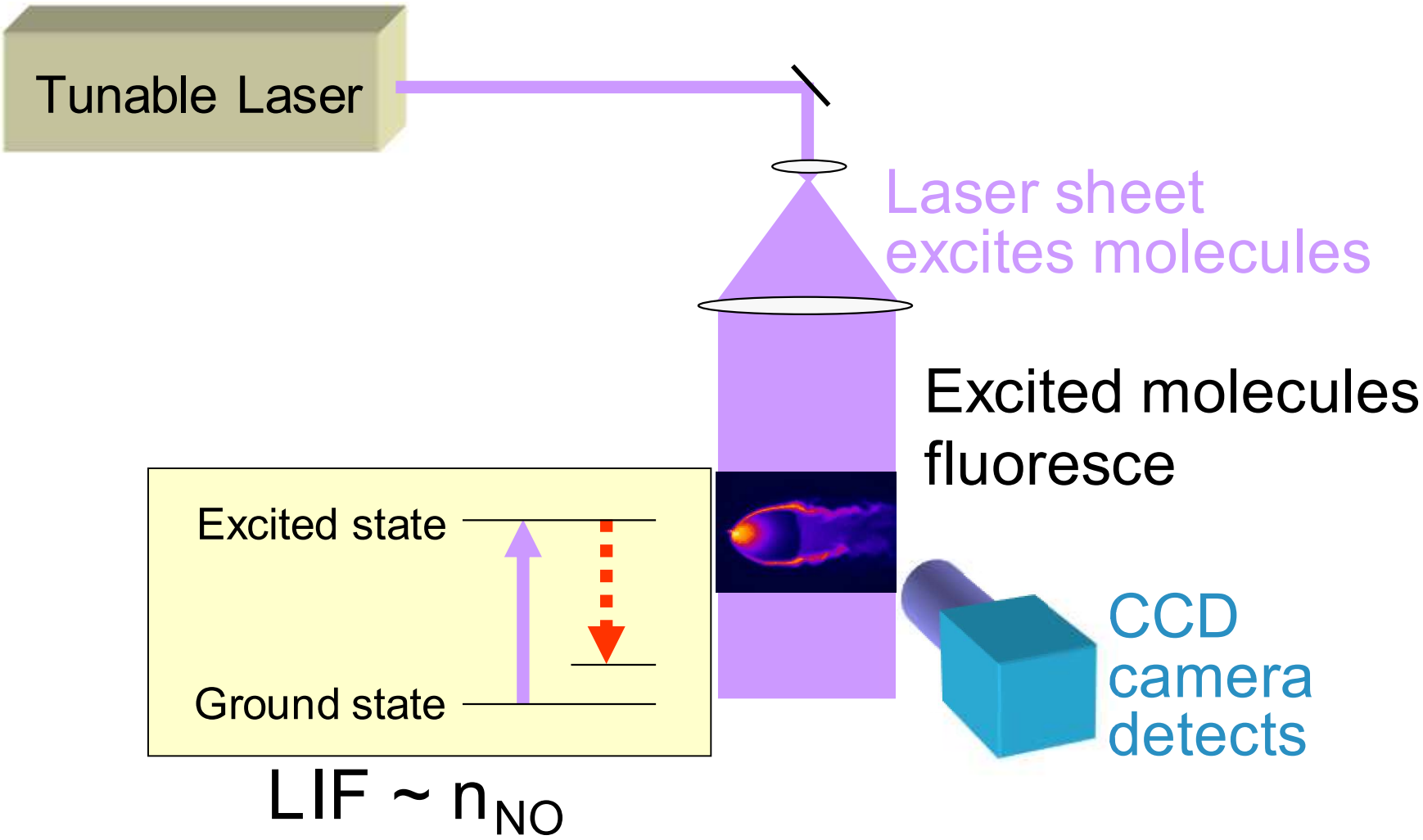

$LIF \sim n_{NO}$

PLIF can probe nonequilibrium

- Commonly used in <u>equilibrium</u> environments
- Useful probe for <u>thermal non-equilibrium</u>:
  - Translational temperature
  - Rotational temperature
  - Vibrational temperature (often $T_{vib} \neq T_{rot} \approx T_{tran}$)
  - Species specific:
    - Different species can have different temperatures (especially vibrational temperatures)
- Can measure, quantify species in <u>chemical non-equilibrium</u> (eg. NO in shock tunnels)
- Can also seed NO into perfect gas flows.
  - Many other tracers can be used, I_2, OH, Kr, etc…

LIF Theory (Two-Level Model)

2

Energy of absorbing species at excited state (2)

1

Energy of absorbing species at ground state (1)

Assumptions:

A. There are only two important states to consider (ground state and excited state). Other levels (rotational and vibrational) are ignored.
B. Prior to excitation, population of absorbers in excited state is negligible (N_2=0)

Two-Level Model Theory

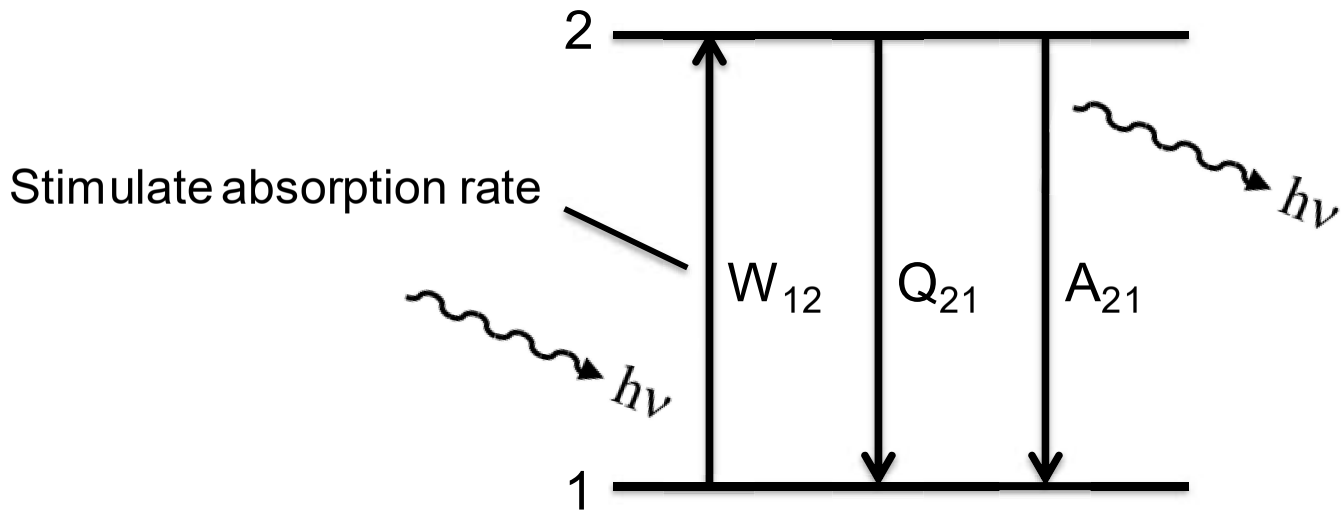

Rate equation: $$\frac{dN_1}{dt} = -\frac{dN_2}{dt} = N_2(Q_{21} + A_{21}) - N_1 W_{12}$$

Conservation of mass for absorbing species: $$N_1 + N_2 = N_s = \chi_s f_B N_T$$

Mole fraction of absorbing species

Total number density

Number density of the absorbing species in the ground state prior to excitation

Boltzmann fraction

Steady State Two-Level Model

- Steady state assumption (e.g. continuous wave laser): $\frac{dN_1}{dt} = -\frac{dN_2}{dt} = 0$
- Solve for N_2: $N_2 = \frac{\chi_s f_B N_T W_{12}}{W_{12} + Q_{21} + A_{21}}$
- Weak excitation assumption: $W_{12} \ll (Q_{21} + A_{21})$
- Integrate spontaneous emission rate: $\int_0^{t_{det}} N_2 A_{21} dt = N_2 A_{21} t_{det}$
- Include the optics of detection to get LIF signal:

$$S_{LIF} = \chi_s f_B N_T W_{12} \left(\frac{A_{21}}{Q_{21} + A_{21}}\right) t_{det} V \frac{\Omega}{4\pi} \eta$$

total number of photons collected

fluorescence yield (Φ)

detection time

volume excited

solid angle

collection efficiency

Concentration of Absorbing Species

$$S_{LIF} = \underline{\chi_s N_T} f_B W_{12} \Phi t_{det} V \frac{\Omega}{4\pi} \eta$$

- To first order, S_{LIF} is proportional to the concentration of the absorbing species
- Qualitative PLIF visualization often used to show the spatial distribution of absorbing species
- (see AIAA Book chapter for measurement strategies for quantitative concentration)

Figure from Inman et al (2013)

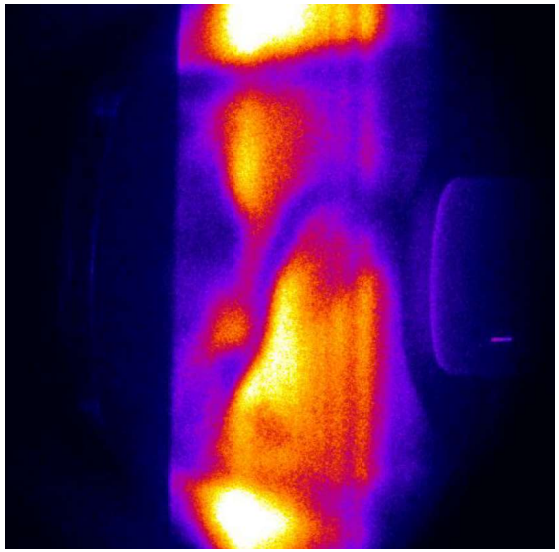

$$S_{LIF} \propto \chi_{NO} N_T$$

PLIF Flow Uniformity Example

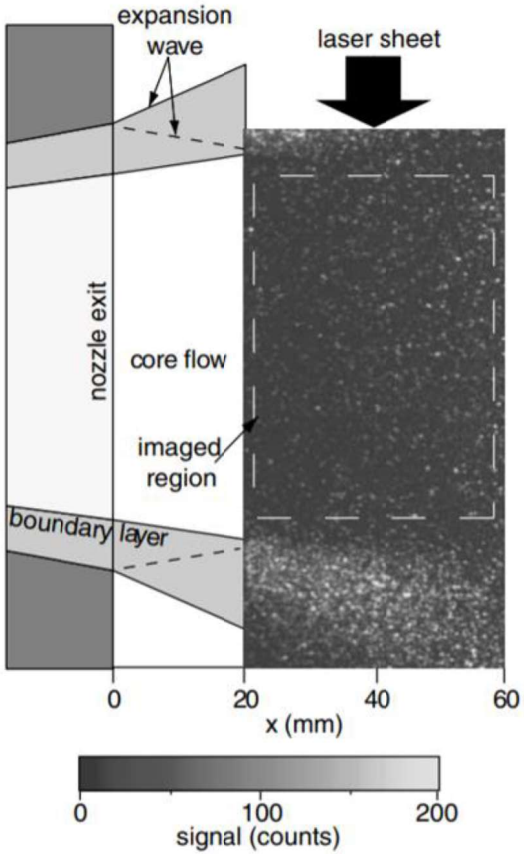

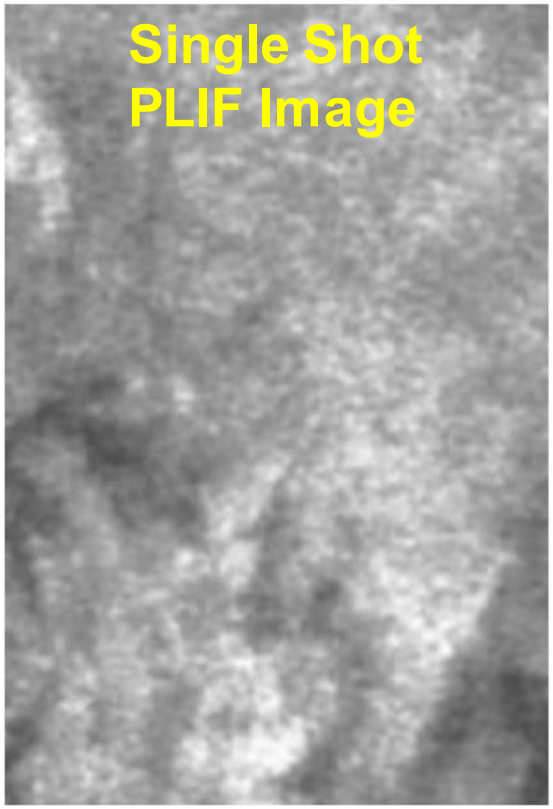

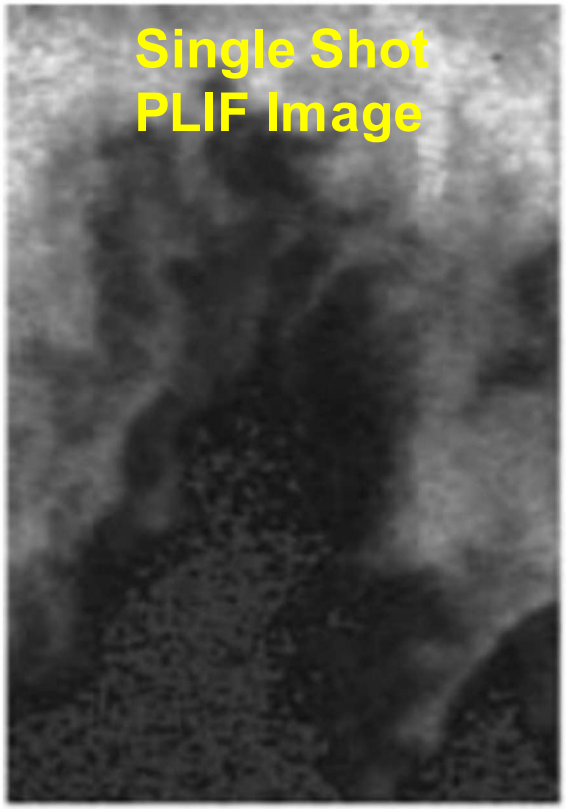

- Flow uniformity in Mach 7.9 flow in T2 free-piston shock tunnel
- PLIF data showed entrainment of cold boundary layer into core flow as source of non-uniformity → nozzle was repaired

O'Byrne, S., Danehy, P. M., and Houwing, A. F. P., "Investigation of hypersonic nozzle flow uniformity using NO fluorescence," *Shock Waves*, Vol. 15, No. 2, 2006, pp. 81–87, doi:10.1007/s00193-006-0013-6.

Boltzmann Fraction

$$S_{LIF} = \chi_s N_T \underline{f_B} W_{12} \Phi t_{det} V \frac{\Omega}{4\pi} \eta$$

- Rotational Boltzmann fraction

$$f_B = \frac{g_j e^{-E_j/k_B T}}{\sum_j g_j e^{-E_j/k_B T}}$$

  - a function of temperature only
  - Peak at 300 K is ~3% for N = 7 (J = 7.5)
- Vibrational and electronic Boltzmann fractions
  - Most molecules in ground state for T < 2000 for atoms, diatomics

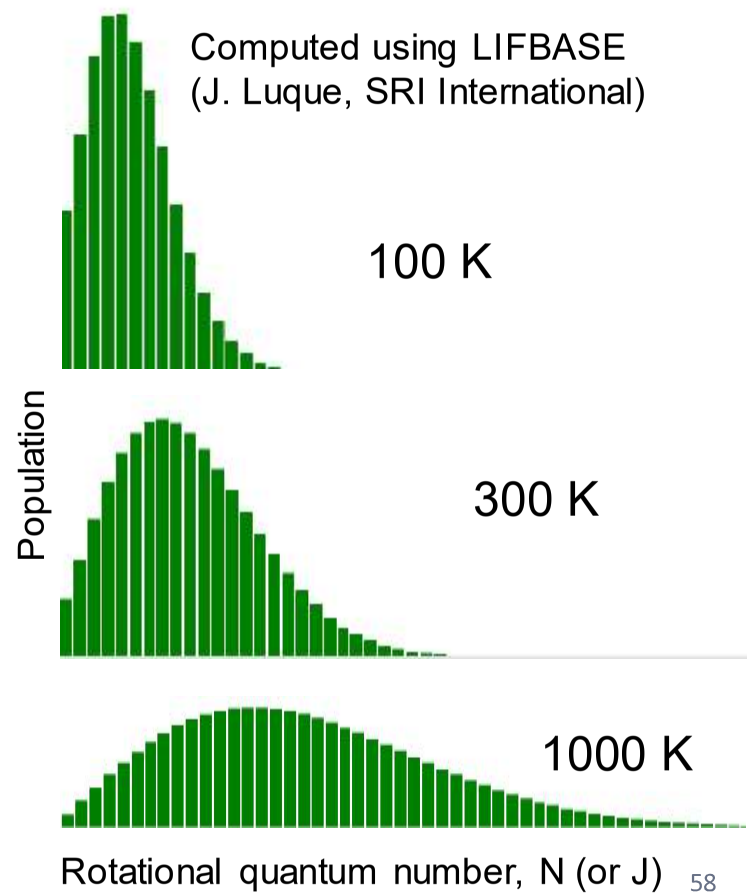

Stimulated Absorption

$$S_{LIF} = \chi_s N_T f_B \underline{W_{12}} \Phi t_{det} V \frac{\Omega}{4\pi} \eta$$

W_{12} is the probability of an <u>absorption</u> transition per sec

$$W_{12} = B_{12} I \underbrace{\int Y_v L_v dv}_{G}$$

laser irradiance

absorption lineshape function

laser spectral profile

Einstein B coefficient

spectral overlap integral

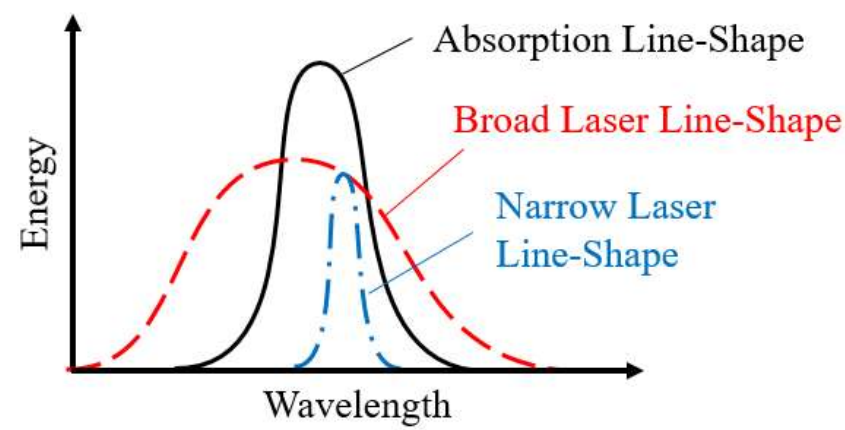

Fluorescence Yield

$$S_{LIF} = \chi_s N_T f_B B_{12} I G \underline{\Phi} t_{det} V \frac{\Omega}{4\pi} \eta$$

The fluorescence yield is affected by collisional quenching

$$\Phi = \frac{A_{21}}{Q_{21} + A_{21}}$$

Probability of an atom/molecule undergoing spontaneous emission per second (Einstein A coefficient)

Probability of a quenching collision per second

Collisional quenching is hard to predict since it depends on many factors

$$Q_{21} = N_T \sum_i \chi_i \sigma_{s,i} v_{s,i}$$

- $N_T = P/k_B T$
- χ is mole fraction
- σ is quenching cross section
- v is mean relative velocity

Two-Level LIF Signal Model and Dependencies

Total number of photons collected

Boltzmann fraction

Total number density

Laser irradiance

$$S_f = \chi_s N_T(P,T) B_{12}(J'',v'') f_B(T,J'',v'') I G(\chi_s,P,T,U) \Phi(\chi_s,\chi_i,P,T) t_{\mathrm{det}} \underbrace{V \frac{\Omega}{4\pi} \eta}_{\text{Optics related}}$$

Mole fraction of tracer species

Overlap integral

Einstein *B* coefficient

Fluorescence yield $\Phi = \dfrac{A_{21}}{Q_{21} + A_{21}}$

- Direct and indirect effects of flow, thermodynamic state, and spectroscopic properties on S_{LIF}
- Carefully designed PLIF experiments can result in quantitative measurements (e.g., T, P, χ_s, ρ, U)

Temperature Sensitivity of S_{LIF}

Effect of Translational Temperature

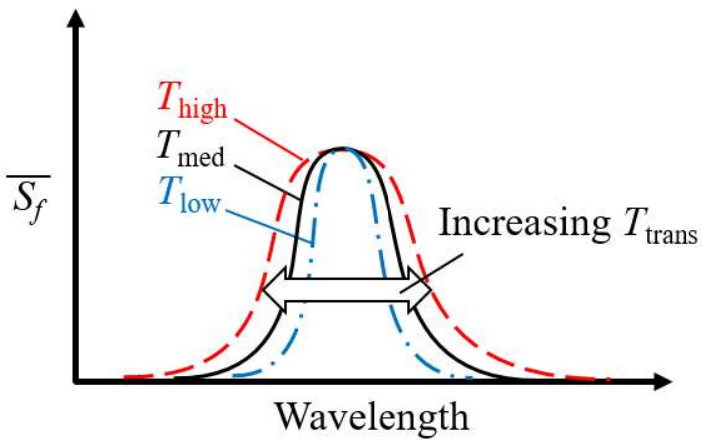

Effect of Rotational Temperature

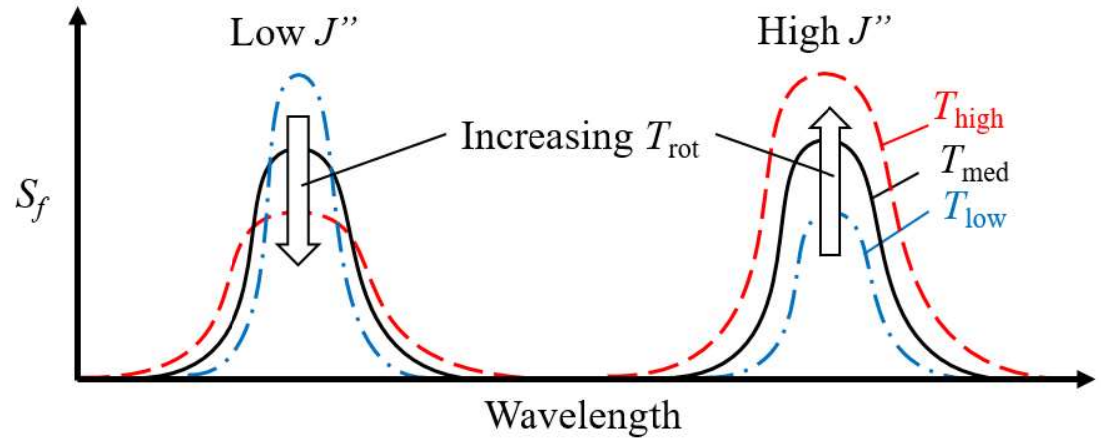

- Broadening of line-shape related to translational temperature (T_{trans})
- Relative amplitudes of high and low J'' transitions related to rotational temperature (T_{rot})

Pressure and Velocity Sensitivity of S_{LIF}

Effect of Pressure

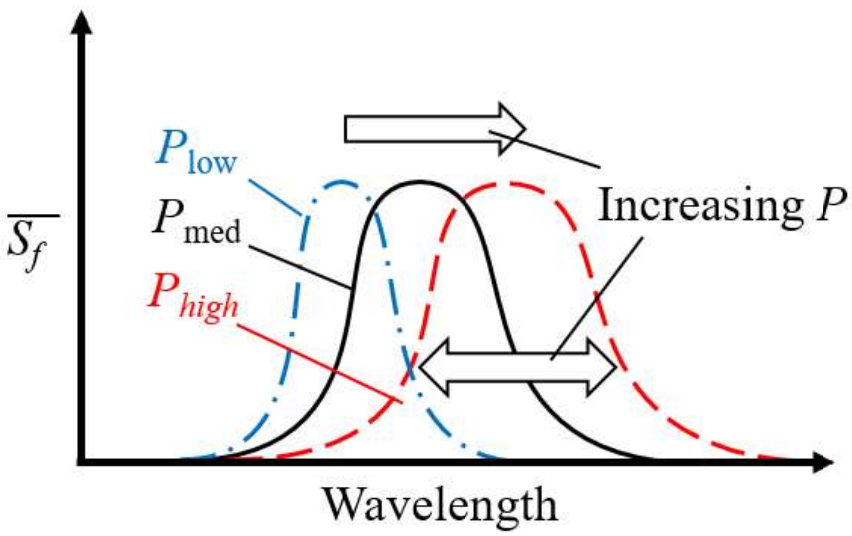

Effect of Gas Velocity

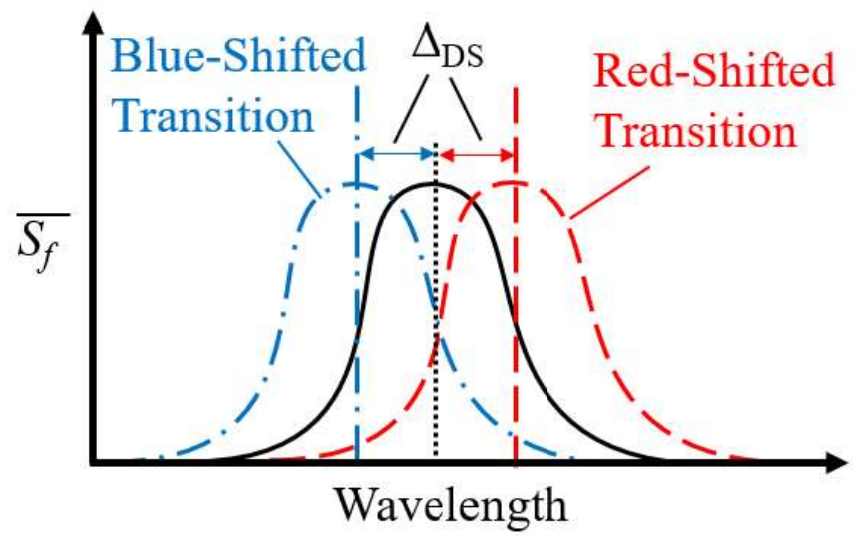

- Increasing pressure broadens and shifts line-shape
  - Pressure can also increase signal (if Q<<A)
- Relative gas velocity towards or away from laser results in a blue or red Doppler shift

Time Dependent S_{LIF} Solution

$$S_{LIF}(t) = S_{LIF}(t_{laser})e^{-(t-t_{laser})/\tau_{LIF}},\ t > t_{laser}$$

photons collected per time

$$\tau_{LIF} = (Q_{21} + A_{21})^{-1}$$

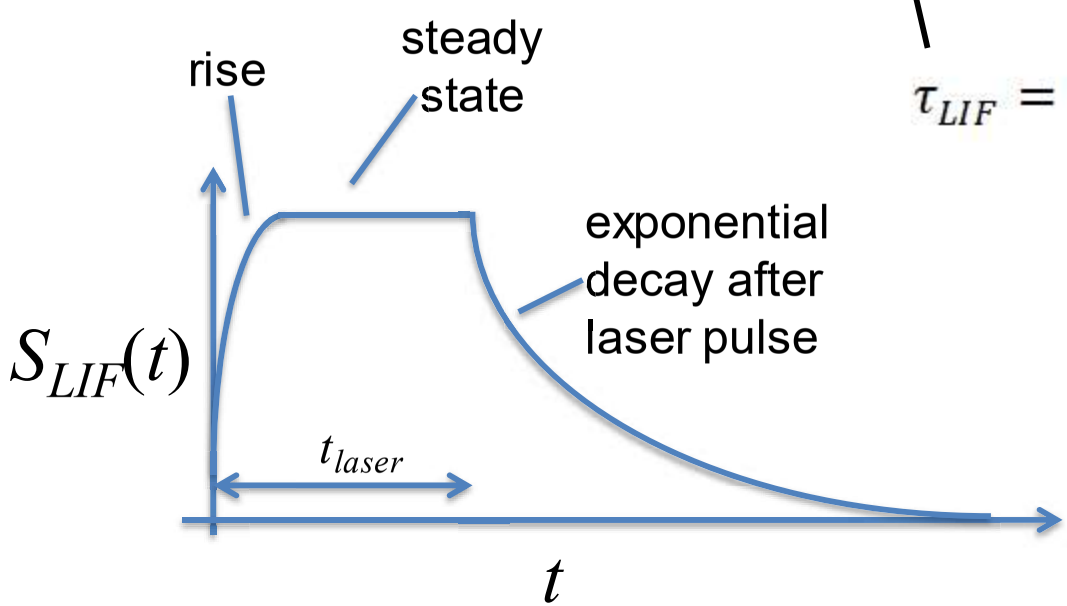

- Laser pulse length is typically ~10 ns
- LIF lifetimes can be a few ns to 100's of ns or longer
  - If you can measure lifetime, you can measure Q!
  - Can measure velocity from long lived decay (MTV)

A real molecule: NO

- NO is a diatomic molecule
  - Electronic
  - Vibration
  - Rotation
    - Not shown
- Absorption and fluorescence take place between electronic states
  - Show rotational and vibrational structure

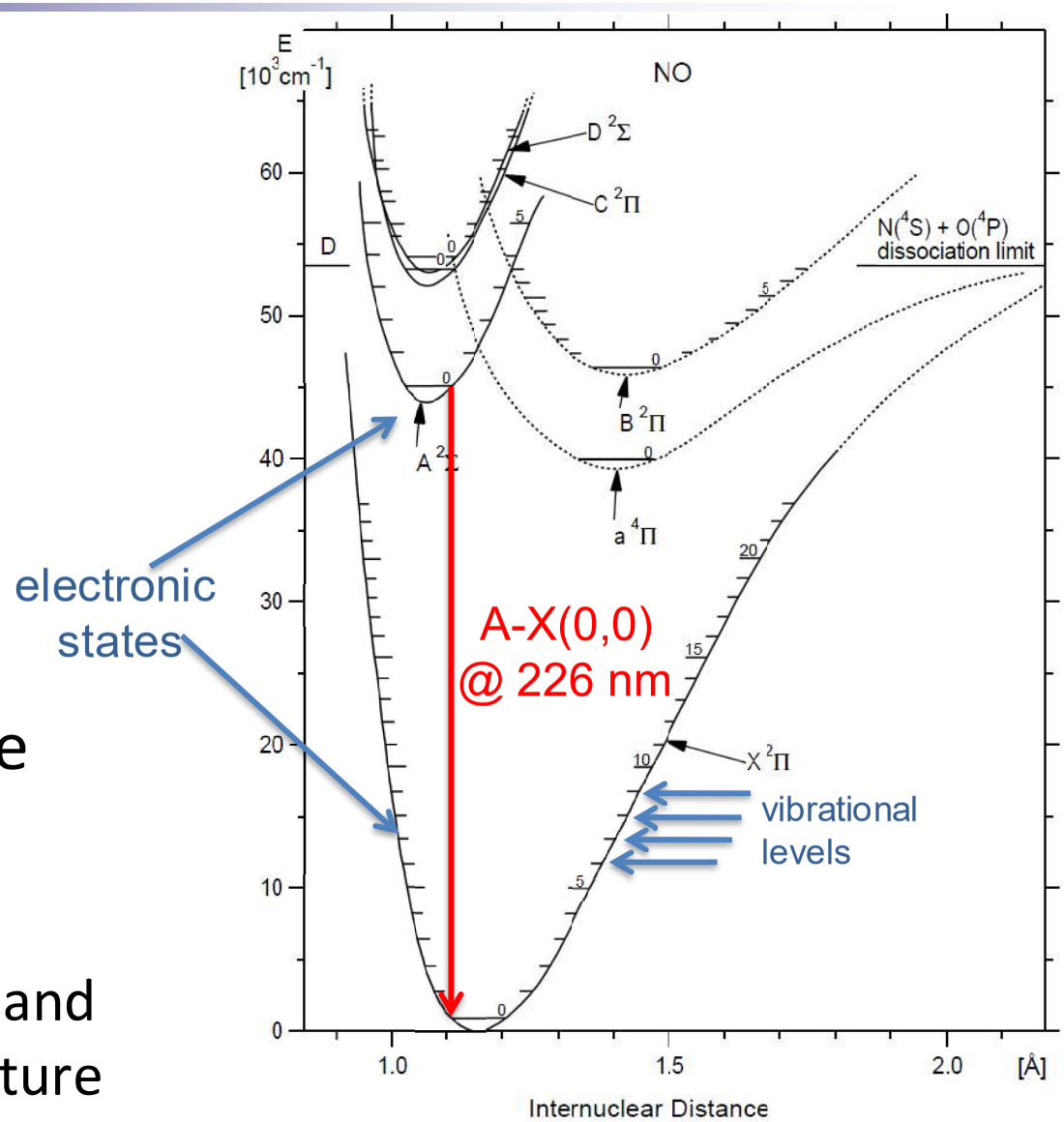

Figure A2.1. Selected potential energy curves that show the electronic structure of NO. In this experiment, we probed transitions in the *A–X* band of NO [adapted from (Scheingraber and Vidal, 1985

LIFBASE Simulation of NO

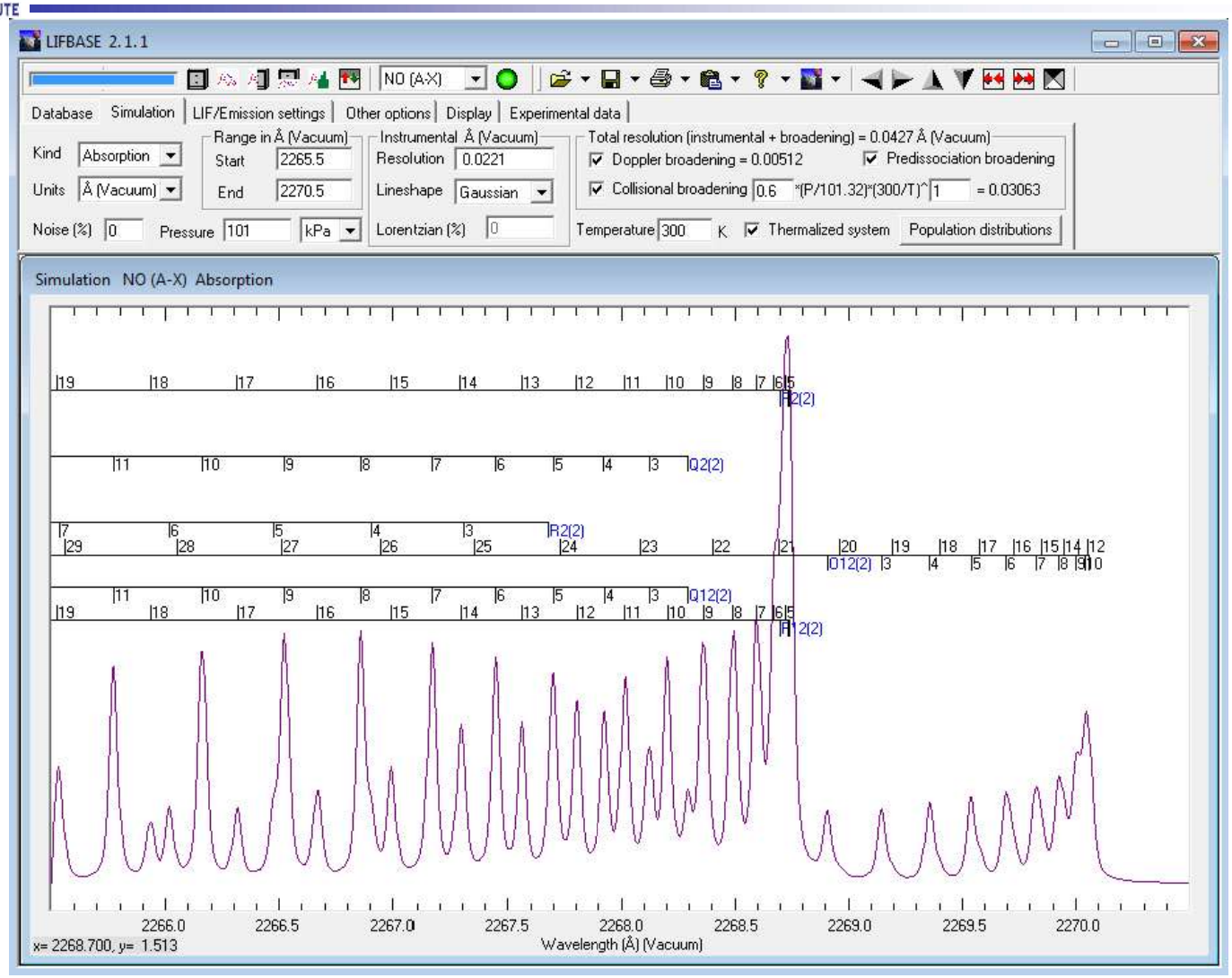

LIFBASE freeware by J. Luque, SRI International

lifbase@yahoo.com

- LIF Excitation Scan between 226.6-227 nm, 1 atm, 300 K
  - Lines all have band names (*O, P, Q, R, S*) and *N*'s or *J*'s (rot quant #)

LIF Temperature Measurements

- Rotational Temperature
  - Ratio of 2 or more rotational lines
  - Describe general case
  - Example in a turbulent base flow
- Vibrational Temperature
  - Ratio of 2 or more vibrational lines
  - Example of freestream characterization
    - Boltzmann plot, where more than 2 lines used
- Translational Temperature

Rotational Lines of NO, 300 K

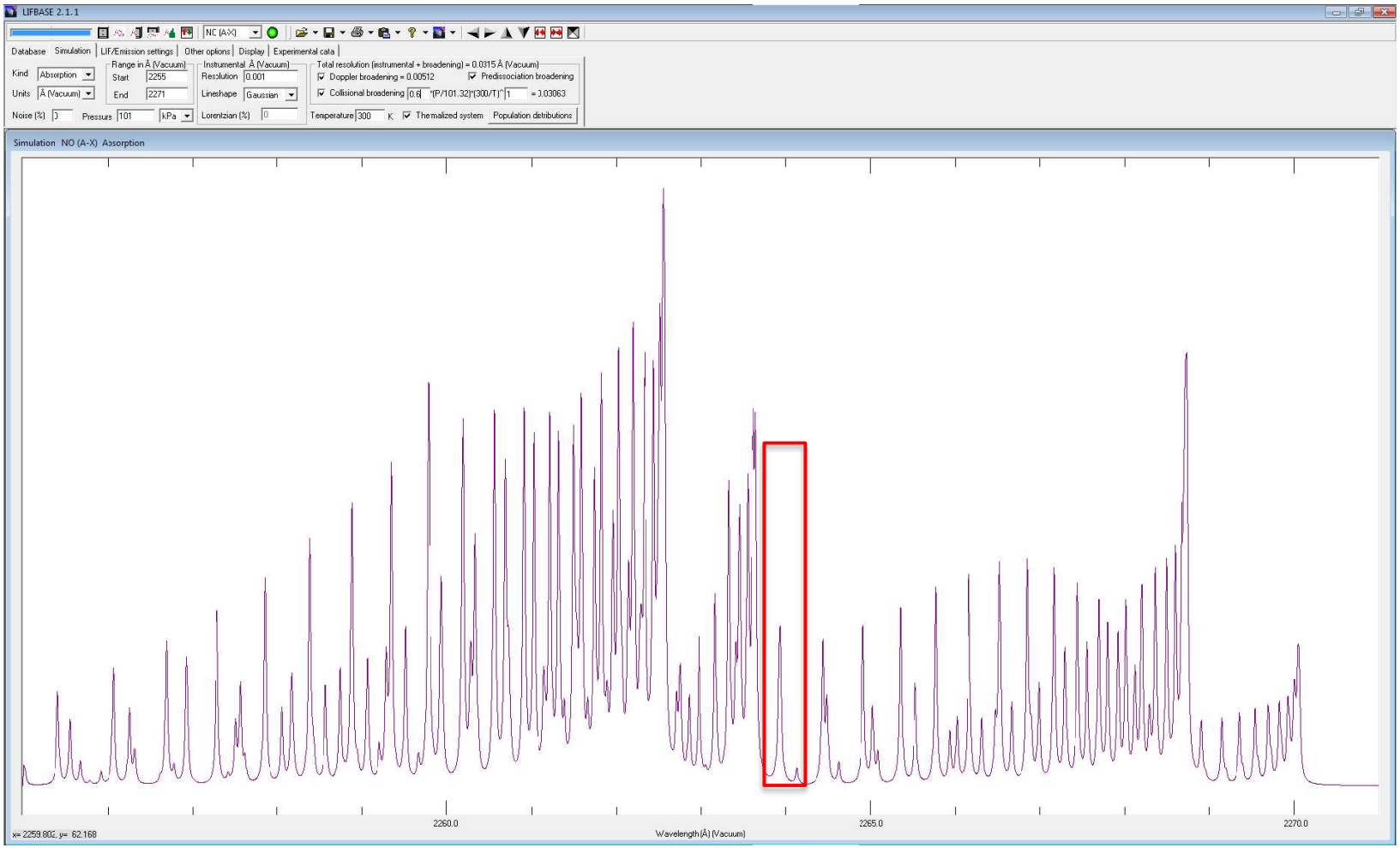

- LIF Excitation Scan between 225-227 nm, 1 atm, 300 K

Rotational Lines of NO, 600 K

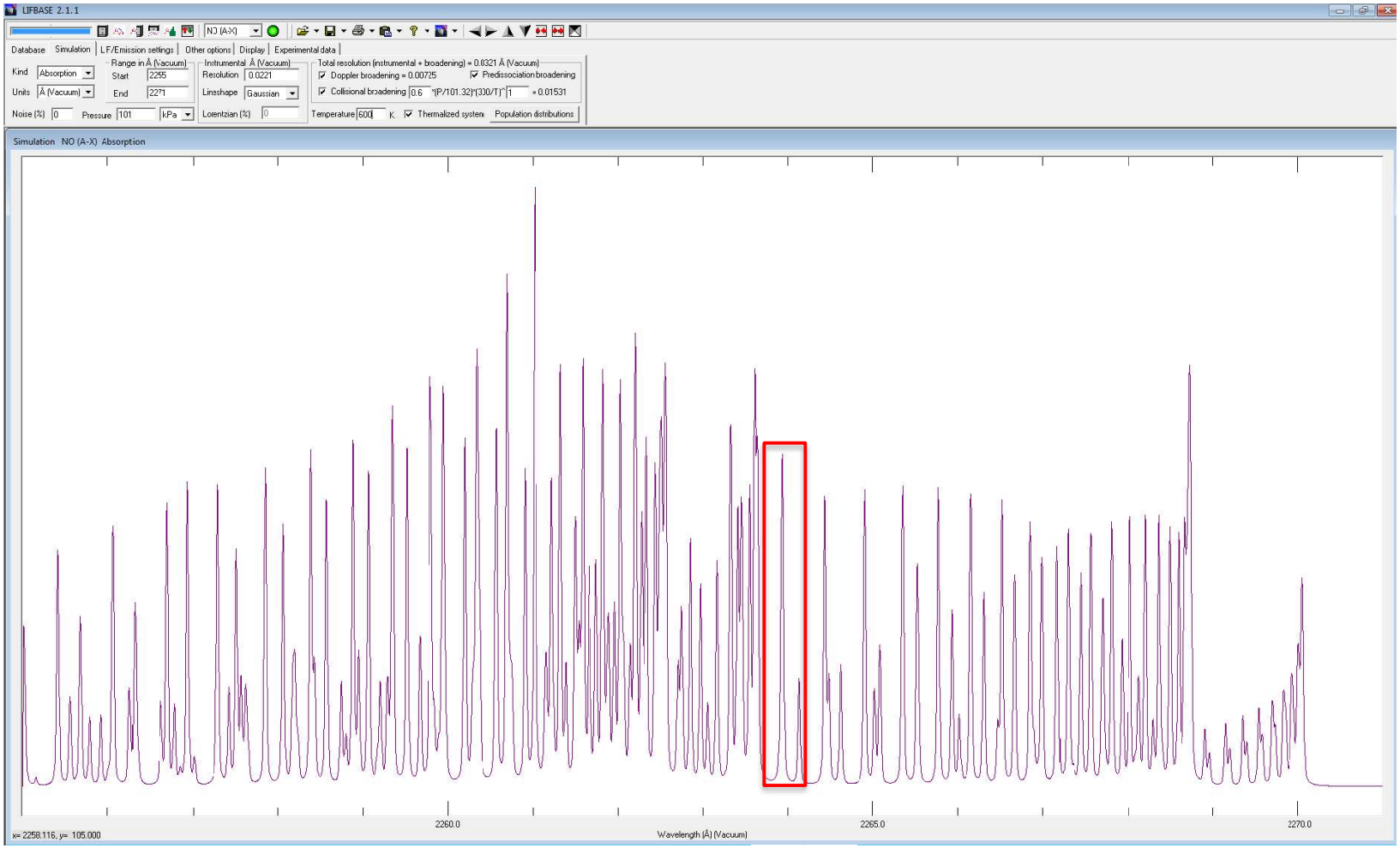

- LIF Excitation Scan between 225-227 nm, 1 atm, 600 K

LIF: Rotational Temperature, T_{rot}

- Recall:

$$S_{LIF} \propto \chi_s f_B(T) B_{12} I G(\chi_s, P, T, U) \Phi(\chi_s, \chi_i, P, T) t_{det}$$

- Obtain LIF or PLIF on two different rotational lines of a molecule: i and j. Take ratio, R:

$$\frac{S_{LIF,i}}{S_{LIF,j}} = R = C \frac{B_{12,i} E_i}{B_{12,j} E_j} \frac{(2J_i+1)\exp[-F_{J,i}/k_B T_{rot}]}{(2J_j+1)\exp[-F_{J,j}/k_B T_{rot}]}$$

Ω, χ_s, η, G, V, N_T and Φ (including Q_{21}) *cancel out!*

- Where:
  - C is a constant
  - E is the laser energy (in mJoules)
  - J is the rotational quantum number
  - F_J is the energy of the state
  - k_B is Boltzmann's constant

LIF: Rotational Temperature, T_{rot}

- Solve for T_{rot}:

$$T_{rot} = \frac{-\Delta E_{rot}}{k_B \ln\left[CR\frac{B_{12,j}E_j(2J_j+1)}{B_{12,i}E_i(2J_i+1)}\right]}$$

- Where:

$$\Delta E_{rot} = (F_{J,i} - F_{J,j})$$

- Temperature sensitivity:

$$\frac{\delta T_{rot}}{T_{rot}} = \frac{k_B T_{rot}}{\Delta E_{rot}} \frac{\delta R}{R}$$

- Suggests to maximize ΔE_{rot} (as long as signals still strong) to minimize error in temperature, δT_{rot}
  - Should choose widely separated states: e.g. J = 3.5 & 35.5

Typical Strategies for T_{rot}

- Typically two approaches:
  - Steady laminar flow
    - Obtain images on one J, then scan laser to another J
    - Ratio images, determine temperature
  - Turbulent flow
    - Two lasers, two cameras (Cumbersome! Expensive!)
    - Acquire two images nearly simultaneously, different J's
    - Need to do this because ratio is a nonlinear function of temperature: $\frac{S_{LIF,i}}{S_{LIF,j}} = R = C\,\frac{B_{12,i}E_i}{B_{12,j}E_j}\,\frac{(2J_i+1)\exp[-F_{J,i}/k_BT_{rot}]}{(2J_j+1)\exp[-F_{J,j}/k_BT_{rot}]}$
    - Typical single-shot temperature measurement precision is ~20% at flame temperatures (Seitzman, 1994)
    - If you use 1 laser/1 camera, →bias errors in turb. Flows
      - (E. R. Lachney, and N. T. Clemens, "*PLIF imaging of mean temperature and pressure in a supersonic bluff wake*," Experiments in Fluids, 24, pp. 354-363, 1998.)
      - Average many measurements to reduce uncertainty

Single laser/camera for T_{rot} in turbulent flow

- Lachney and Clemens (1998) used 1 laser / 1 camera to map mean T_{rot} in a base flow.
- NO uniformly seeded in N_2 at Mach 3
- Chose: $J = 8.5$ and $J = 10.5$

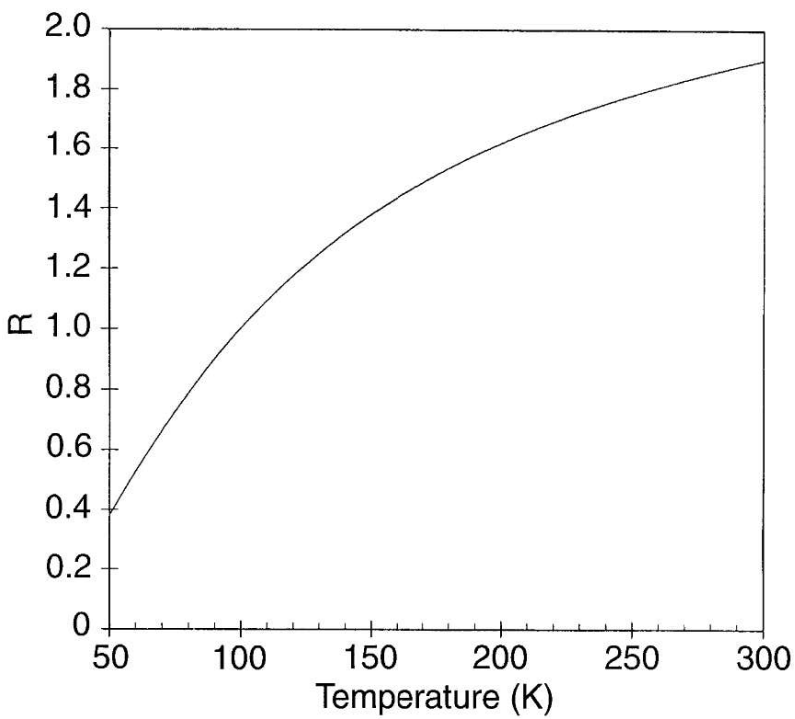

Ratio of lines, used to measure T_{rot}

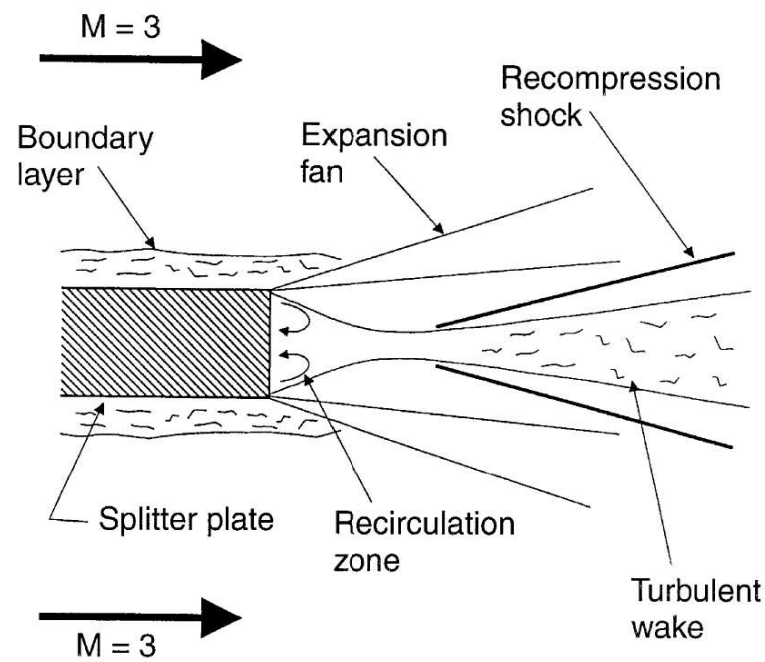

Turbulent supersonic wake flow

Single laser/camera for T_{rot} in turbulent flow

- Lachney and Clemens (1998):

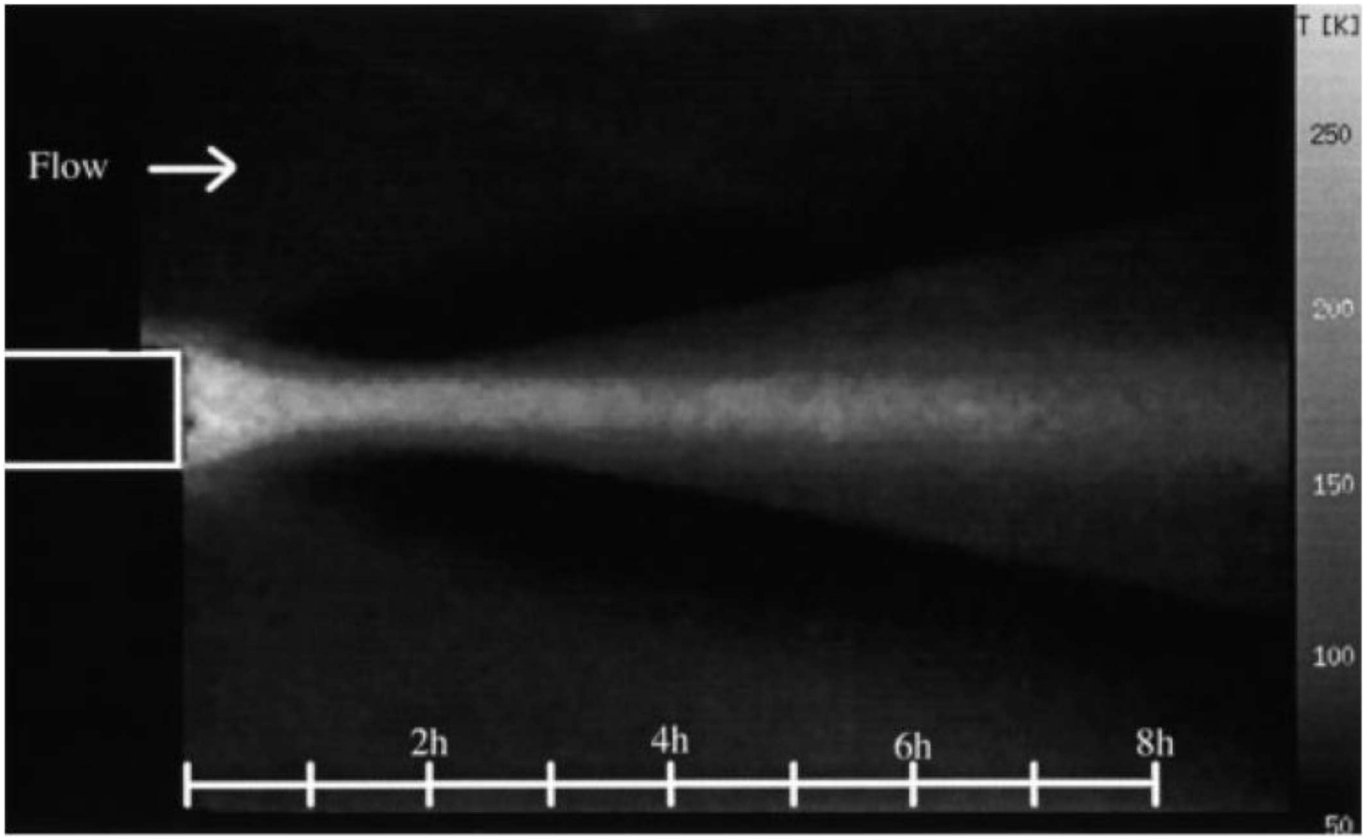

Turbulent supersonic wake flow temperature measurement

Agreed with temperatures inferred from probe measurements to within 11%

E. R. Lachney, and N. T. Clemens, "*PLIF imaging of mean temperature and pressure in a supersonic bluff wake*," Experiments in Fluids, 24, pp. 354-363, 1998

Vibrational Bands of NO

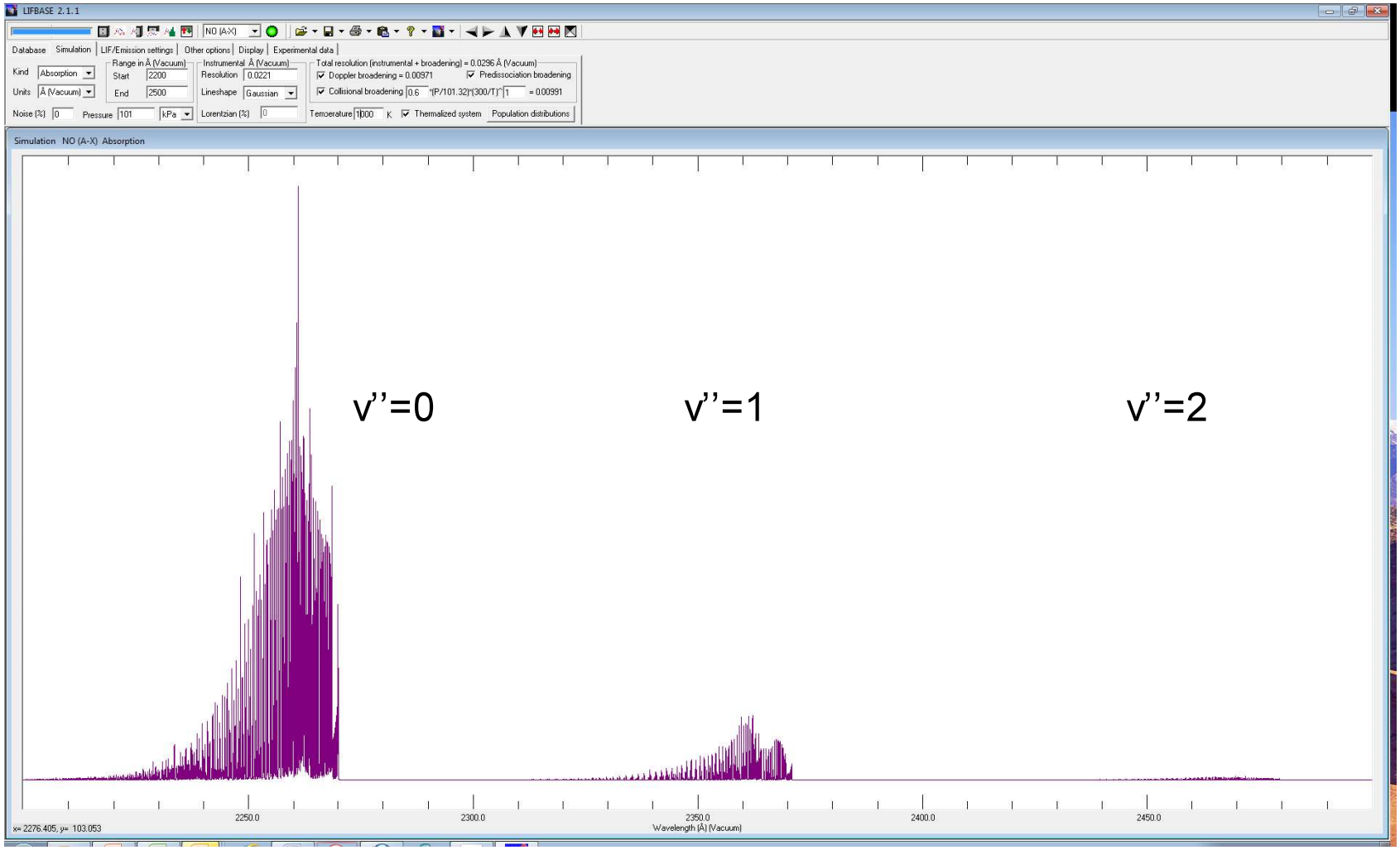

- Three vibrational bands: T = 1000 K
  - Vibrational bands have quantum number, *v*

Vibrational Bands of NO

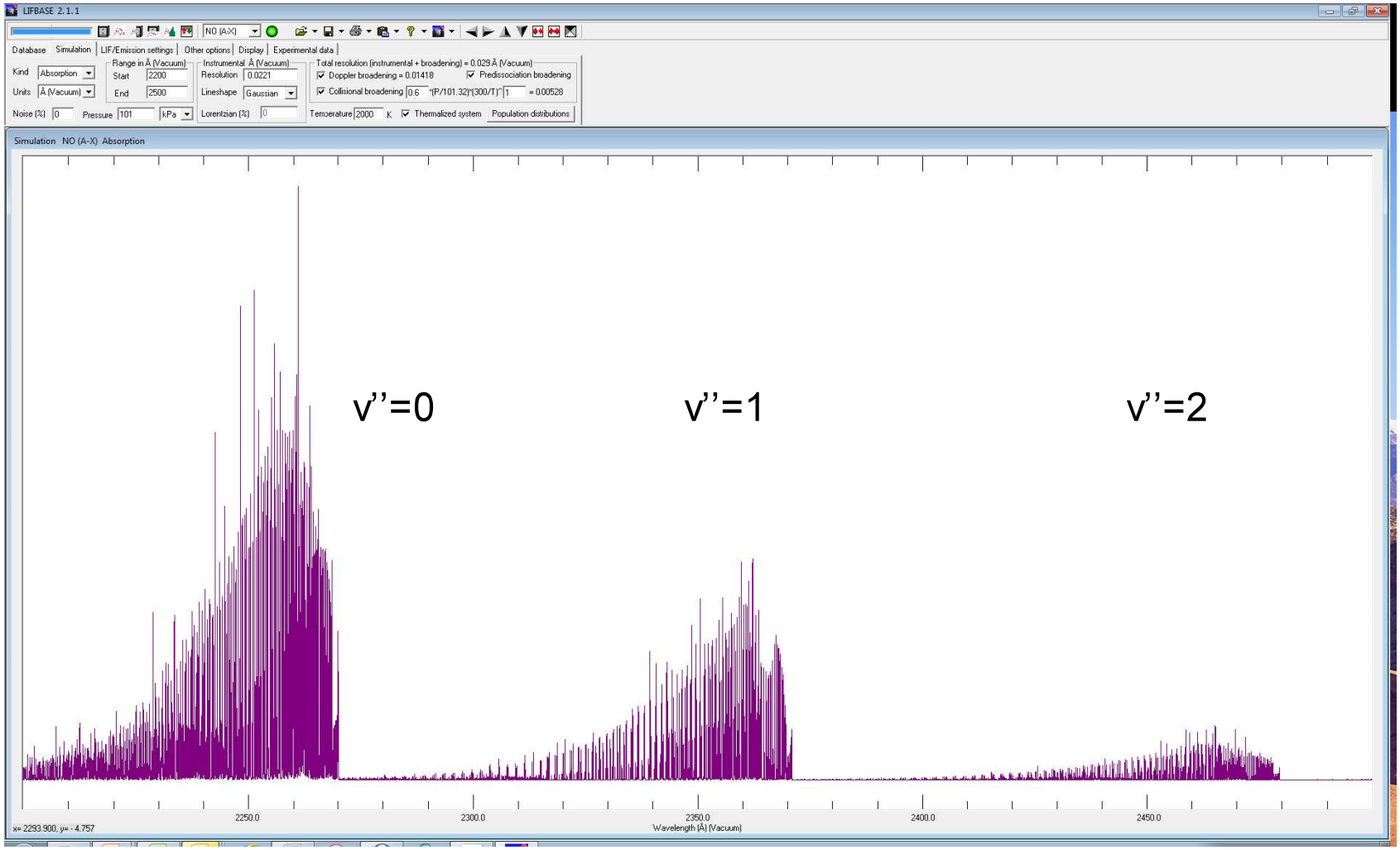

- Three vibrational bands: T = 2000 K

Vibrational Temperature T_{vib} Measurement

- A similar approach can be made to obtain vibrational temperature measurements
  - Typically excite the same rotational line (*J*) in 2 or more vibrational bands ($F_j \approx$ constant)
  - Can do 2 line measurements as before
  - Can use a Boltzmann Plot:
    - Graph:

$$\ln\left[\frac{S_{LIF,i}}{B_{12,i}E_i(2J_i+1)\exp[-F_{J,i}/k_BT_{rot}]}\right] \quad \text{versus} \quad G_{v,i}$$

vibrational energy of states probed

    - Slope is: $-1/(k_BT_{vib})$

If $F_j \approx$ constant then T_{vib} can be determined independent of T_{rot}

Vibrational Temperature T_{vib} Measurement

- Vibrational temperature measured in a nozzle exit flow verifying vibrational nonequlibrium ($T_{vib} \neq T_{rot}$)

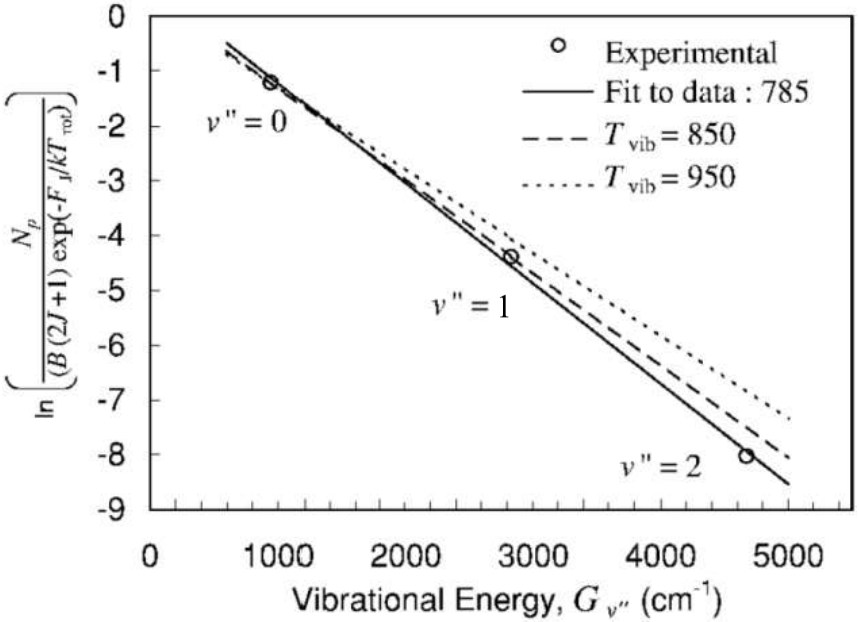

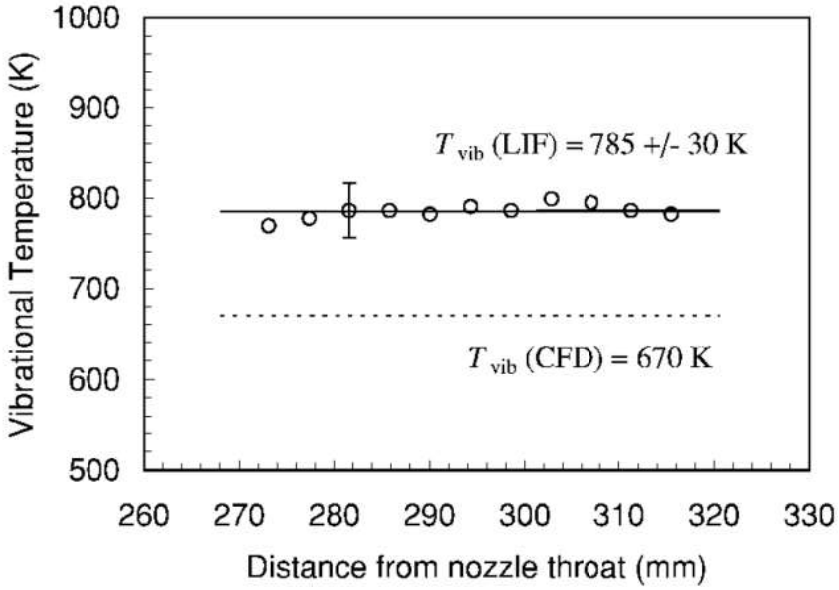

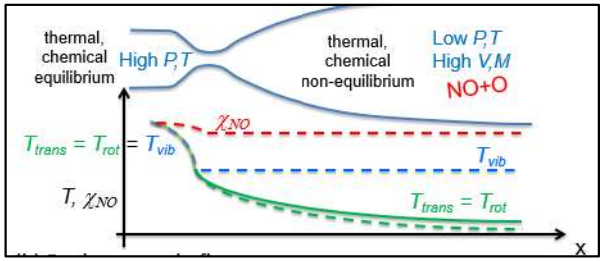

$T_{rot} \approx 400$ K and decreasing with distance

P. C. Palma, P. M. Danehy, and A. F. P. Houwing, "*Fluorescence Imaging of Rotational and Vibrational Temperature in Shock-Tunnel Nozzle Flow*," AIAA Journal, 41(9), September 2003

Translational Temperature

- Can measure T_{trans} (and P) from width and shapes of spectral lines
- Spectral lines have a shape
  - Molecular motion leads to:
    - Doppler Broadening (inhomogeneous)
    - Gaussian shape
    - FWHM: $\Delta\nu_D = \frac{\nu_0}{c}\sqrt{\frac{8\ln(2)k_B T}{m}}$
  - Collisions lead to:
    - Pressure Broadening (homogeneous)
    - Lorentzian shape
    - FWHM: $\Delta\nu_P = \frac{P}{101{,}325}\cdot\left[2\gamma\cdot\chi_i\cdot\left[\frac{295}{T}\right]^{0.75}+\ldots\right]$
  - Combination is: Voigt
    - Convolution (if $\Delta\nu_P, \Delta\nu_D$ comparable)
    - Formulas in manuscript

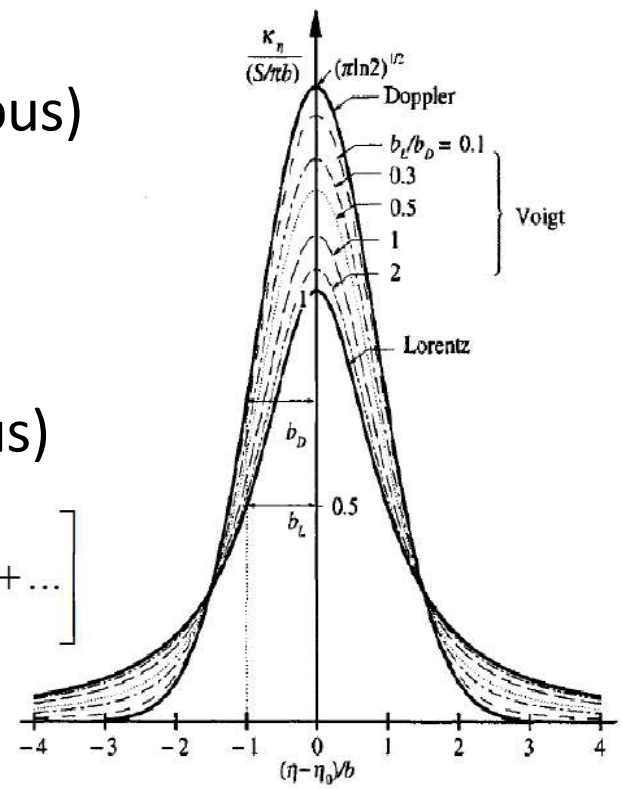

Modest, M: *Radiation Heat Transfer*, Academic Press, Elsevier Science, USA, 2003

Translational Temperature

- If using a very narrow linewidth laser…

  $$\Delta\nu_L << \Delta\nu_P, \Delta\nu_D$$

  …can neglect laser width
  - Semiconductor diode laser
- Scan laser frequency across a transition
  - Argon atom at 810.4 nm
  - Turbulent inductively coupled plasma (ICP) torch
- Fit measured LIF spectrum
  - Have homogeneous (Stark) and Doppler broadening
  - Determine n_e and T

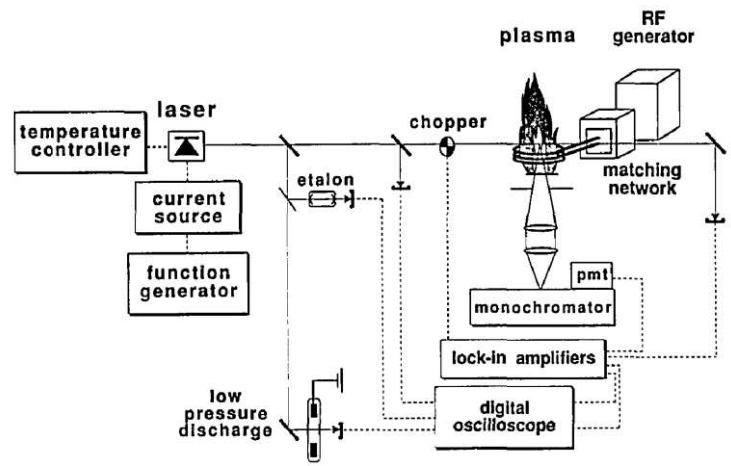

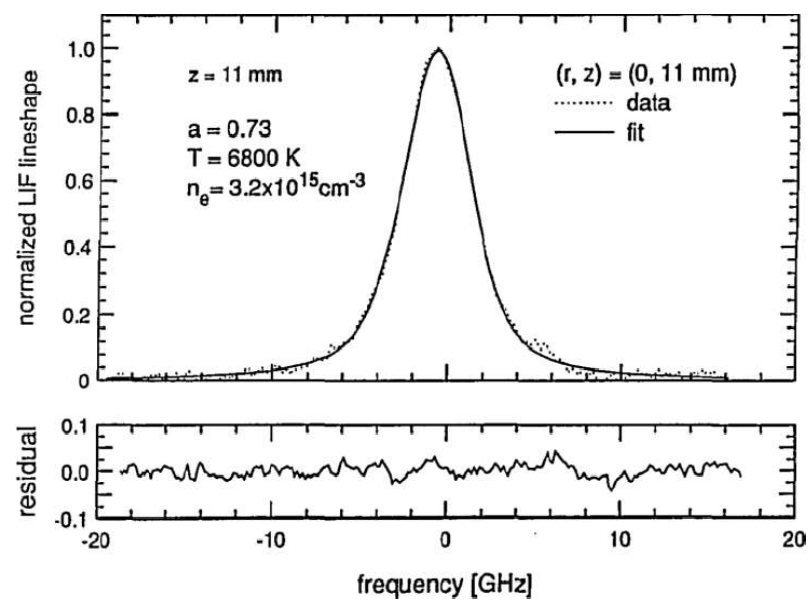

D. S. Baer, H. A. Chang, and R. K. Hanson, "*Fluorescence diagnostics for atmospheric-pressure plasmas using semiconductor lasers*," Journal of the Optical Society of America B, 9(11), pp. 1968-1978, November, 1992

LIF Thermometry Example in an Arcjet

Experimental Setup

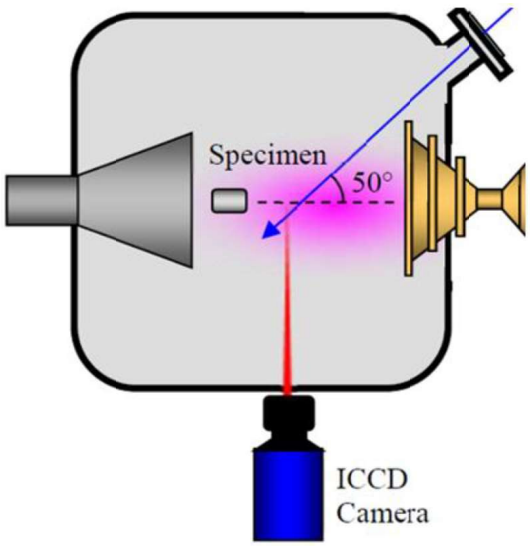

O-atom LIF Spectra

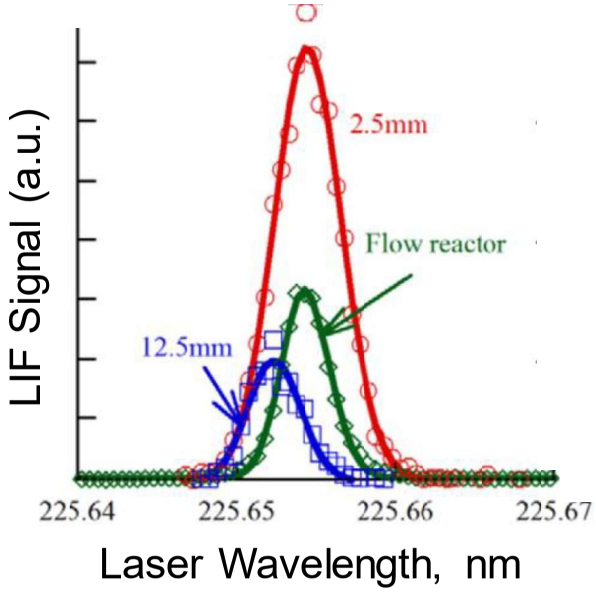

Resulting Measurement

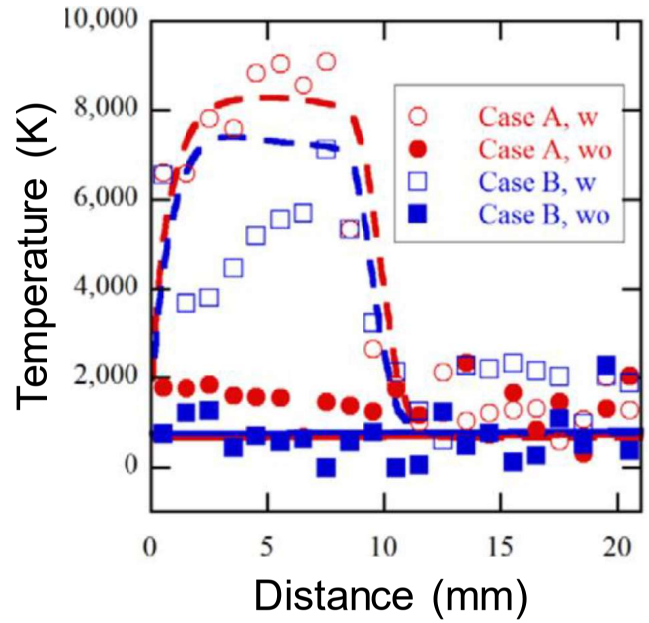

- Translational temperature measured from O-atom LIF in 750kW arc heated wind tunnel at the JAXA Chofu Space Center
- Large scatter typical for arcjets
- See also extensive O-, N-LIF work at NASA Ames Research Center

Takayanagi, H., Kato, S., Sakai, T., Mizuno, M., Fujii, K., Fujita, K., Matsui, M., and Yamagiwa, Y., "Translational temperature distribution measurements in high enthalpy flows by laser-induced fluorescence," AIAA 2013-0741, *51st AIAA Aerospace Sciences Meeting*, Grapevine, TX, 2013.

PLIF Pressure Measurement: Mach 3

Experimental Setup

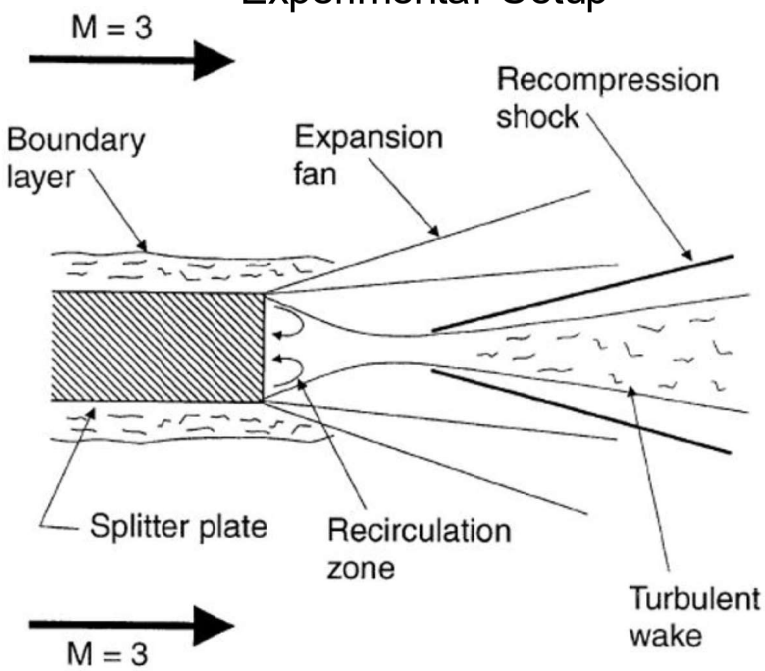

Resulting Pressure Measurement

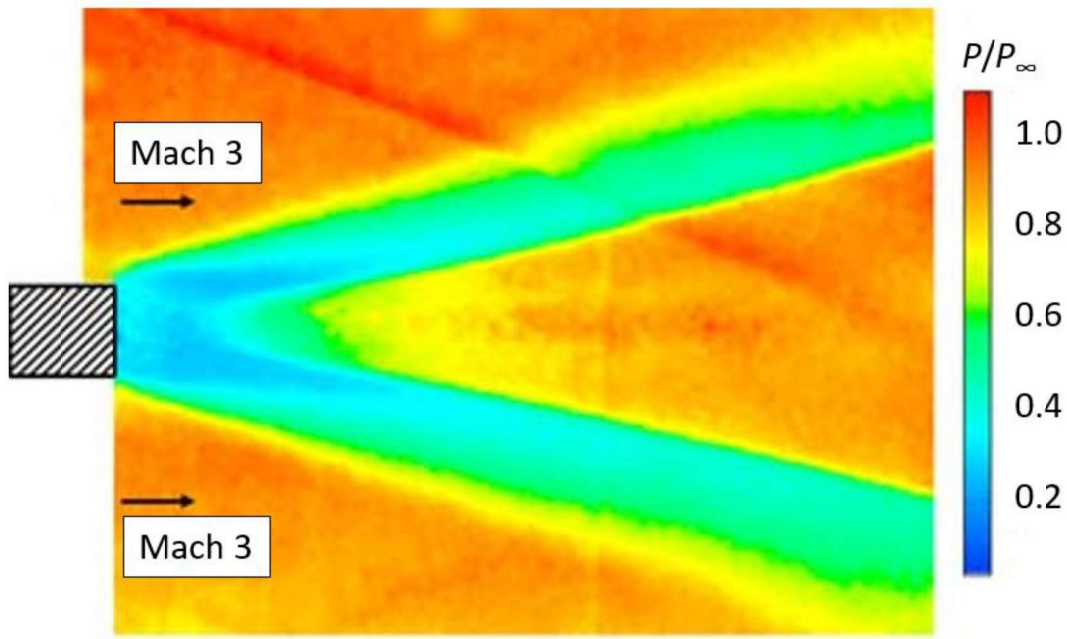

- Pressure measured in near wake of thick plate in Mach 3 Flow
- Pressure dependence of the LIF signal through N_T was exploited in the low-quenching limit (Q<<A).

Lachney, E. R., and Clemens, N. T., "PLIF imaging of mean temperature and pressure in a supersonic bluff wake," *Experiments in Fluids,* Vol. 24, 1998, pp. 354-363

LIF-based Velocimetry Techniques

- Doppler shift
  - Based on laser frequency relative to absorption line

This Section

- Molecular tagging velocimetry (MTV)
  - aka Flow tagging velocimetry
  - Time of flight
  - Single-laser and multi-laser methods

Next Section

Doppler Shift Velocimetry

- The Doppler shift:

$$\Delta\nu = \frac{U}{c}\nu_0$$

Wikipedia "Doppler Shift"
http://creativecommons.org/licenses/by-sa/3.0/deed.en

- Can be used to measure velocity with LIF
  - Relative shift between laser and absorbing molecules
  - Angle of detection does not matter for LIF
- The overlap integral, G, which describes the overlap of the laser's spectrum with a line
  - L_ν is laser's spectral shape, typically modeled as Gaussian or Lorentzian
  - Y_ν is the transition's absorption line shape, can be shifted by Doppler shift

$$G = \int L_\nu Y_\nu d\nu$$

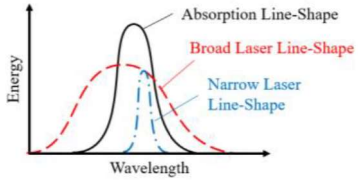

Doppler-based LIF Velocimetry

- Direct laser sheet into the flow
- Acquire images or signal at different laser frequencies
  - Choose frequencies near an absorption line
  - Measure absorption lineshape at each point
  - Reference data acquired simultaneously

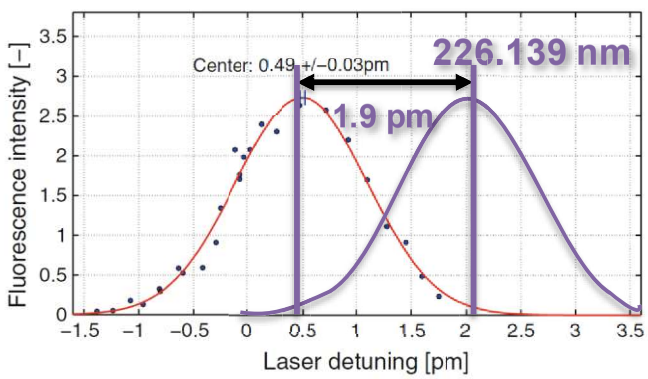

  - Measure from two different directions to get two different velocity components
  - Do need to consider pressure shift

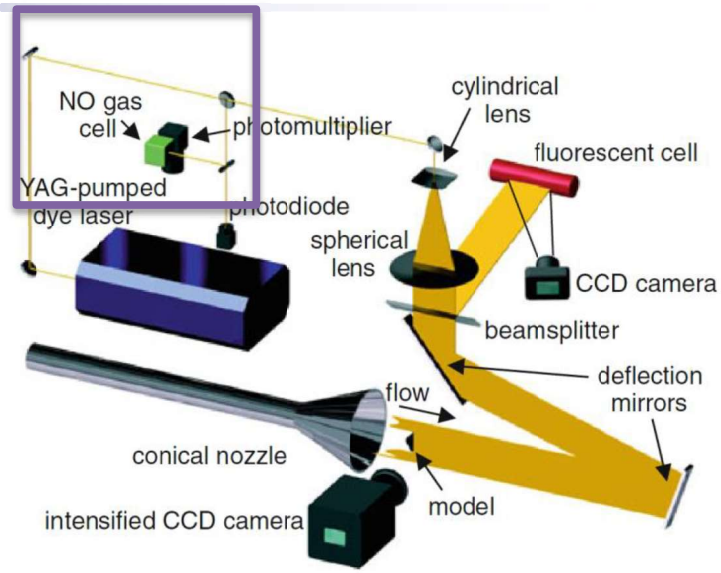

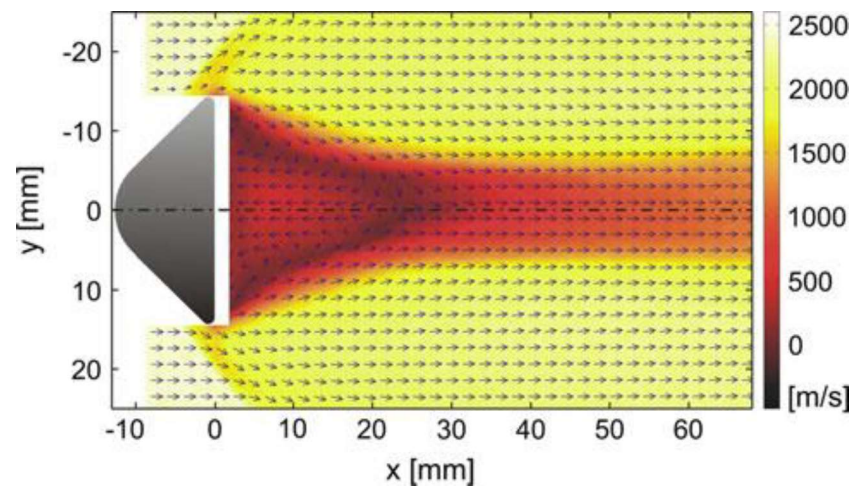

R. Hruschka, S. O'Byrne, and H. Kleine, "*Two-component Doppler-shift fluorescence velocimetry applied to a generic planetary entry probe model*," Experiments in Fluids, 48, pp. 1109-1120, 2010

Doppler Shift Velocimetry

- Benefits
  - Capable of providing 1- or 2-component velocity maps
  - Relatively easy to implement

- Drawbacks
  - Typically not time resolved
  - Typically requires reference measurement
  - Spectral shift resulting from increased pressure needs to be accounted for
  - Requires a gas ‘seed’ to either be naturally present or introduced into the flow

Quantitative PLIF Conclusions

- Advantages
  - Qualitative flow visualization usually obtained
  - Fine spatial resolution, 2D or 3D
  - Short gate times (freeze flow)
  - High speed possible (10 kHz – 1 MHz)
  - High signal-to-noise ratio
  - Multi-parameter measurements possible: T, V, P, χ
- Disadvantages
  - Expensive high-power lasers (laser safety)
  - Need to seed tracer species (many are toxic)
  - Sometimes difficult to isolate property of interest in quantitative technique

Molecular Tagging Velocimetry

Daniel Reese, National Institute of Aerospace, Virginia USA
Paul Danehy, NASA Langley Research Center, Virginia, USA
Craig Johansen, The University of Calgary, Canada
Brett Bathel, NASA Langley Research Center, Virginia, USA

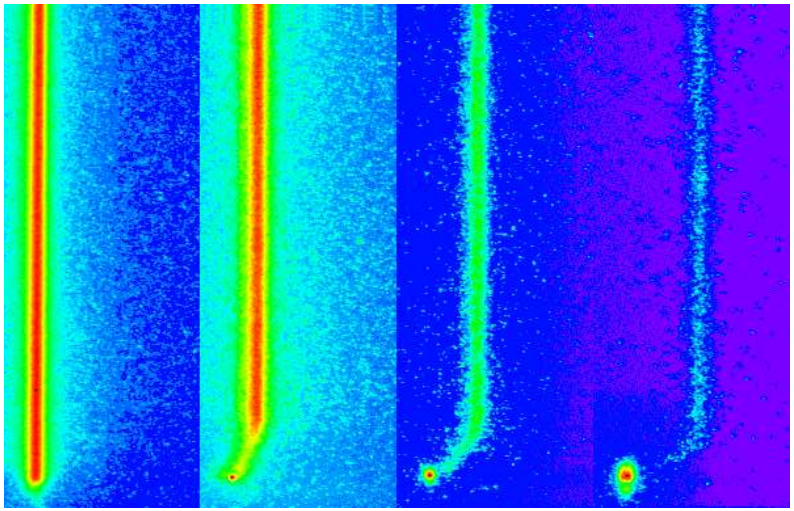

NASA and The Australian National University

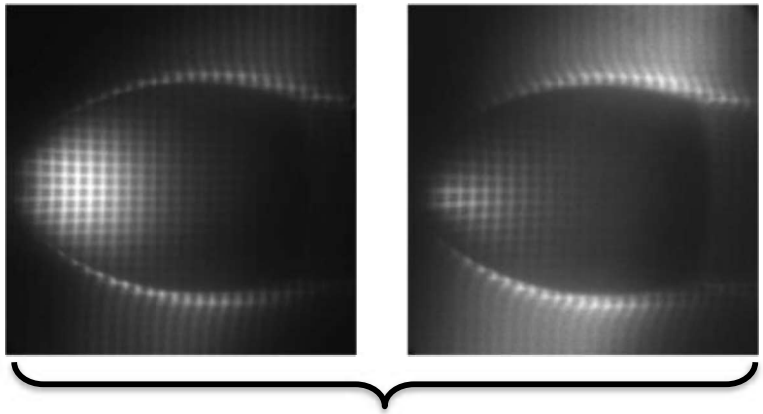

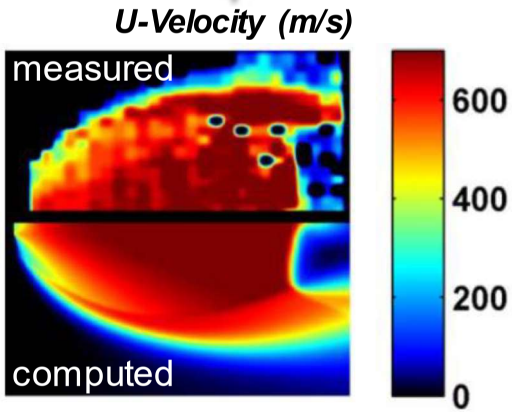

Texas A&M

Molecular Tagging Velocimetry

MTV Theory

- Laser excites (tags) gas
- Tagged point/line is imaged at t=0
- Gas advects downstream with flow
- Tagged line is imaged at $t=\Delta t$
- Displacement Δx is determined from image pair
- Velocity estimated from $V= \Delta x/ \Delta t$

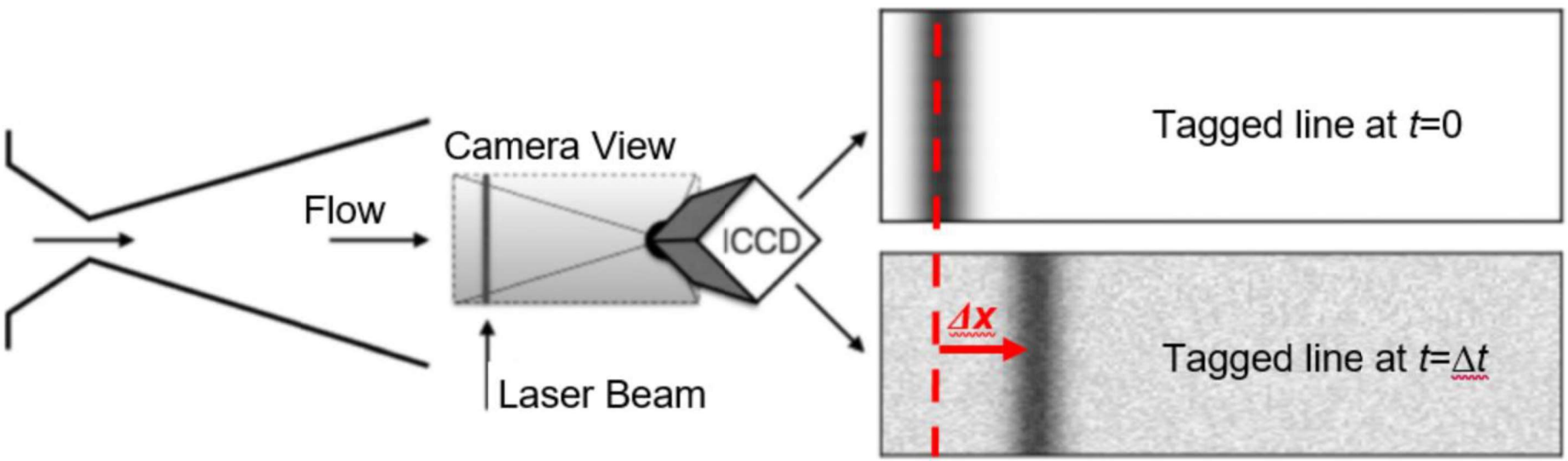

Matos PS, Barreta LG, Martins CA. Velocity and NO-Lifetime Measurements in an Unseeded Hypersonic Air Flow. ASME. J. Fluids Eng. 2018; 140(12):121105-1-121105-8. doi:10.1115/1.4039863.

Single-Laser MTV

- Biacetyl (Hiller et al, 1984; Koochesfahani, 2007)
- Acetone (Lempert, 2002)
- NO (Danehy, 2003; Hsu, 2009; Bathel, 2011)
- I_2 (Balla, 2013)
- N_2 using FLEET (*Femtosecond laser electronic excitation tagging*) (Michael, 2011)
  - Does not require seeding
  - Does require an expensive fs laser

- *LIF lifetime must be long enough so molecules still emit light after (slightly) moved*

LIF Molecular Tagging Velocimetry (MTV)

Single-laser LIF MTV

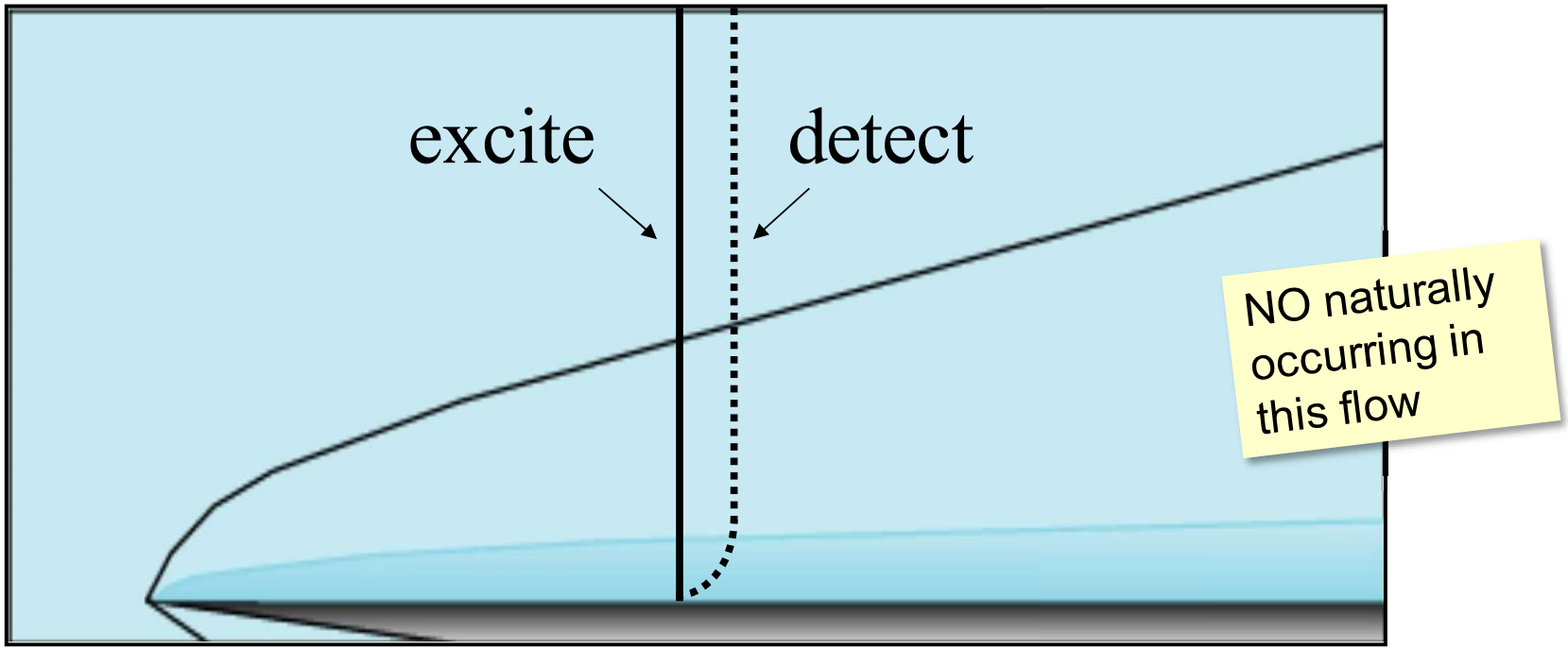

- Boundary layer: slow moving gas near surface
  - Important: heat transfer, drag, separation, etc.
- Instantaneous measure of 1 velocity component
  - Can be extended to 2 or 3 components

P. M. Danehy, S. O'Byrne, A. F. P. Houwing, J. S. Fox, and D. R. Smith, "*Flow-Tagging Velocimetry for Hypersonic Flows Using Fluorescence of Nitric Oxide*," AIAA Journal, 41(2), February 2003

Experimental Setup: Top View

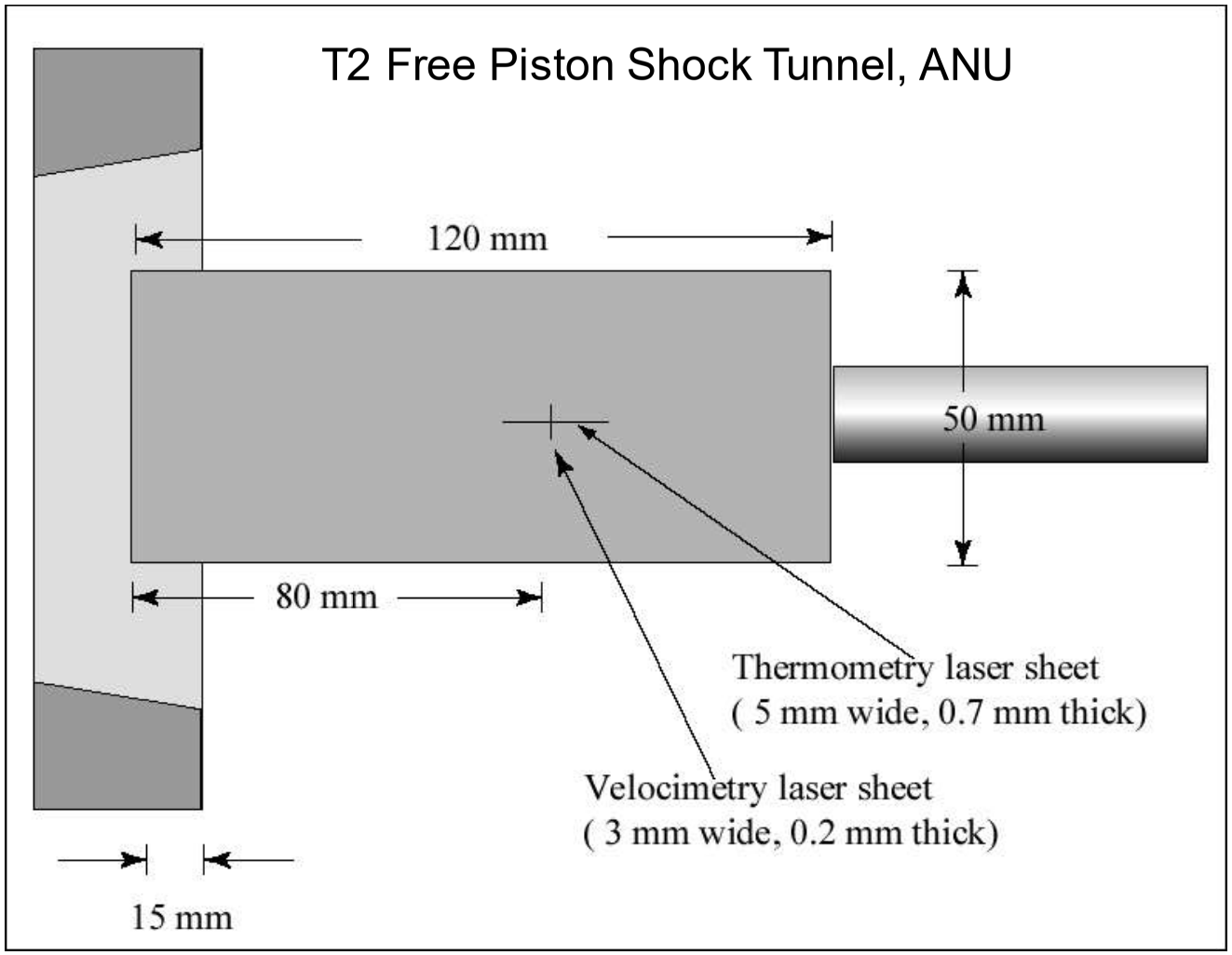

Velocity ~ 3000 m/s; Mach Number = 7, laminar boundary layer

MTV: Delayed Images

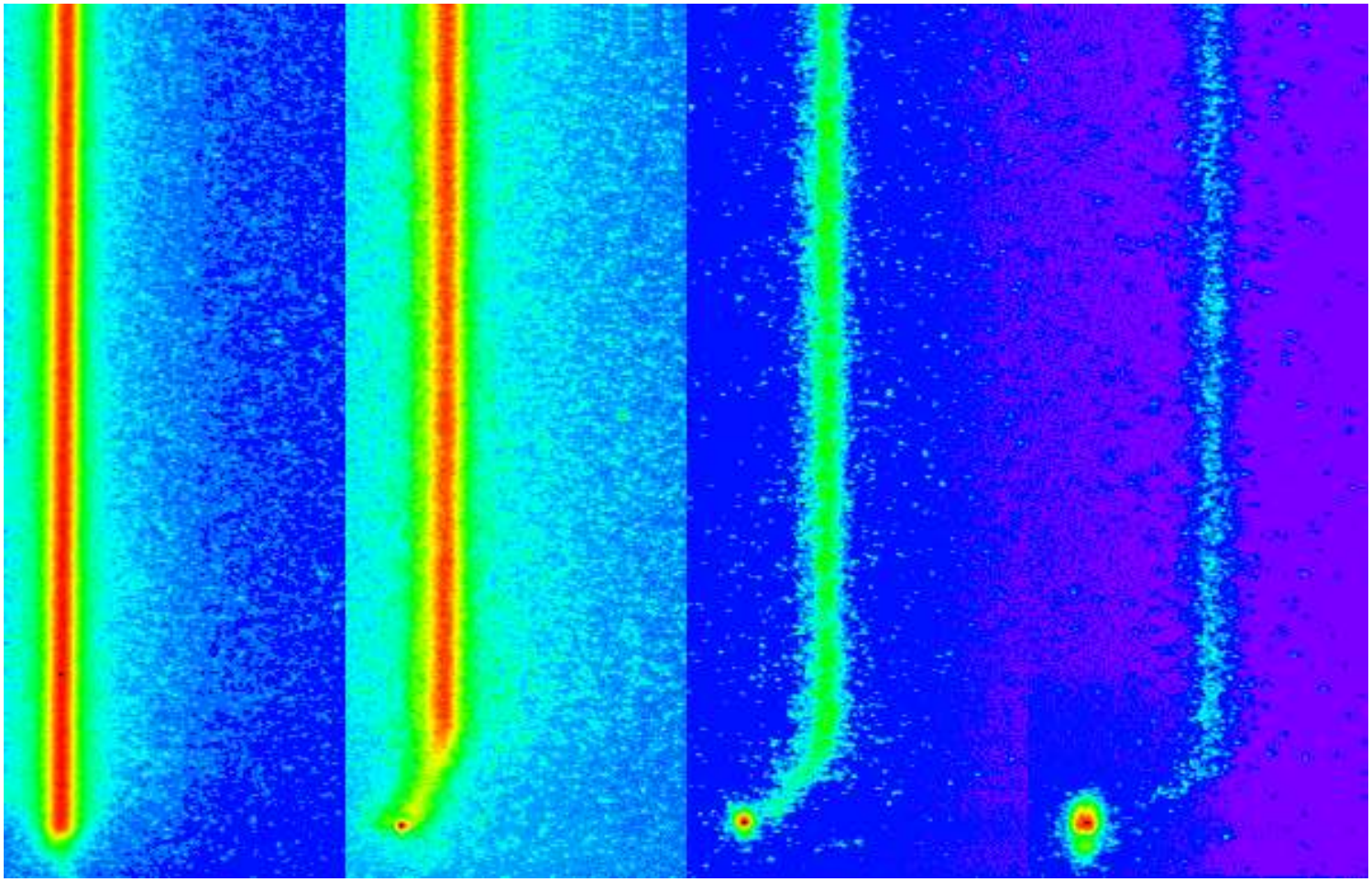

Delay = 0 | 250 ns | 500 ns | 750 ns | ln(data) shown here

- Measurements performed on successive tunnel runs

P. M. Danehy, S. O'Byrne, A. F. P. Houwing, J. S. Fox, and D. R. Smith, "*Flow-Tagging Velocimetry for Hypersonic Flows Using Fluorescence of Nitric Oxide*," AIAA Journal, 41(2), February 2003

Average of Single-Shot Measurements

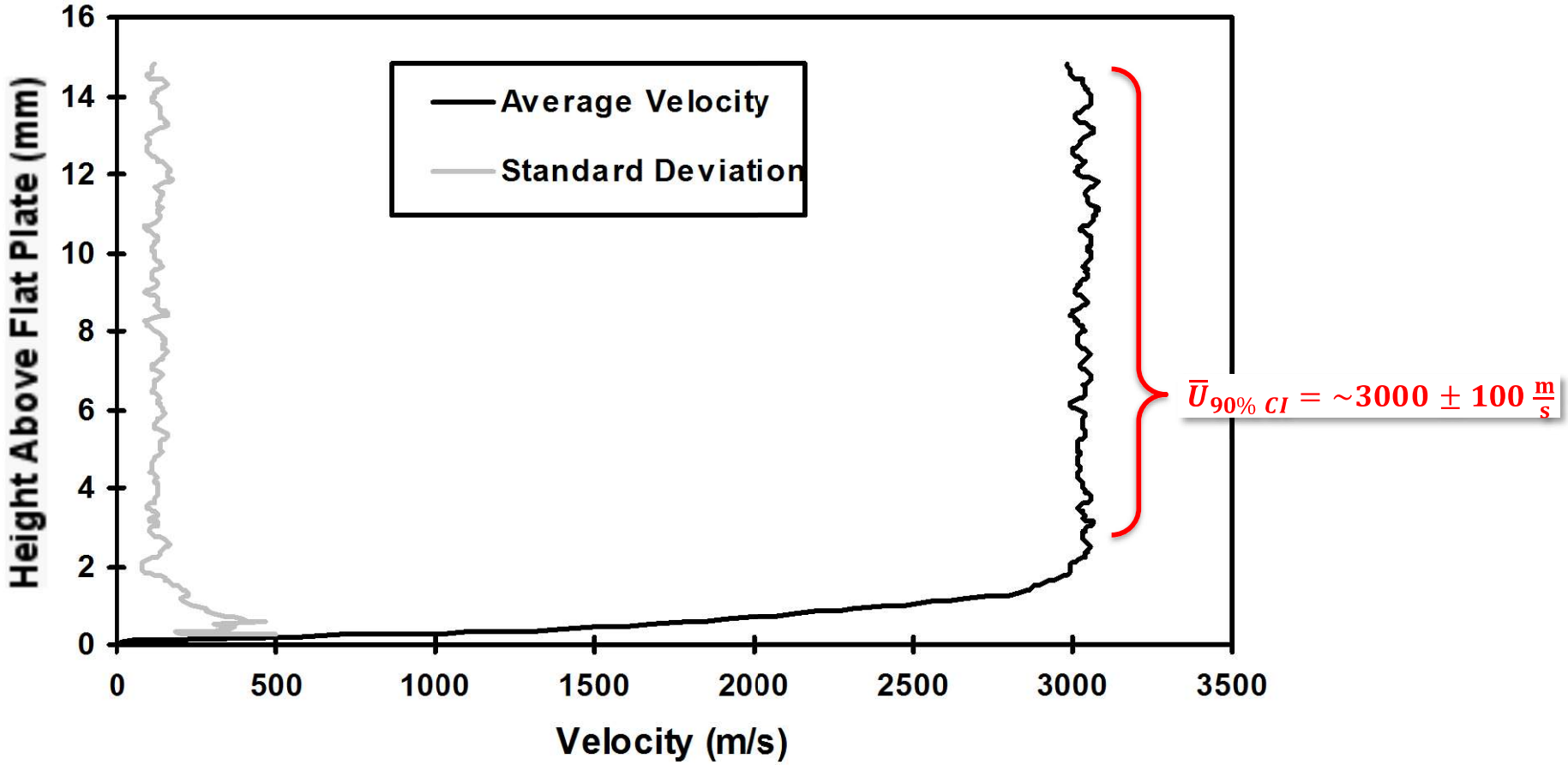

- Freestream velocity is uniform at 3035±60 m/s.
- 95% boundary layer thickness is 1.4±0.1 mm.
- Single shot measurement precision: ~60 m/s out of ~3000 m/s (2%)
  - spatially averaged uncertainty (freestream region) ~100 m/s (3%)

Single-laser MTV: NO PLIF

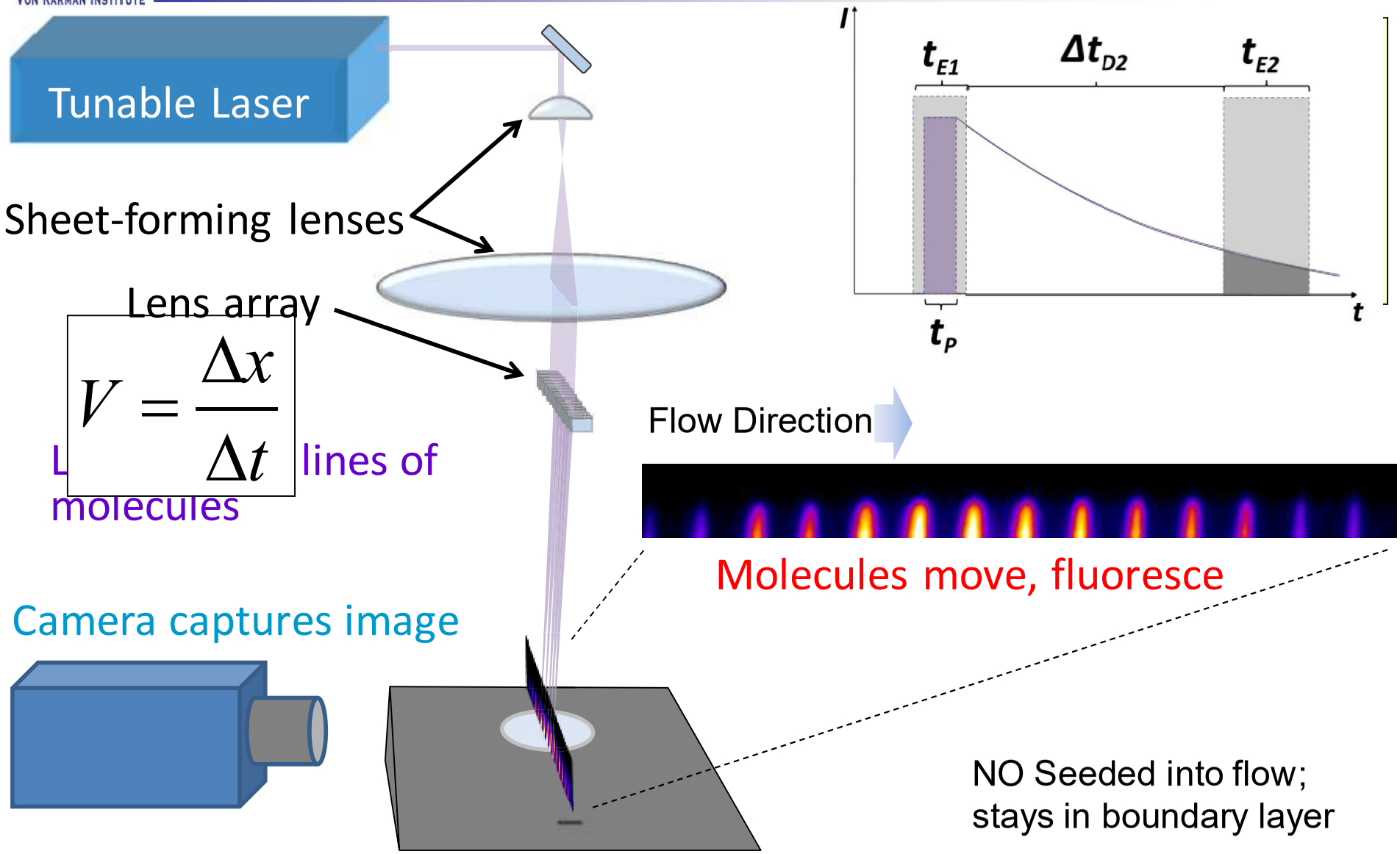

Single-laser MTV

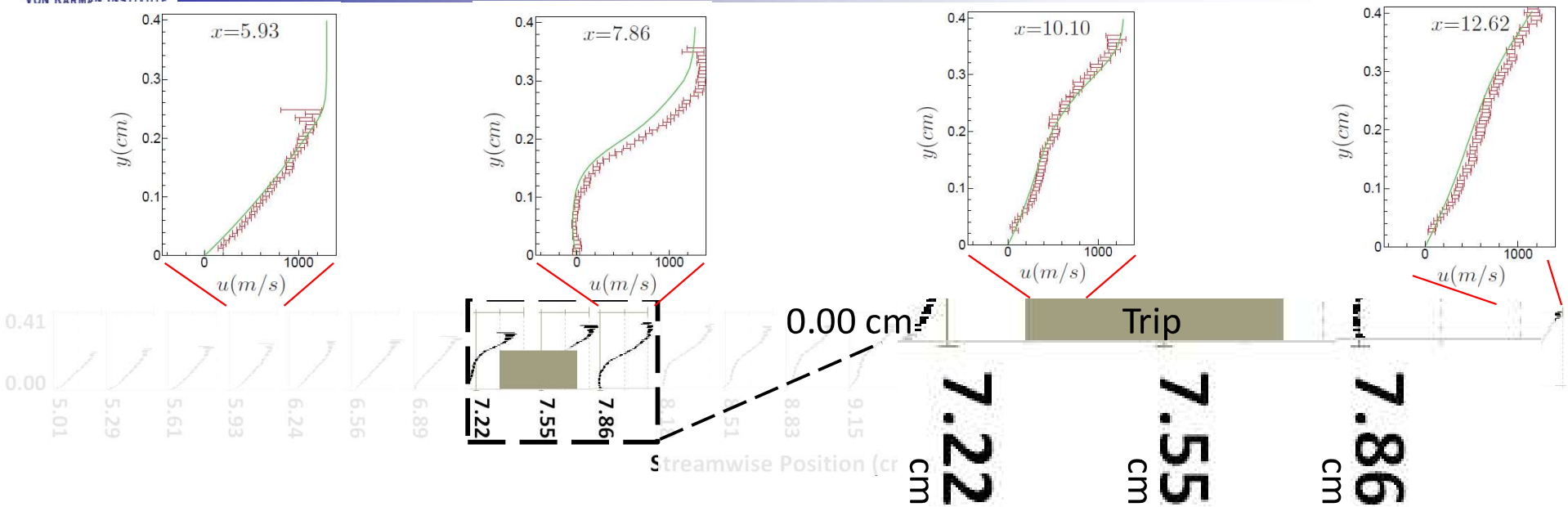

- **Velocity Measurement Improvements**
  - Instantaneous (<1 μs), single-component measure of 25 profiles simultaneously
  - Developed thorough uncertainty analysis methodology
  - Uncertainties in mean: as good as 3% of freestream (~1000 m/s) for 38 images
  - Data used in subsequent CFD study by Iyer et al. of Univ. of Minnesota (AIAA 2011-566)

B. F. Bathel, P. M. Danehy, J. A. Inman, S. B. Jones, C. B. Ivey, C. P, and Goyne, "*Velocity Profile Measurements in Hypersonic Flows Using Sequentially Imaged Fluorescence-Based Molecular Tagging*," AIAA Journal, 49(9), September 2011

Doppler-shift & MTV with NO PLIF

NO LIF Spectra

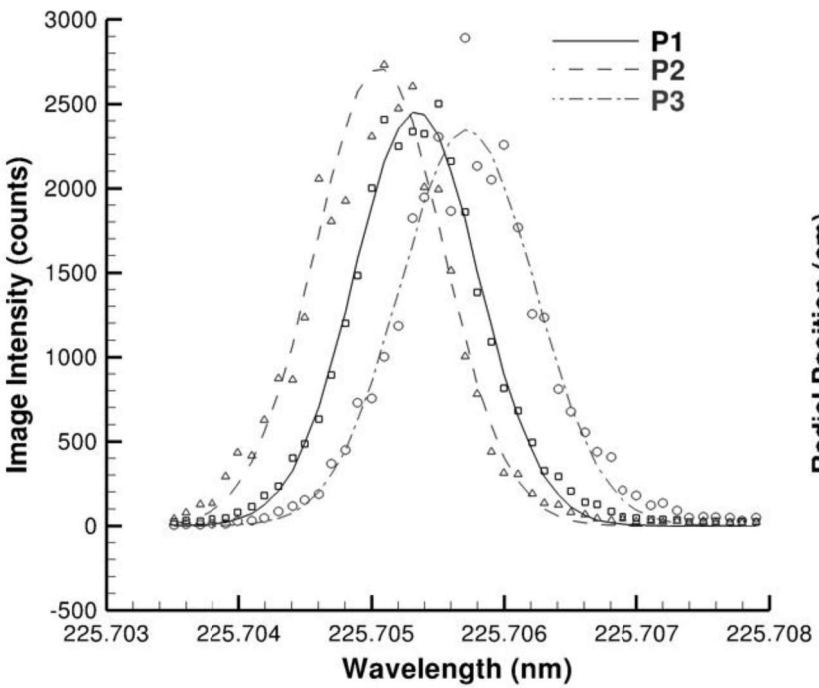

Velocity Contour Map and Vector Field

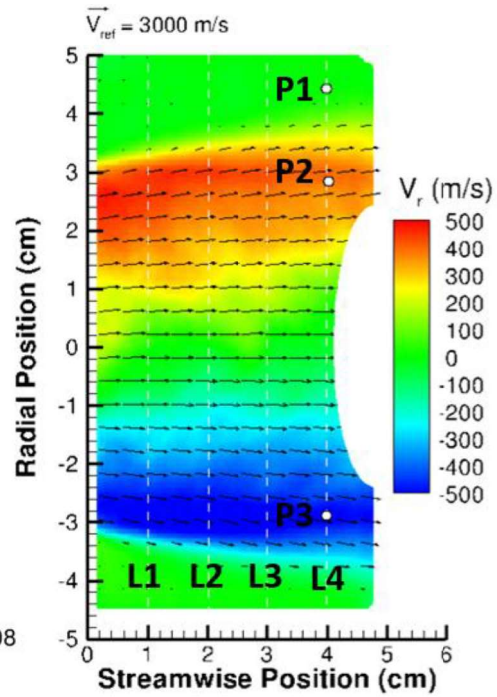

Radial Velocity Profiles

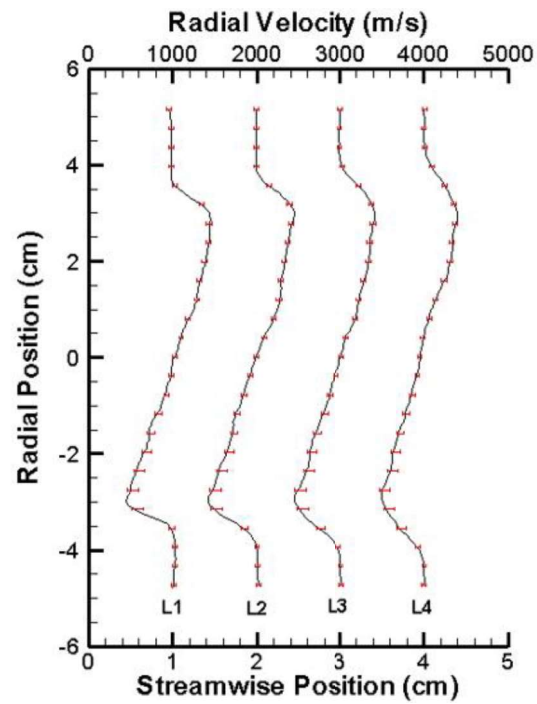

- Radial velocity measured with Doppler Shift
- Axial Velocity measured with MTV.
- Combined for complete velocity field

Mach 5 arcjet flow in HyMETS arcjet

Inman, J., Bathel, B., Johansen, C., Danehy, P., Jones, S., Gragg, J., and Splinter, S., "Nitric oxide planar laser-induced fluorescence measurements in the Hypersonic Materials Environment Test System," *AIAA Journal*, Vol. 51, No. 10, 2013, pp. 2365-2379, doi:10.2514/1.J052246

Single-laser MTV: FLEET

- Simple principle:
  - Works with N_2 in air or N_2 flows
  - Femtosecond laser is focused down to a line or spot
  - Gas glows for 10's of μs
- Originally developed at Princeton:
  - Air jet at room temperature, atmospheric pressure
  - Non-linear process
- Recently applied to transonic cryogenic flow at NASA Langley
  - Tracking of spot provided 2-D velocimetry [Burns et al.]
  - ~1 m/s accuracy and precision

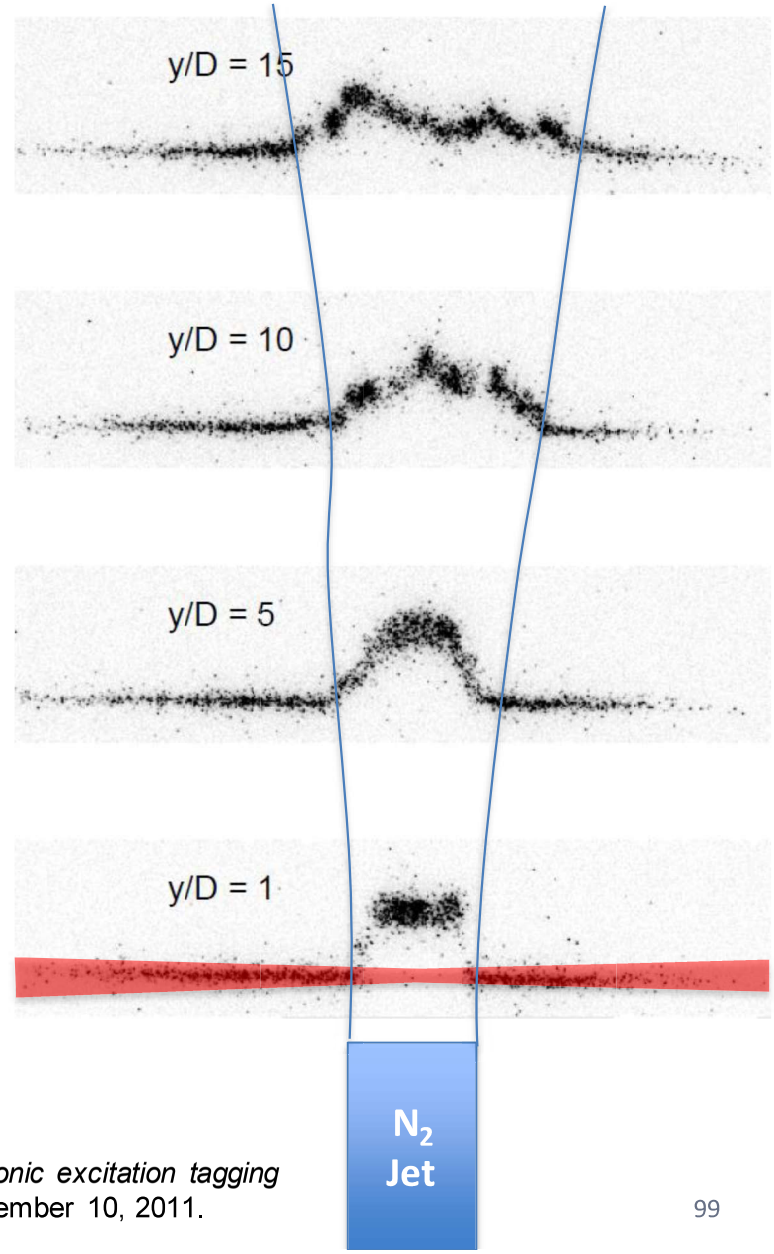

J. Michael, M. Edwards, A. Dogariu, and R. Miles, "*Femtosecond laser electronic excitation tagging (FLEET) for quantitative velocity imaging in air*," Applied Optics, 50(26), September 10, 2011.

Single-laser MTV: FLEET in AEDC

- 800 nm laser used to write FLEET line
- Unseeded measurements at 1kHz in both air and nitrogen
- Time-resolved velocity measurements at Mach 10 and 14 agree with the T9 prediction

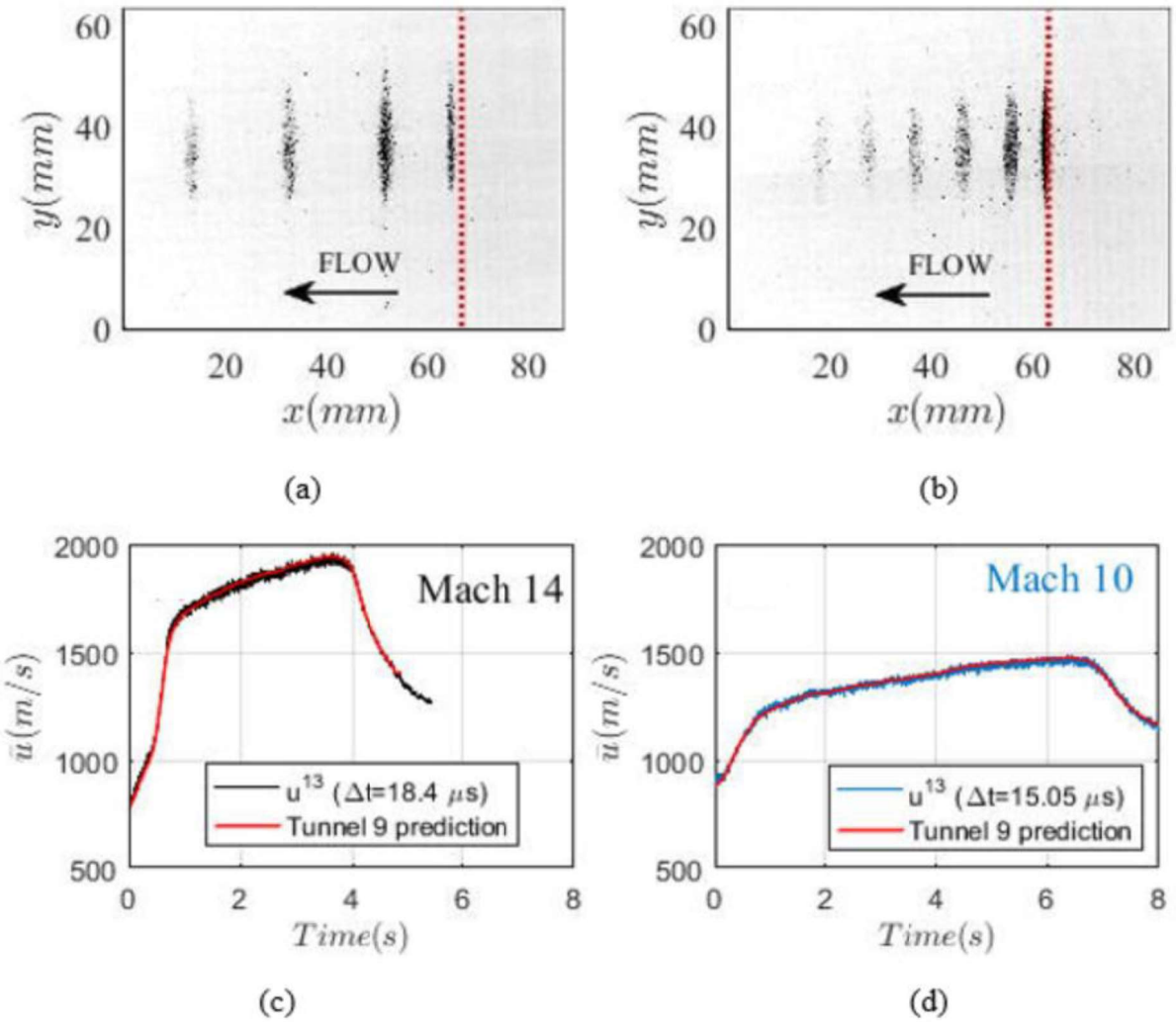

L. E. Dogariu, A. Dogariu, R. B. Miles, M. S. Smith, and E. C. Marineau. Non-intrusive Hypersonic Freestream and Turbulent Boundary-Layer Velocity Measurements in AEDC Tunnel 9 using FLEET. In 2018 AIAA Aerospace Sciences Meeting, Kissimmee, Florida, USA, 2018. AIAA 2018-1769.

Single-laser MTV

- Benefits
  - Near-Instantaneous measurement (~1 μsec)
  - Capable of providing velocity information along a line (1-component) or at grid points (2-component)
  - 'Seedless' methods available
  - Relatively simple to setup and perform

- Drawbacks
  - Reduced spatial resolution compared to Doppler shift approach
  - Operational limits often dictated by fluorescence lifetime
  - Potential for model damage
  - Potential for altering thermodynamic state of gas

Multilaser MTV

- Typically, one laser generates a line, series of lines or a grid pattern by dissociation, ionization (LEI), vibrational excitation (RELIEF), photolysis, bleaching or other process. Additional laser(s) read out pattern.
  - Example: Excimer laser at 193 nm+N_2+O_2→NO
  - *Air Photolysis and Recombination Tracking (APART)*
    - Dam et al, Optics Letters, 26 (1), pp. 36-38 2001
- A list of partner species used in the photolysis writing and reading process includes:

  H_2O-OH, N_2O-NO, O_2-O_3, N_2/O_2-NO, and NO_2-NO

- Method can use air constituents (N_2/O_2, O_2, N_2) or can be seeded (H_2O, N_2O, NO_2, Na, Kr, etc.).
  - We have used NO_2→NO to study transition

Multilaser MTV

- NO_2 to NO Photolysis
- NO LIF excitation

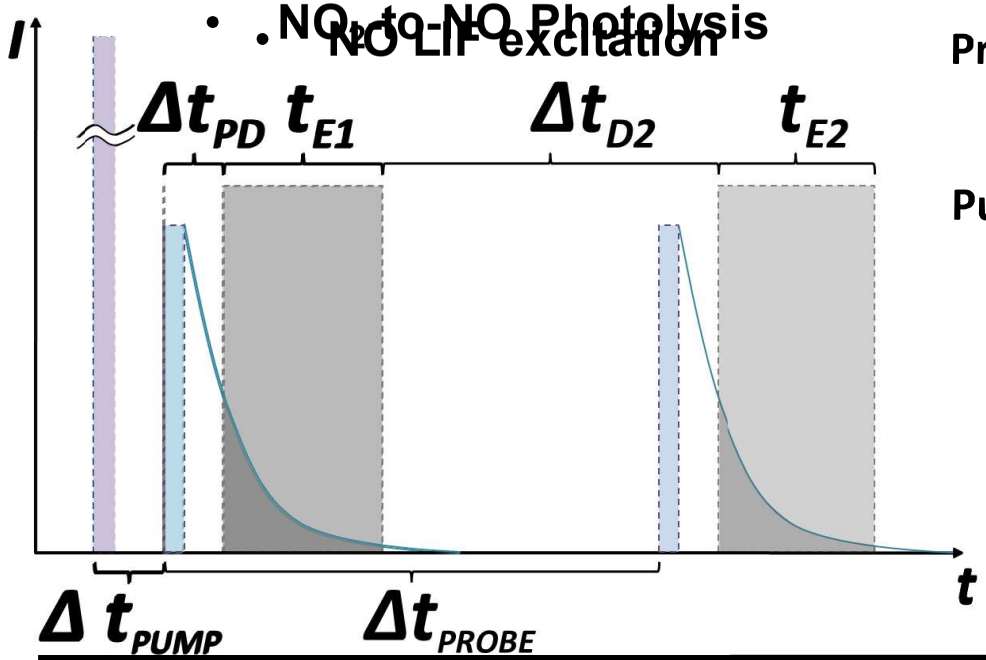

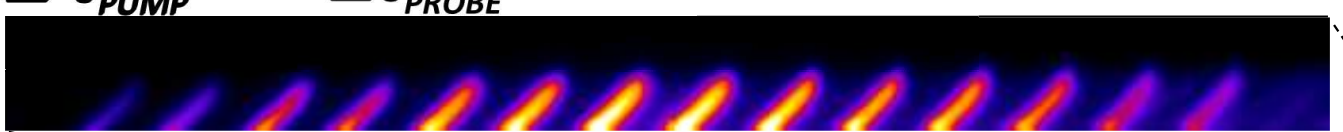

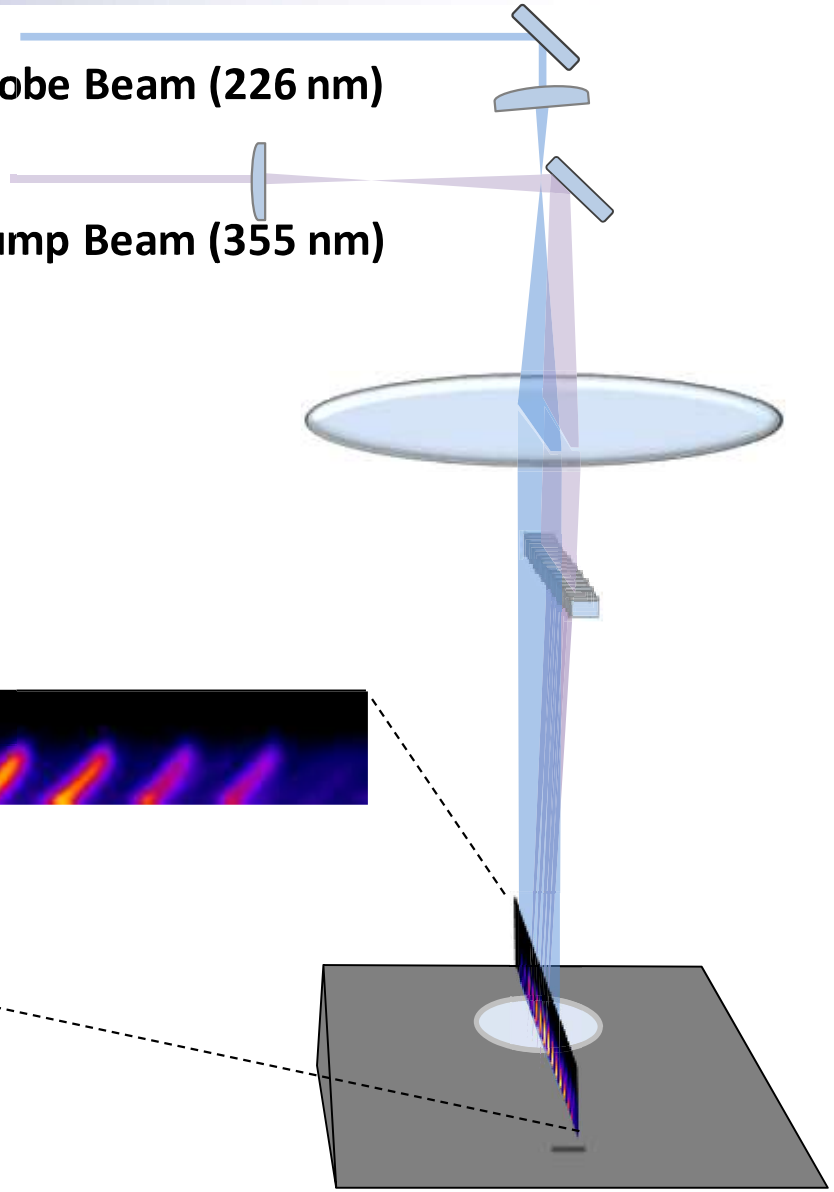

(for details of velocimetry method, see Bathel et al, AIAA-2011-3246 and others incl. TAMU[149], OSU[150], etc.)

Multi-laser MTV: KTV in AEDC

- Krypton Tagging Velocimetry (KTV)
- Line written using 214.7 nm laser and read using 769.5 nm sheet
- Used to obtain velocity profiles at Mach 10 and 14
- Time-resolved velocity measurements agree with the T9 conventional method

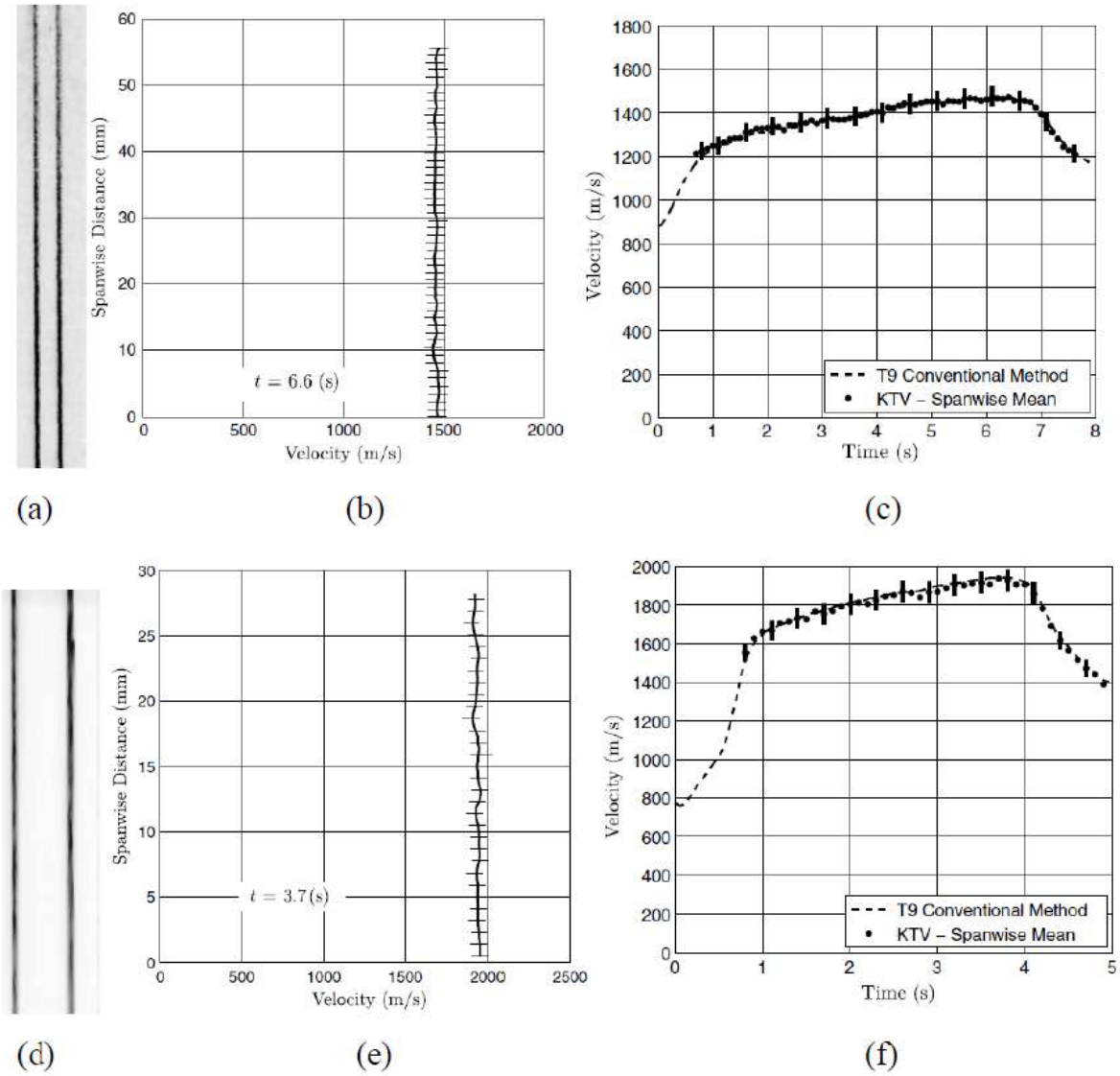

Mustafa, M. A., Parziale, N. J., Smith, M. S., and Marineau, E. C., "Nonintrusive Freestream Velocity Measurement in a Large-Scale Hypersonic Wind Tunnel," *AIAA Journal*, Vol. 55, No. 10, 2017, pp. 3611–3616. doi: 10.2514/1.J056177

Multi-laser MTV: HTV

- Vitiated high enthalpy test facility at Wright Patterson AFB (Research Cell 19)
- 7 x 7 grid written using 193 nm laser to dissociate H_20 and produce OH tracer molecules
  - Hydroxyl Tagging Velocimetry (HTV)
- Grid read at delayed time, 282 nm sheet
- Used to obtain velocity profiles of supersonic flow over a cavity (σ ~20 m/s)

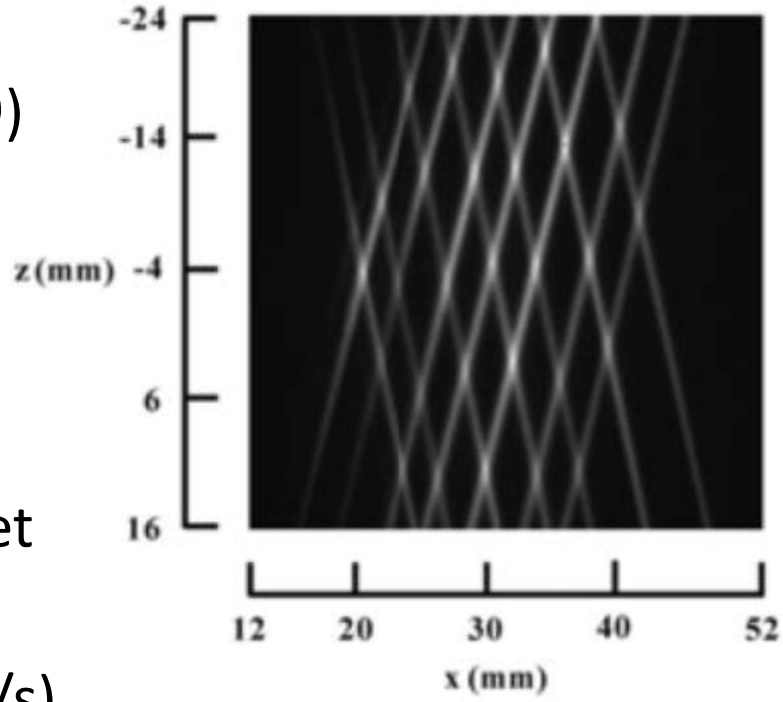

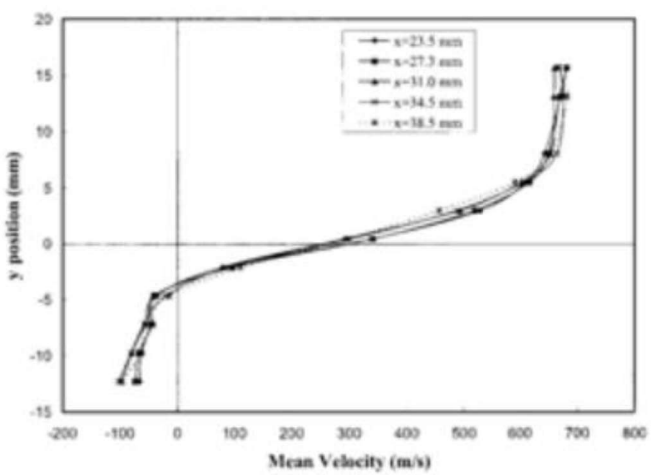

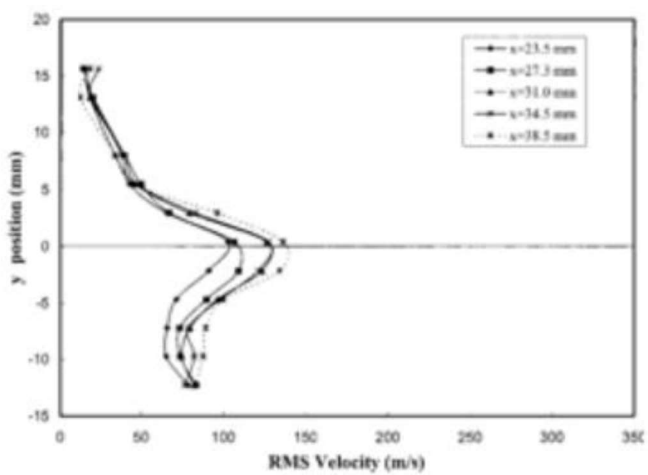

Pitz, R. W., Lahr, M. D., Douglas, Z. W., Wehrmeyer, J. A., Hu, S., Carter, C. D., Hsu, K. Y., Lum, C., and Koochesfahani, M. M., "Hydroxyl Tagging Velocimetry in a Supersonic Flow Over a Cavity," *Applied Optics*, Vol. 44, No. 31, 2005, pp. 6692–6700. doi:10.1364/AO.44.006692

3 laser MTV: measure u, v, T

- Texas A&M has used 3 laser technique with crossed beam pattern for 2-component velocity and temperature in an underexpanded N_2 jet flow with NO_2:
  - VENOM: vibrationally excited nitric oxide monitoring
  - Excite to v' = 1 state

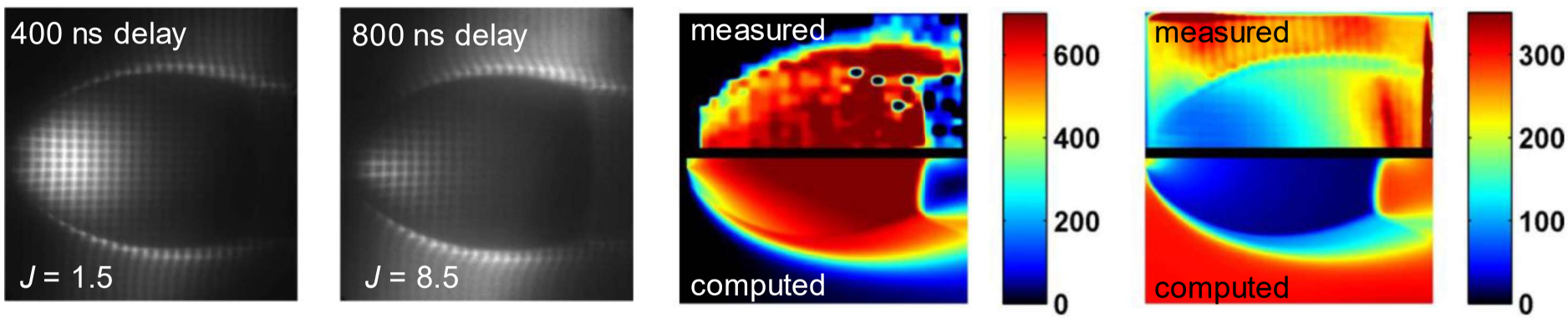

Raw data images

U-Velocity (m/s)
(~5% uncertainty)

Temperature (m/s)
(~9-35% uncertainty)

R. Sánchez-González, R. Srinivasan, R. D. W. Bowersox, and S. W. North, "*Simultaneous velocity and temperature measurements in gaseous flowfields using the vibrationally excited nitric oxide monitoring technique: a comprehensive study*," Applied Optics, 51(9), pp. 1216-1228, March 20, 2012

Multilaser MTV: Unseeded

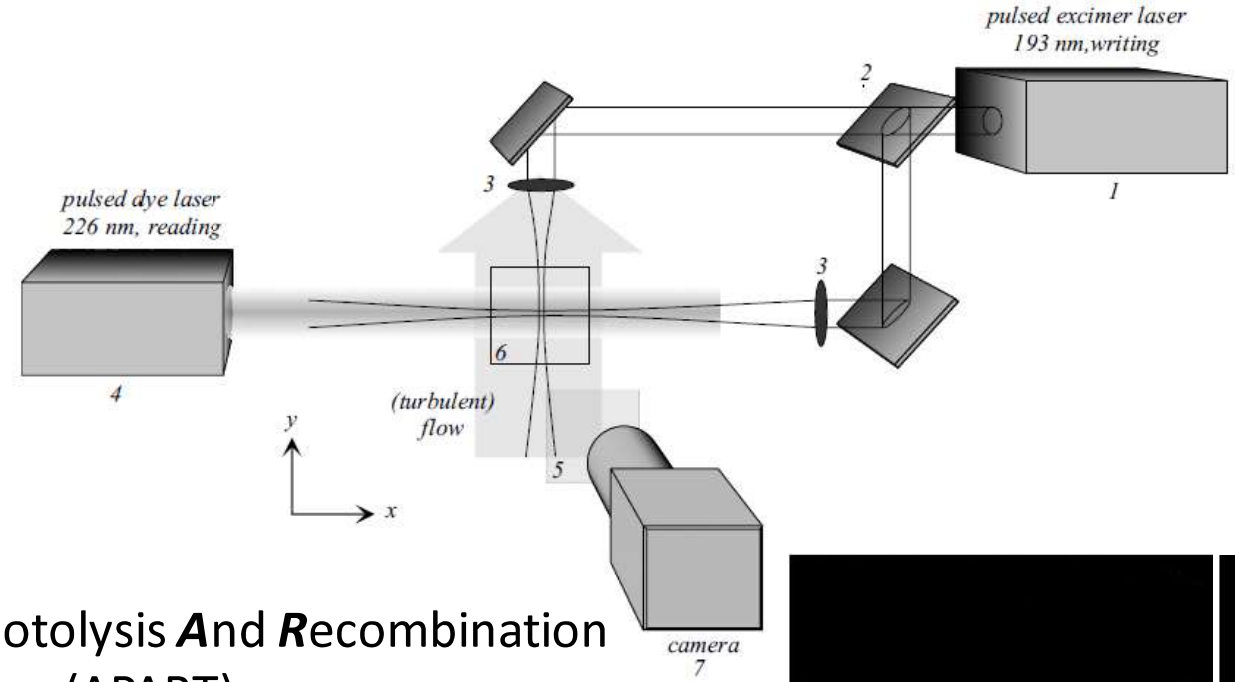

- ***A***ir ***P***hotolysis ***A***nd ***R***ecombination ***T***racking (APART)
  - Nitric oxide generated in unseeded air via dissociation by UV excimer laser beam
  - NO then probed with LIF excitation wavelengths

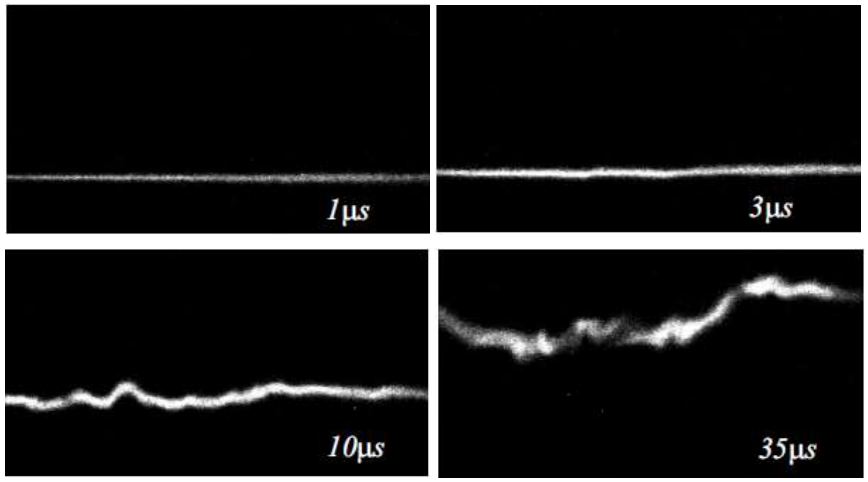

J. Bominaar, M. Pashtrapanska, T. Elenbaas, N. Dam, H. ter Meulen, and W. van de Water, *"Writing in Turbulent Air,"* Physical Review, 77, 2008.

Multilaser MTV: Unseeded

- ***R***aman ***E***xcitation and ***L***aser-***I***nduced ***E***lectronic ***F***luorescence (RELIEF)
  - O_2 vibrational excitation via Raman pumping
  - UV Excimer laser used to probe 1st vibration state of oxygen
  - Works for flows where T < ~750 K

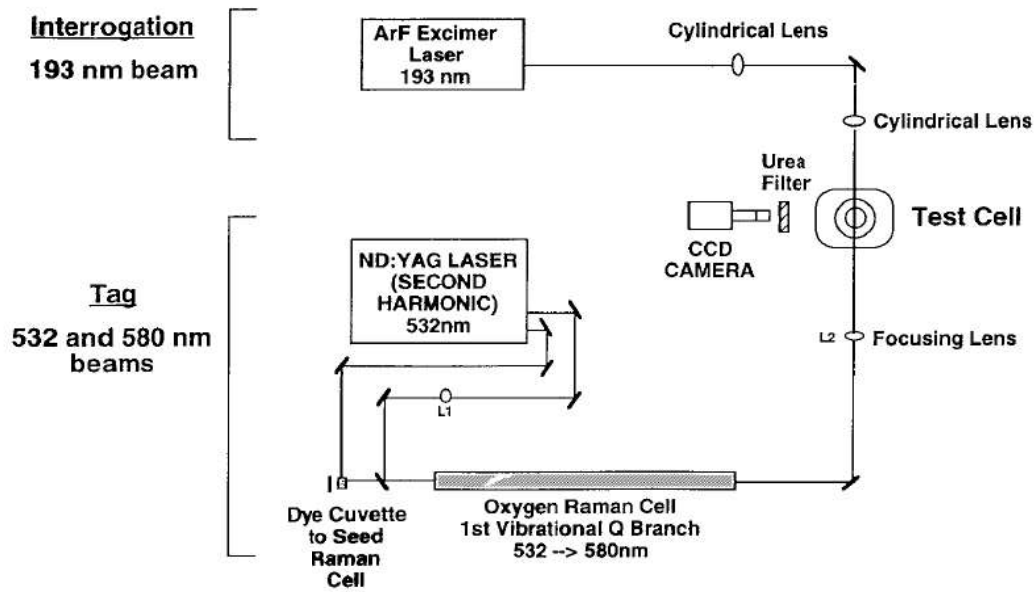

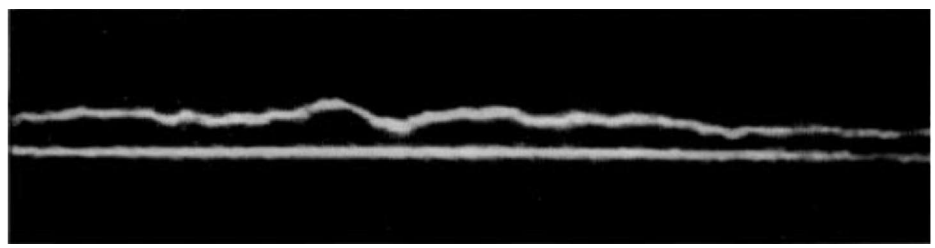

R. Miles, J. Grinstead, R. Kohl, and G. Diskin, *"The RELIEF flow tagging technique and its application in engine testing facilities and for helium-air mixing studies,"* Measurement Science & Technology, 11, pp. 1272-1281, 2000.

Three-laser MTV: uncertainty & design

- **Analysis**
  - Uncertainty for high s/n data
    - Mean: 1% of edge velocity (~1300 m/s) in 200 images
    - Single-shot: 1-2% of edge velocity
  - Measurement within 100 μm from wall

- **Tradeoffs for experiment design**
  - Accuracy and precision improve with probe delay
  - Spatial resolution worse with longer probe delay
    - Can use longer delay for slow flow
  - Current configuration requires relatively large blowing rates for adequate signal-to-noise
    - May be significant wall-normal velocity component

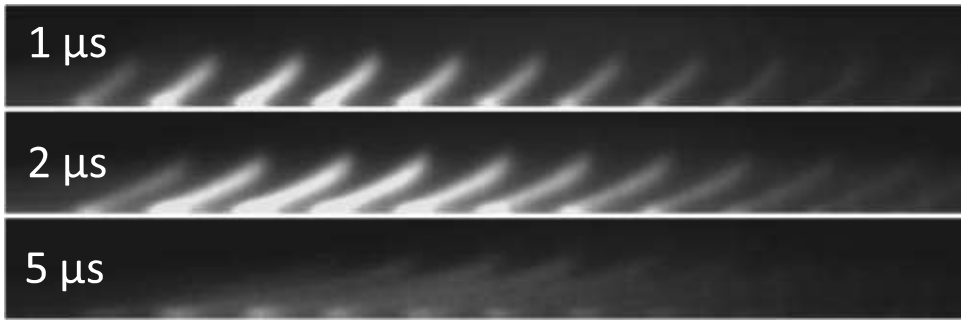

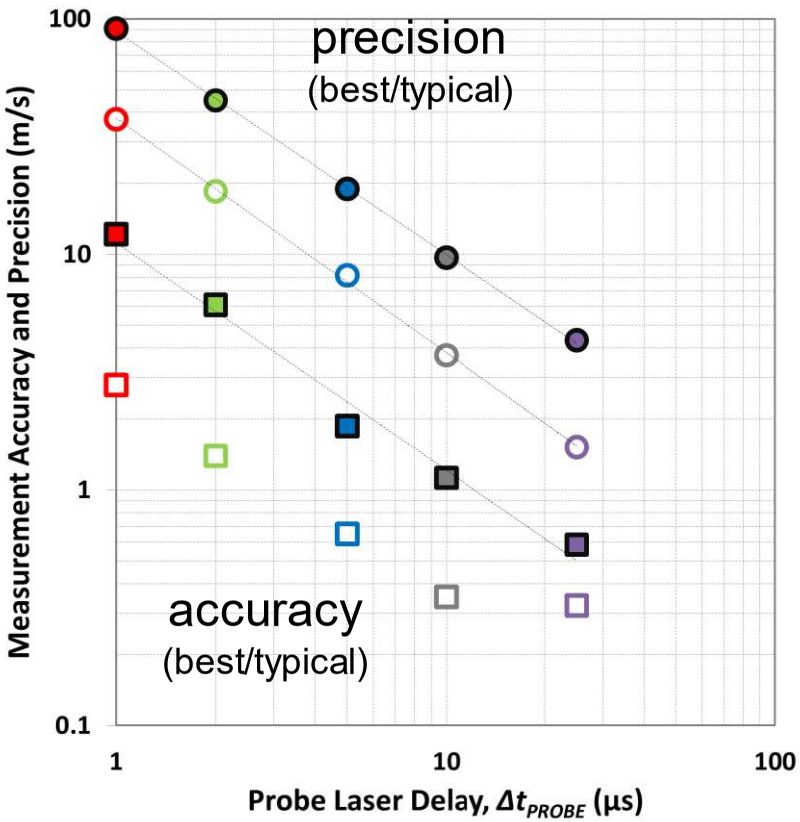

Data obtained at static, low pressure conditions

Multi-laser MTV

- Benefits
  - Capable of providing instantaneous velocity along a line (1-component) or at grid points (2-component)
  - Several 'seedless' methods available
  - Not limited by fluorescence lifetime (works in high *P*)
  - Can have higher accuracy and precision vs single laser methods
- Drawbacks
  - More complicated setup – requires multiple lasers
  - Reduced spatial resolution compared to Doppler shift approach
  - Potential for model damage
  - Altering thermodynamic state of gas

Focused Laser Differential Interferometry

***Nicholas Parziale**, Stevens Institute of Technology, Hoboken NJ USA*
***Paul Danehy**, NASA Langley Research Center, VA, USA*

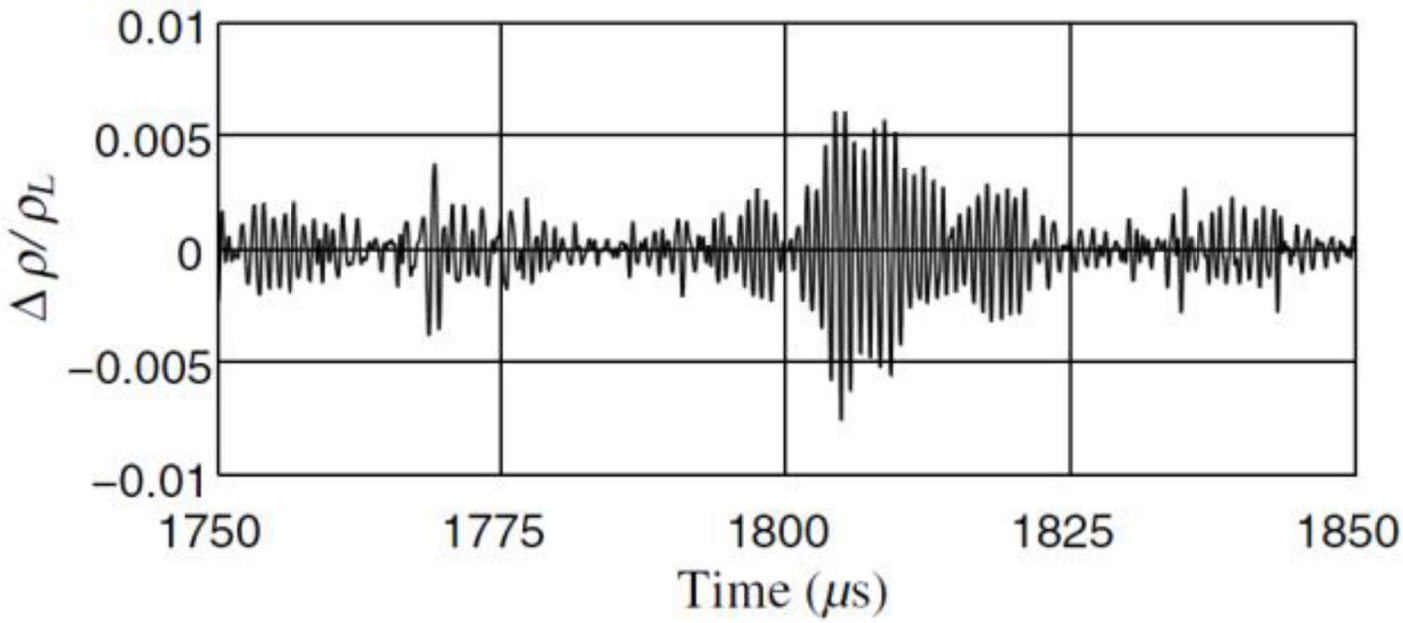

Focused Laser Differential Interferometry

- Interferometry is very sensitive to density

$$n - 1 = K\rho$$

  - Typically is path-averaged over the line of sight
  - LDI, using two parallel beams has been used to study development of laser-heated spots in transitional flow (Salyer, Collicott, Schneider, 2000)
    - *But LDI is sensitive to any changes along the path of the laser*
- Focused LDI (FLDI) is most sensitive at the focus point of the two beams
  - Originally by Smeets and George, 1973
  - Recently implemented at Caltech

FLDI Setup at Caltech

- Laser beam split into two using a polarizer (P1) and Wollaston prism (W1).
  - Also slightly deflected
  - Two spots focus into flow at A
- Two light beams travel mainly through same flow
  - Beams separated $0.35\ mm$
  - $\pm 10\ mm$ long interaction length
- Beams recombined (W2), made to interfere (P2) and detected (D)
  - $20\ MHz$ time response

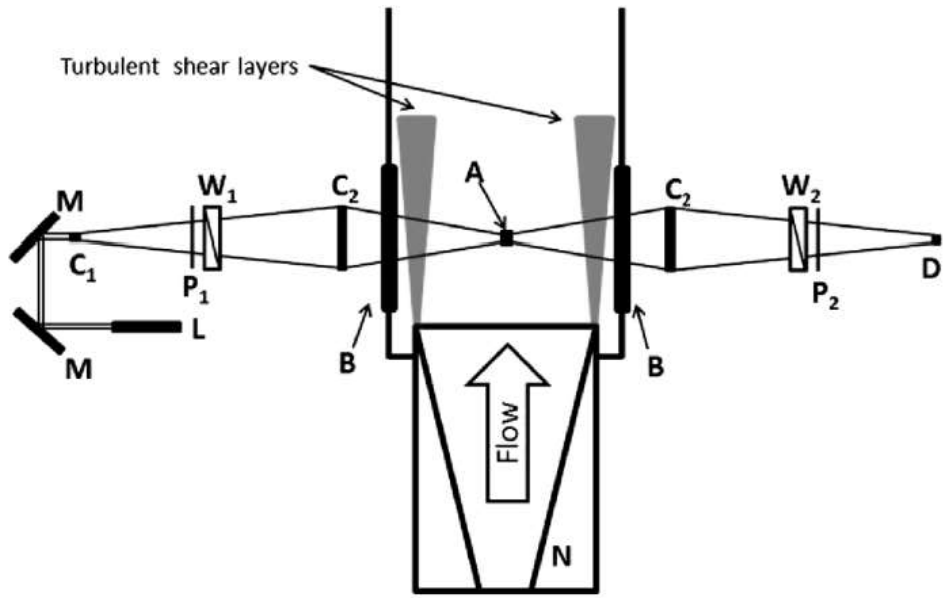

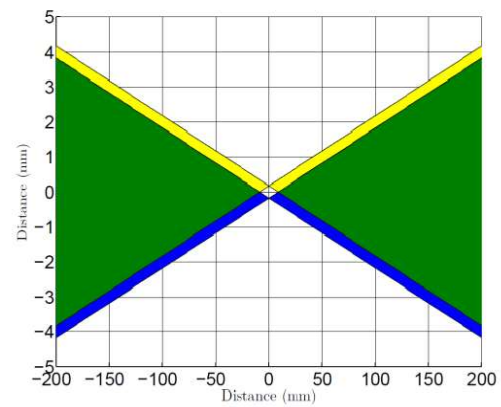

Computed light pattern at probe region

N. J. Parziale, J. E. Shepherd, and H. G. Hornung, "Differential Interferometric Measurement of Instability in a Hypervelocity Boundary Layer," AIAA J., Vol. 51, No. 3, p. 750-753, March 2013

FLDI Results: Cone BL

- FLDI was used in T5 free piston shock tunnel
  - Boundary layer development on a cone

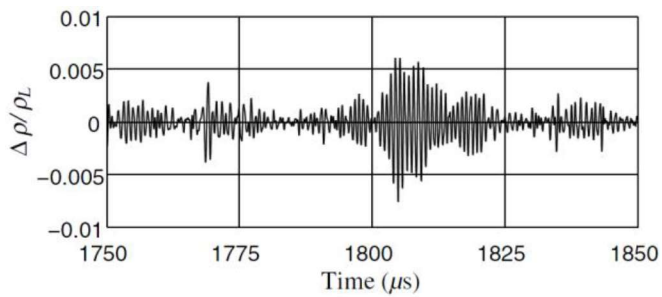

  - $1.17\ MHz$ instability wave measured with FLDI
    - $0.5\ mm$ above surface of cone with $1\ mm$ thick BL
  - Accuracy in $\frac{\Delta\rho}{\rho}$ is $\sim 30\%$ but precision is $\sim 0.5\%$
  - Sensitivity is that between the two measurement locations instead of more common fluctuation about mean

N. J. Parziale, J. E. Shepherd, and H. G. Hornung, "Differential Interferometric Measurement of Instability in a Hypervelocity Boundary Layer," AIAA J., Vol. 51, No. 3, p. 750-753, March 2013

FLDI Results: Tunnel Freestream

- FLDI was used in T5 free piston shock tunnel
  - Freestream noise measurement

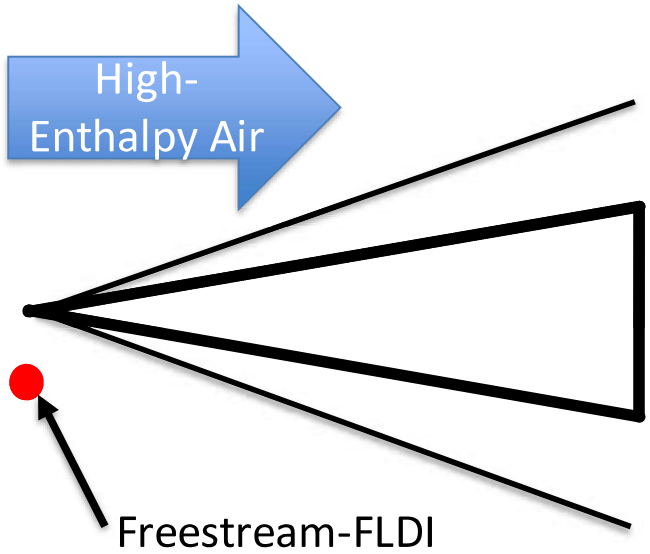

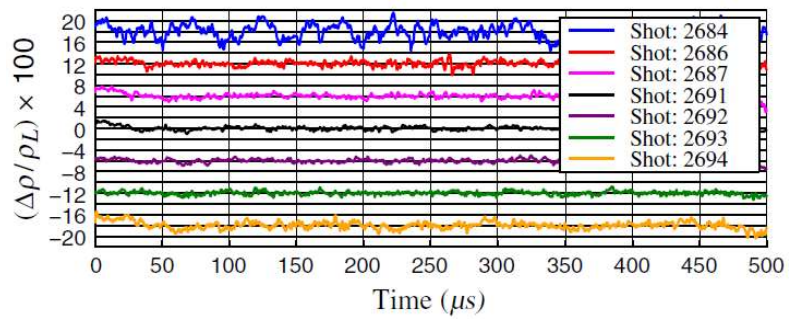

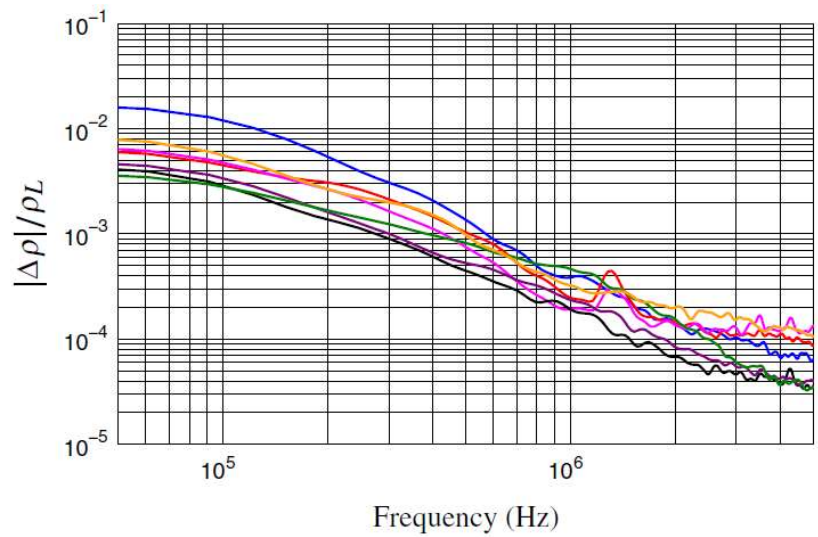

Parziale, N. J., Shepherd, J. E., and Hornung, H. G., "Free-stream density perturbations in a reflected-shock tunnel," Experiments in Fluids, Vol. 55, No. 2, 2014, pp. 1–10. doi: 10.1007/s00348-014-1665-0

FLDI Results: Cone BL Development

- FLDI was used in T5 free piston shock tunnel
  - Boundary layer development on a cone.

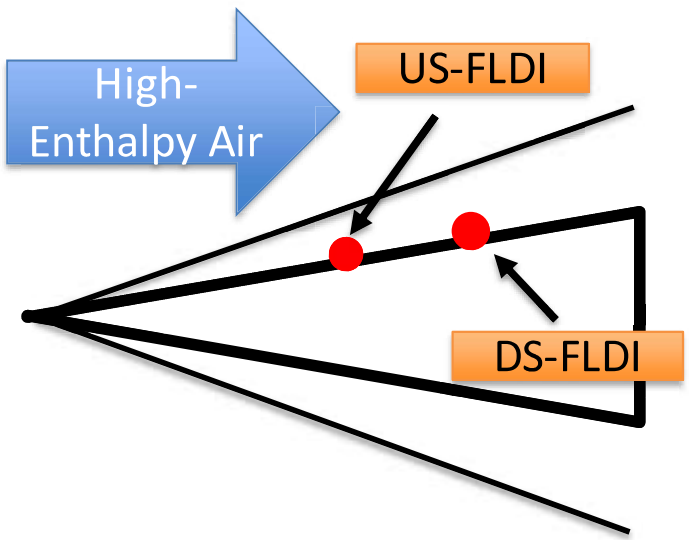

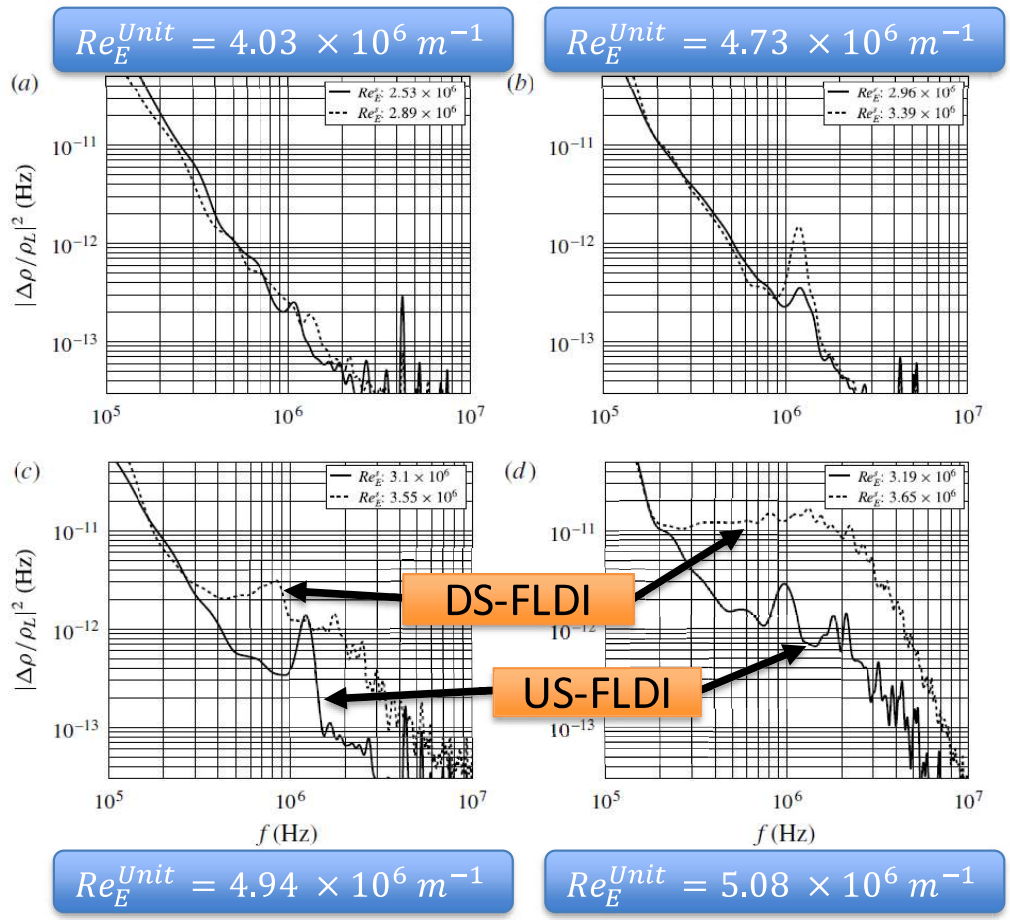

Parziale, N. J., Shepherd, J. E., and Hornung, H. G., "Observations of hypervelocity boundary-layer instability," Journal of Fluid Mechanics, Vol. 781, 2015, pp. 87–112. doi: 10.1017/jfm.2015.489

FLDI Results: Tunnel Freestream

- Used in NASA 20 Inch Mach 6 Air Tunnel
  - Compared freestream noise measurements to other techniques (PCB, Kulite)

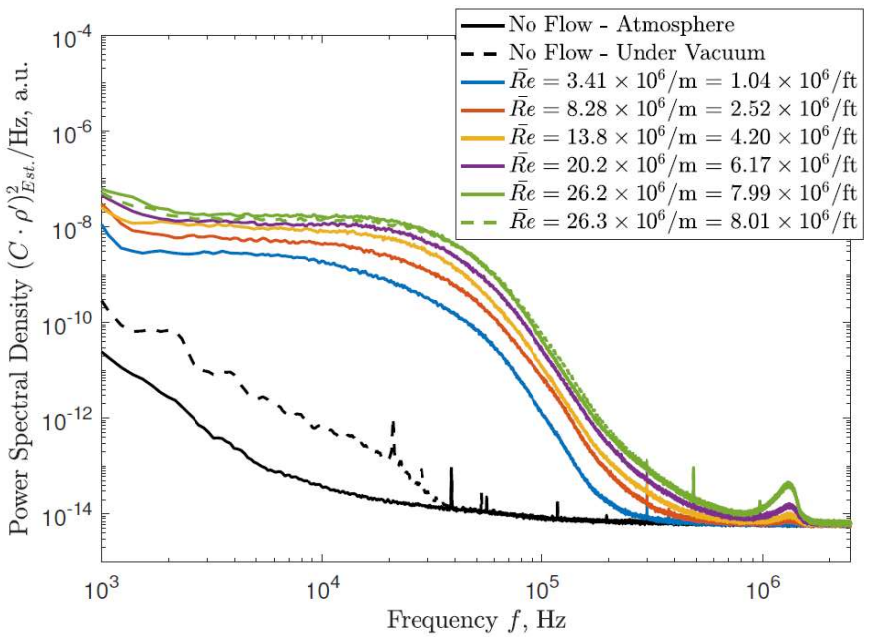

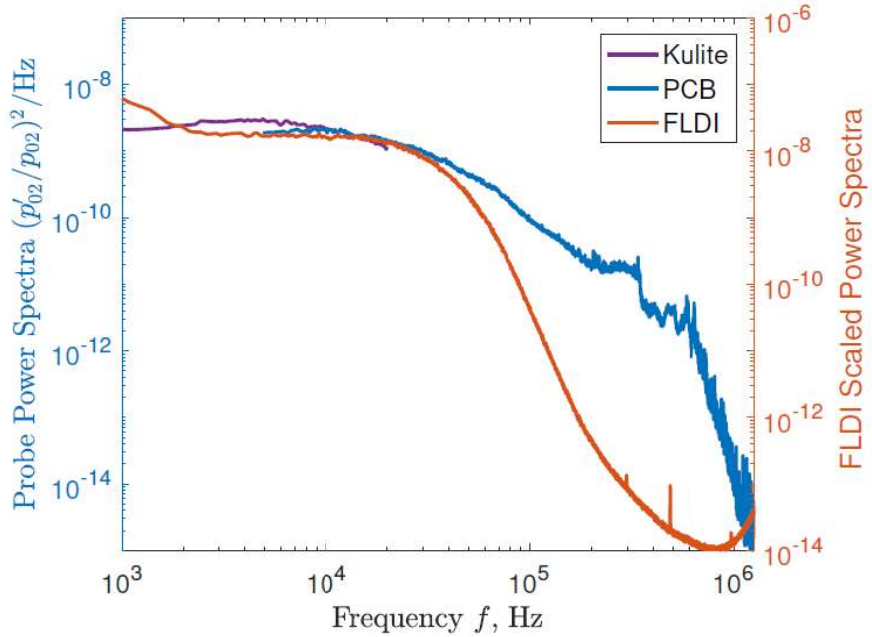

Chou, A., Leidy, A., King, R. A., Bathel, B. F., and Herring, G., "Measurements of Freestream Fluctuations in the NASA Langley 20-Inch Mach 6 Tunnel," AIAA Aviation Forum, AIAA 2018-3073, Atlanta, Georgia. doi: 10.2514/6.2018-3073

FLDI Results: Two-Point Cone BL

- Used in NASA 20 Inch Mach 6 Air Tunnel
  - 2nd-mode instability in hypervelocity boundary layer

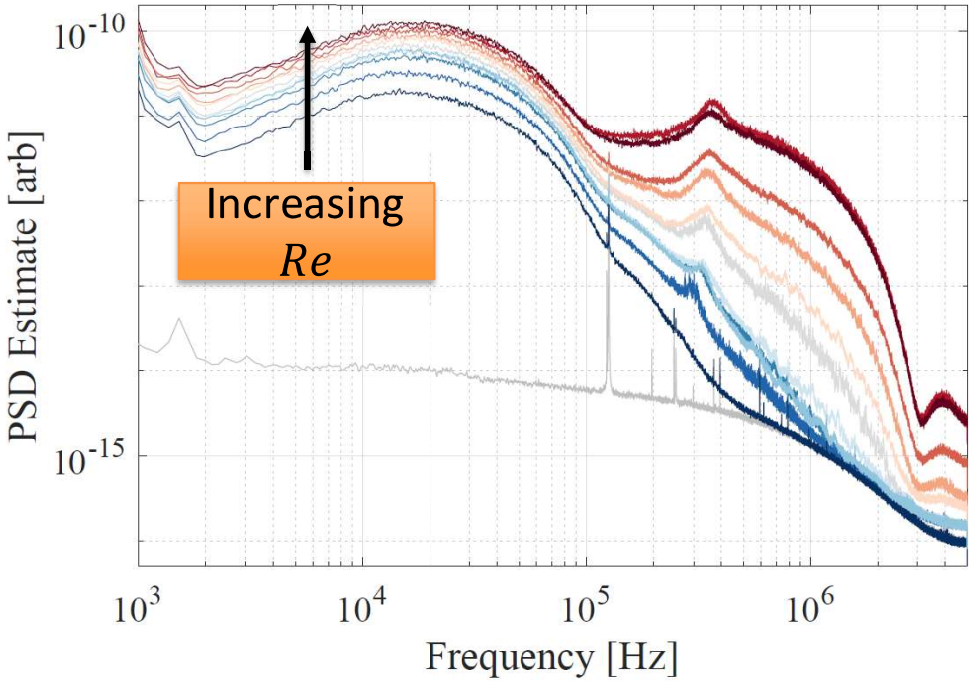

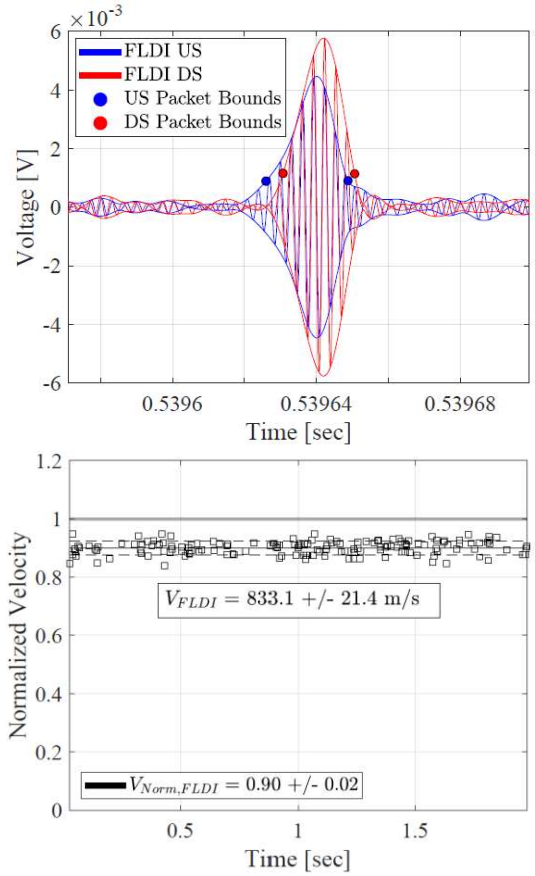

Weisberger, J. M., Bathel, B. F., Herring, G. C., King, R. A., Chou, A., and Jones, S. B., "Two-Point Focused Laser Differential Interferometry Second-Mode Measurements at Mach 6," AIAA Aviation Forum, AIAA 2019-2903, Dallas, TX. doi: 10.2514/6.2019-2903

Laser Scattering Techniques

Paul Danehy, *NASA Langley Research Center, VA, USA*
Timothy Fahringer, *National Institute of Aerospace, Hampton VA, USA*

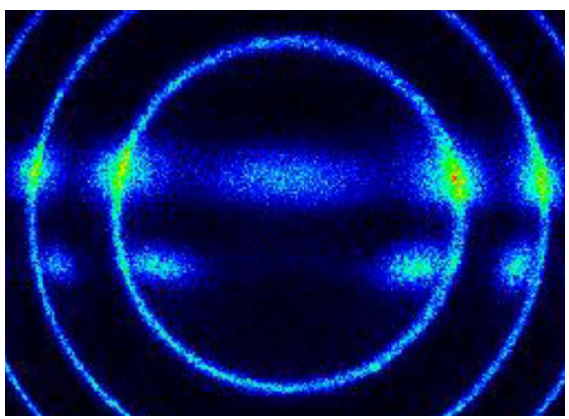

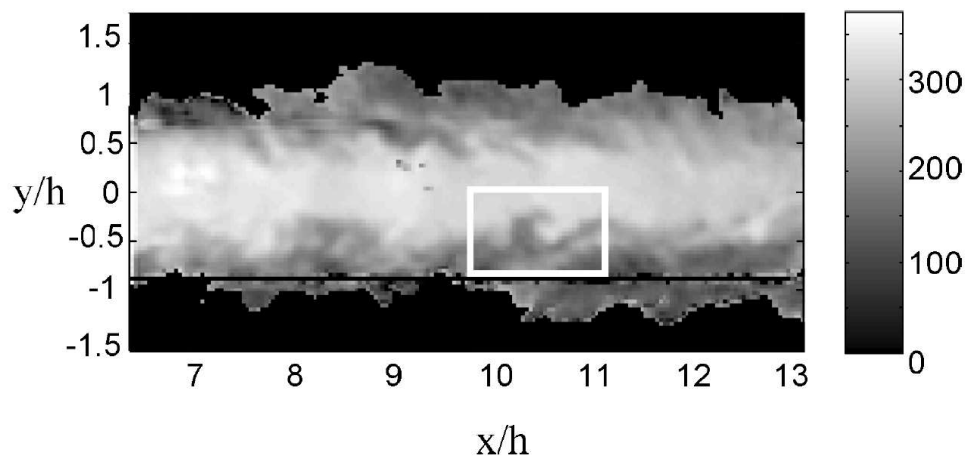

Laser Scattering Techniques

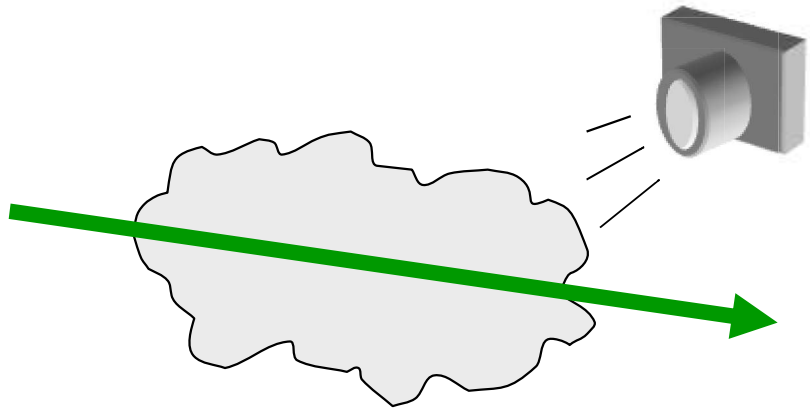

- When light passes through a gas:
  - LIF is a *resonant* absorption/emission process
  - Mie, Rayleigh and Raman are <u>*scattering*</u> processes
    - Mie Scattering: $d \geq \lambda$ (d is the particle size)
    - Spontaneous Rayleigh and Raman scattering: $d << \lambda$
- Will provide physical interpretation for Rayleigh and Raman
  - Classical description in AIAA chapter
  - There is also a quantum treatment

Will discuss Mie later: DGV and PIV

Rayleigh Scattering

- Rayleigh scattering:
  - Electric field causes electron cloud to oscillate with respect to the nucleus: <u>induced dipole</u>

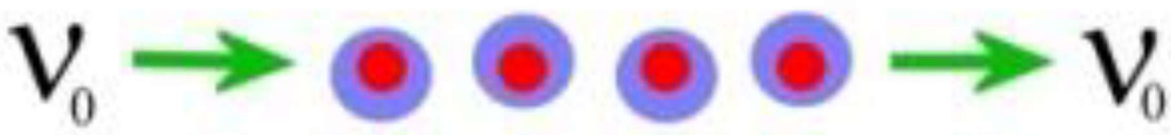

http://www.timkelf.com/Research/ResearchSERS.html

  - An oscillating dipole acts like an antenna: radiates!
    - Radiation is perpendicular to oscillation

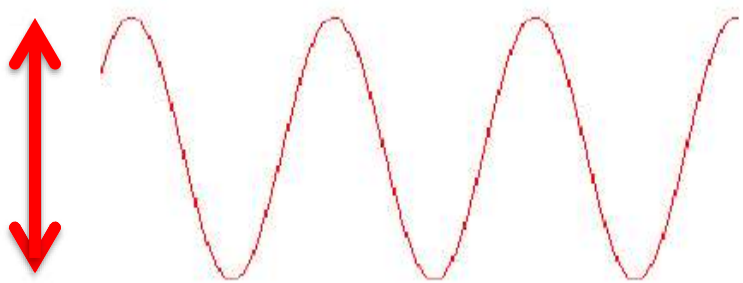

Rayleigh Scattering

- Very weak process
  - 1 photon in 0.1 million scatters / meter at STP
- Wavelength dependence: $1/\lambda^4$

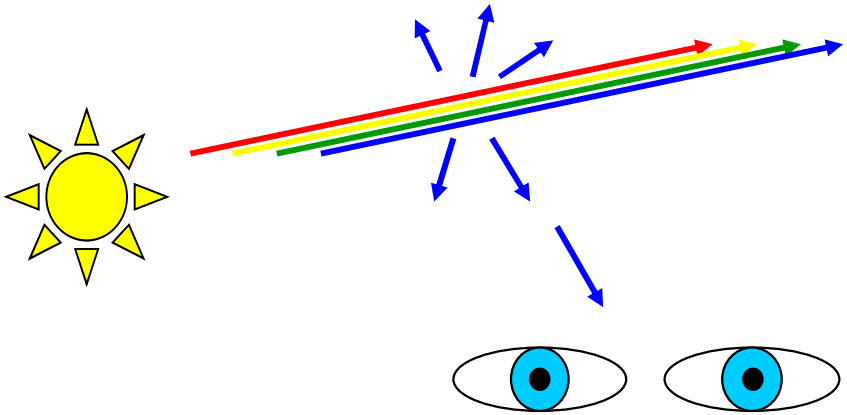

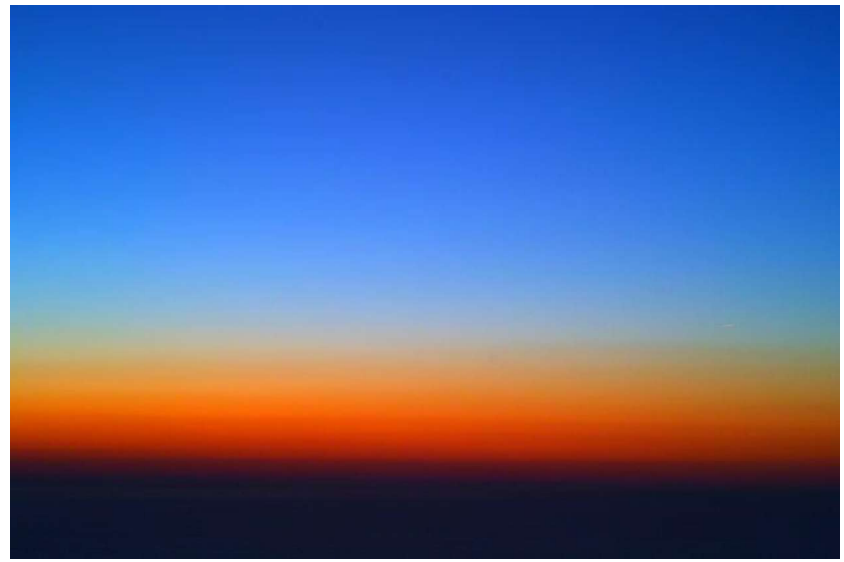

Rayleigh scattering in the atmosphere after sunset, picture taken over the ocean, at 500m altitude.
http://ms.wikipedia.org/wiki/Selerakan_Rayleigh

- Causes blue sky and red sunsets
  - Mie scattering from aerosols also contributes

Raman Scattering

- Similar to Rayleigh scattering but molecules gain or lose energy during scattering process
- Raman x1000 lower probability than Rayleigh

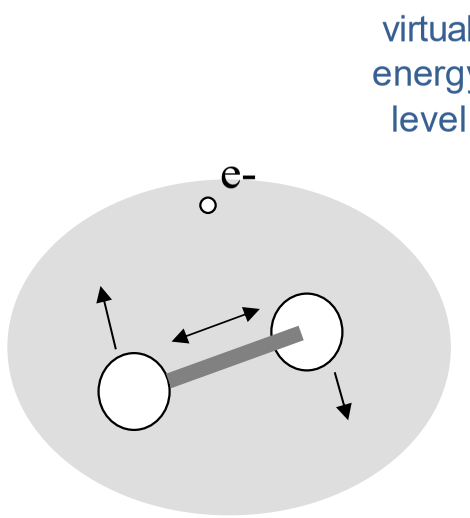

N_2 molecule

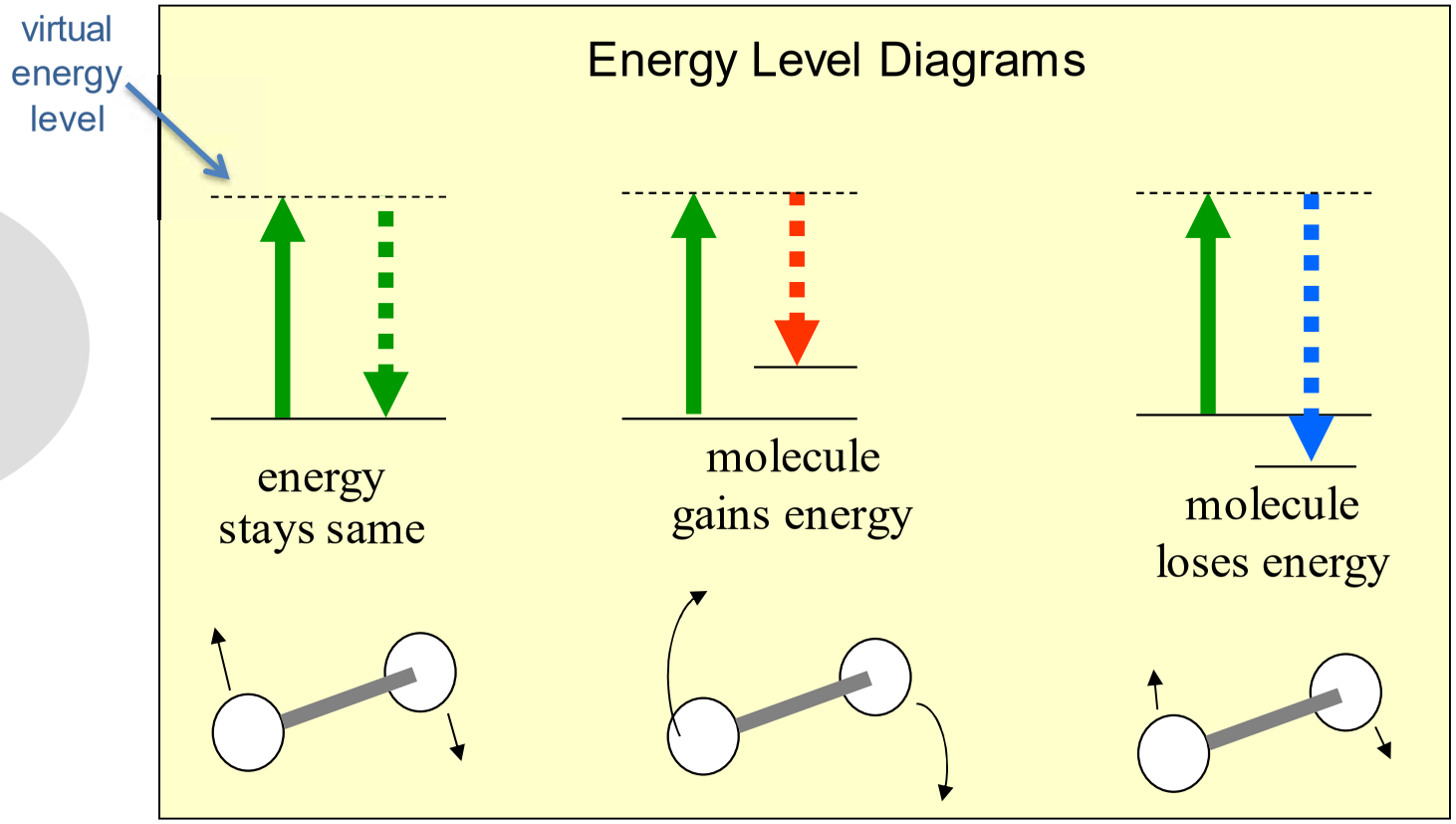

Raman Scattering

- Raman scattering results in a frequency shift
  - Molecule vibrating at frequency ν_{mol}

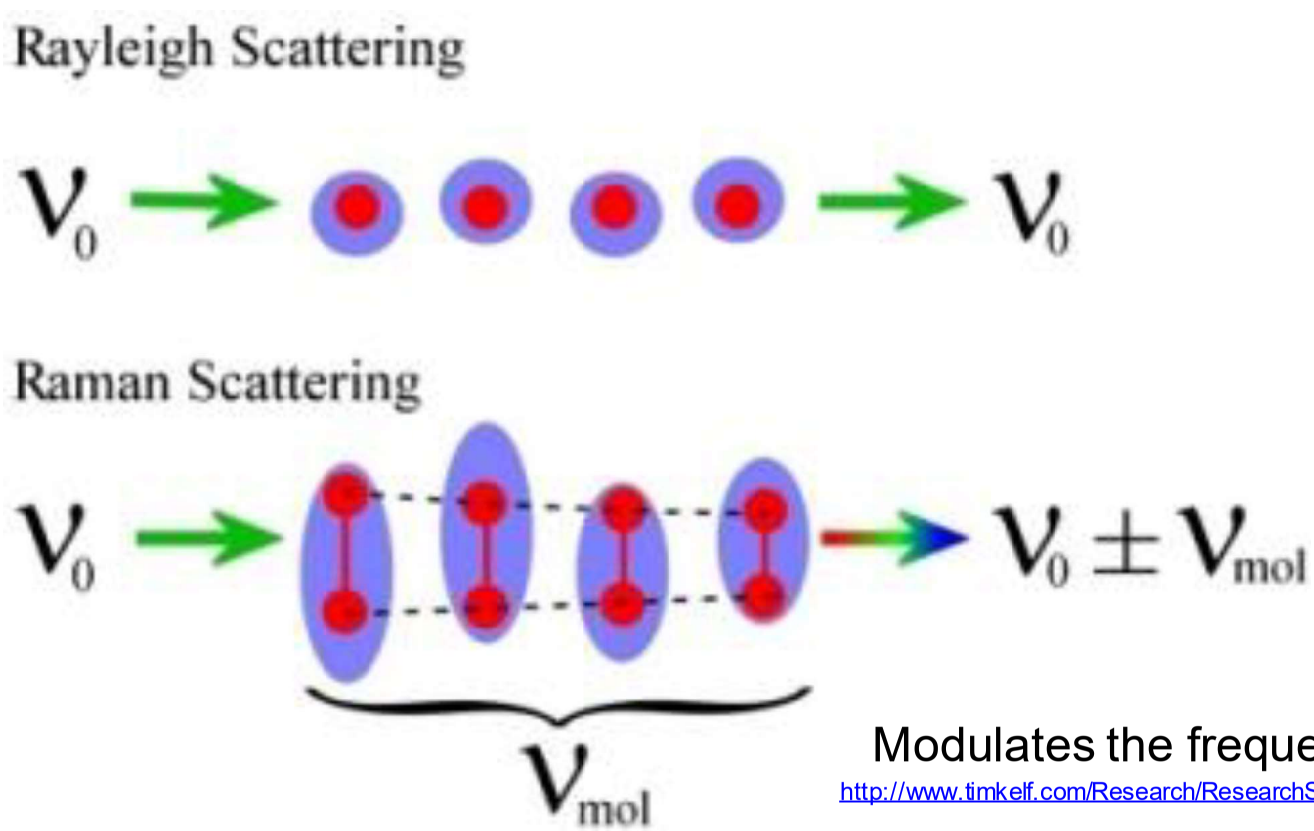

Modulates the frequency

http://www.timkelf.com/Research/ResearchSERS.html

Mie, Rayleigh and Raman Scattering

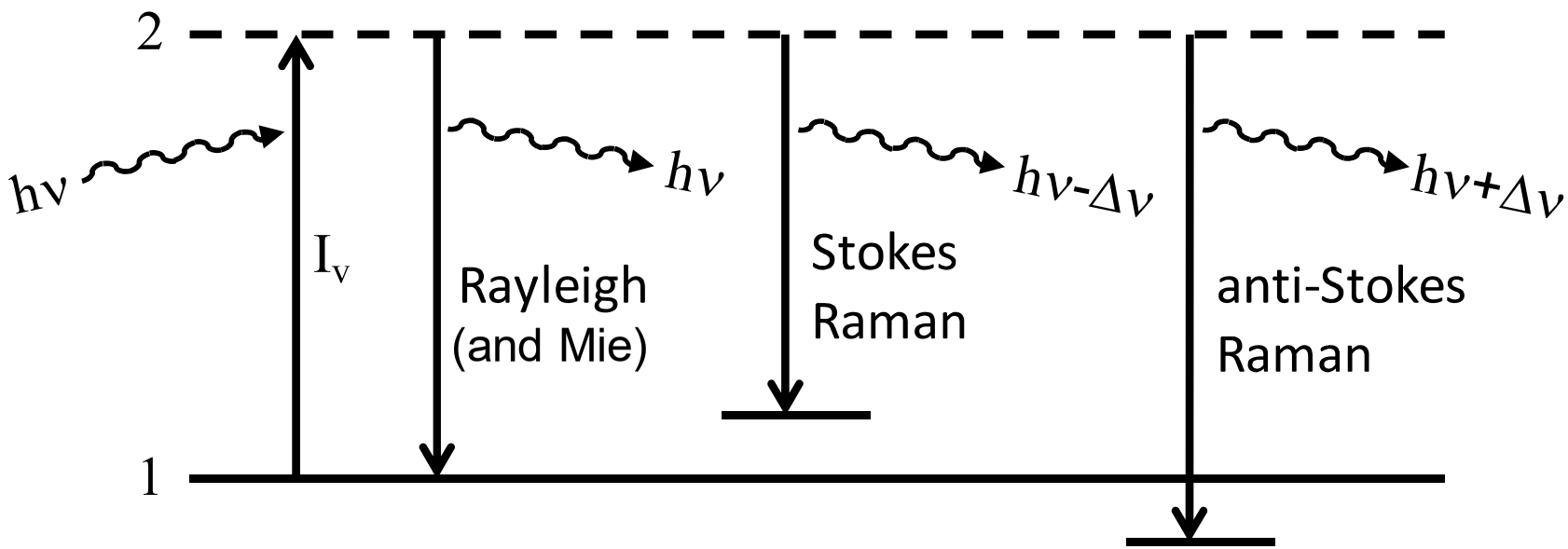

- Energy level diagram:
  - Stokes Raman: energy absorbed by molecule
  - anti-Stokes Raman: energy lost by molecule
    - Initial state must not have been a ground state

Rayleigh and Raman Spectra

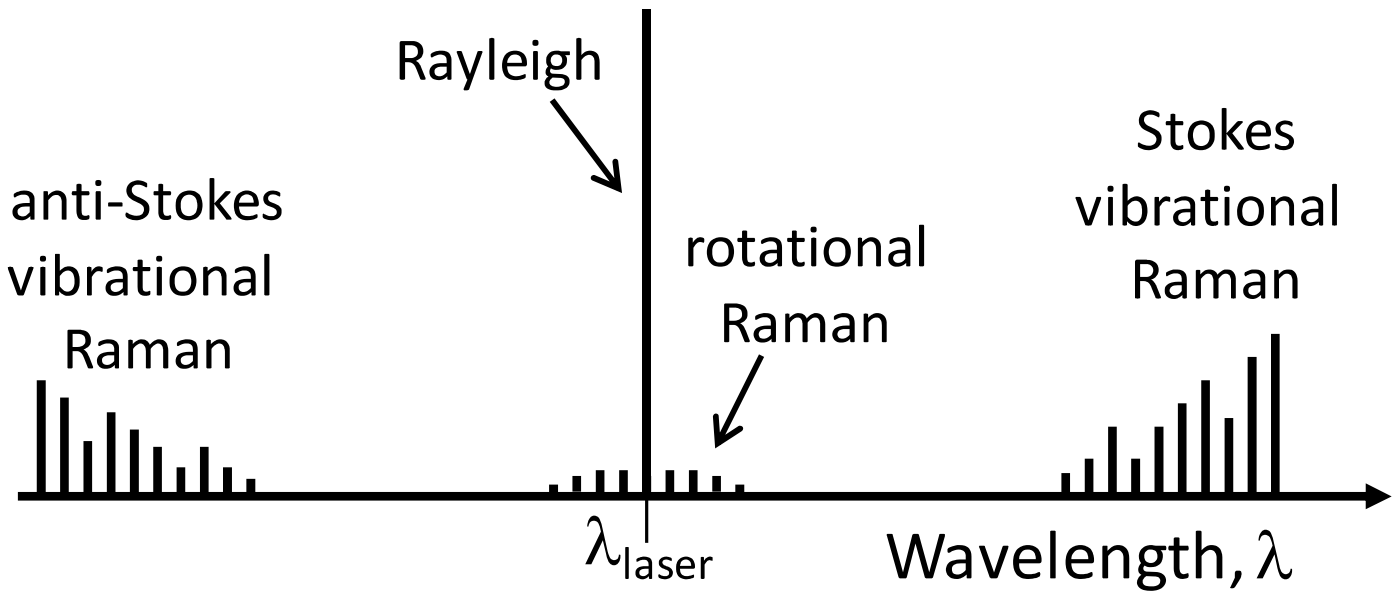

- Rayleigh: near laser's wavelength
- Raman: frequency shift depends on molecule, state (sensitive to <u>concentration</u> and <u>temperature</u>)
  - Rotational Raman
  - Vibrational Raman

Rayleigh Spectrum

- Rayleigh Scattering is at or near the laser's wavelength.
  - Doppler broadened (~$T^{1/2}$)
  - Can be Doppler shifted (~V)
  - Signal proportional to N (~ρ)

$$I_{zz}^{\Omega} = \left(\frac{\partial\sigma}{\partial\Omega}\right)_{zz} NI$$

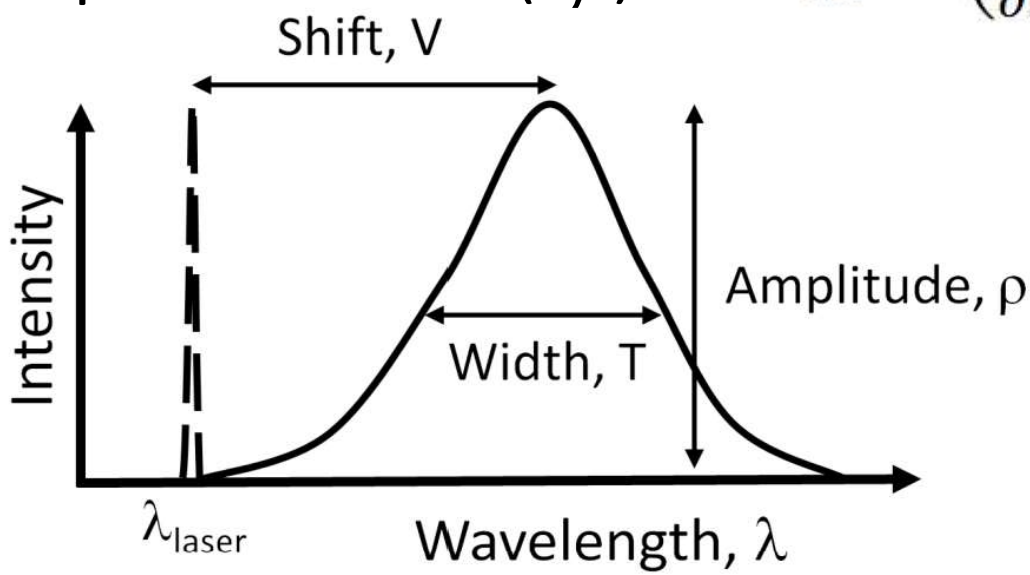

  - Can potentially measure these simultaneously
    - Requires high spectral resolution

Rayleigh and Raman Examples

- Rayleigh
  - Velocimetry, multi point
  - V, T, ρ, single point
  - V, T, ρ, imaging
  - ρ measurement (and infer T)

- Raman
  - Concentration
  - Temperature

Rayleigh Velocimetry

- Rayleigh scattering velocimetry can measure selected velocity components
  - Measured component is bisector between incident laser and collection optics

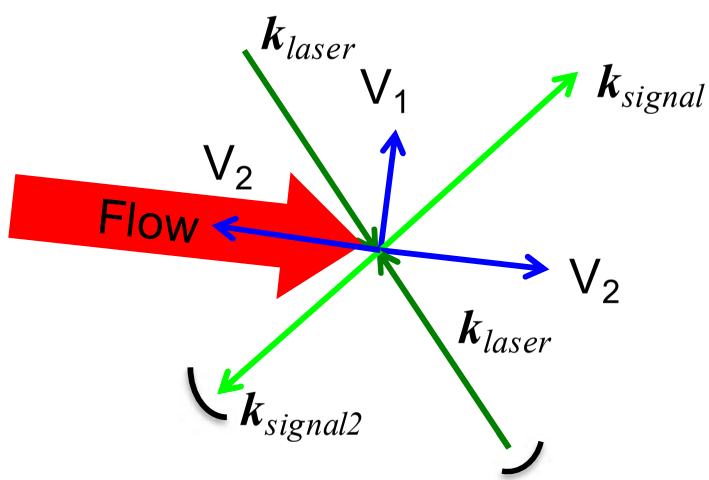

Wave vector:

$k = 2\pi/\lambda$

D. Bivolaru, P. M. Danehy, R. L. Gaffney, Jr. and A. D. Cutler, "Direct-View Multi-Point Two-Component Interferometric Rayleigh Scattering Velocimeter," 46th AIAA Aerospace Sciences Meeting and Exhibit, Reno, Nevada, AIAA Paper 2008-236, January 7-10, 2008

  - Can measure multiple velocity components by adding additional detection angles or laser beams

Rayleigh Velocimetry

- Rayleigh scattering velocimetry has been performed different ways, always requiring a high resolution device to resolve the Doppler shift
  - I_2 filter in front of CCD
    - Imaging capability
    - limited dynamic range
  - Fabry Perot etalon
    - PMT based (faster)
    - CCD based (multi-point)
  - Combined I_2 filter and Fabry Perot etalon
  - See manuscript for references

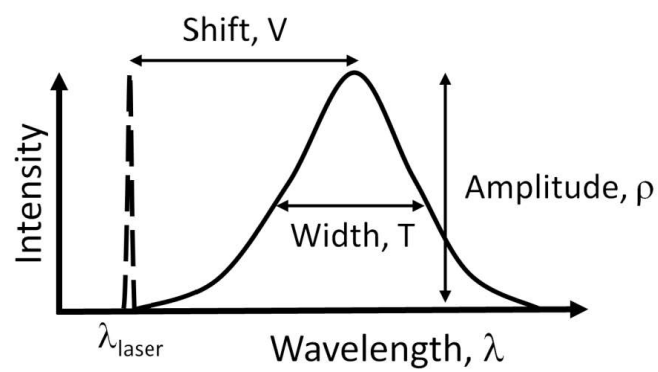

Rayleigh Velocimetry using Fabry-Perot Etalon

- Velocimetry using a Fabry Perot Interferometer (FPI) with CCD camera

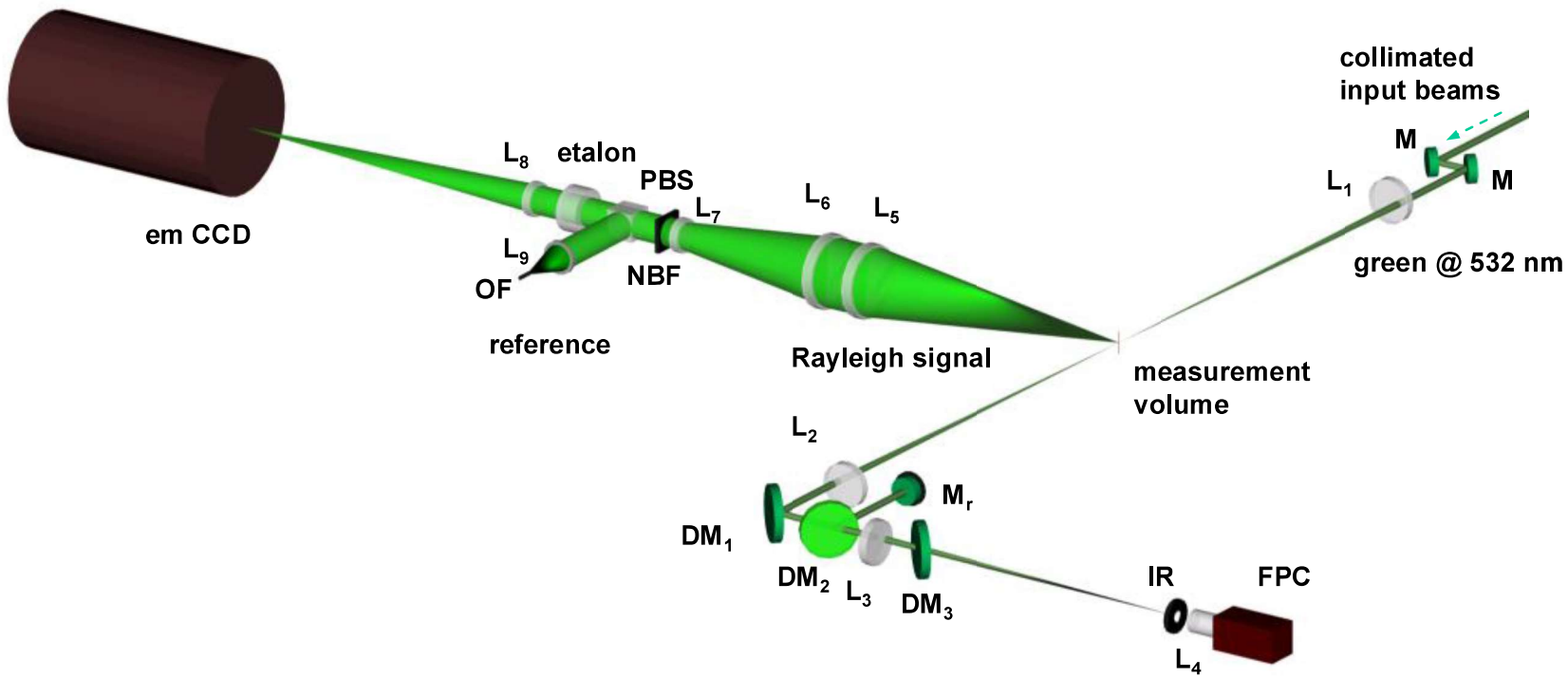

- D. Bivolaru, P. M. Danehy, R. L. Gaffney, Jr. and A. D. Cutler, "Direct-View Multi-Point Two-Component Interferometric Rayleigh Scattering Velocimeter," 46th AIAA Aerospace Sciences Meeting and Exhibit, Reno, Nevada, AIAA Paper 2008-236, January 7-10, 2008

Rayleigh Velocimetry using Fabry-Perot Etalon

one-component system

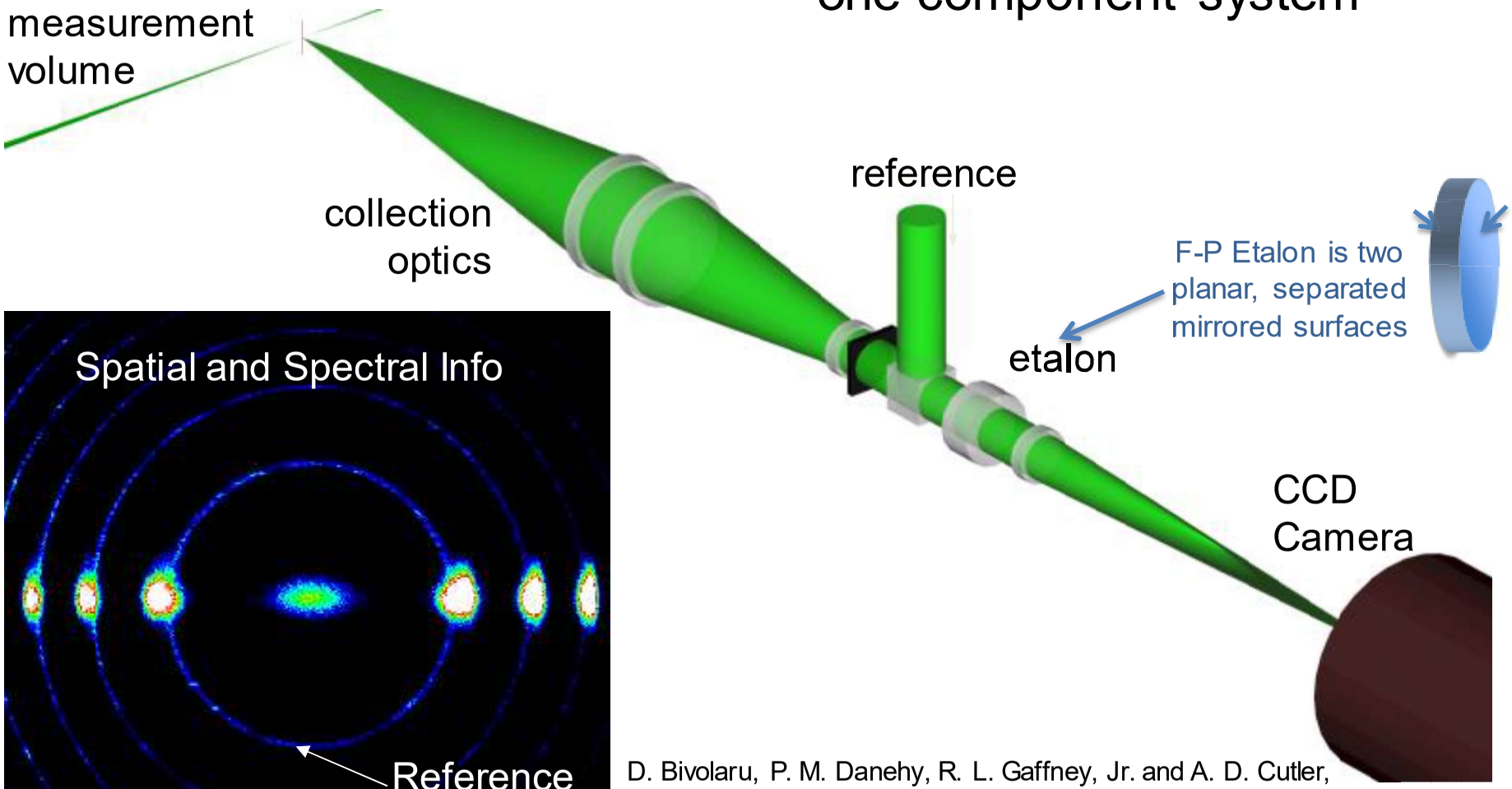

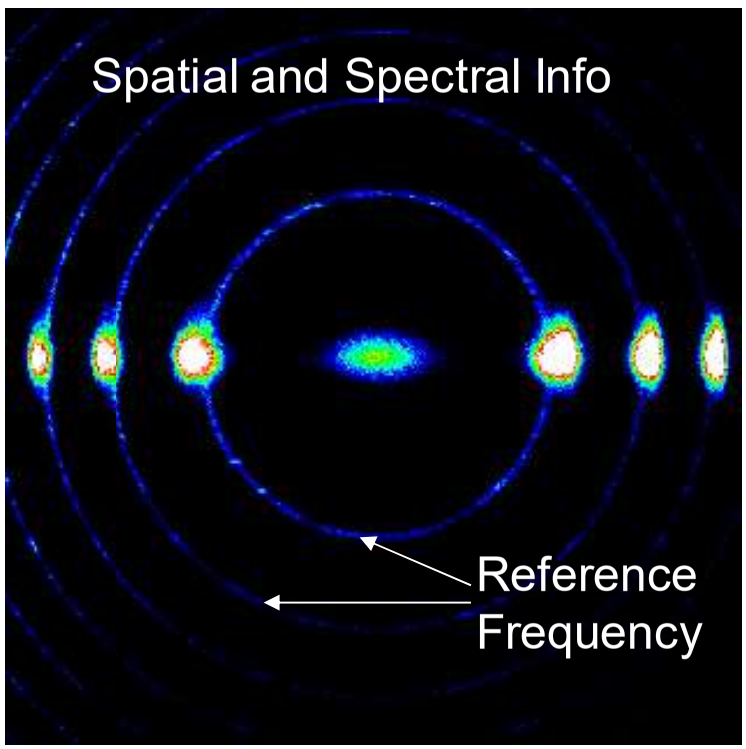

D. Bivolaru, P. M. Danehy, R. L. Gaffney, Jr. and A. D. Cutler, "Direct-View Multi-Point Two-Component Interferometric Rayleigh Scattering Velocimeter," 46th AIAA Aerospace Sciences Meeting and Exhibit, Reno, Nevada, AIAA Paper 2008-236, January 7-10, 2008

Rayleigh Scattering Image Processing

D. Bivolaru, P. M. Danehy, R. L. Gaffney, Jr. and A. D. Cutler, "Direct-View Multi-Point Two-Component Interferometric Rayleigh Scattering Velocimeter," 46th AIAA Aerospace Sciences Meeting and Exhibit, Reno, Nevada, AIAA Paper 2008-236, January 7-10, 2008

Raw image data

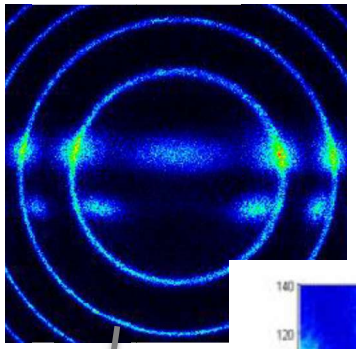

Import to Matlab®

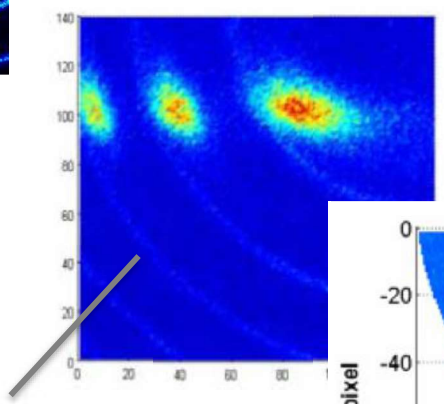

x-y to r-y transform

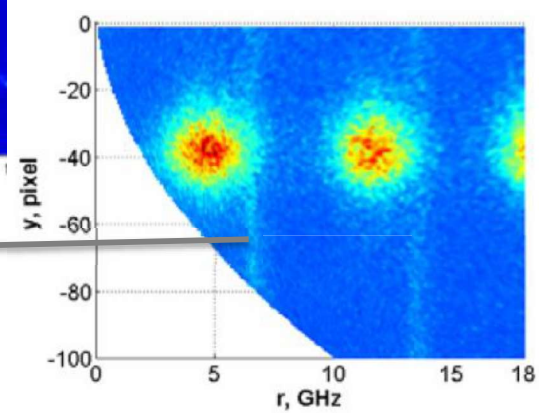

Circles provide reference
(7.5 GHz etalon)

Combine to spectrum and fit

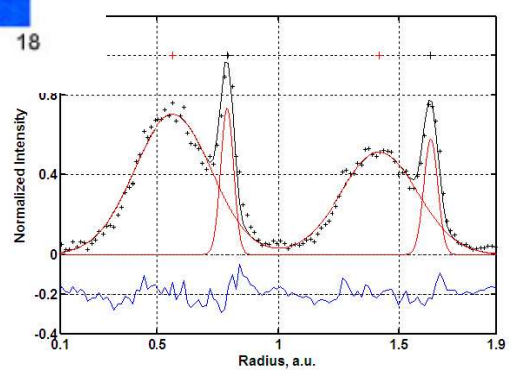

- Significant image processing is required

Rayleigh Scattering Velocity Results

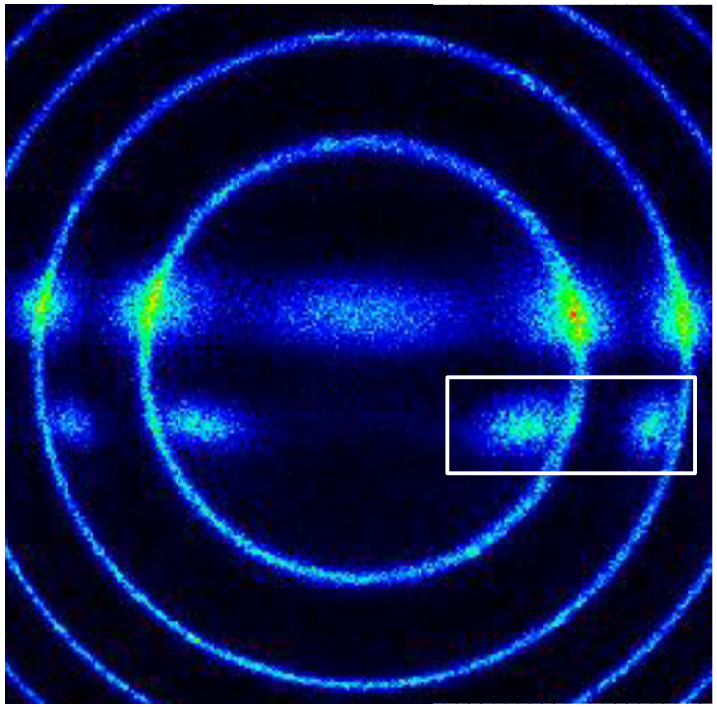

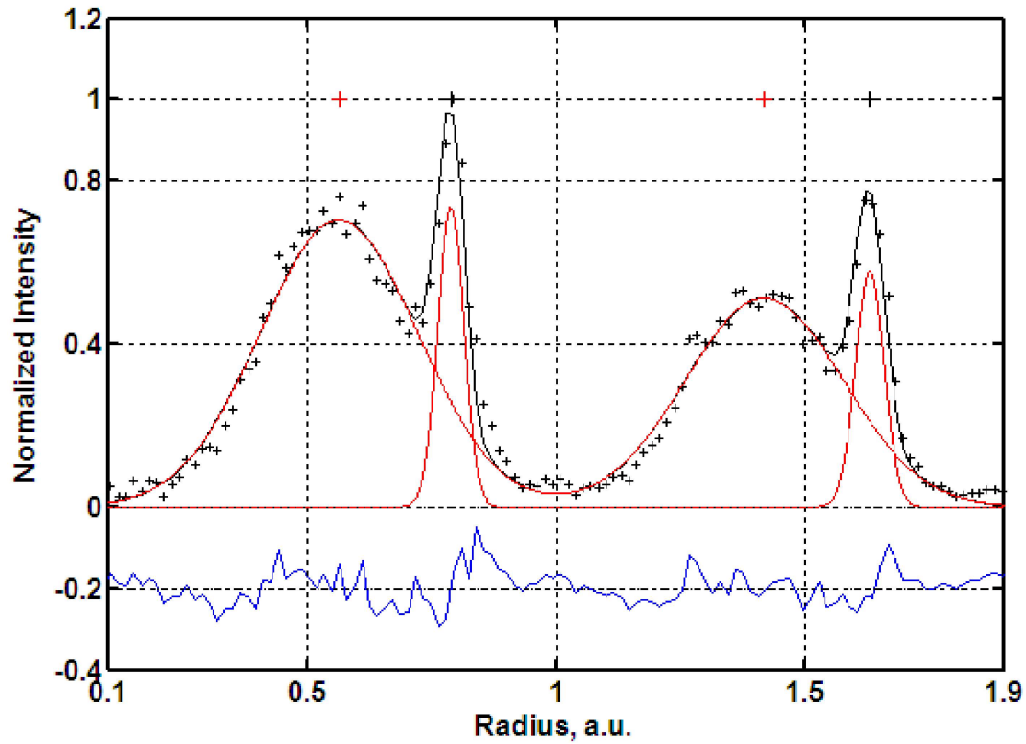

- *Rayleigh scattering in a large scale (6 cm diameter) Mach 1.6 H_2-air combustion heated jet operating at Mach 5.5 enthalpy at NASA Langley*

  Velocity precision of ~40 m/s out of 1200 m/s, (3%)
  The dynamic range of the instrument was ~3000 m/s
  - precision 1% of dynamic range

D. Bivolaru, P. M. Danehy, R. L. Gaffney, Jr. and A. D. Cutler, "Direct-View Multi-Point Two-Component Interferometric Rayleigh Scattering Velocimeter," 46th AIAA Aerospace Sciences Meeting and Exhibit, Reno, Nevada, AIAA Paper 2008-236, January 7-10, 2008

134

Rayleigh Velocimetry (I_2 filter)

- Instead of an etalon, use I_2 filter → 2D imaging

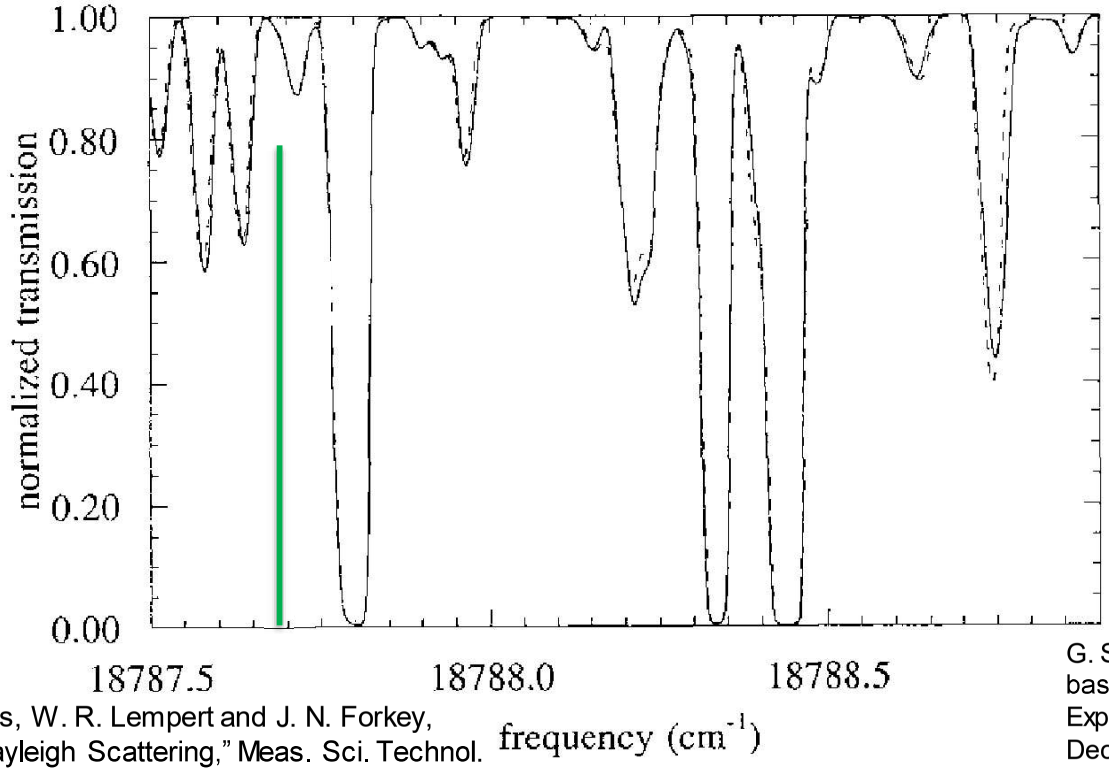

I_2 absorption near 532 nm

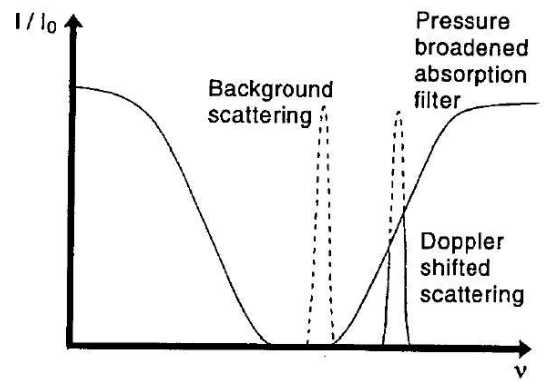

R. B. Miles, W. R. Lempert and J. N. Forkey, "Laser Rayleigh Scattering," Meas. Sci. Technol. p. R33-R51, v.12, 2001

G. S. Elliott, M. Samimy, S. A. Arnette "A molecular filter based velocimetry technique for high speed flows," Experiments in Fluids, Volume 18, Issue 1-2, pp 107-118, December 1994

- Gas cell, filled with low-pressure N_2 plus some I_2 crystals; control temperature to determine absorption
- Scan Nd:YAG laser frequency (or fixed)

Rayleigh Imaging of T, V, ρ (or P)

- Direct YAG laser sheet into a Mach 2 jet

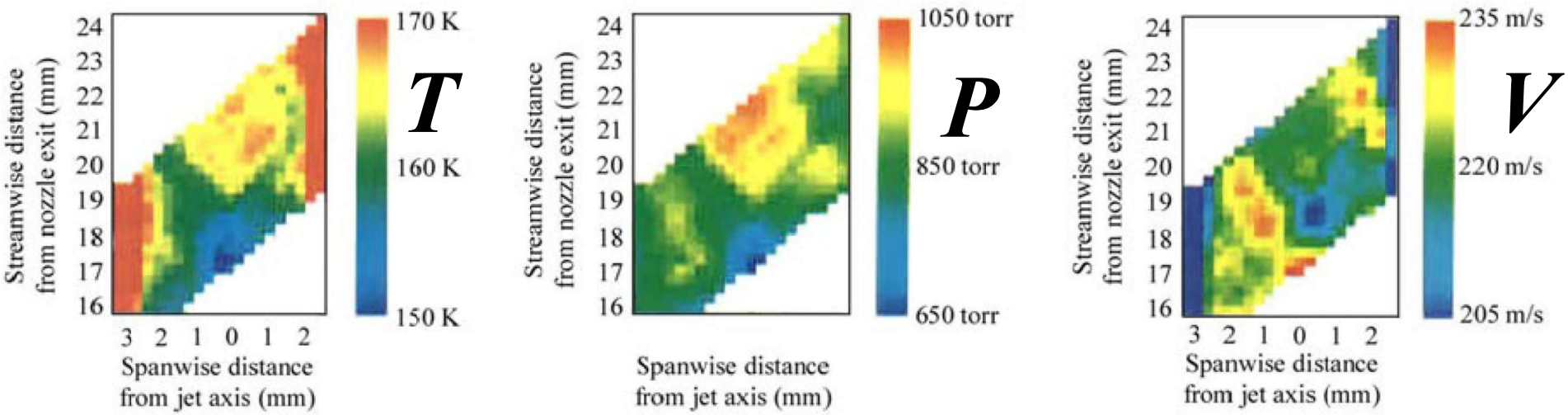

R. B. Miles, W. R. Lempert and J. N. Forkey, "Laser Rayleigh Scattering," Meas. Sci. Technol. p. R33-R51, v.12, 2001

- Scanned laser frequency, determine T, V, ρ (report P) based on measured spectrum at each pixel
- Same method can be used for velocimetry from particles (usually fixed frequency, multiple detection angles)
  - Planar Doppler Velocimetry (PDV) or Doppler Global Velocimetry (DGV)

Rayleigh Scattering: ρ

- Rayleigh scattering has a spectrum:
  - Sensitive to T, V, ρ
  - Prior examples used Fabry Perot Etalon or I_2 cell to observe spectrum
  - These devices reject signal, making them less sensitive detectors of ρ.
- Collect *all* of the scattering
  - Less equipment/less setup/simpler
  - Bigger signal
  - Can do single point or imaging
  - Only sensitive to ρ.
    - (If you know P and composition you can convert ρ to T.)

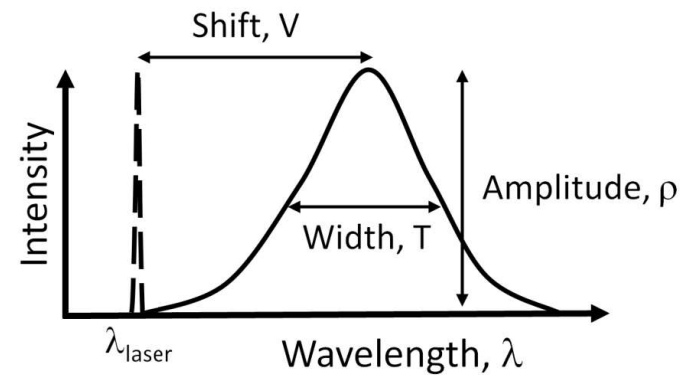

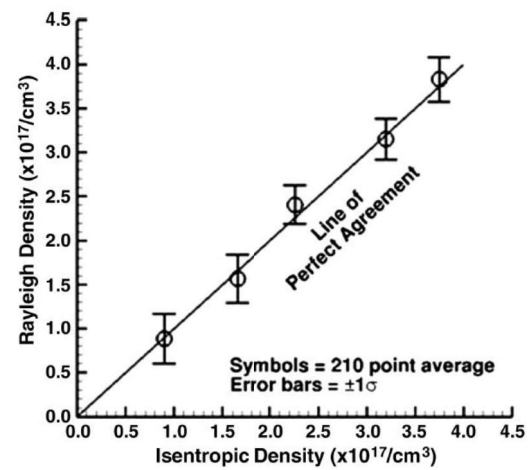

Using a UV laser (e.g. ArF at 193 nm) allows measurements to be made at low pressures (e.g. 1/300 atmospheric density)

Balla, R. Jeffrey, and Joel L. Everhart. "Rayleigh scattering density measurements, cluster theory, and nucleation calculations at Mach 10." AIAA Journal 50, no. 3 (2012): 698-707.

Raman Spectroscopy

- Raman spectrum obtained in a CH_4-air flame:
  - Average of 500 pulses using stretched 0.5 J/pulse, 532 nm
    - Stretch 10 ns pulse to 500 ns to avoid laser-induced breakdown

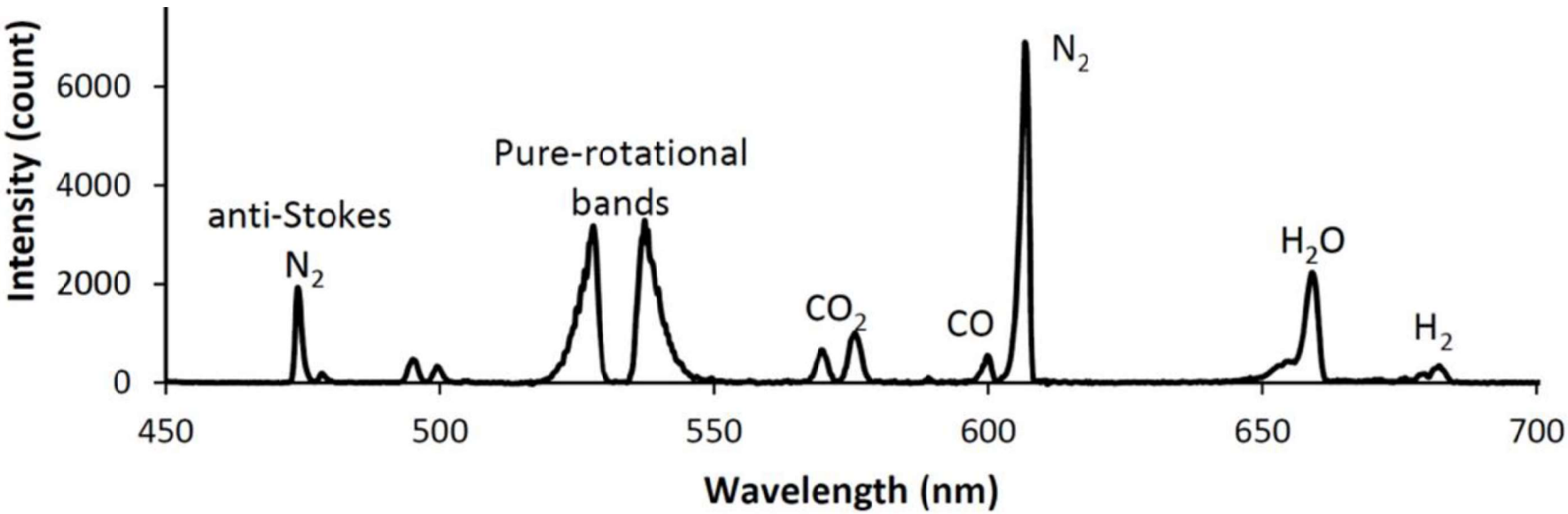

Figure courtesy of Jun Kojima, NASA Glenn Research Center (Jun.J.Kojima@nasa.gov)

- Can measure species (N_2, CO, CO_2, H_2, H_2O) from such spectra &temperature from Stokes/anti-Stokes

Raman Concentration Measurement

(and Rayleigh Temperature and LIF concentration)

- Example of Raman concentration measurements in a subsonic turbulent CH_4/air flame at Sandia National Laboratories, California
  - 4 Nd:YAG lasers at 532 nm to produce 1.8 Joules/pulse, focused to a point

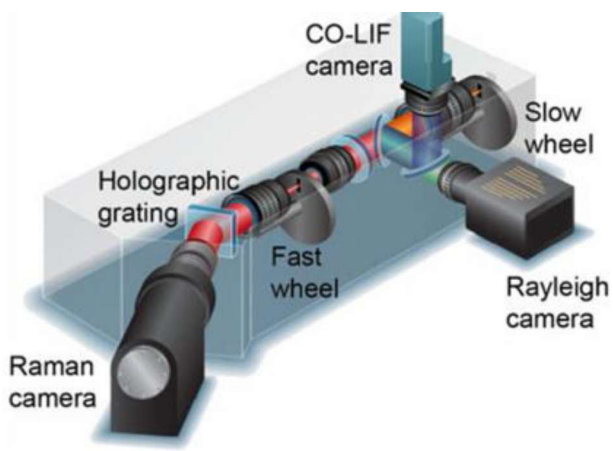

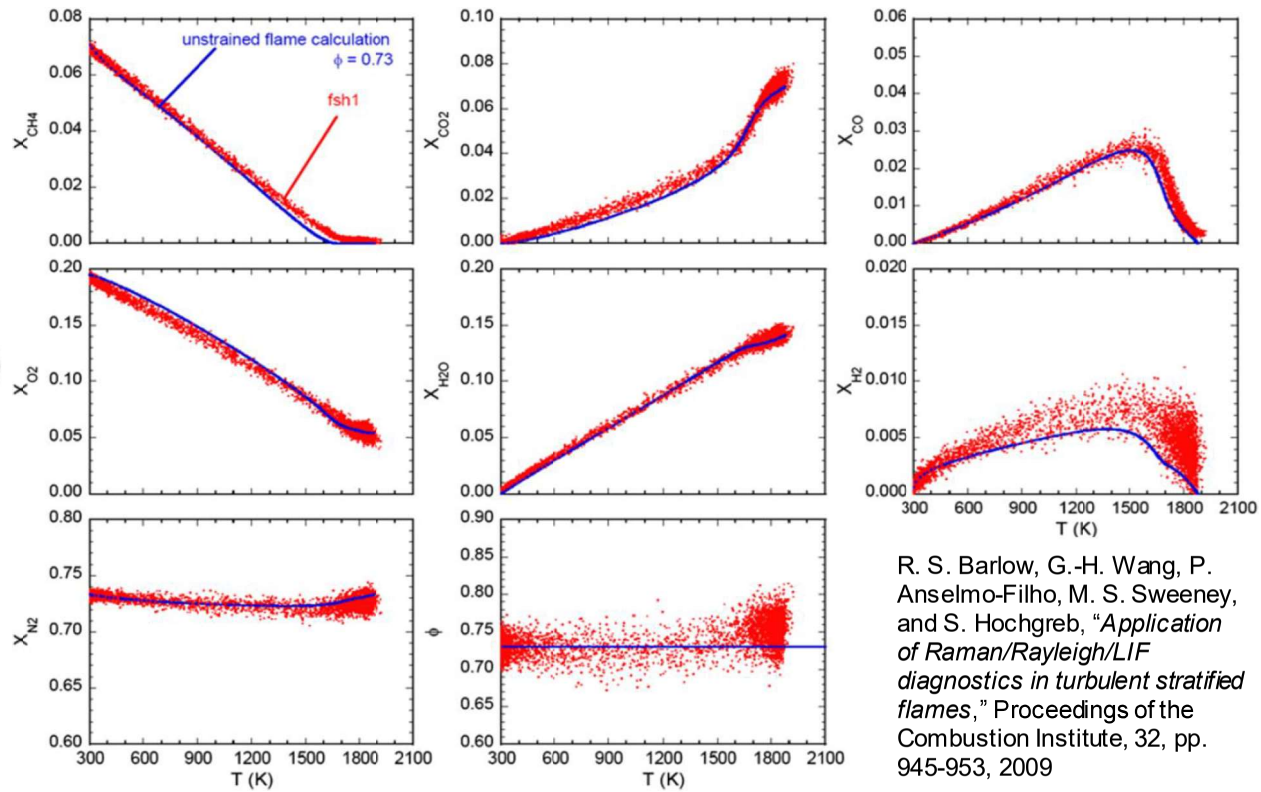

χ_i precision ~0.7% to 7.5%
T precision ~0.75%

R. S. Barlow, G.-H. Wang, P. Anselmo-Filho, M. S. Sweeney, and S. Hochgreb, "*Application of Raman/Rayleigh/LIF diagnostics in turbulent stratified flames*," Proceedings of the Combustion Institute, 32, pp. 945-953, 2009

- Raman/Rayleigh/LIF line imaging (~10 pixels / mm along the 6-mm-long probe volume)
  - N_2, O_2, CH_4, CO_2, H_2O and H_2 from Raman, CO from 2 photon LIF
  - Temperature from Rayleigh density measurement (idea gas law)

Raman Temperature Measurement

- Several ways to measure temperature with Raman
  - none as precise as CARS (3%)

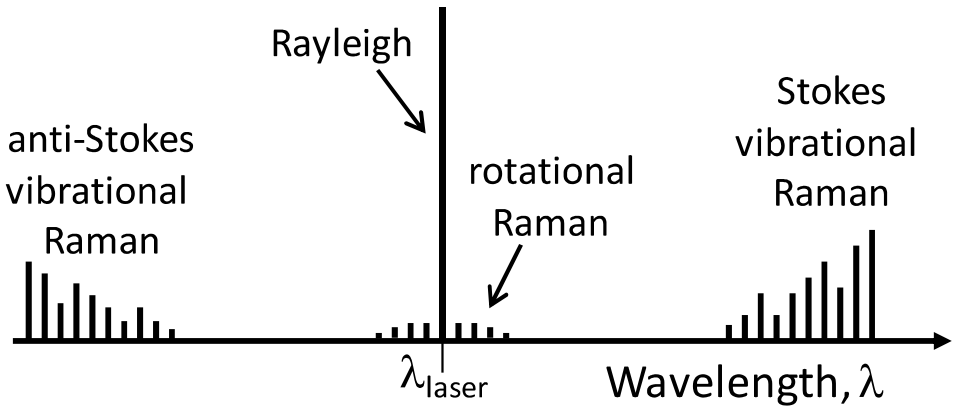

- <u>Rotational Temperature</u> from pure-rotational Raman (see Kojima, 2008)
- <u>Vibrational temperature</u> measurements
  - Only good above 700 K
  - Stokes / anti-Stokes vibrational Raman
    - Low resolution, so can measure concentrations at same time
    - ~20% precision in measurements along a line (Wehrmeyer, 1996)
  - Spectrally resolved vibrational band (Sharma et al, 1993)

Raman Temperature Measurement

- Raman temperature measurement from spectrally resolved vibrational N_2 band.
  - Excited with KrF Excimer laser 0.25 J at 248 nm (25 ns pulse)

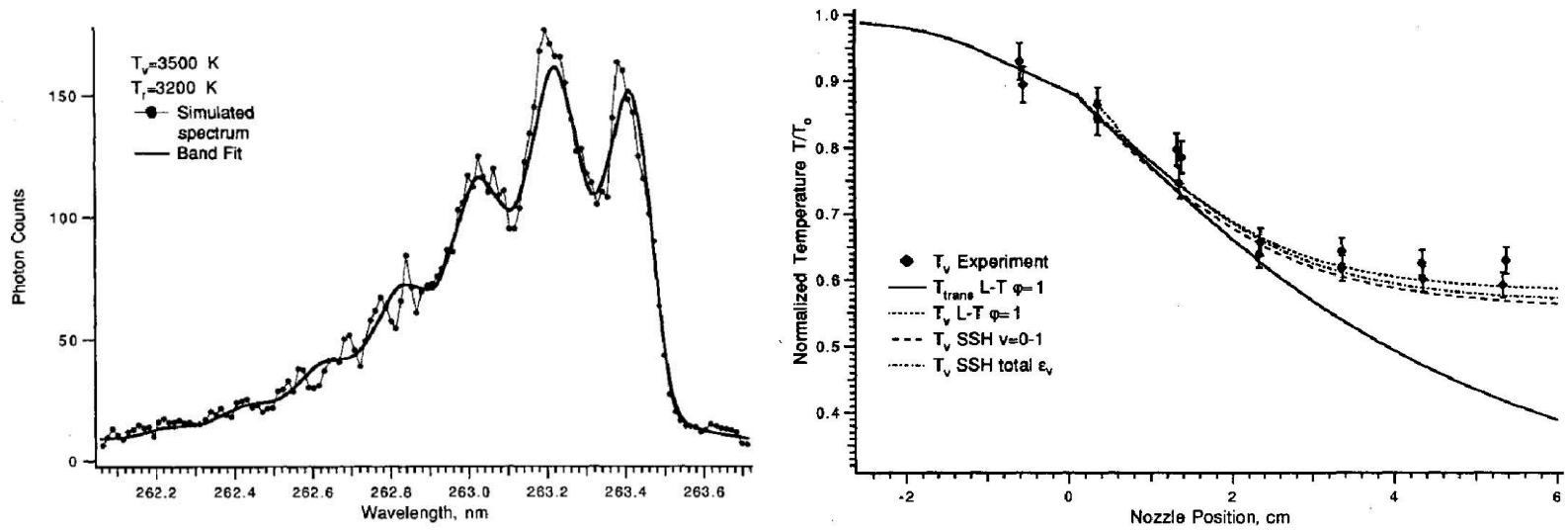

S. P. Sharma, S. M. Ruffin, W. D. Gillespie and S. A. Meyer, "Vibrational Relaxation Measurements in an Expanding Flow Using Spontaneous Raman Scattering," J. of Thermophys. and Heat Trans. Vol. 7, No. 4, Oct.-Dec. 1993

  - Single shot precision ~5% (not explicitly stated)
    - More precise than Stokes/anti-Stokes but cannot measure species concentrations with same instrument.

Advantages and Disadvantages: Rayleigh & Raman

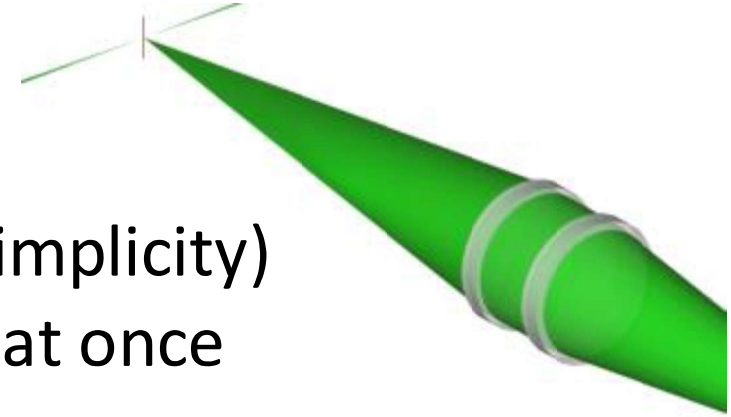

- Advantages:
  - No seeding required
  - Only one color of laser used (simplicity)
  - Multiple properties measured at once
    - T, V, ρ for Rayleigh
    - T, many species for Raman
    - Can do Raman and Rayleigh together and with LIF
- Disadvantages:
  - Weak signal:
    - Requires very high power laser
      - stretched to avoid laser induced breakdown
    - Requires large windows, big, close collection optics
    - Usually singe point or line measurements
  - Temperature less accurate & precise than CARS

Doppler Global Velocimetry

- Velocity Measurement based on the Doppler Shift.
  - Mie Scattering.
  - Doppler shift is directly proportional to particle velocity.
- Each view measures 3 components of velocity
  - Unit vector bisects camera and laser directions.
  - 3 views are required to calculate orthogonal velocity components.
- An atomic/molecular-vapor cell is used to determine the frequency of light at each pixel.
  - Laser tuned to the midpoint of an absorption feature.
  - Darker pixels indicate higher speed.
  - Brighter pixels indicate lower speed.
  - Dynamic range limited to span of absorption feature.
    - Typically 500 MHz corresponding to 350 m/s
- Velocity Uncertainty
  - $\pm$2-3 m/s typically
  - $\pm$0.5 m/s optimally

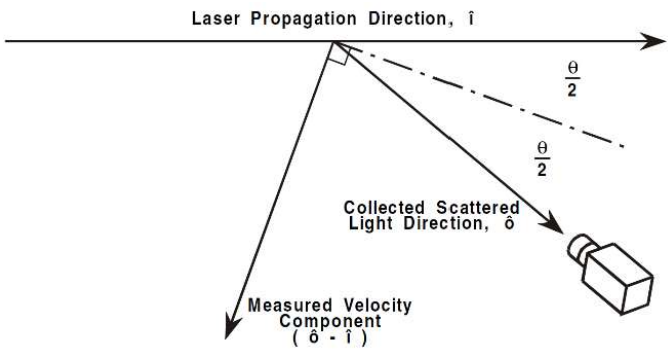

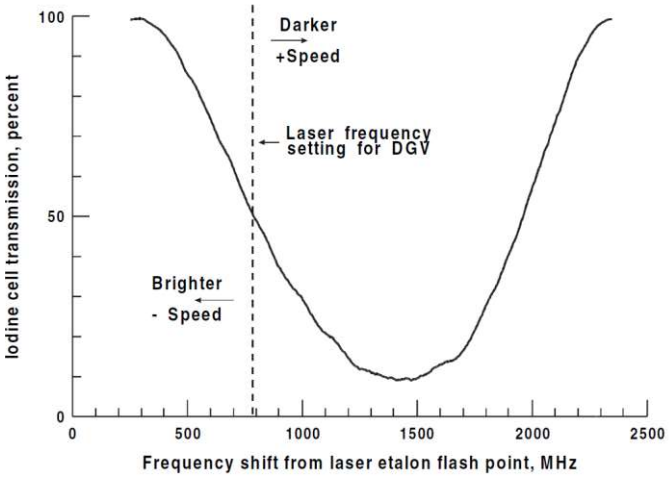

Meyers, J. F., Lee, J. W., and Schwartz, R. J., "Characterization of measurement error sources in Doppler global velocimetry,"

Measurement Science and Technology, vol 12, 2001

Doppler Global Velocimetry

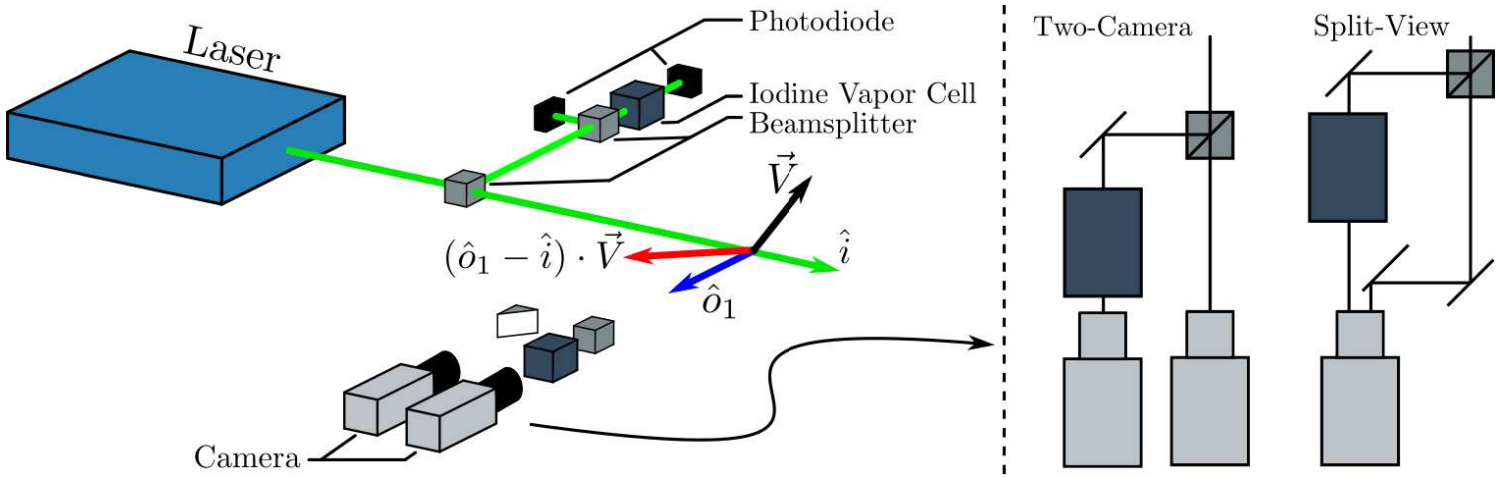

Typical experimental configuration includes:

- Laser frequency monitor or Laser frequency lock
- Reference/Signal camera system.
  - Two-camera system (High Resolution, Low Complexity)
  - Split-view system (Low cost)
- Reference – Signal view mapping is large source of error:
  - Beam splitter ratio (variations of 3-5% can lead to ± 7 m/s error)
  - Image alignment (0.1 pixel leads to ± 5m/s error)

Advantages to DGV

- Does not need to image individual particles
  - Large fields of view
  - Small particles
- High resolution
  - 1 pixel = 1 velocity measurement.

Disadvantages

- Large number of views/optical access
- Optical complexity for cameras

Doppler Global Velocimetry

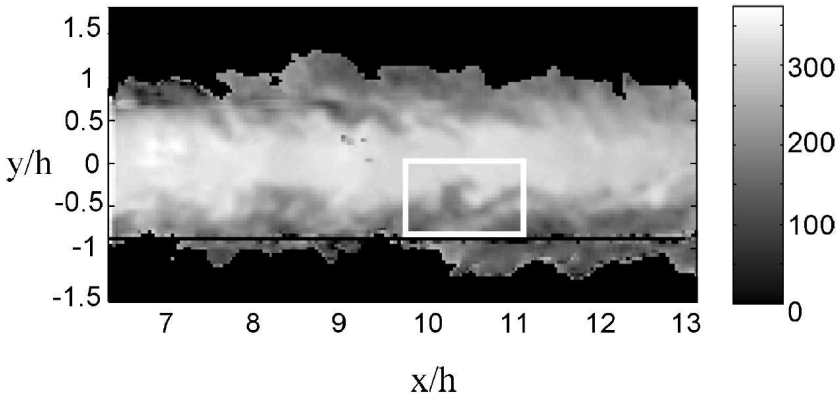

Thurow, B. S., Jiang, N., Lempert, W. R., and Samimy, M., "Development of Megarhertz-Rate Planar Doppler Velocimetry for High-Speed Flows," *AIAA Journal*, vol 43, 2005.

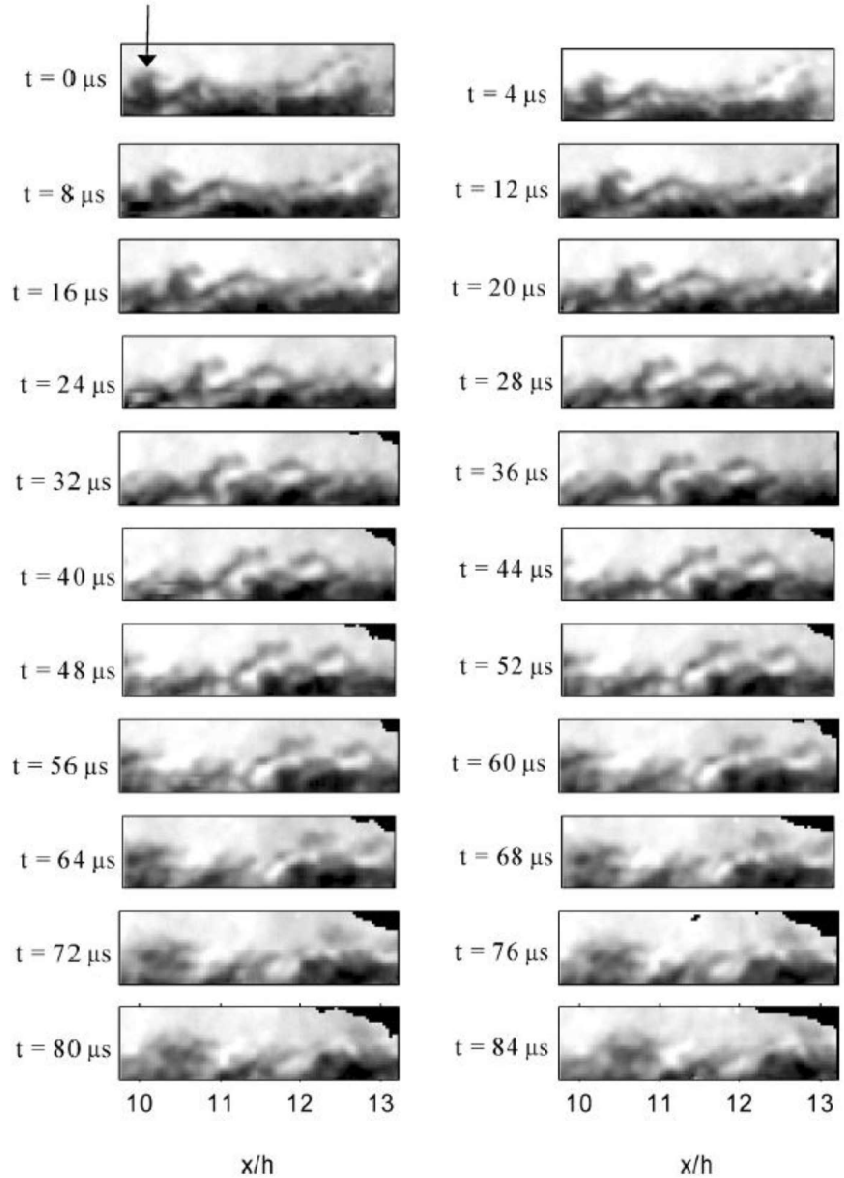

- Mach 2.0 jet
  - Rectangular jet (38.1 x 12.7 mm)
  - Acetone particles (~50 nm)
- Pulse-Burst Laser
  - 28 pulses/images per burst
  - 250 kHz
  - 9 mJ/pulse
- Estimated total error of 13 m/s (4%)

Advantages / Disadvantages of DGV

- Advantages
  - High signal levels
  - Large fields of view (compared to Rayleigh)
  - Sensitive to velocity: High precision possible

- Disadvantages
  - Particles / fog required
  - Signal and laser same wavelength: interference
  - Only measure 1 parameter (velocity)
  - Limited dynamic range (cross-correlation DGV [Lowe, VT] extends this)

Coherent anti-Stokes Raman Spectroscopy (CARS)

Paul Danehy, *NASA Langley Research Center, Virginia, USA*
Chloe Dedic*, University of Virginia, Charlottesville, VA, USA*
Andrew Cutler, *The George Washington University, USA*

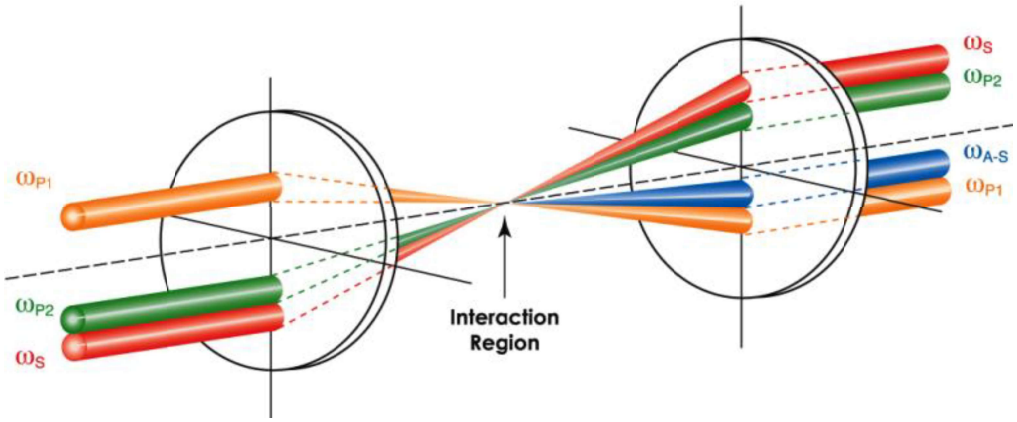

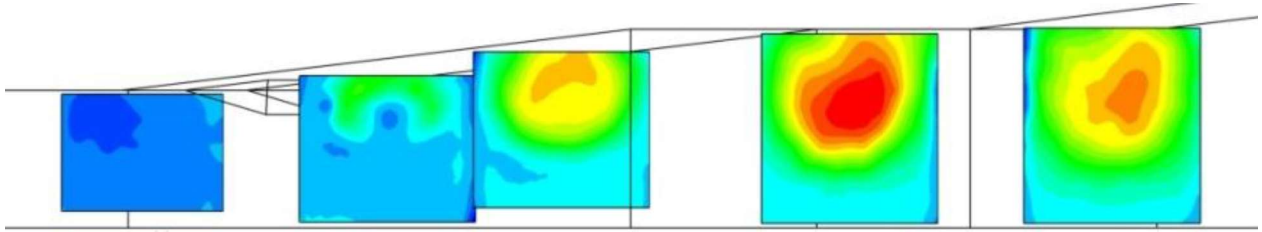

Polarization

When an electric field is applied to a medium…
- Displacement in electron clouds around atom/molecules
- Electric dipole is induced (separation of charges)

Polarization: sum of the dipole moments per unit volume

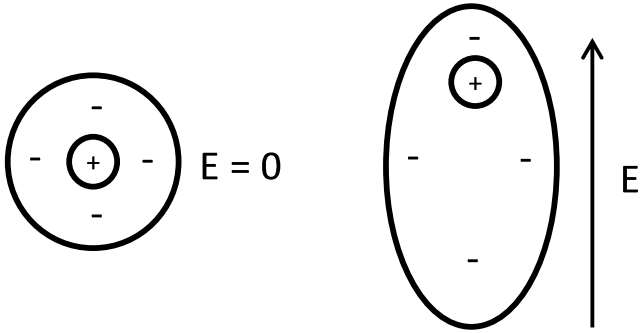

Electric displacement:

$$\mathbf{D} = \epsilon \mathbf{E}$$

$$\mathbf{D} = \epsilon_0 \mathbf{E} + \mathbf{P}$$

ε: electric permittivity of a medium

Polarization:

$$\mathbf{P} = \epsilon_0 \chi^{(1)} \mathbf{E} + \text{higher-order terms}$$

Electric polarization in the medium is different than the polarization of the electric field!

Polarizability: how easily electrons can be moved in response to the applied electric field

Polarization

Expanding the macroscopic polarization to consider higher-order terms:

$$P(\omega) = \epsilon_0 \chi^{(1)}(\omega) E_1(\omega_1) + \epsilon_0 \chi^{(2)}(\omega) E_1(\omega_1) E_2(\omega_2) + \epsilon_0 \chi^{(3)}(\omega) E_1(\omega_1) E_2(\omega_2) E_3(\omega_3) + \ldots$$

- Total polarization induced has a nonlinear dependence on the incoming field amplitudes in the higher order terms
- Connection to the index of refraction

Second-order polarization: only in anisotropic media (crystal)
- Second harmonic generation
- Sum-frequency or difference-frequency mixing

Third-order polarization: in isotropic medium (glass, gases)
- Kerr effect (intense electric field modifies index of refraction)
- four-wave mixing, etc.

$$\vec{P}^{(3)}(t, \vec{r}) = \epsilon_0 \chi^{(3)} E_1(t, \vec{r}) E_2(t, \vec{r}) E_3(t, \vec{r})$$

Polarization

Considering linear Raman scattering versus stimulated Raman scattering/CARS…

Instead of relying on a change in polarizability from a naturally occurring vibration/rotation, we can drive the change in polarizability (drive the coherence) using two electric fields, scatter from this prepared coherence with the third

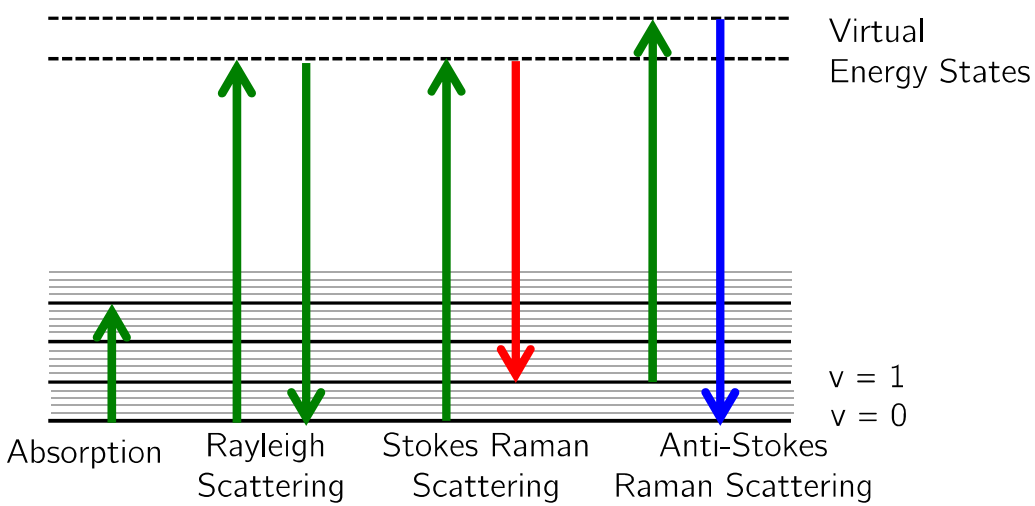

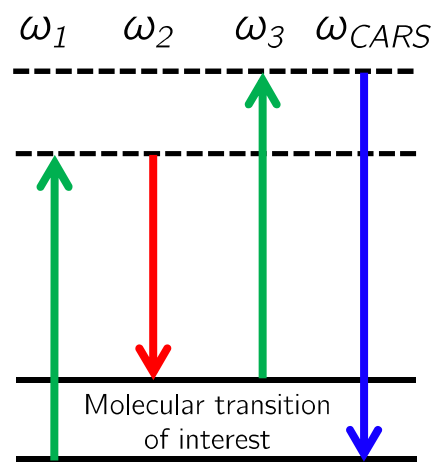

"Raman-active":
Change in polarizability

Thus, three waves incident on a medium, medium response (phased array of oscillators) produces a fourth wave radiated by the induced nonlinear polarization

Induced electric field

Full representation of an electric field:

$$E(\mathbf{r}, t) = E(t)e^{i(\mathbf{kr} - \omega_0 t + \phi)}$$

For the induced molecular dipoles to build up constructively, the generated electric field must:

1) Satisfy conservation of energy
2) Propagate in-phase and in the same direction (conservation of momentum)

Conservation of energy

- Conserving photon energy

$$\omega_p - \omega_s + \omega_{probe} - \omega_{CARS} = 0.$$

Plus or minus

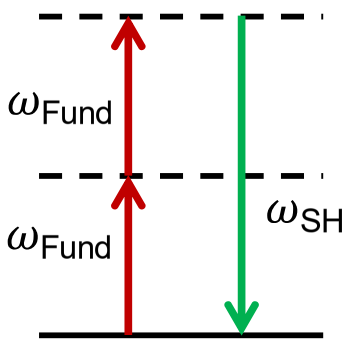

Second Harmonic Generation

ω_{SH} = 2*$\omega_{Fund.}$

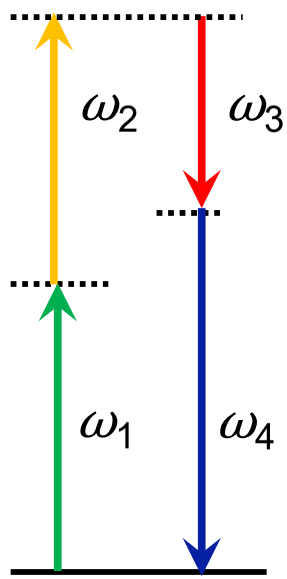

Nonresonant 4-wave mixing

$$\omega_1 + \omega_2 - \omega_3 - \omega_4 = 0$$

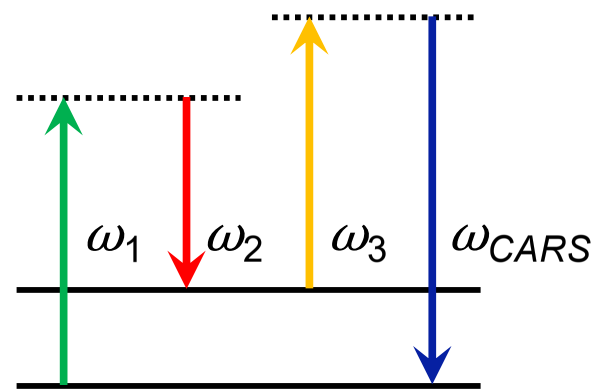

CARS

$$\omega_1 - \omega_2 + \omega_3 - \omega_{CARS} = 0$$

Conservation of momentum

- The induced molecular dipoles must be “in-phase”
- All have to propagate in the same direction or they destructively interfere
- Direction is dictated by “phase-matching”
- Conserving photon momentum

$$\vec{k}_1 + \vec{k}_2 - \vec{k}_3 - \vec{k}_4 = 0$$

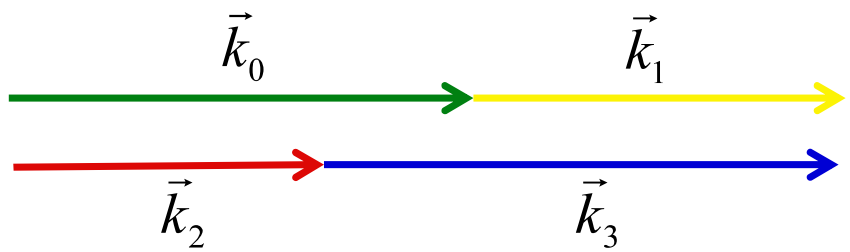

Collinear Phase-Matching

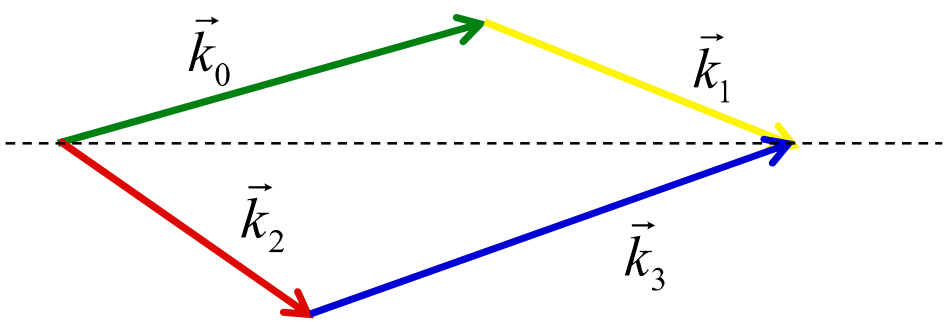

Planar Phase-Matching

Conservation of momentum: phase matching

- *Ensuring that the light wavefronts 'match up'.*

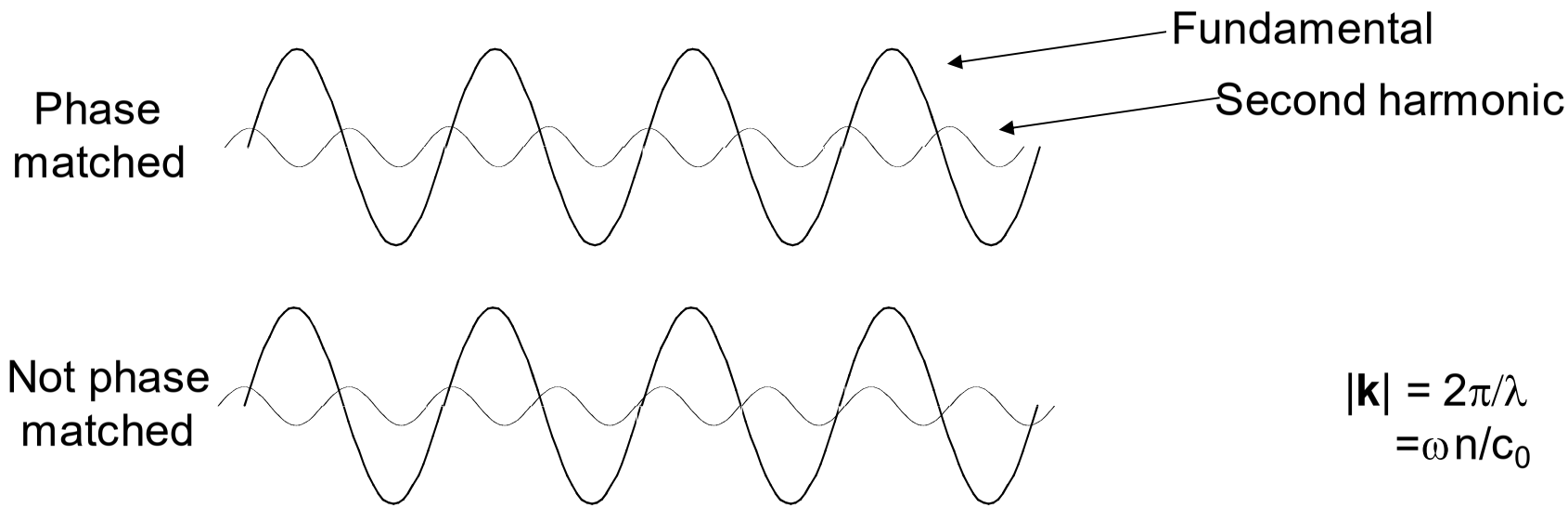

$|\mathbf{k}| = 2\pi/\lambda$
$= \omega n/c_0$

- Dispersion causes deconstructive interference
- New photons generated are out of phase with previous ones: resulting in loss

What is CARS?

Broadband N_2 CARS

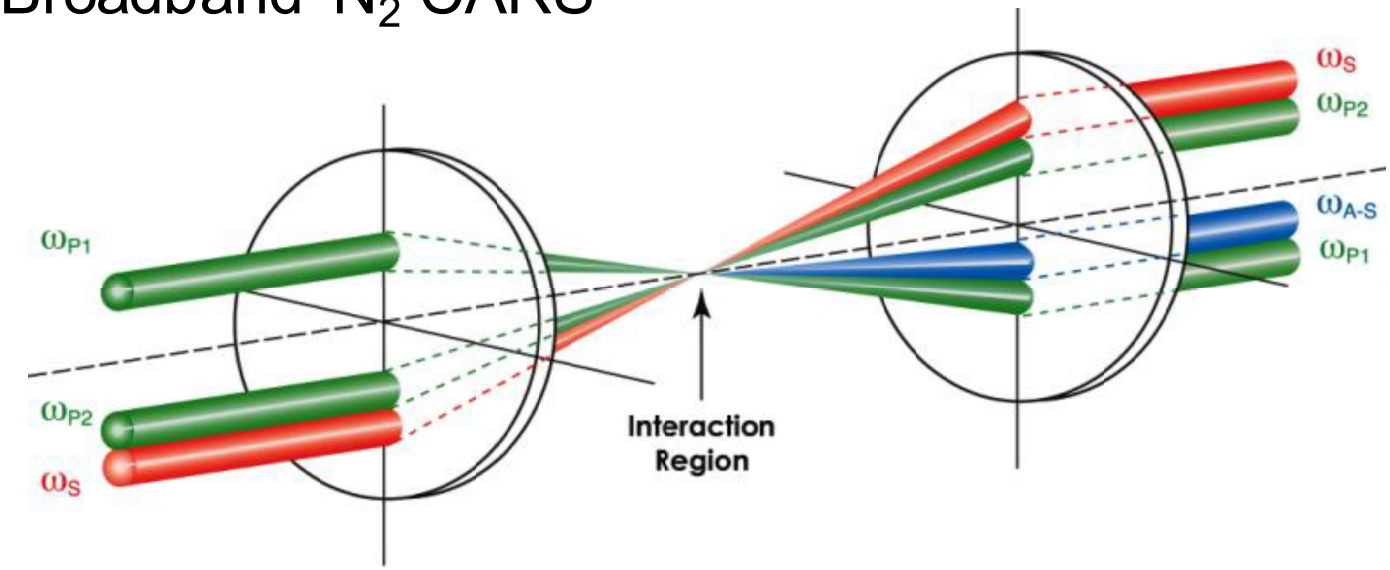

Spectrally-broad red beam +
Spectrally-narrow green beams =
Single-shot blue CARS spectrum

$$I_{CARS}(\omega_4) \propto |P^{(3)}_{res}(\omega_4)|^2 = |\epsilon_0 \chi^{(3)}_{CARS} E_1(\omega_1) E_2(\omega_2) E_3(\omega_3)|^2$$

CARS Energy Level Diagram (conservation of energy)

- 3 laser pulses: 2 Green (532 nm) and 1 Red (607 nm)
  - Frequency difference between Green and Red Probes N_2 vibrational Raman Shift

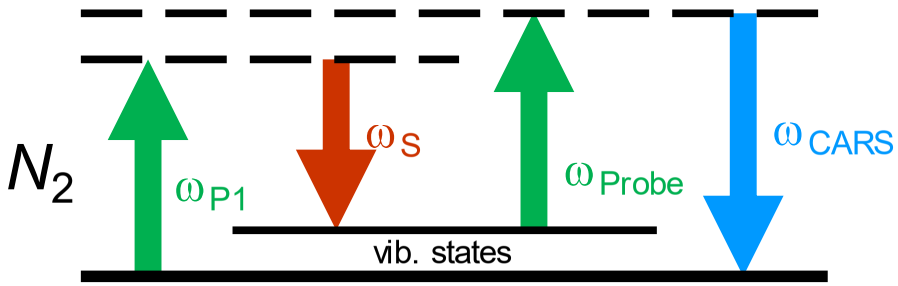

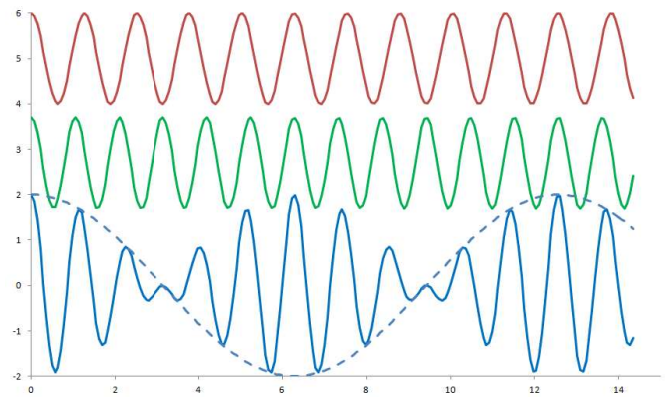

- Result: CARS signal beam at 473 nm.
  - Spatially, spectrally, temporally filter this signal
    - Good technique for luminous flows
  - Send to spectrometer equipped with CCD camera
  - Measured CARS spectra can be compared to a library of theoretical spectra on a single-shot basis (10 ns)

CARS Temperature Sensitivity

Boltzmann Distribution

$$\Delta\rho_{i\to f} = \frac{g_f}{\sum_m g_m e^{\frac{-E_m}{k_B T}}}\left[e^{\frac{-E_i}{k_B T}} - e^{\frac{-E_f}{k_B T}}\right]$$

S-branch (Rotational CARS)

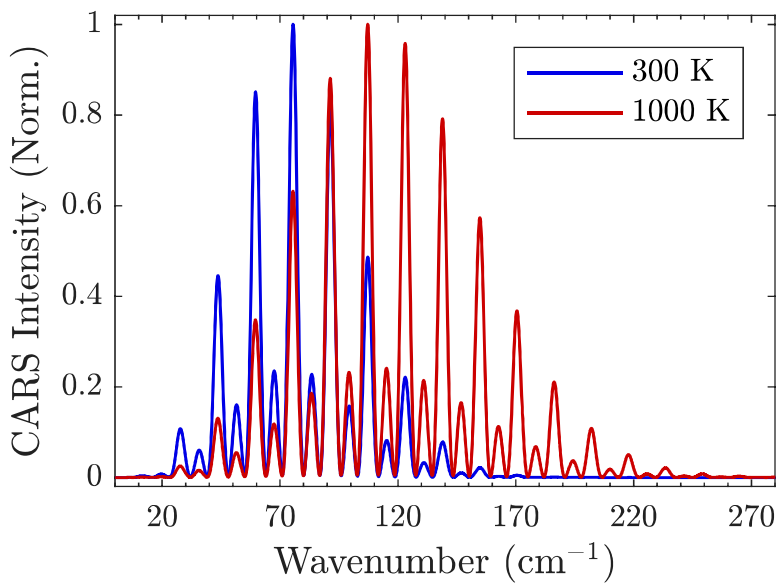

Q-branch (Rovibrational CARS)

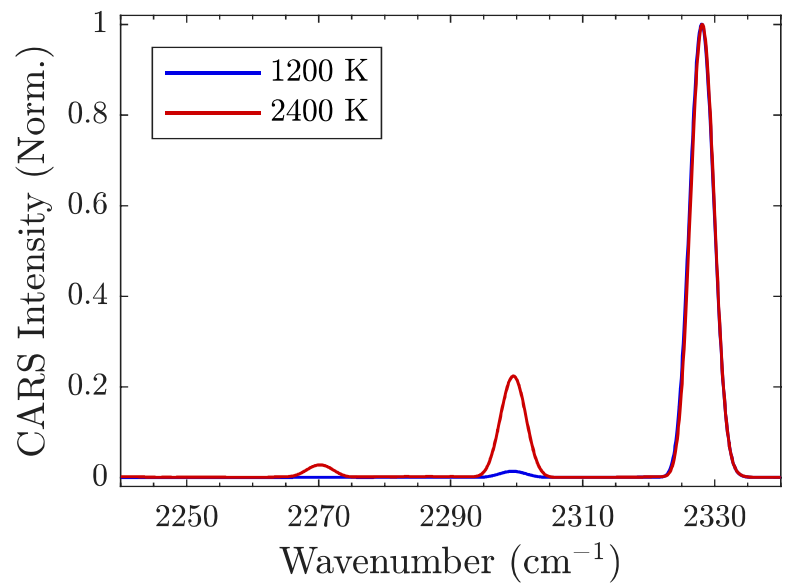

Concentration Sensitivity

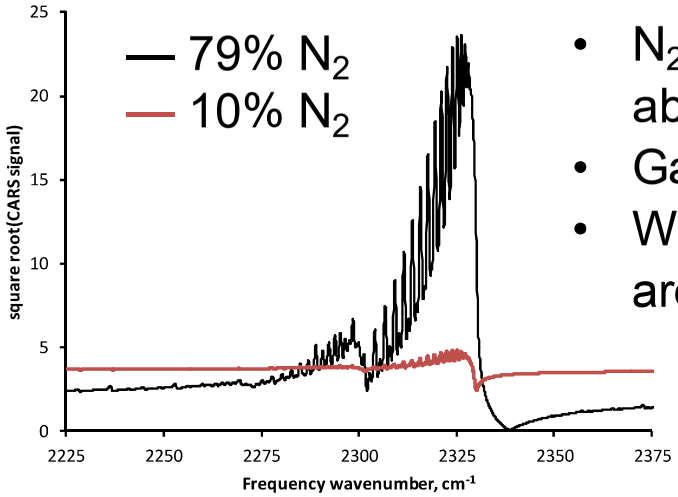

- N_2 common target because it is relatively inert and abundant in the atmosphere
- Gas composition impacts resonant and nonresonant
- When Raman frequencies from multiple molecules are simultaneously excited…

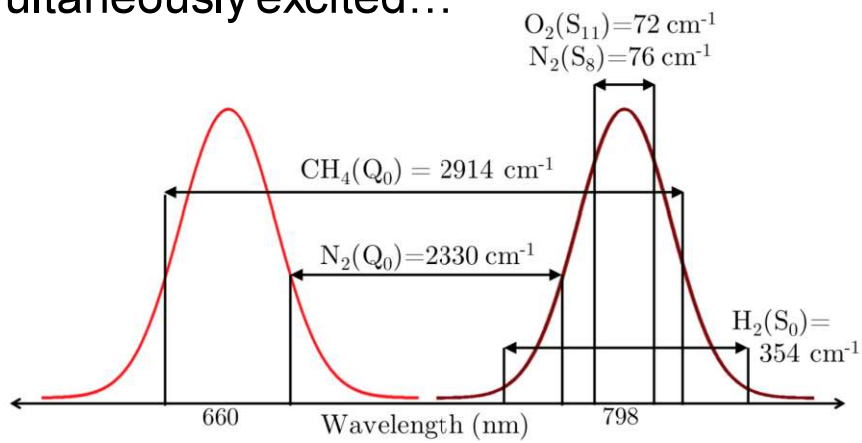

Dedic, Miller, Meyer, *Opt. Lett.*, 2014

Spectrally **isolated** transitions

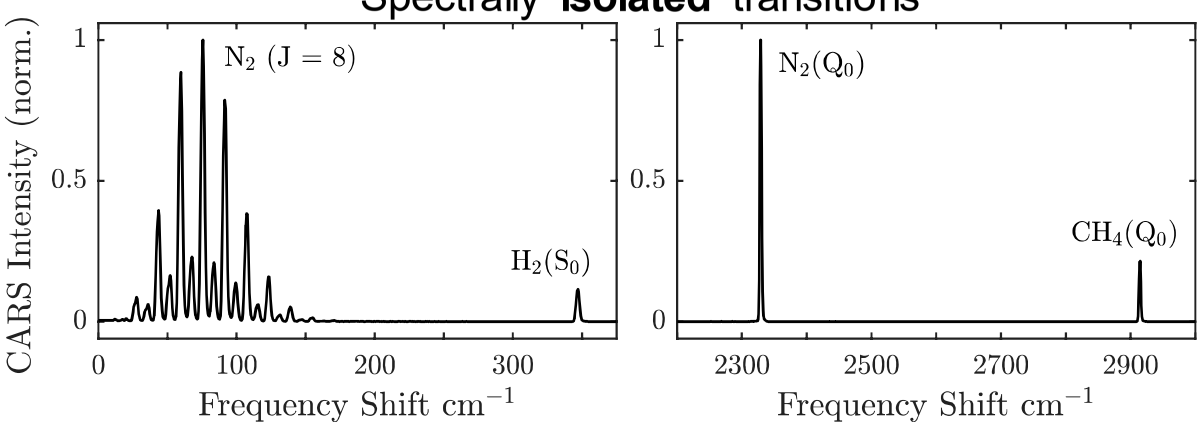

Spectrally **overlapping** transitions

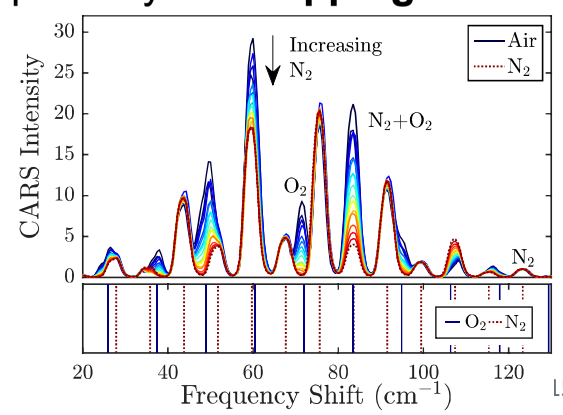

Dual-Pump ns CARS: N_2, O_2, H_2, …

- (ns) Pump and probe pulses can reverse rolls to access more species

Green "pump" excites **N_2**
Raman Shift (2330 cm^{-1})

Yellow "pump" excites **O_2**
Raman Shift (1555 cm^{-1})

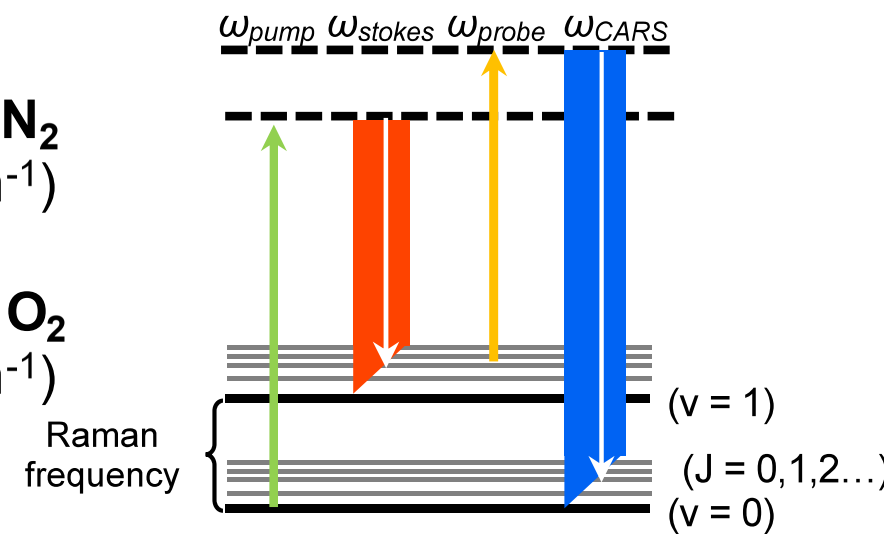

- Result: Two different spectral regions of Raman Shift appear coincident in the 490 nm CARS beam.
  - Depending on gas environment, species other than N_2 and O_2 appear (H_2 pure rotational, …)

O'Byrne et al., AIAA Journal, 2007
Weikl et al., App. Opt., 2009
Tedder et al, Appl. Opt., 2010
Cutler et al., J. Prop. Power, 2014

Typical Dual-Pump CARS Spectra and Fits

Single-shot spectra (black) shown with best fit (red)

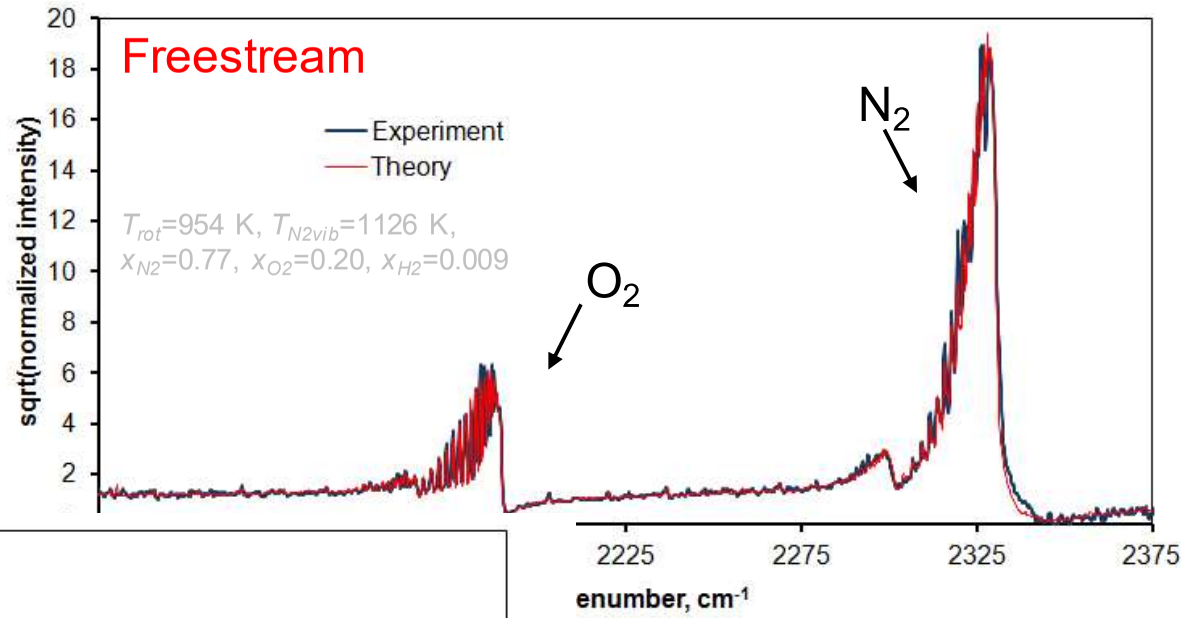

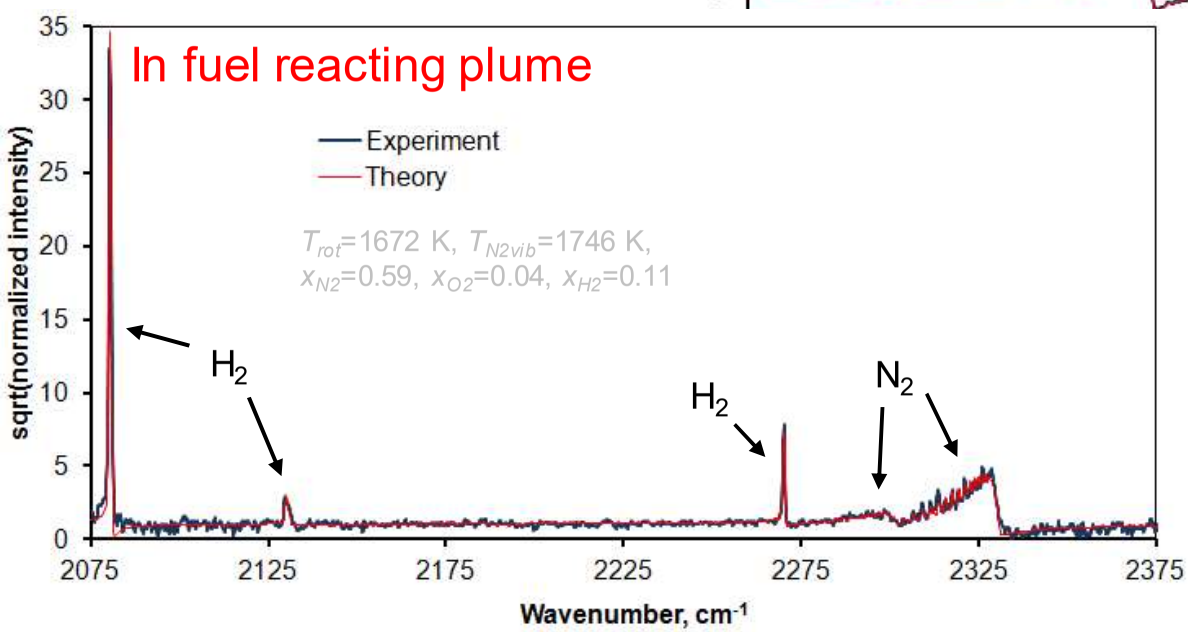

Measurement obtained:

- In UVa Scramjet (Conf C)
- φ=0.18, Plane 2, z/H=0
- in10 ns (instantaneous)
- at 20 Hz repetition rate
- Measurement volume = 1.7 x 0.2 x 0.2 mm^3

CARS Experimental setup

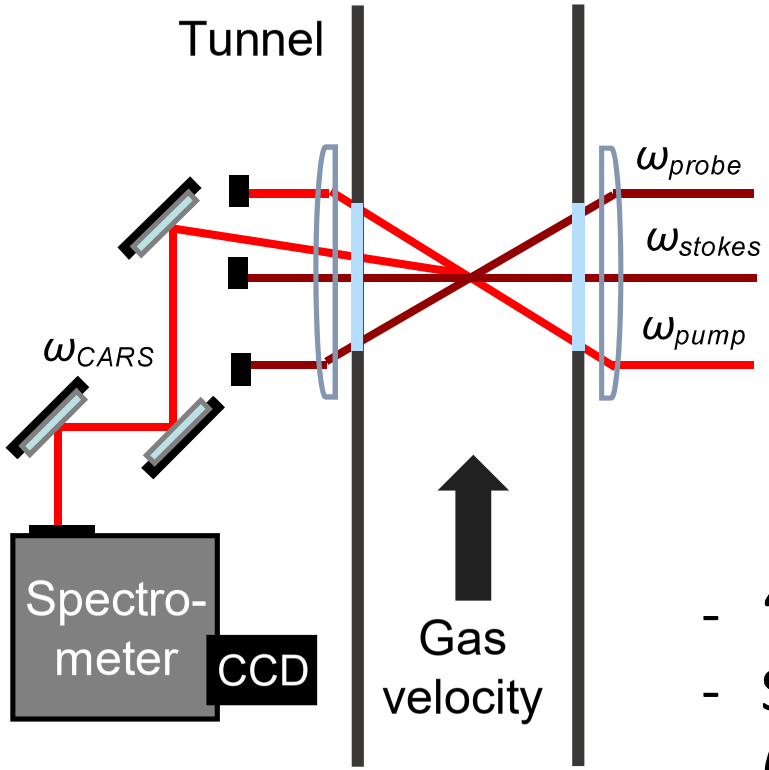

- "Pitch and catch" geometry
- Spatially-resolved measurement (ellipsoidal probe volume)
- Single-laser-shot temporal precision ~ 10 ps – 10 ns

CARS Phase Matching Geometries

Choice of phase matching configuration impacts ***spatial resolution***…

- Collinear CARS:
  - Poor spatial resolution (2-10 mm)

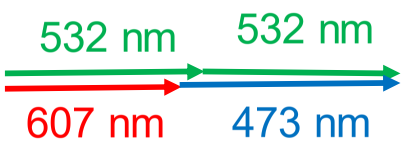

- (Planar) BoxCARS:

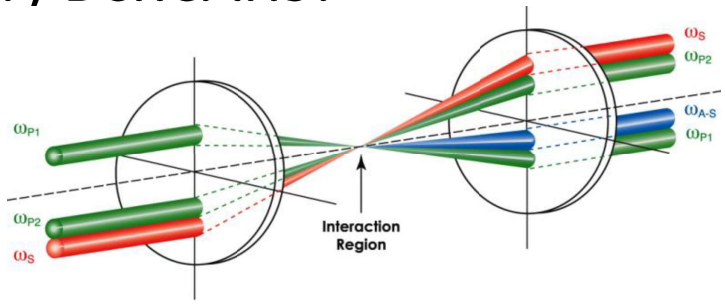

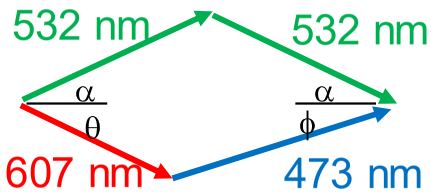

- Folded BoxCARS:

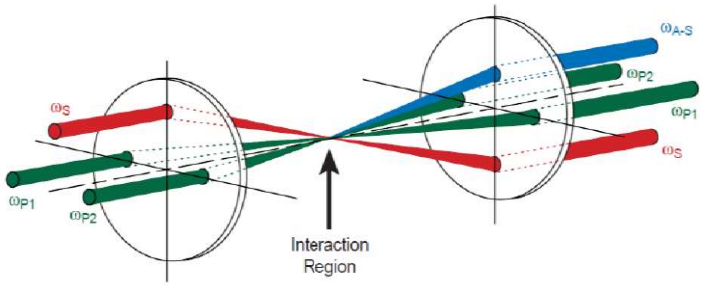

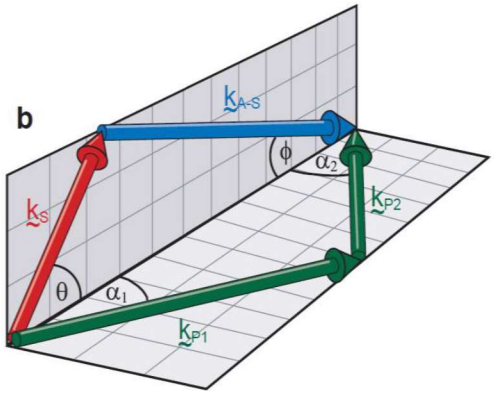

  - Best spatial resolution (1.5 mm x 0.1 mm x 0.1 mm) but lower signals and affected by beam steering from turbulence

NASA/GWU Mobile CARS System

→ Simplifies/speeds set up in facility

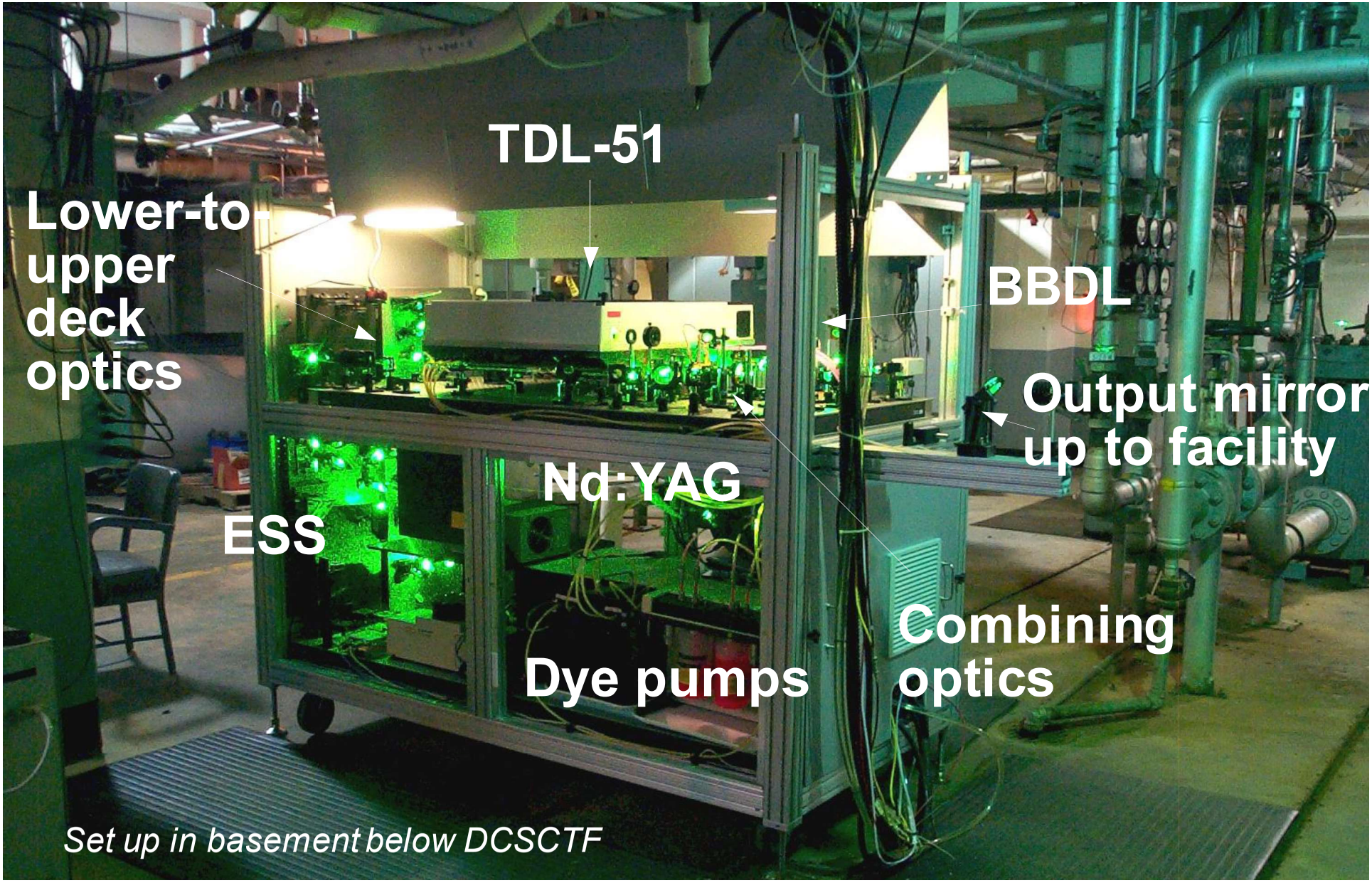

Set up in basement below DCSCTF

Features of NASA/GWU Mobile CARS System

- YAG laser plus 2 dye lasers on single cart
- Transmission and receiving optical stages
- Can put system on a truck and moved to facilities
- Measures T_{rot}, T_{vib}, N_2, O_2, H_2 mole fractions at 20 Hz.
  - Quantified accuracy, precision
- Fully automated data acquisition
  - Remote operation of system
  - X-Y (-Z) probe volume traverse capability
  - Input test matrix; system acquires and saves data for hours until complete
  - Laser power automatically adjusted to prevent saturation effects (detector saturation, Stark broadening, Raman pumping)
  - Beam alignment monitors; remote control alignment
- Beam shaping capability to maintain alignment measurement in turbulent flows and amidst mechanical vibrations
  - 10x improvement compared to USED CARS

Currently at UVa: Optical System

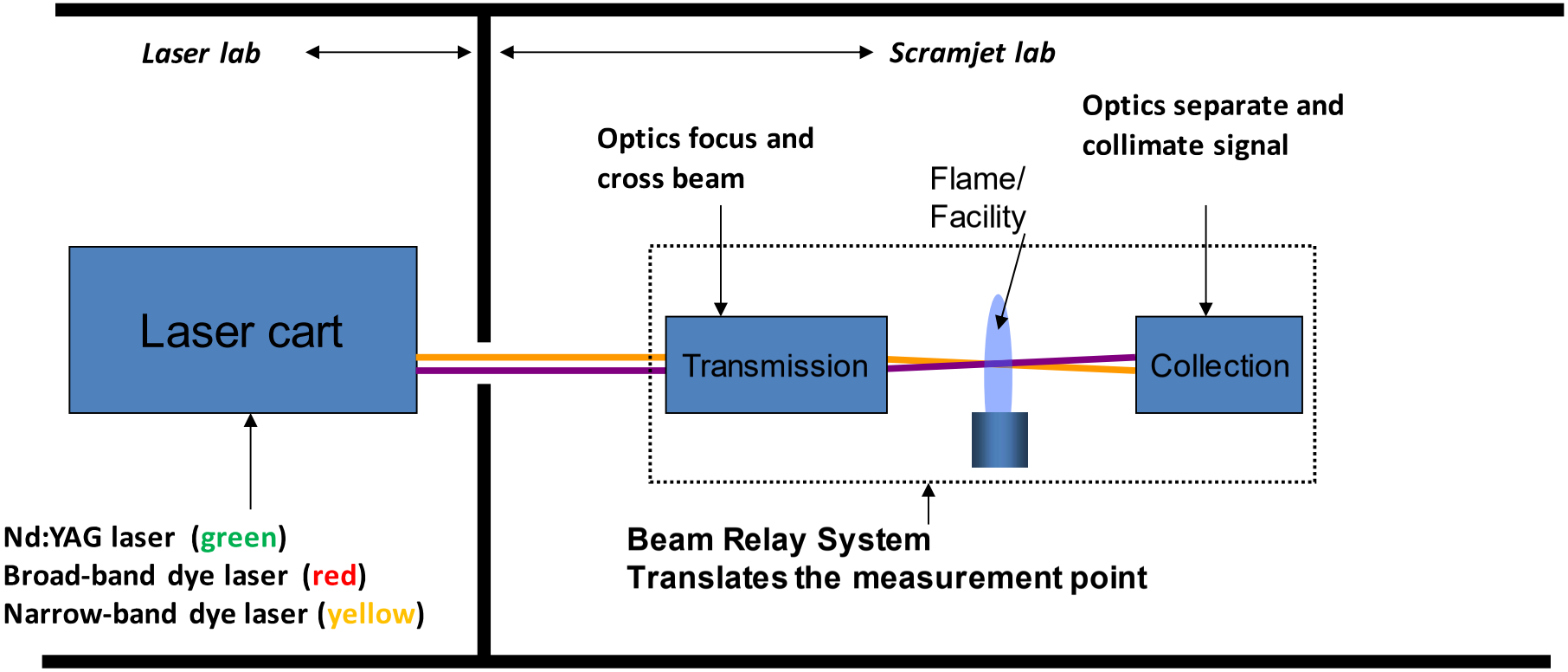

Transmission stage and test section at UVa

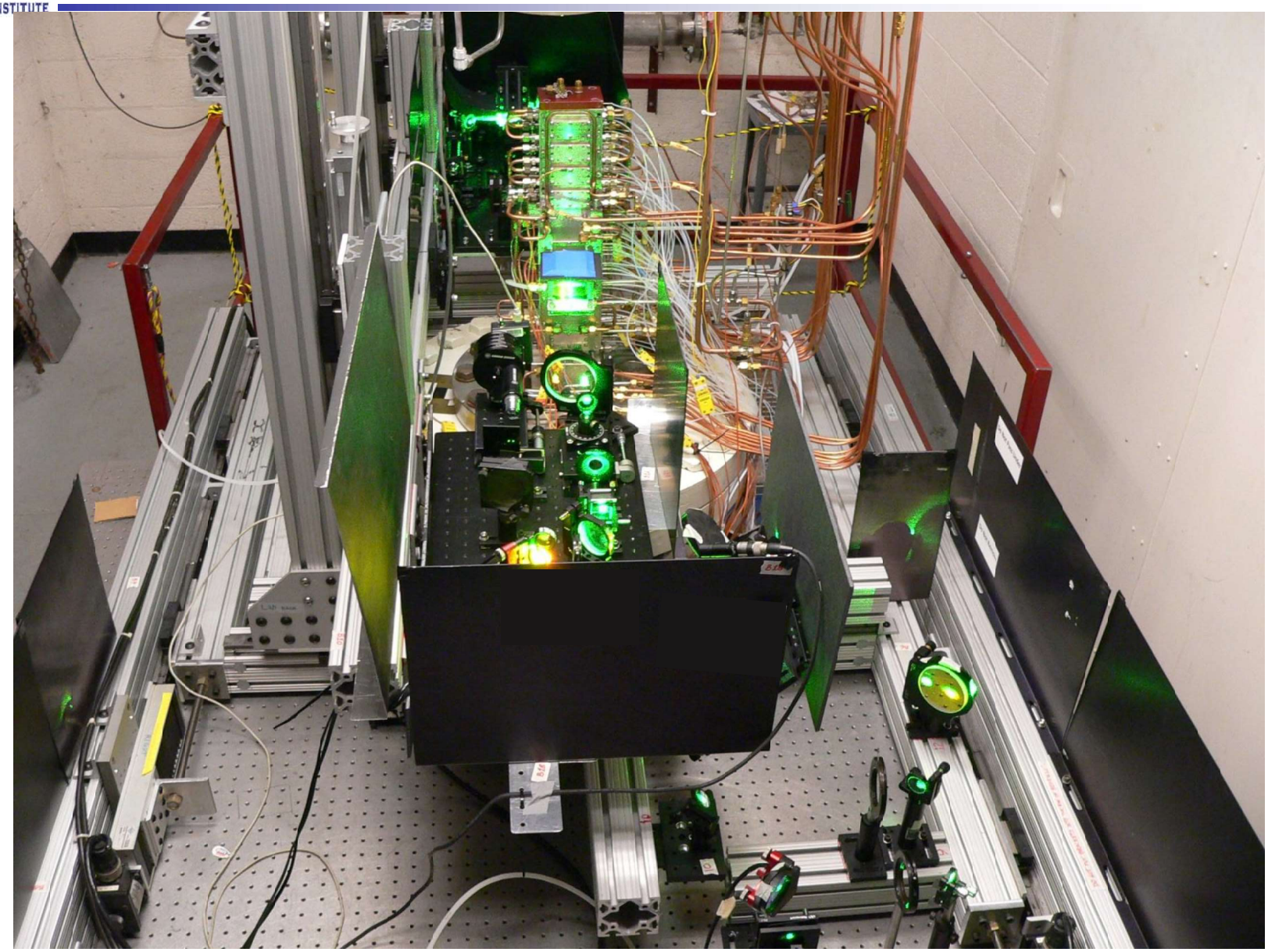

Facility / Dual Mode Scramjet at UVa

UVASCF Test Section

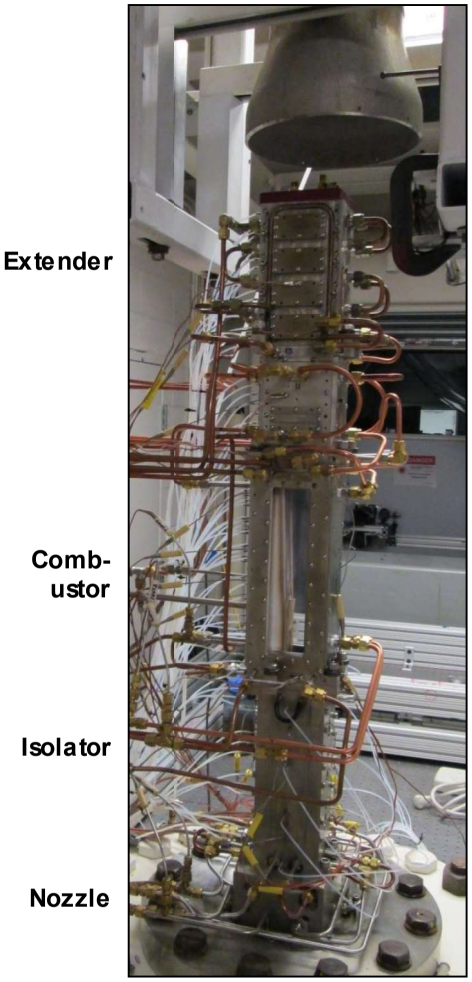

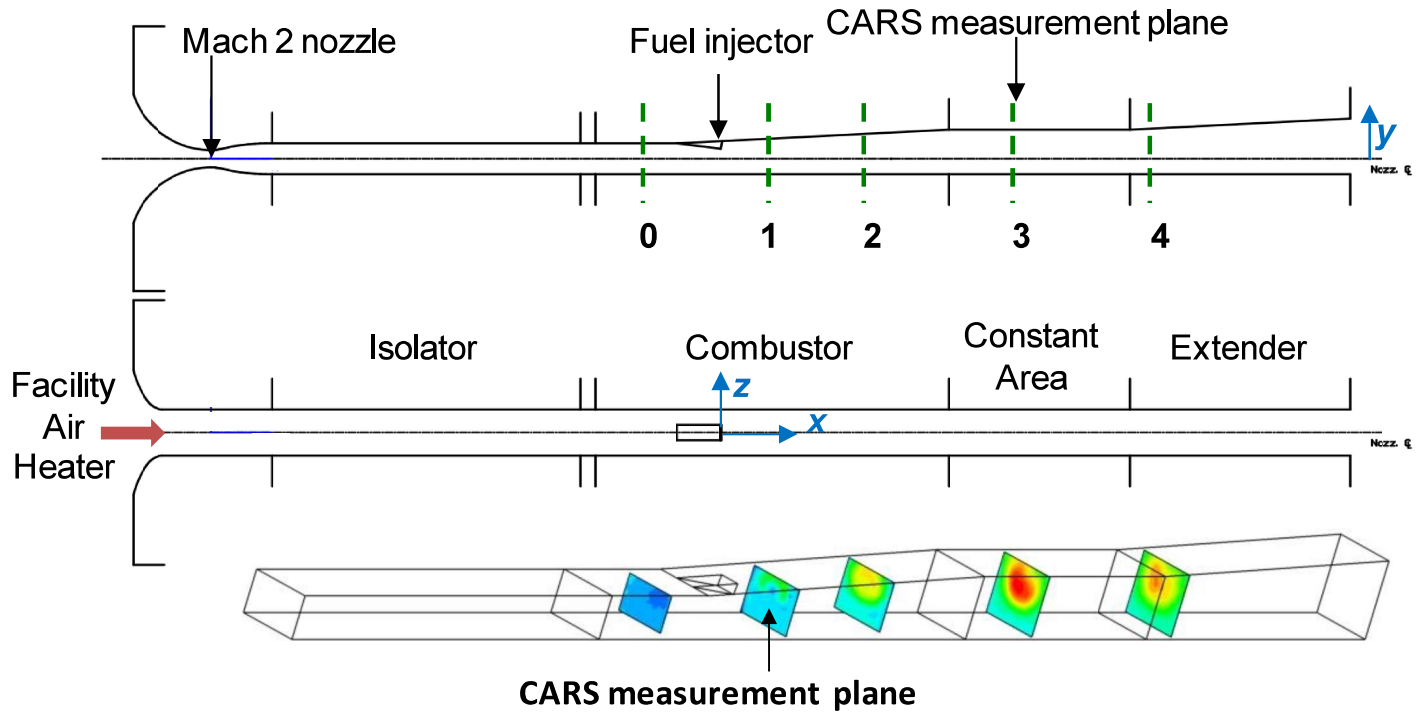

- Electrically heated clean air, nominal T_t = 1200 K, M = 2 nozzle
- Long test times allow large data sets at steady inflow conditions
- Highly turbulent flowfield
- Good optical access

Nonequilibrium: CARS T_{rot} and T_{vib}

Mean Rotational Temperature

H_2 fuel, Config. C

***φ*=0.18**

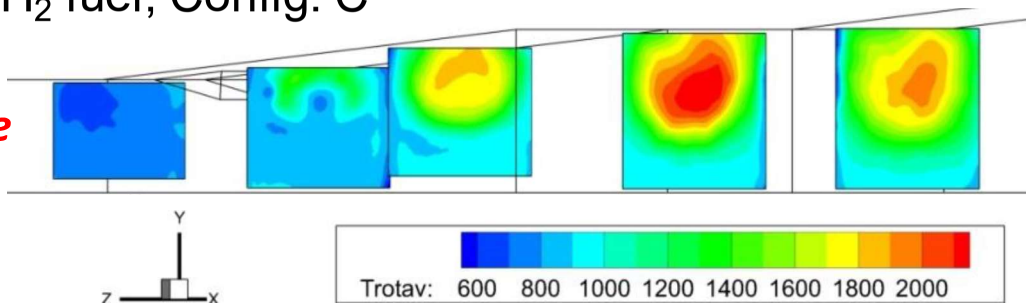

Mean Vibrational Temperature

***φ*=0.18**

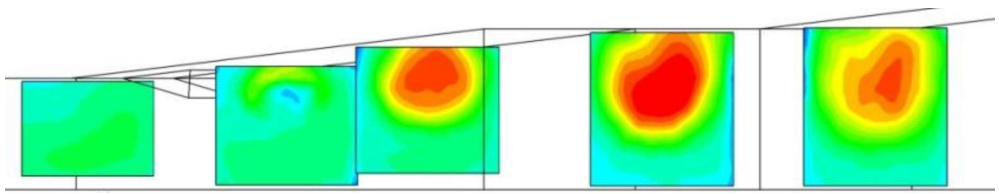

Cutler et al., AIAA-2013-0335, 2013
Cutler et al., AIAA Journal, 2015

- Nonequilibrium within the clean-air UVa combustion tunnel
- Temperature maps constructed by translating CARS system
- Vibrational temperatures frozen near the heater stagnation temp.

Cutler et al., Comb. Flame, 2019

Quantitative measurement of T, concentrations of O_2, CO_2, C_2H_4

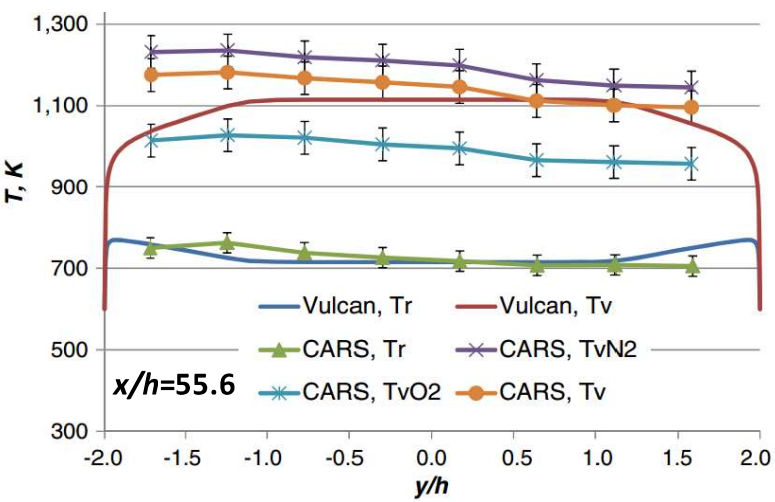

Vibrational Temperature

Vibrational O_2 and N_2 T's "lumped" together to validate the vibrational nonequilibrium model implemented in VULCAN code by R. Baurle (NASA).

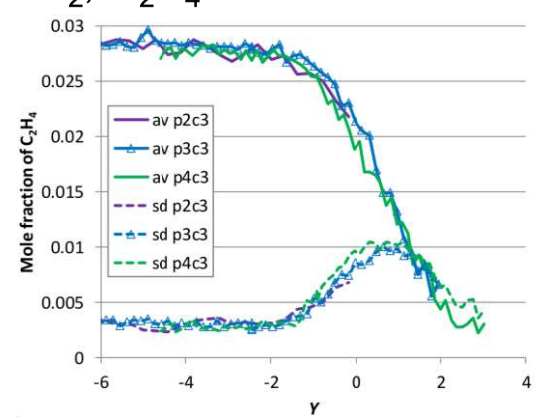

ns CARS vs. Hybrid fs/ps CARS

ns CARS

Hybrid fs/ps CARS

Frequency:

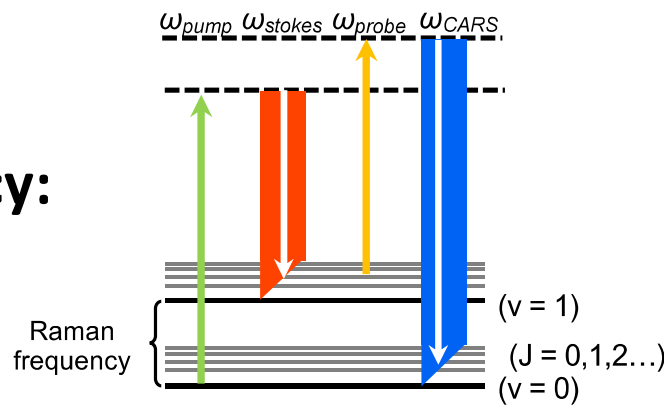

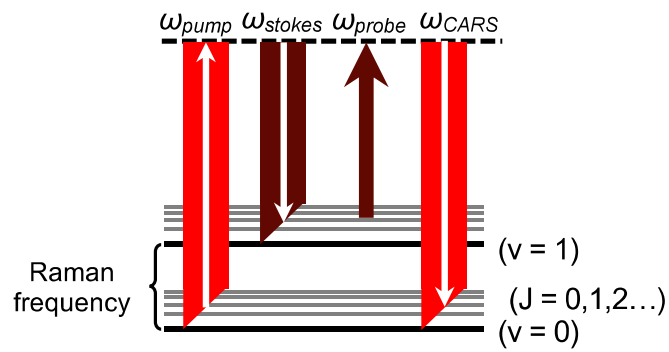

Time:

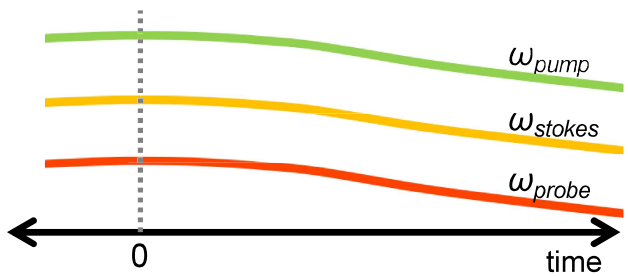

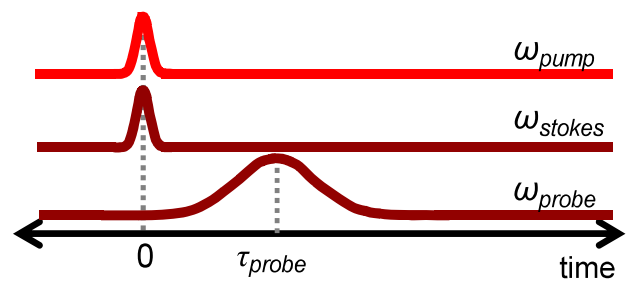

Advantages:

- Wide range of species can be targeted simultaneously using a broadband dye laser, dual-pump excitation
- Use nonresonant signal when all but one major species is measured
- Has been successfully applied to supersonic tunnel measurements

- Insensitive to collisions—improved accuracy in unknown collisional environment
- Inherent broadband excitation to access multiple transitions
- Temporally suppress nonresonant signal
- Stable laser source enables improved measurement precision (1%)
- kHz laser sources: faster data collection

Time-Response of fs CARS

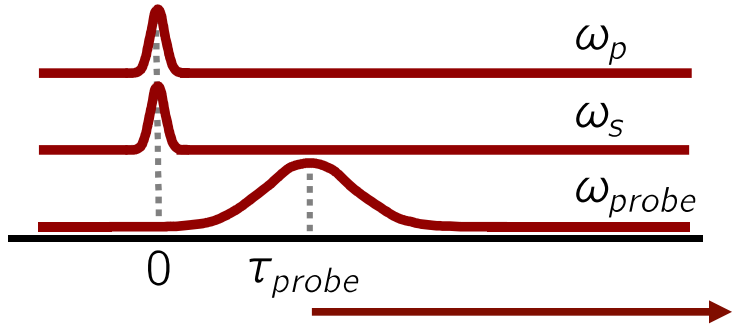

Delay probe pulse to sample the
time response of Raman excitation

S-branch (Rotational CARS)

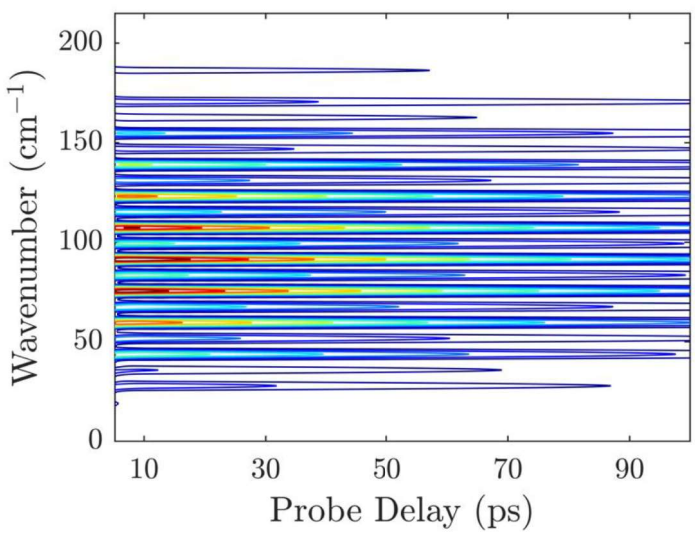

Q-branch (Rovibrational CARS)

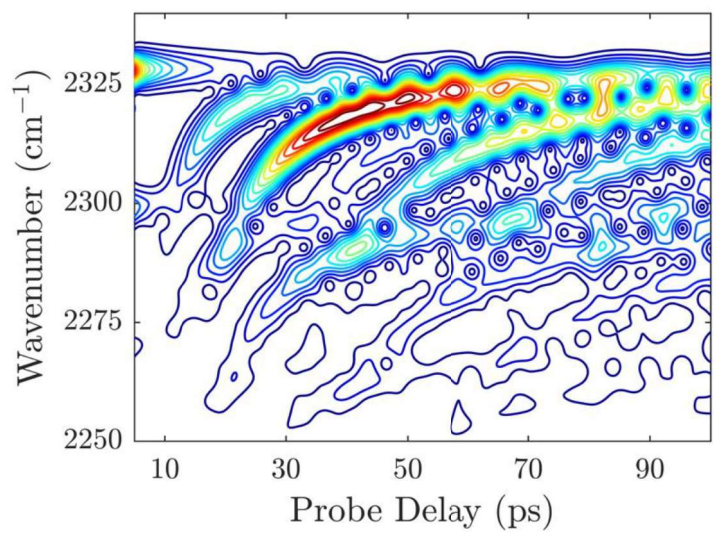

170

Time-Response of fs CARS

Raman transition intensities at 2000 K

S-branch (Rotational CARS)

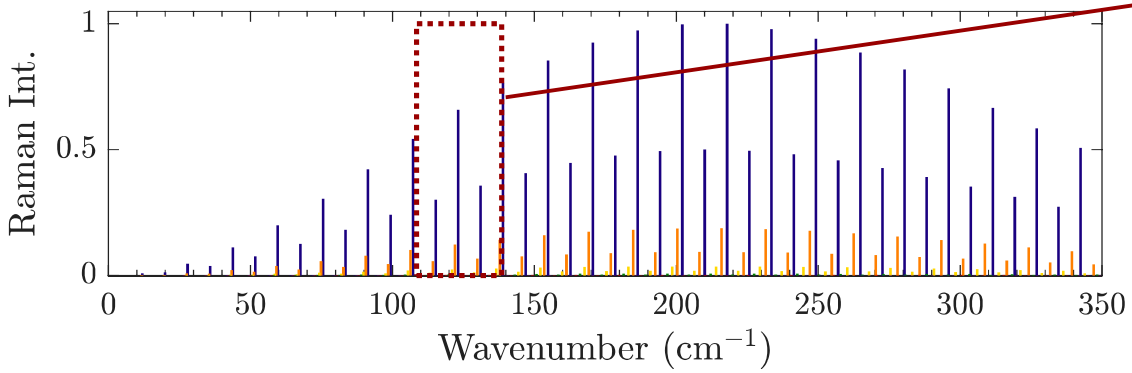

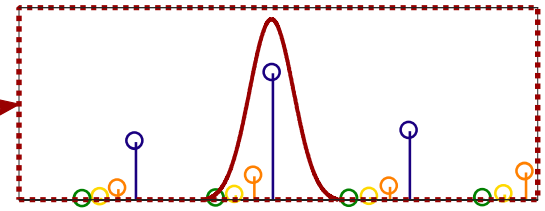

30 cm^{-1}

Well-separated transitions – each transition decays exponentially

Q-branch (Rovibrational CARS)

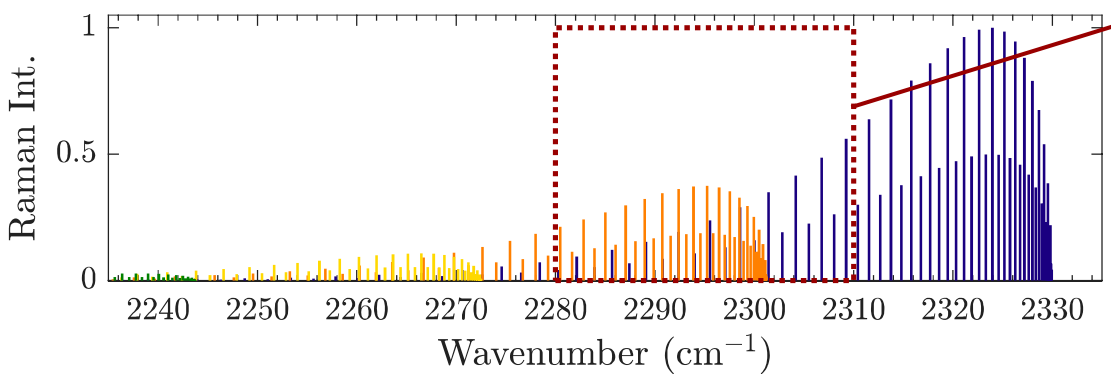

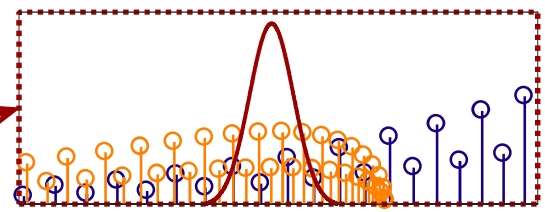

30 cm^{-1}

Overlapping transitions – complex time response

fs/ps CARS of dielectric barrier discharge

Single-shot nonequilibrium measurements in a **nonthermal plasma**

C.E. Dedic, T.R. Meyer, J.B. Michael, *Optica*, Vol. 4, No. 5, 2017

C.E. Dedic, PhD, Iowa State University, 2017

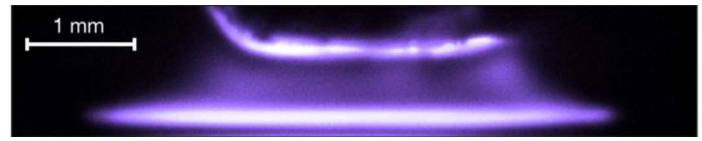

Single laser source with pulse shaping to form ps pulse

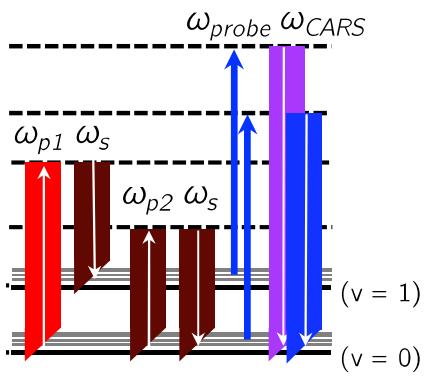

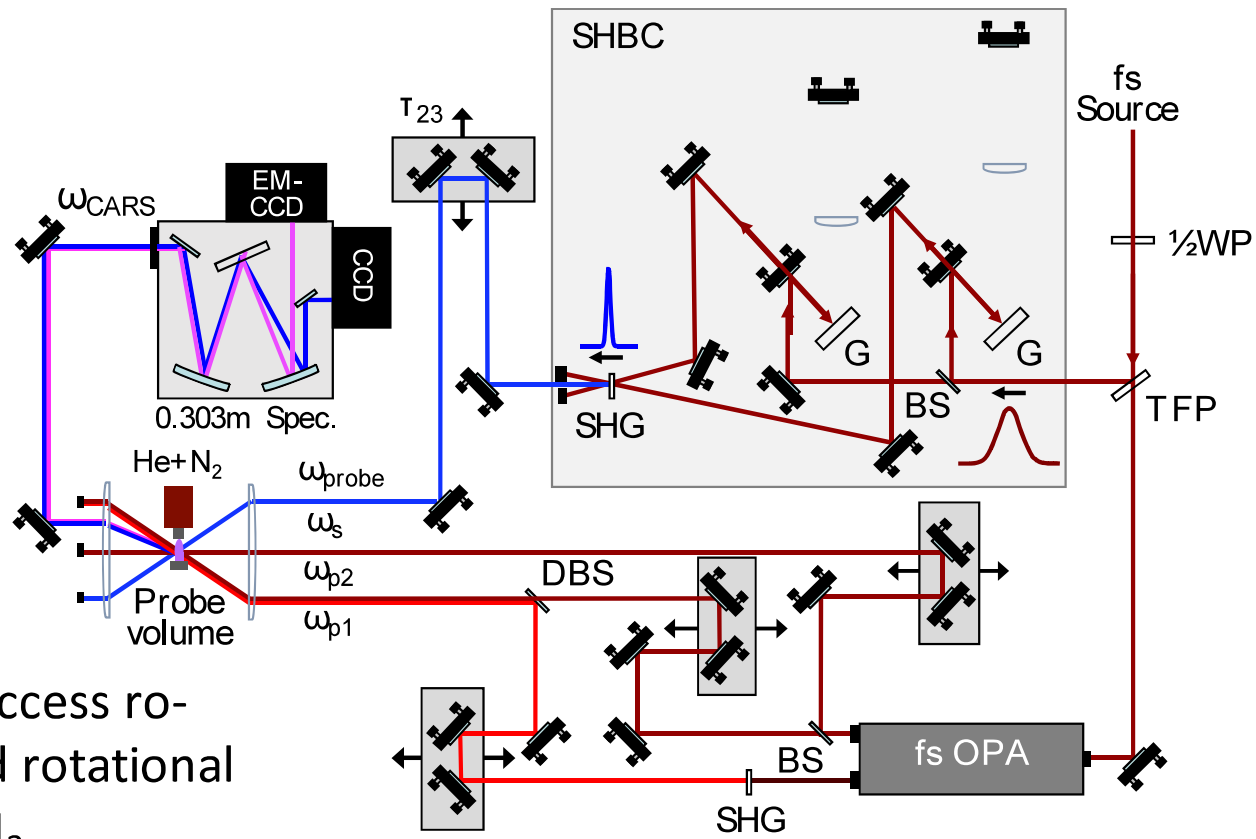

Dual-pump excitation to access ro-vibrational (Q-branch) and rotational (S-branch) transitions of N_2

Sample fs/ps CARS spectra

Single-shot, S-branch **Single-shot, Q-branch**

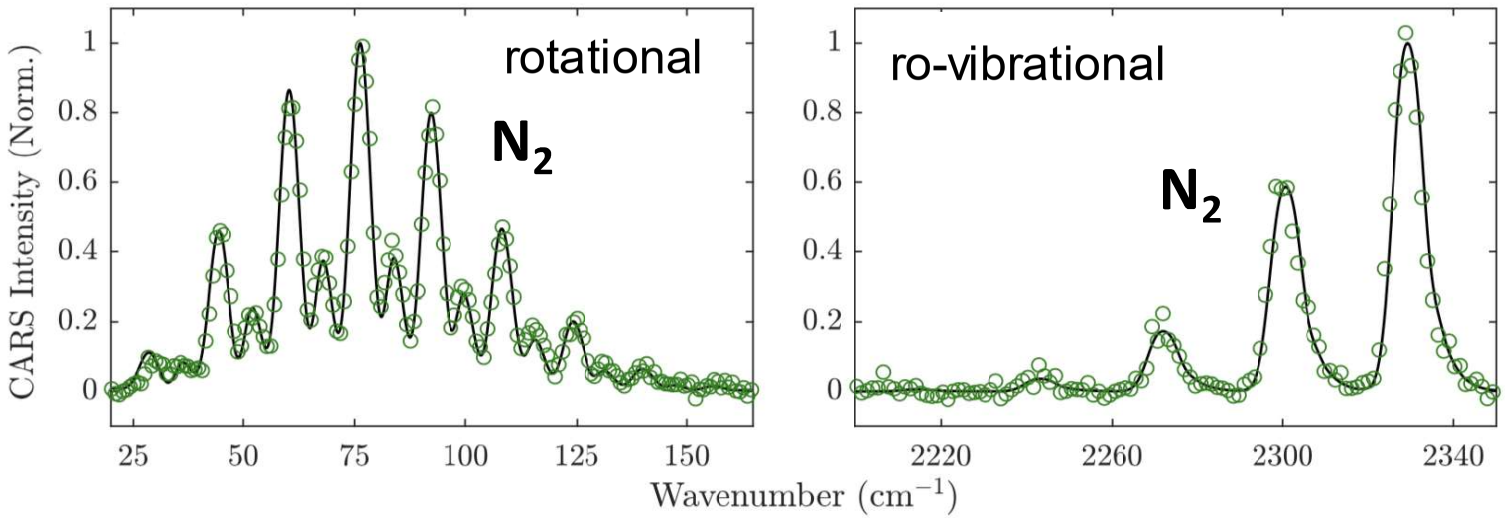

- Atmospheric pressure plasma
- Dual-pump excitation of S- and Q-branch simultaneously
- Sensitive, separate rotational temperatures from S-branch
- Q-branch (vibrational) has **less spectral resolution than ns CARS** due to probe pulse width (3 cm^{-1} vs. <0.01 cm^{-1})

C.E. Dedic, T.R. Meyer, J.B. Michael, *Optica*, Vol. 4, No. 5, 2017

T_{rot} and T_{vib} measurements

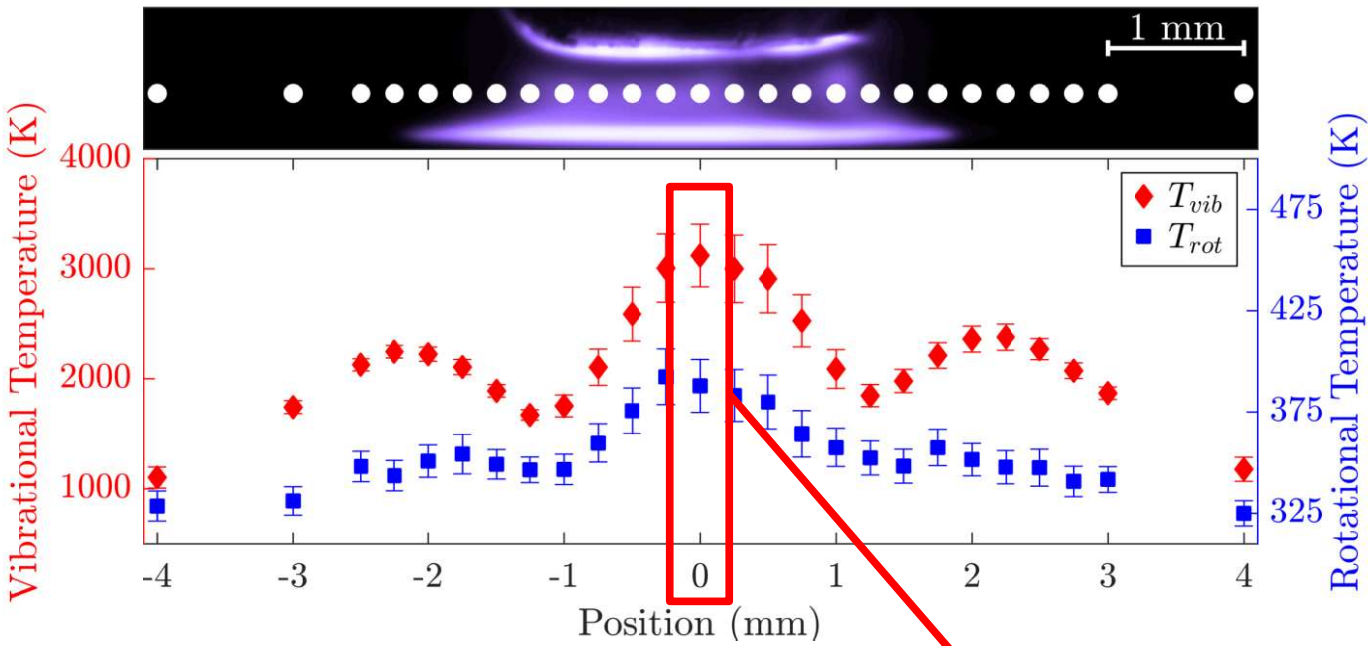

400 single-shot spectra

T_{rot} = 388 K T_{vib} = 3120 K

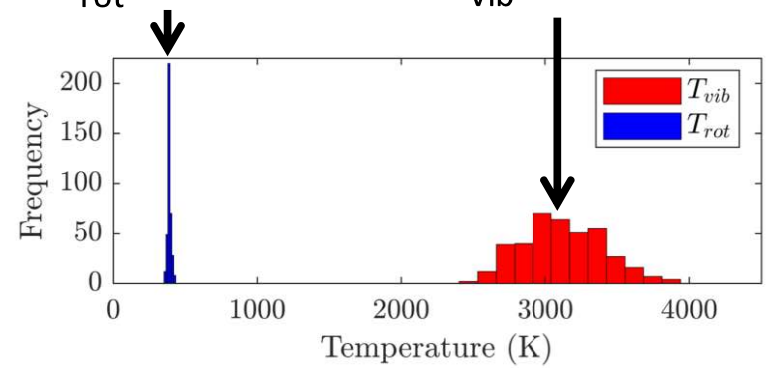

- CARS can measure vibrational and rotational energy state populations of the **ground electronic state N_2(X)**
- **Single shot** measurements show fluctuations in **T_{vib}** due to unstable plasma (**σ=11.3%),** Stable **T_{rot}** (**σ=3.9%**)

Comparison: CARS and emission spectroscopy

- Comparison of CARS to traditional plasma emission spectroscopy
- Emission is **path-integrated** and **non-directional**, causing spatial uncertainty
- Rotational temperature measurement **less sensitive**
- Emission measures the populations in excited electronic states—unlike CARS which measures the N_2(X) ground state—potentially leading to **measurement bias**

N_2(B,*v*←C,*v*+2) emission

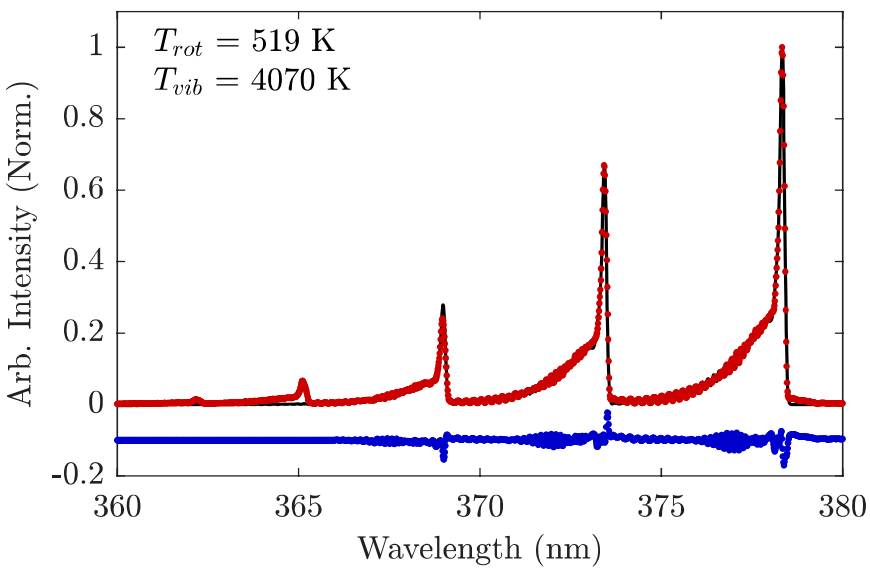

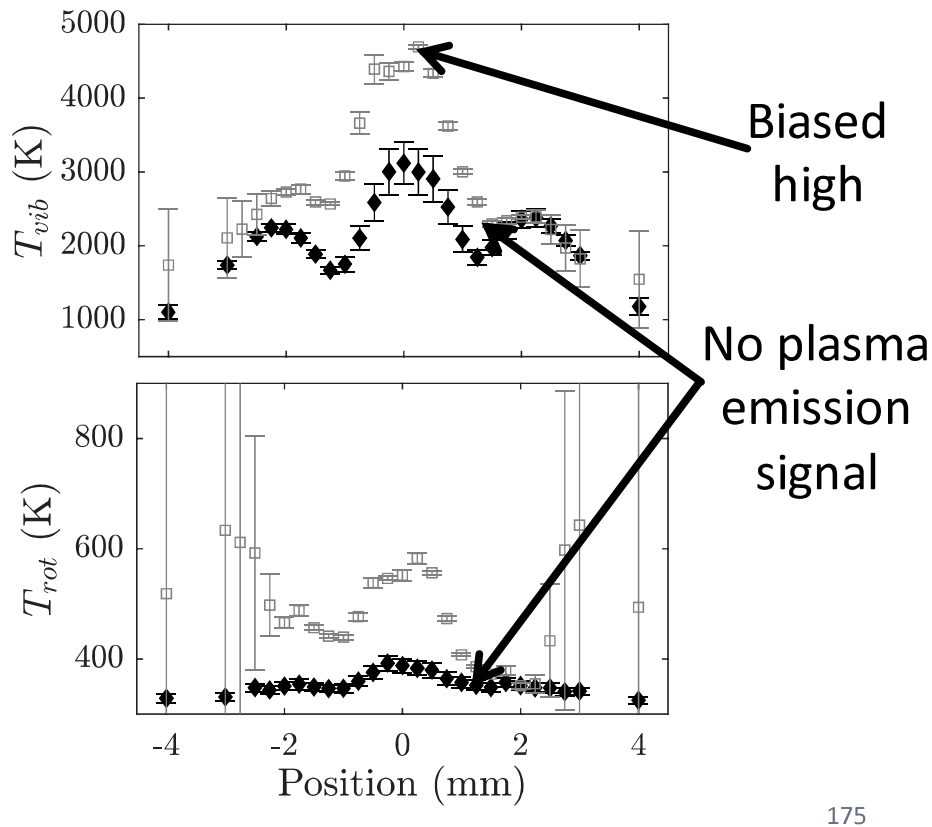

fs/ps CARS in a supersonic jet

- 2-probe scheme to enable **single shot** measurement of temperature and pressure
- BOXCARS phase-matching configuration with **offset** probe pulses
- Probe 1 is delayed to **minimize nonresonant** interference, Probe 2 is delayed to **maximize pressure sensitivity**

Dedic et al., AIAA SciTech, 2019

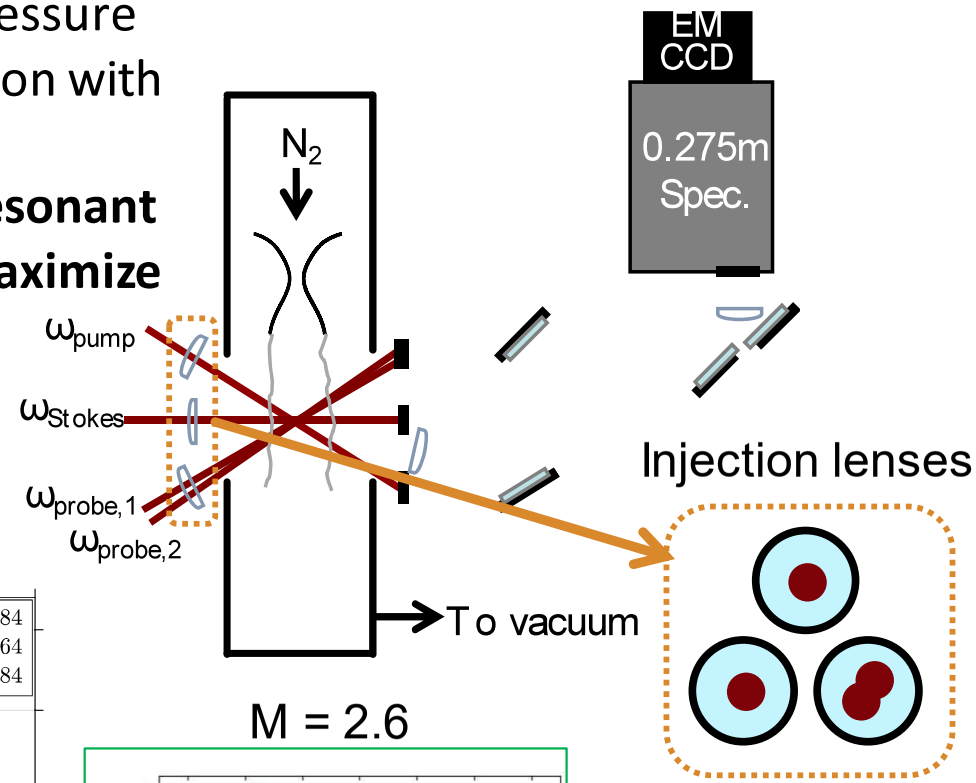

Temperature results for 3 nozzles:

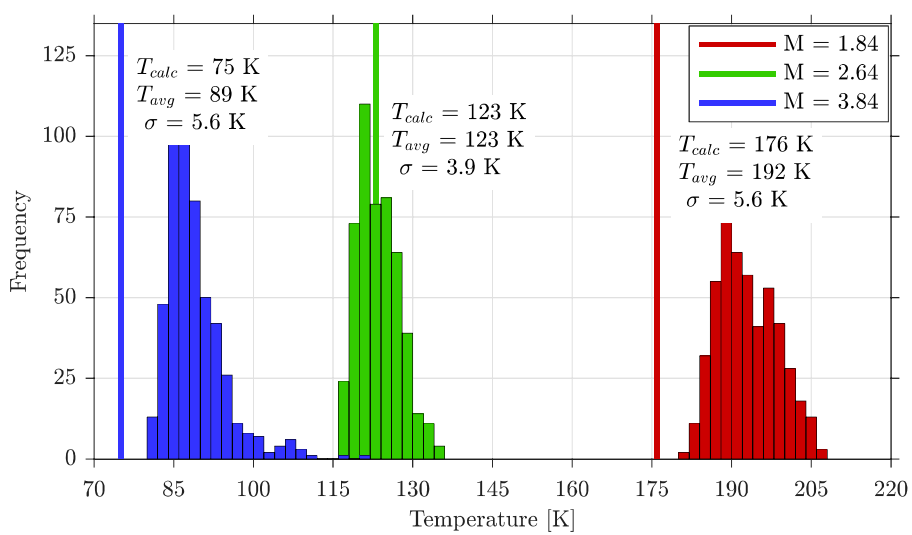

M = 2.6

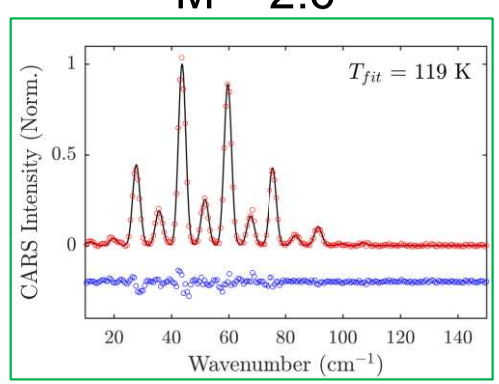

Pressure results: M = 3.84

- Two sample spectra pairs from the **Mach 3.84 jet**
- Although both temperatures match, very different pressures

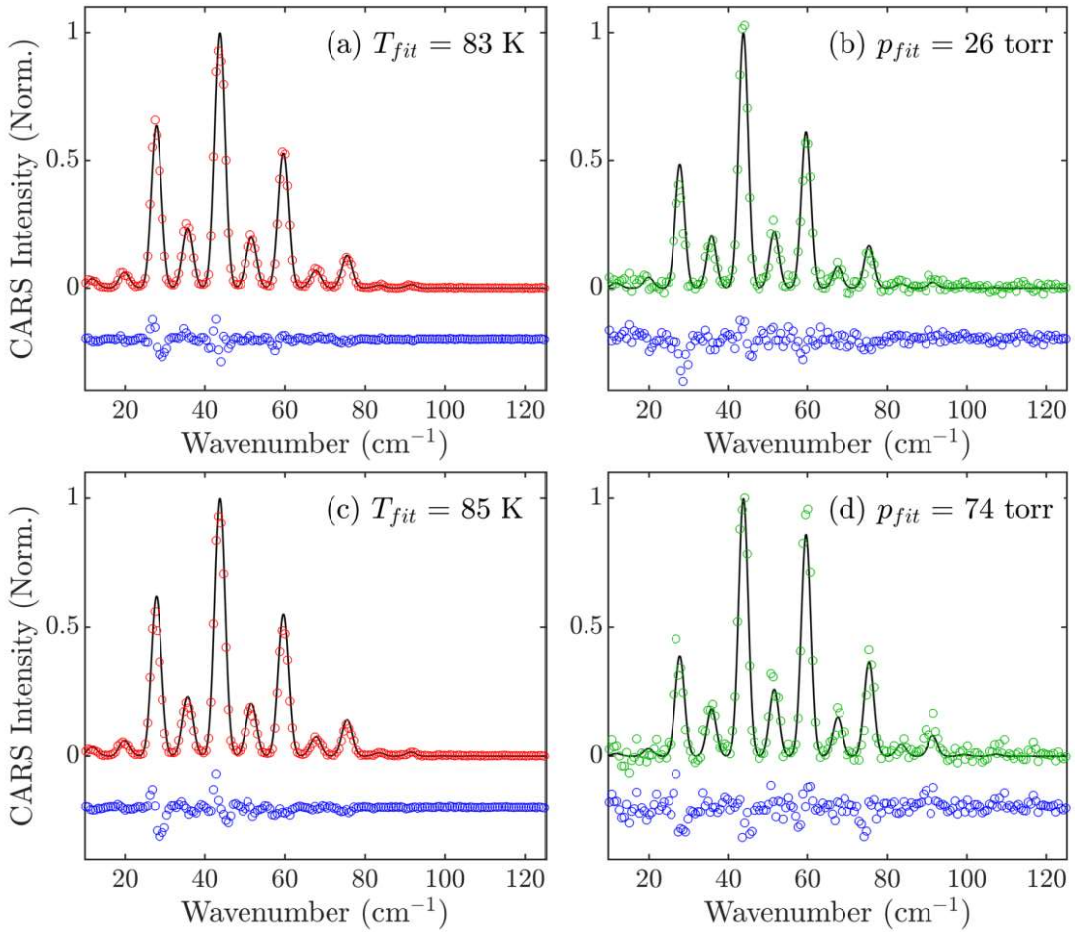

T_{fit} = **83 K**
p_{fit} = **26 torr**
SNR_{early} = 1040
SNR_{late} = 86

T_{fit} = **85 K**
p_{fit} = **74 torr**
SNR_{early} = 950
SNR_{late} = 60

Extending fs/ps CARS to 1,2-D

Single-shot 1-D Temperature profiles

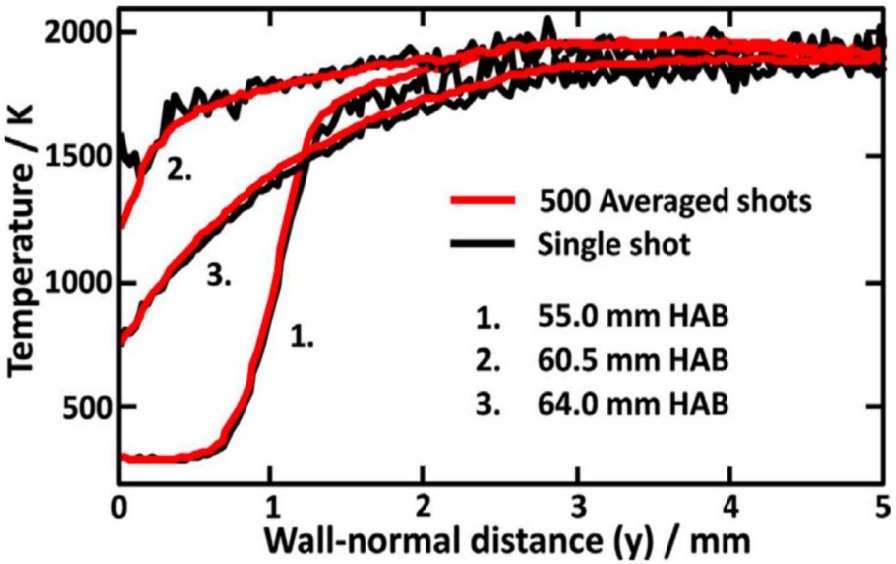

Optical Setup

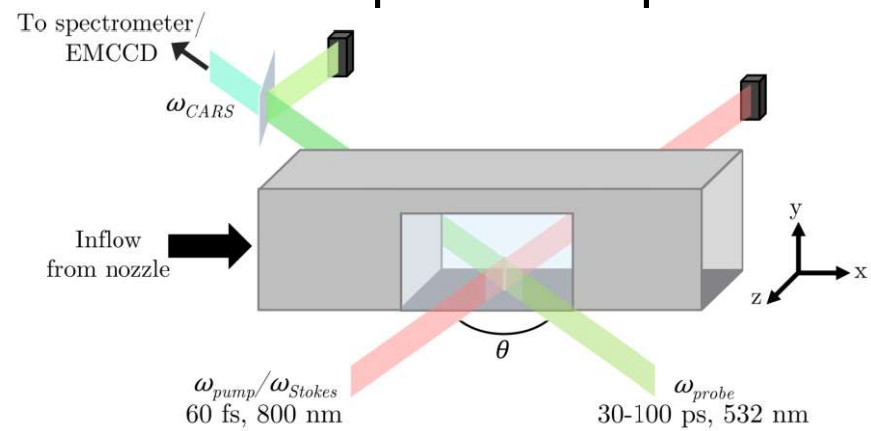

A. Bohlin, C. Jainski, B.D. Patterson, A. Dreizler, C.J. Kliewer,
Proceedings of the Combustion Institute, Vol. 36, No. 3, 2017.

- Single-shot and shot-averaged measurements in a wall-stabilized flame
- Simplified two-beam setup, requires two amplified lasers (fs and ps)
- **Spatial resolution** along the 5 mm measurement line of **35 μm,** with **2-3% precision at any single point**
- Measurements within 30 μm of wall
- 2D measurements also possible (Sandia, AFRL)

Advantages/Disadvantages of CARS

- CARS is a relatively accurate and precise temperature and species measurement technique for reacting and nonequilibrium flows
  - Temp. Accuracy 1-3%; Precision 1-3%
- CARS can be performed through small windows or slots but need access on 2 sides.
- Relatively complicated technique, theoretically and experimentally
  - Takes months to analyze data carefully.
- Seedless, spatially resolved
- Quantify nonequilibrium distributions while sampling the ground-electronic states
- Is being extended to much faster measurements ~10 kHz with fs CARS
  - Recently: 2 beam CARS, CARS imaging (Sandia, AFRL)
- Has been performed using optical fibers to deliver the laser beams, both in ns and ps regimes

Multi-Species Measurement: Dual-Pump CARS

Conventional Broadband CARS

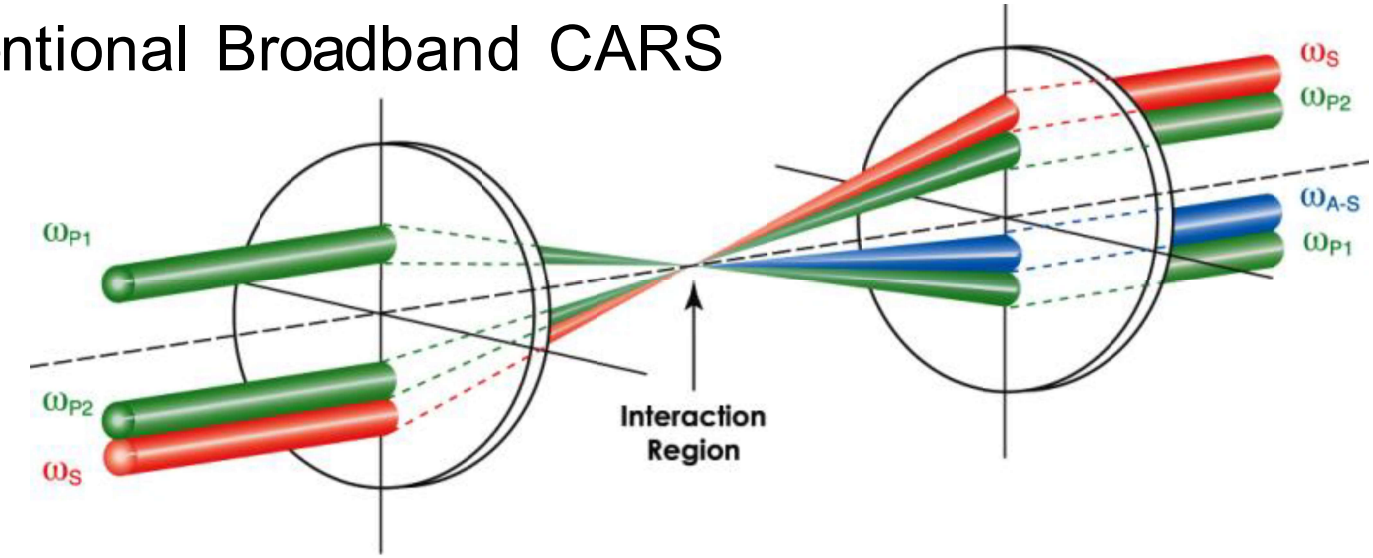

Dual-Pump CARS (Lucht and co-workers)

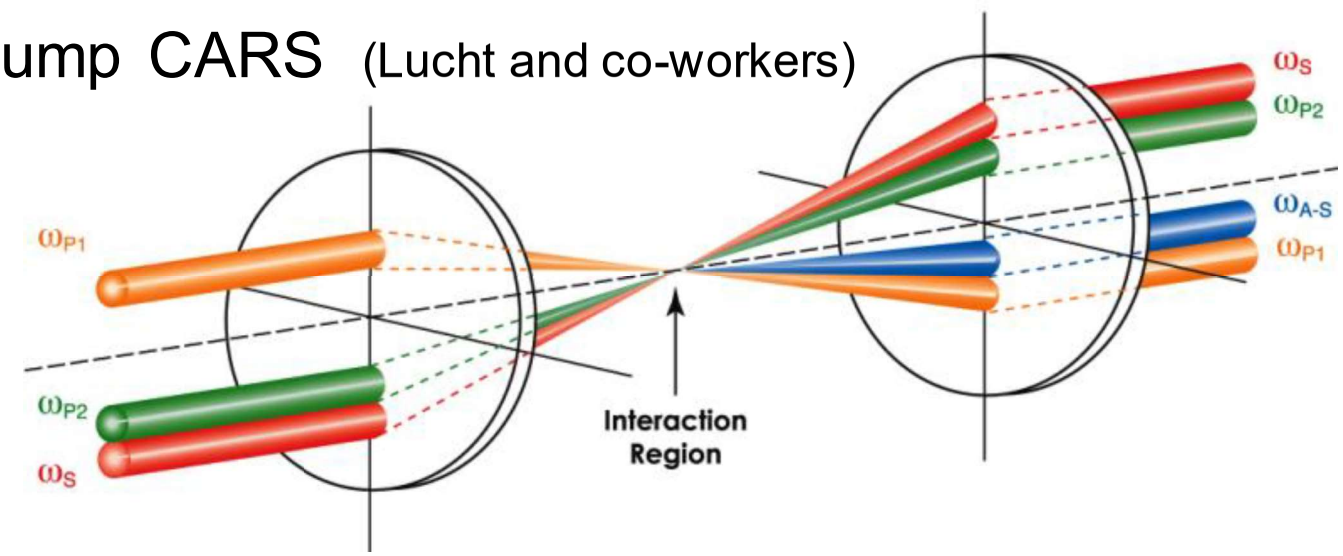

Intro: Nonlinear Optics

– **Second Harmonic Generation (SHG)**

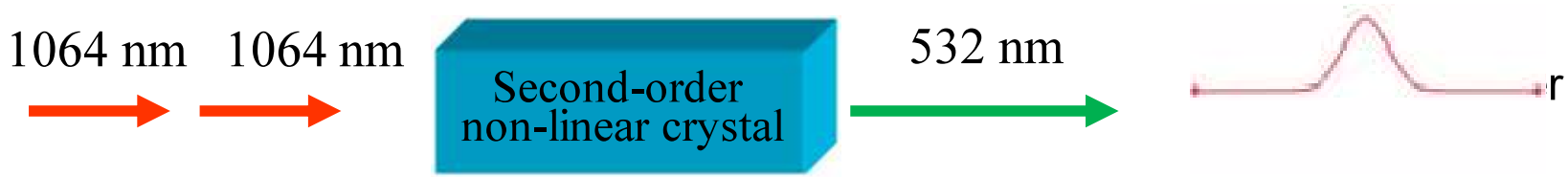

– Solved using the Wave Eqn:

$$\nabla^2 \mathbf{E} - \frac{1}{c^2}\frac{\partial^2 \mathbf{E}}{\partial t^2} = \mu_0 \frac{\partial^2 \mathbf{P}_{\mathrm{NL}}}{\partial t^2}$$

– Assume SVEA and 1st Born Approx:

$$I_{\omega_2} \propto \frac{d^2 P_{\omega_1}^2 L^2}{\mathrm{A}^2}$$

– d is a coefficient, P is power, L is length, A is area

Non-linear Susceptibility

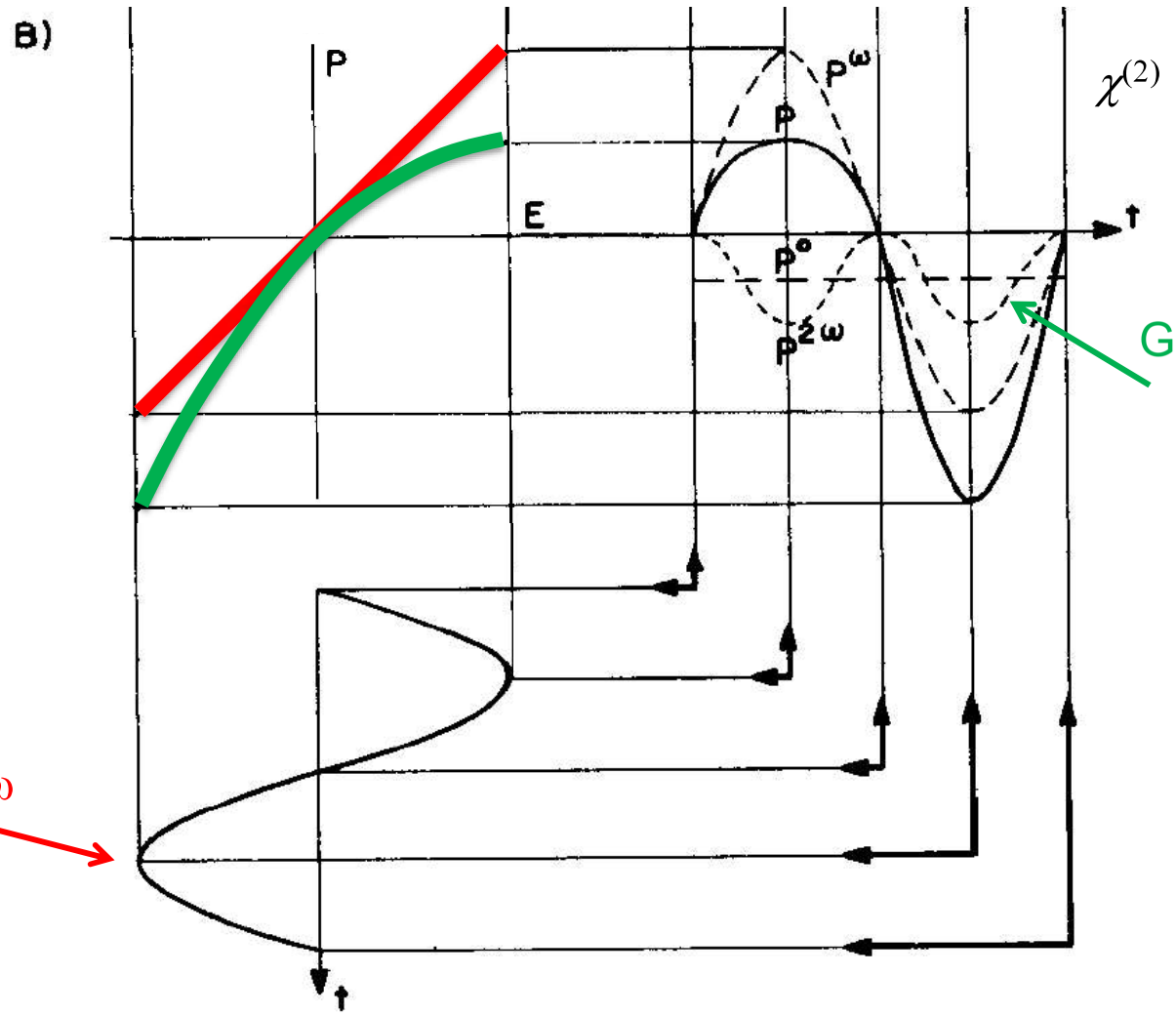

G.C. Baldwin "An introduction to nonlinear optics." *New York: Plenum Press,* (1969).

- Non-linear effects: Intense electric fields of one frequency can generate a **P** at another

CARS Phase Matching (conservation of momentum)

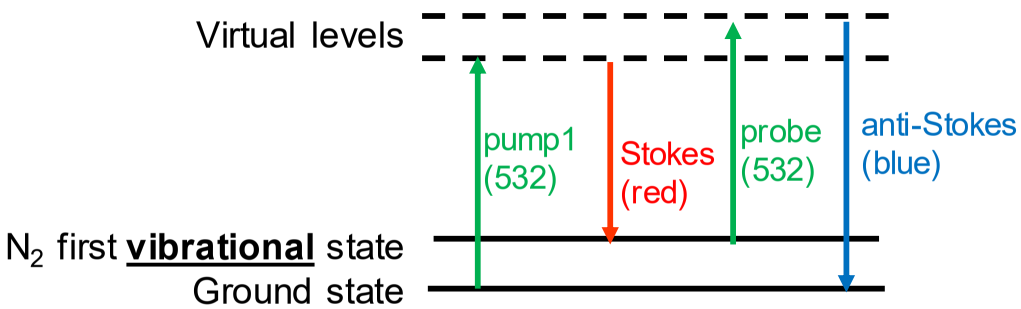

Planar Boxcars Geometry

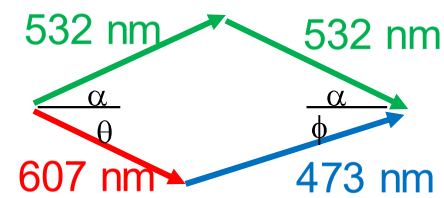

$$k_{p1} + k_{p2} = k_S + k_{A-S}$$

It is straight forward to compute the CARS phase matching angles:

N2 cars		adjust inpu	
	lambda	wavenum	angle (degrees
stokes	607	16474.46	**3.963**
pump 2	532	18796.99	**3.500**
pump 1	532	18796.99	**3.500**
anti stokes	473.4956	21119.52	**3.091**
			0.023576939
N2 Raman =	2322.528	cm-1	0.023576939
(nominal N2 = 2330 cm-1)			*3.00927E-20*

Different molecules require different angles (can get multiple signals at different spatial locations: Dual-Stokes)

CARS Theory 1

- Non-linear effects:
  - Intense electric fields of one frequency can generate a P at another
  - $P = \varepsilon_0 (\chi E + \chi^{(2)} E^2 + \chi^{(3)} E^3 + \ldots)$
  - $\chi^{(2)}$ = 2nd order susceptibility
    - Only media lacking a centre of symmetry (ie, no gases, liquids)
  - $\chi^{(3)}$ = 3rd order susceptibility
    - All dielectric media
  - Generally ($\chi E >> \chi^{(2)} E^2 >> \chi^{(3)} E^3$)

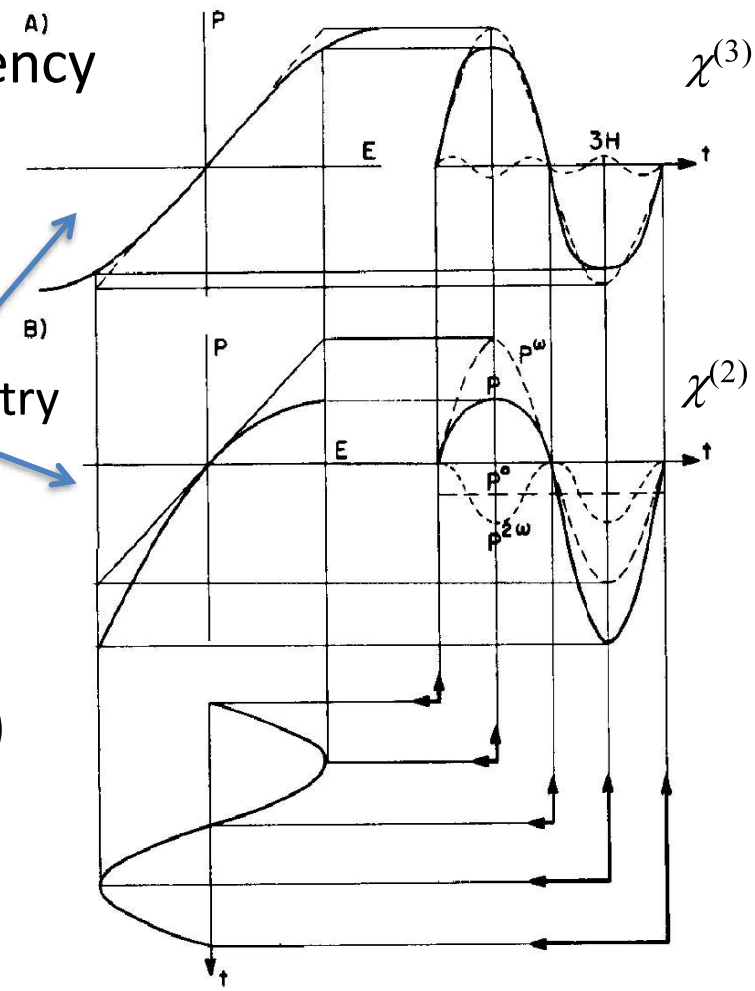

G.C. Baldwin "An introduction to nonlinear optics." *New York: Plenum Press*, (1969).

CARS Theory 2

- Polarization generated at CARS signal frequency:

$$P^{(3)}(\omega_{signal}) = \epsilon_0 \chi_{CARS} E(\omega_{pump}) E(\omega_{Stokes}) E(\omega_{probe})$$

- Substitute into the wave equation. Result:

$$I_{signal} \propto I_{pump} I_{Stokes} I_{probe} |\chi_{CARS}|^2 L^2$$

- To obtain large signals, want long L, high laser power (tight focus) and strong resonance

$$\chi_{CARS} = \sum_j \frac{K_j \Gamma_j}{2\Delta\omega_j - i\Gamma_j} + \chi_{nr} \text{ where } K_j \propto N \Delta_j \left(\frac{\partial\sigma}{\partial\Omega}\right)_j$$

- Γ_j is damping coefficient, N is number density, Δ_j is the population difference
  - N→ concentration; Δ_j→Temperature sensitivity

Particle Image Velocimetry

***Jordi Estevadeordal**, North Dakota State University, Fargo, ND, USA*

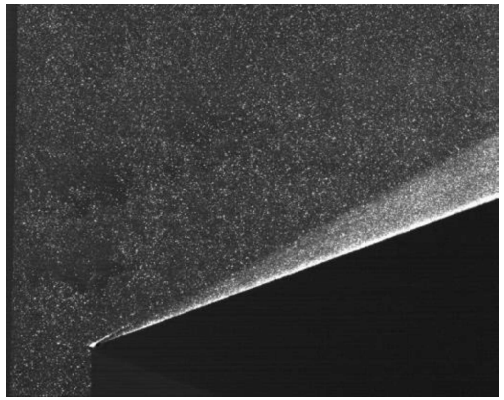

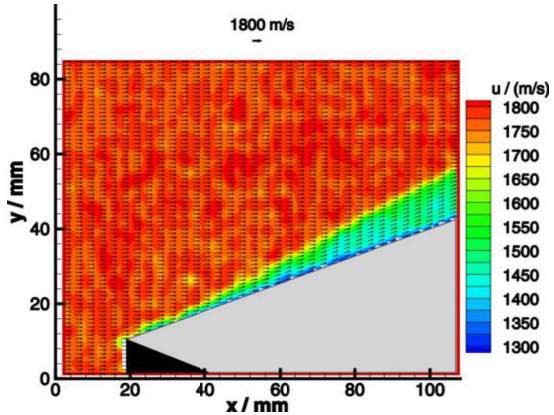

REF: Havermann, M., Haertig J., Rey C., George A., "*PIV Measurements in Shock Tunnels and Shock Tubes," In: Particle Image Velocimetry. Topics in Applied Physics,* Vol. 112. Springer, Berlin, Heidelberg, 2007

Particle Image Velocimetry

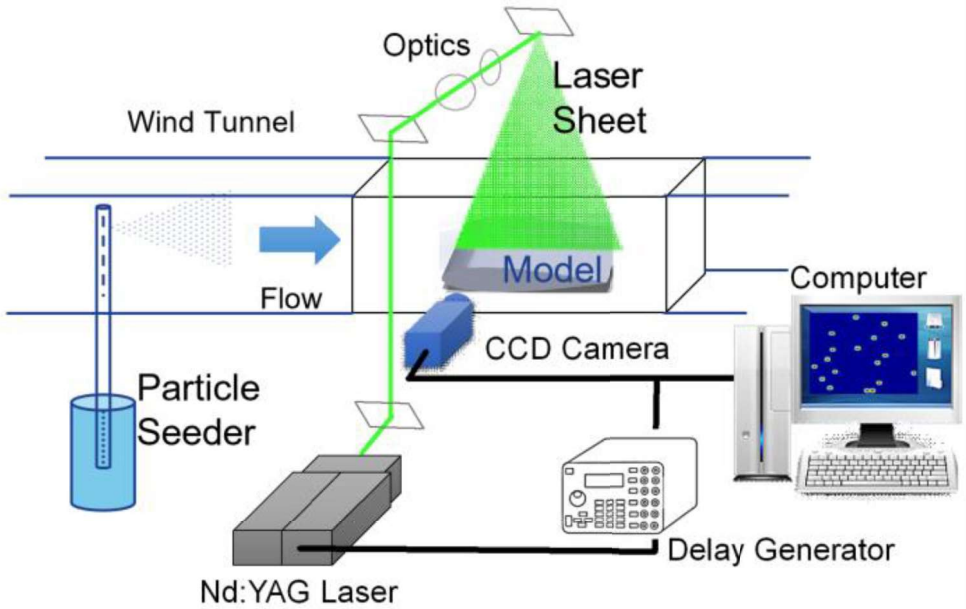

Standard PIV system

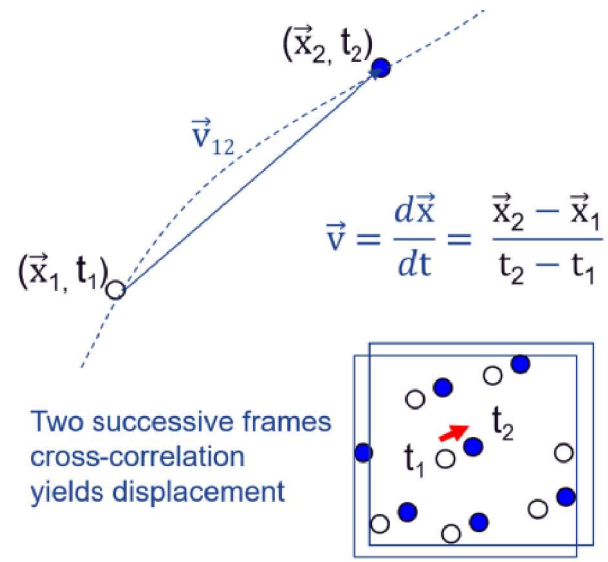

Velocity calculation principle

- Laser-sheet pulses illuminate the particle seeded flow and 'freeze their motion'
- 2+ images are acquired and velocity is calculated from the particle displacements
- <u>Lasers</u>: Nd:YAG, Burst-Mode (100 kHz), <u>Cameras</u>: CCD, CMOS (100 kHz)

PIV has a Standardized setup and is capable of '4D' velocity rendering

Particle Image Velocimetry

Processing Vector Field in successively small interrogation subregions:

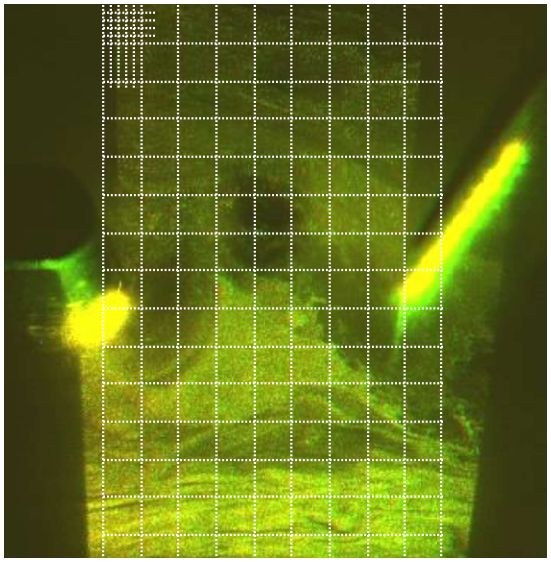

Seeded flow double exposure from transonic compressor flow.

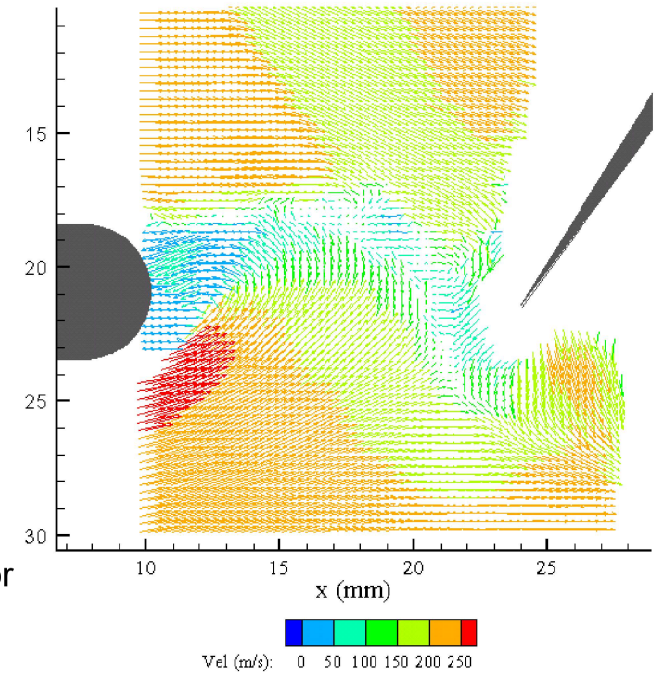

High-resolution Vector Field

Estevadeordal, J., Gogineni, S., Goss, L., Copenhaver, B., Gorrell, S. *"Study of Wake-Blade Interactions in a Transonic Compressor Using Flow Visualization and DPIV*," J. Fluids Eng 124(1), 166-175 (2001)

PIV can render High-Resolution Vector Fields to particle levels

PIV Particle Seeding

- Particles have sizes on the order of the light wavelength and are much brighter than molecules
  - Light Scattering in Mie Regime (much brighter than Rayleigh)

  however
  - Hinder other molecular property measurements (T, density)
  - May not follow the flow motion faithfully

- Particle seeding types (for submicron particle generation):
  - Fluidized Bed (Solid Al_2O_3, TiO_2)
  - Aerosols (Liquid atomizers –DEHS, 'Smoke Generators' -Mineral Oil)
  - Sprays (CO_2) clean seeding

- Particle response quantification: (τ_f: flow time scale τ_p: particle time response)
  - Stokes Number $\mathrm{St} = \frac{\tau_p}{\tau_f}$ (< 0.1 for acceptable flow tracking)
  - e.g. time Response $\tau_p = d_p^2 \frac{\rho_p}{18\mu_f}(1 + 2.7Kn_d)$ (*) includes compressibility effects

* τ_p is the particle response time, d_p is the diameter, ρ_p is the particle density, μ_f is the fluid kinematic viscosity, and Kn_d is the Knudsen number (ratio of molecular mean free path and the d_p) that takes into account the rarefaction effects in compressible flows.

PIV particle seeding challenges are accentuated at high-speeds

PIV Particle Seeding

Sample Image of Particle Field at Mach 2.5 shock

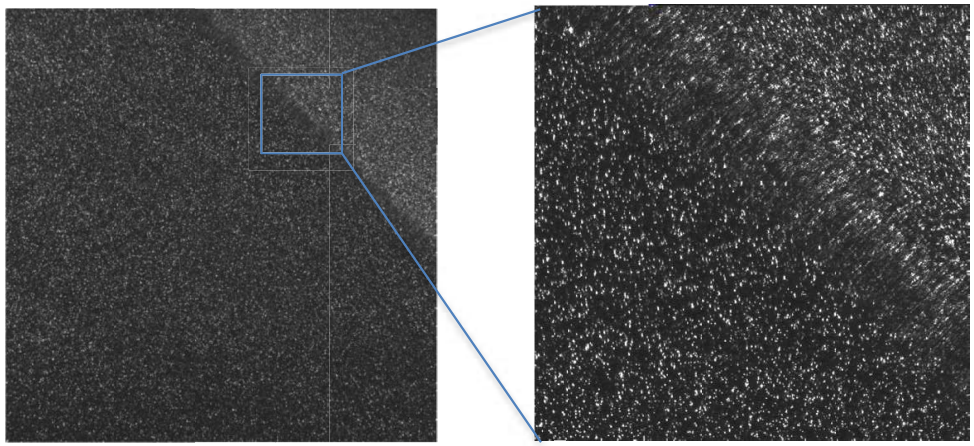

Particle field undergoing a shock in a Mach 2.5 flow and closed-up image of the shock region (Courtesy of Dr. S. Beresh of Sandia National Laboratories, NM)

- High-speed phenomena having rapid flow changes, turns, shocks, high frequencies, and gradients yields <u>particle lag</u> and <u>aero-optical distortion that need be corrected</u>

High-speed phenomena can introduce high particle lag and aero-optical distortions

PIV Application Examples

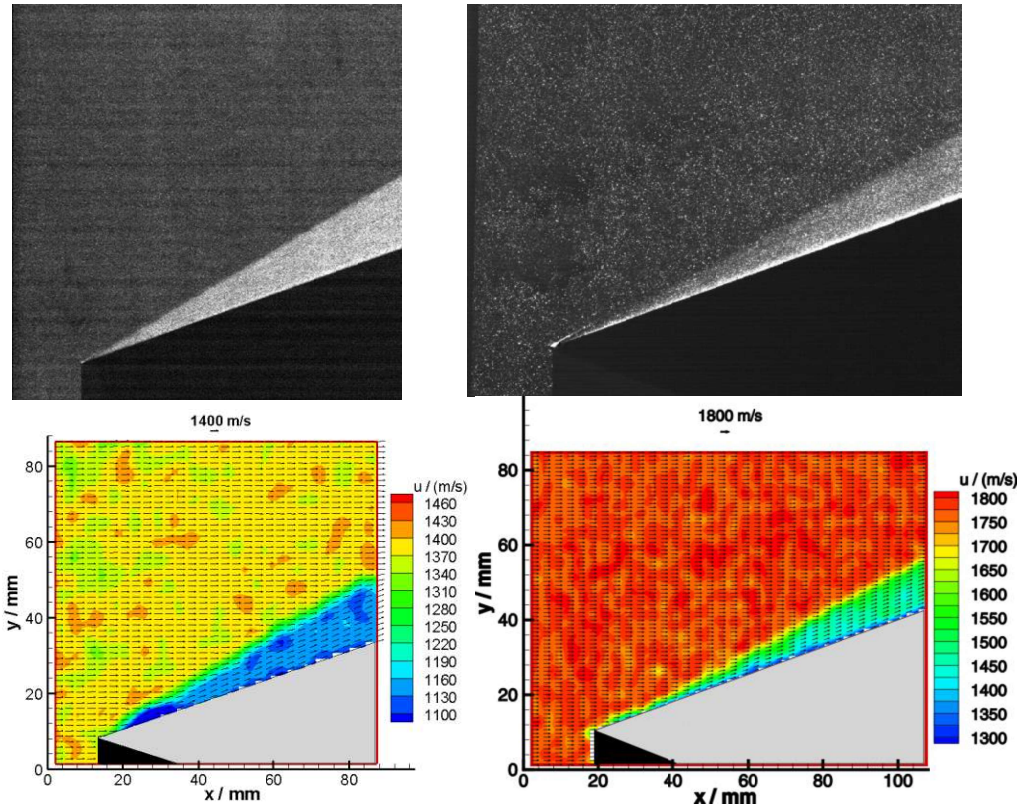

EXAMPLE:
Raw images and PIV results for **<u>Mach 4.5 (left) and Mach 6 (right)</u>** of flow over a 20° wedge.

REF: Havermann, M., Haertig J., Rey C., George A., "*PIV Measurements in Shock Tunnels and Shock Tubes,*" *In: Particle Image Velocimetry. Topics in Applied Physics,* Vol. 112. Springer, Berlin, Heidelberg, 2007

PIV captures general high-speed flow velocity features but can smear details near sharp changing phenomena like shocks and boundary layers

Application Examples

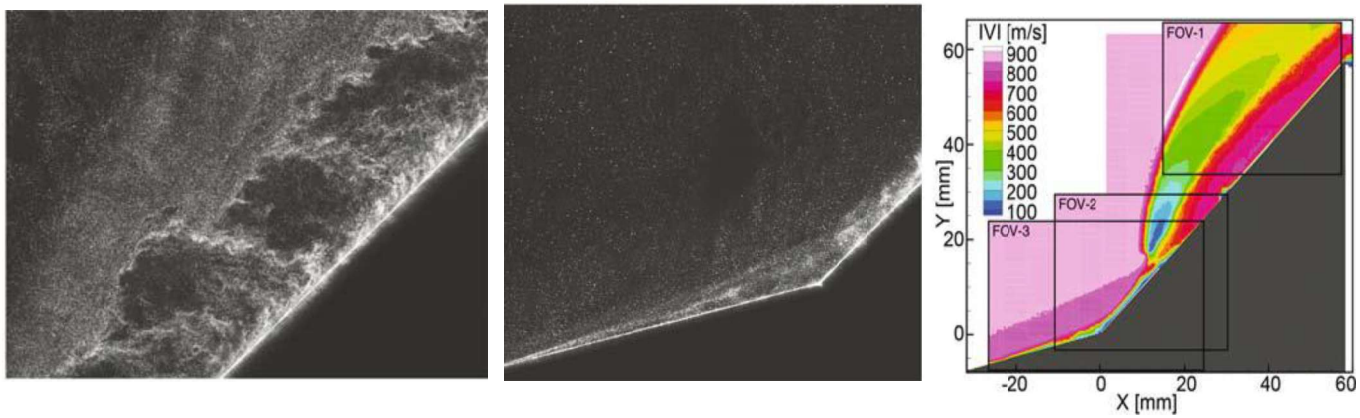

EXAMPLE: **Hypersonic Mach 7 Flow** at Hypersonic Test Facility Delft (HTFD): Double Ramp Flow Visualization and PIV samples. Reproduced with permission from the authors

REF: Scarano, F., "Overview of PIV in Supersonic Flows," *In: Particle Image Velocimetry. Topics in Applied Physics*, Springer, Berlin, Heidelberg , January 2008

PIV captures general high-speed flow velocity features but can smear details near sharp changing phenomena like ramps and boundary layers

Application Examples

EXAMPLE:
Sequence of velocity fields with vorticity extracted from a 2.5 ms burst velocity fields acquired at **25 kHz**, measuring a **Mach 3.7 jet issuing into a Mach 0.8 crossflow.**
Reproduced with permission of the authors

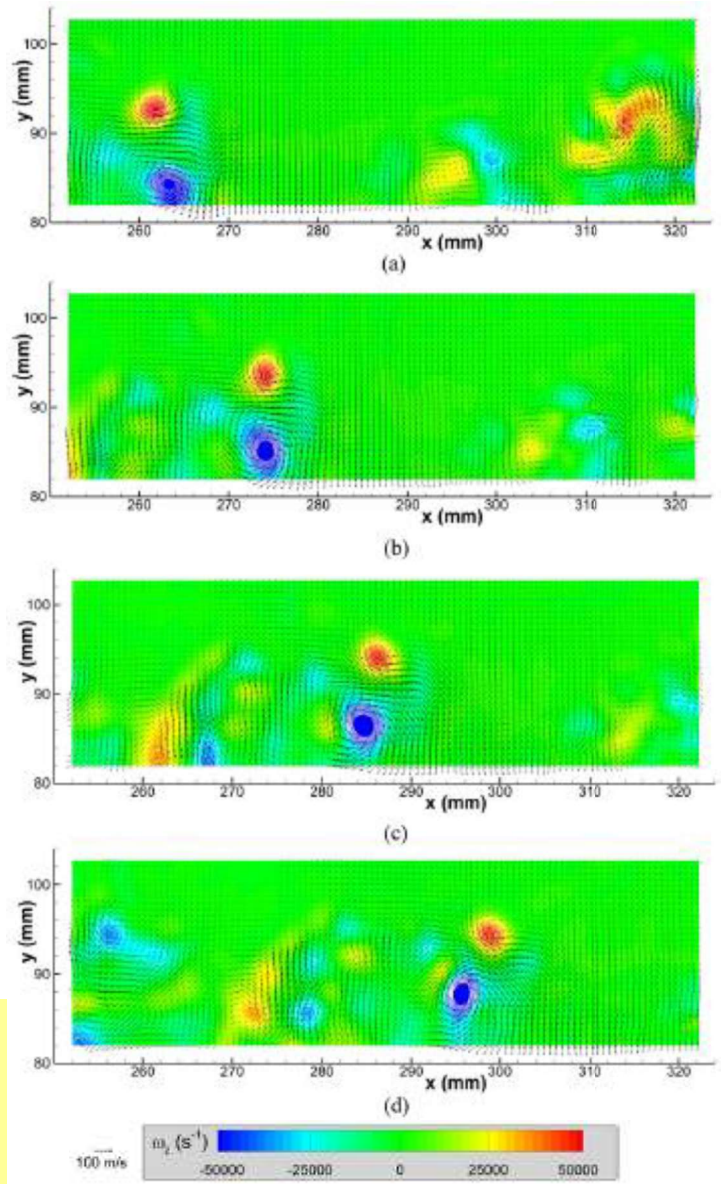

REF:

Beresh, S., Kearney, S., Wagner, J., Guildenbecher, D., Henfling, J., Spillers, R., Pruett, B., Jiang, N., Slipchenko, M., Mance, J., and Roy, S., "*Pulse-burst PIV in a high-speed wind tunnel,*" *Meas. Sci. Technol.,* Vol. 26, 2015, doi: 10.1088/0957-0233/26/9/095305

PIV recent advances in high-rep-rate lasers/cameras allow capturing high-speed flow phenomena

PIV Summary

- Advantages
  - Capable of multidimensional measurement
    - Time-resolved three velocity components in volumes
      - (time resolved volumetric PIV '4D')
  - Software well developed and commercial available.
  - Relatively easy to implement

- Disadvantages
  - Requires Particles seeding:
    - Particle lag
    - Aero-optical Distortion in high speed phenomena
  - Laser and signal at same wavelength, causing interference.
  - Hinders measurement of other properties at same time

Optical Emission Spectroscopy

***Brett Cruden**, AMA Inc. at NASA Ames Research Center, Moffett Field, CA, USA*
***Paul Danehy,** NASA Langley Research Center, VA, USA*
***Michael Winter**, University of Kentucky, KY, USA*

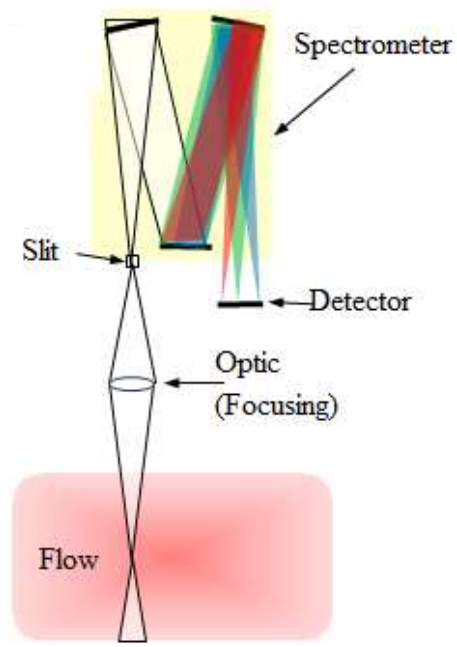

Emission Spectroscopy Configurations

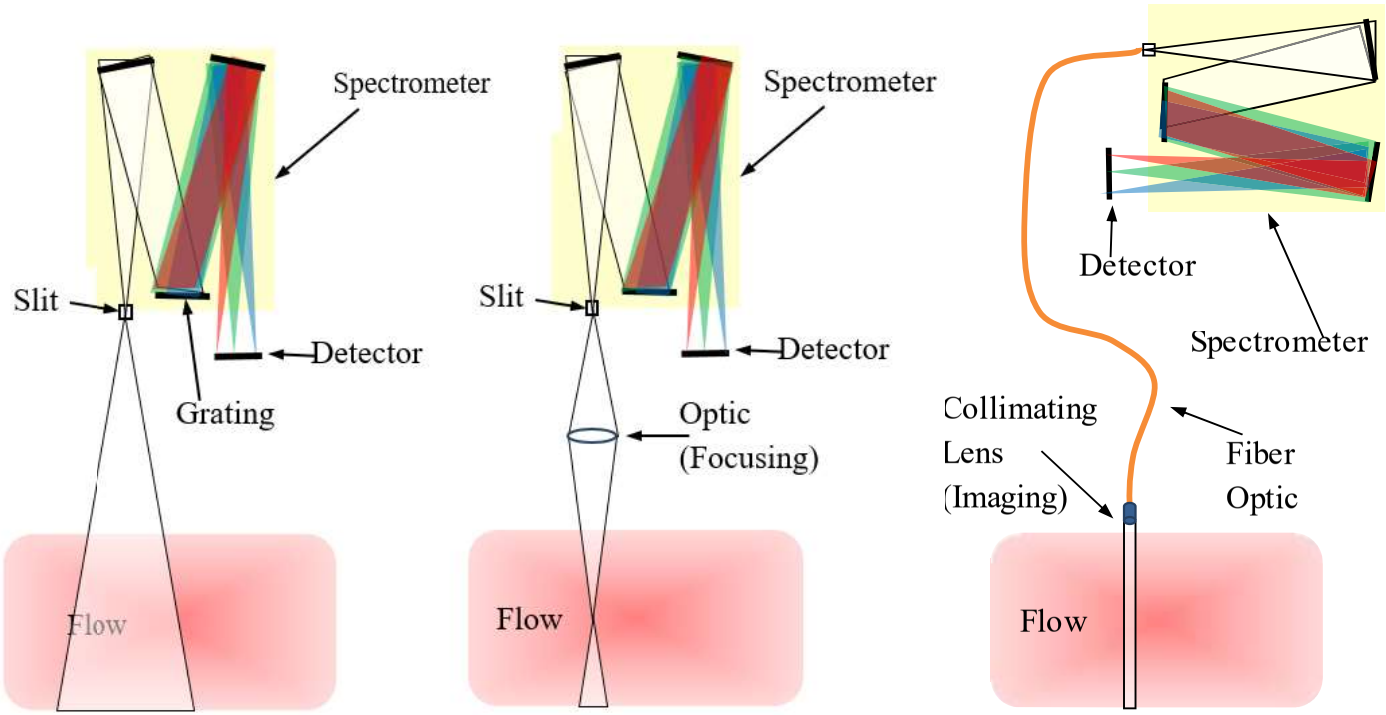

- Flow emits radiation in all directions, spectrometer measures light that is collected
- Collection volume is conical, but is modified by use of optics
  - Data is still line-integrated, averaged over the collection cone
- Spectrometer separates incoming light by wavelength (Note: No laser is used!)

Emission of Atoms and Molecules

Characteristics:

- Line position
- Line strength/intensity
- Line shape

from $\Delta E = E_{upper} - E_{lower} = h\,\nu$,

→ ν or λ for known energy levels

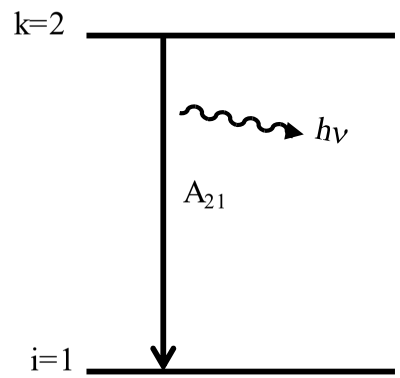

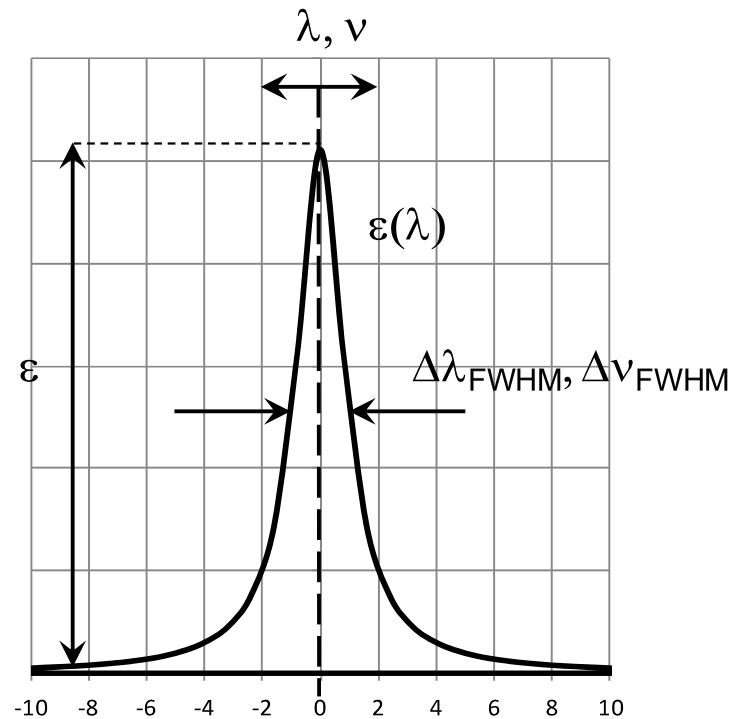

valid in general (atoms and molecules)

$$\varepsilon_{21} = \frac{h\nu}{4\pi} A_{21}\, n_2$$

number of transitions
→ depends on energy of the upper state

one photon/transition
→ depends on energy difference

In equilibrium, the density n_k is related to n through the Boltzmann distribution:

Emission of Atoms: Electronic Excitation

Characteristics:

- Line position
- Line strength/intensity
- Line shape

from $\Delta E = E_{upper} - E_{lower} = h\nu$,

→ ν or λ for known energy levels

valid in general (atoms and molecules)

$$\varepsilon = \frac{h\nu}{4\pi} A_{ki} n_k$$

Number of different states which share the same energy
Depends on the total angular momentum J which is the value of the vector addition of the orbital angular momentum L and the spin momentum S
g = 2 J + 1

Degeneracy of the state k

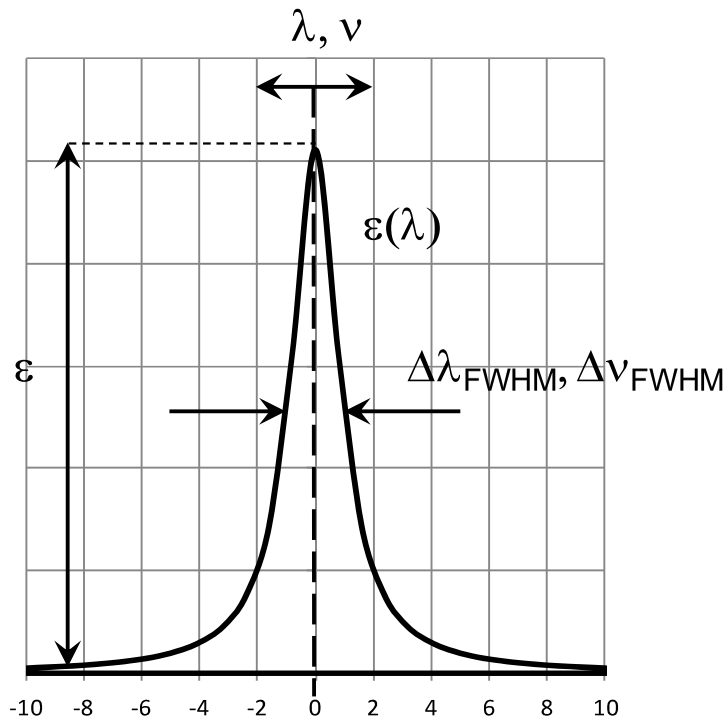

Population density of the excited state k

$$n_k = \frac{g_k}{U(T_{ex})} n_0 \exp\left(-\frac{E_k}{kT_{ex}}\right)$$

excitation energy of the state k

electronic excitation temperature (in equilibrium gas temperature)

Partition function

$$U(T_{ex}) = \sum_i g_i \exp\left(-\frac{E_i}{kT_{ex}}\right)$$

Total density of the species under consideration

In equilibrium, the density n_k is related to n through the Boltzmann distribution:

Emission of Atoms: Electronic Excitation

Characteristics:

- Line position
- Line strength/intensity
- Line shape

from $\Delta E = E_{upper} - E_{lower} = h\,\nu$,

→ ν or λ for known energy levels

valid in general (atoms and molecules)

$$\varepsilon = \frac{h\nu}{4\pi} A_{ki} \; n_k$$

$$= \frac{h\nu}{4\pi} A_{ki} \frac{g_k}{U(T_{ex})} n_0 \exp\left(-\frac{E_k}{kT_{ex}}\right)$$

for electronic excitation in equilibrium

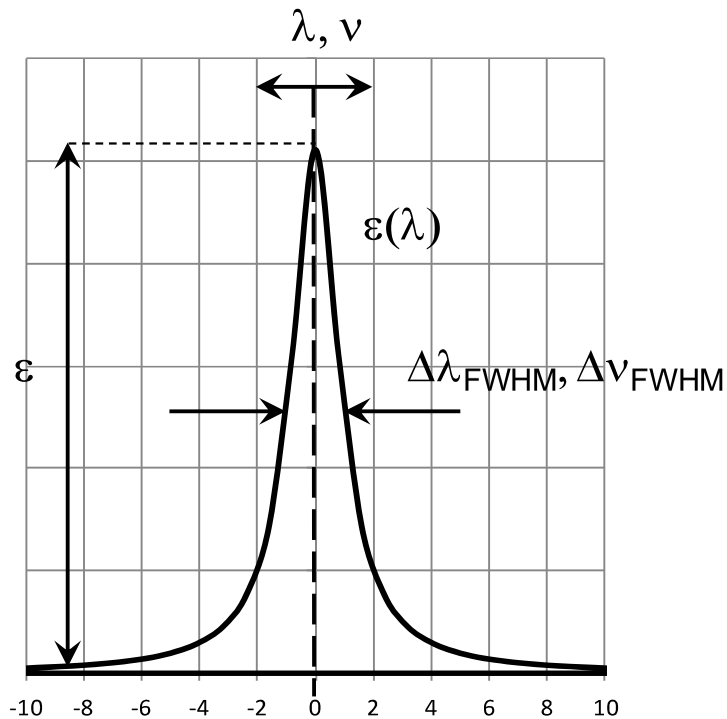

information on the transition (from quantum mechanics, e.g. from tables)

information about the thermodynamic condition of the plasma

In equilibrium, the density n_k is related to n through the Boltzmann distribution:

Electronic Excitation Temperature

Theoretically, the ratio of two lines would be sufficient to determine the excitation temperature, but it is often in doubt if the electronic excitation is in equilibrium.

$$\ln\left(\frac{I_{ki}}{\nu A_{ki} g_k}\right) + const = -\frac{E_k}{kT_{ex}}$$

→ Plot $\ln\left(\frac{I_{ki}}{\nu A_{ki} g_k}\right)$ vs E_k → straight line with slope -1/kT (Boltzmann Plot)

If points are indeed on a straight line → Boltzmann valid → T can be determined

BUT: Even if Boltzmann seems valid, the apparent excitation temperature might not be an equilibrium temperature:

Alternate method to determine Temperature is to use spectral fitting with a theoretical model of the emitter.

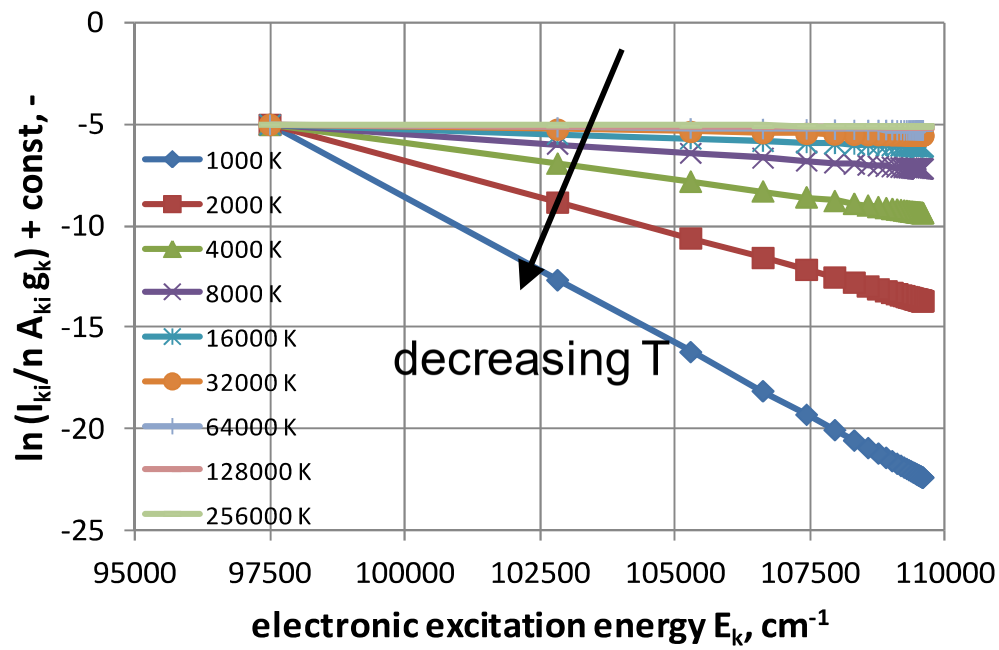

Emission from Molecules

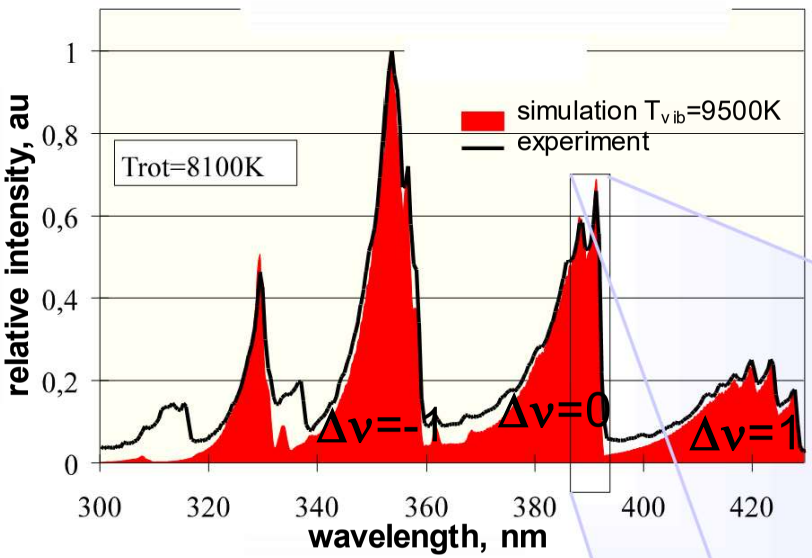

Molecule emission shows some shape but looks like a continuum

- Ratio of the different vibrational systems governed by T_{vib}
- Ratio within one vibrational transition (e.g. 0-0 → V_u=0, V_l=0) governed by T_{rot}

High spectral resolution →Single lines like atoms but more ...

→ rotation and vibration

N2+ B-X system

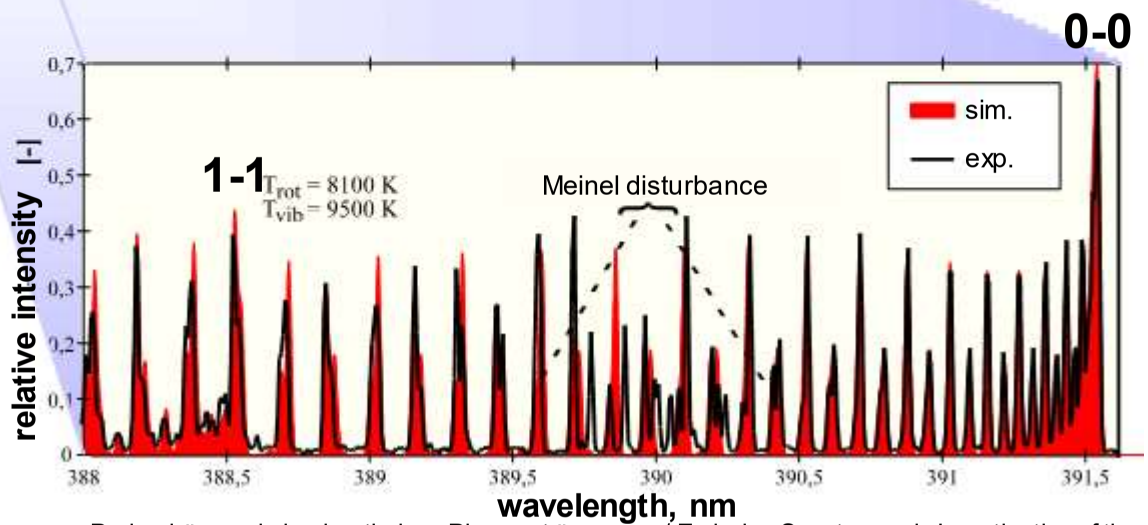

Winter, M.: Emissionsspektroskopische Untersuchung der Umströmung von Probenkörpern in hochenthalpen Plasmaströmungen / Emission Spectroscopic Investigation of the Flow Field around a Blunt Body in a High Enthalpy Flow, Dissertation (in German), Universität Stuttgart, Germany, Dec. 2006.

Emission from Molecules

• Each electronic level of a molecule is described by a potential curve in terms of energy vs. inter nuclear distance.

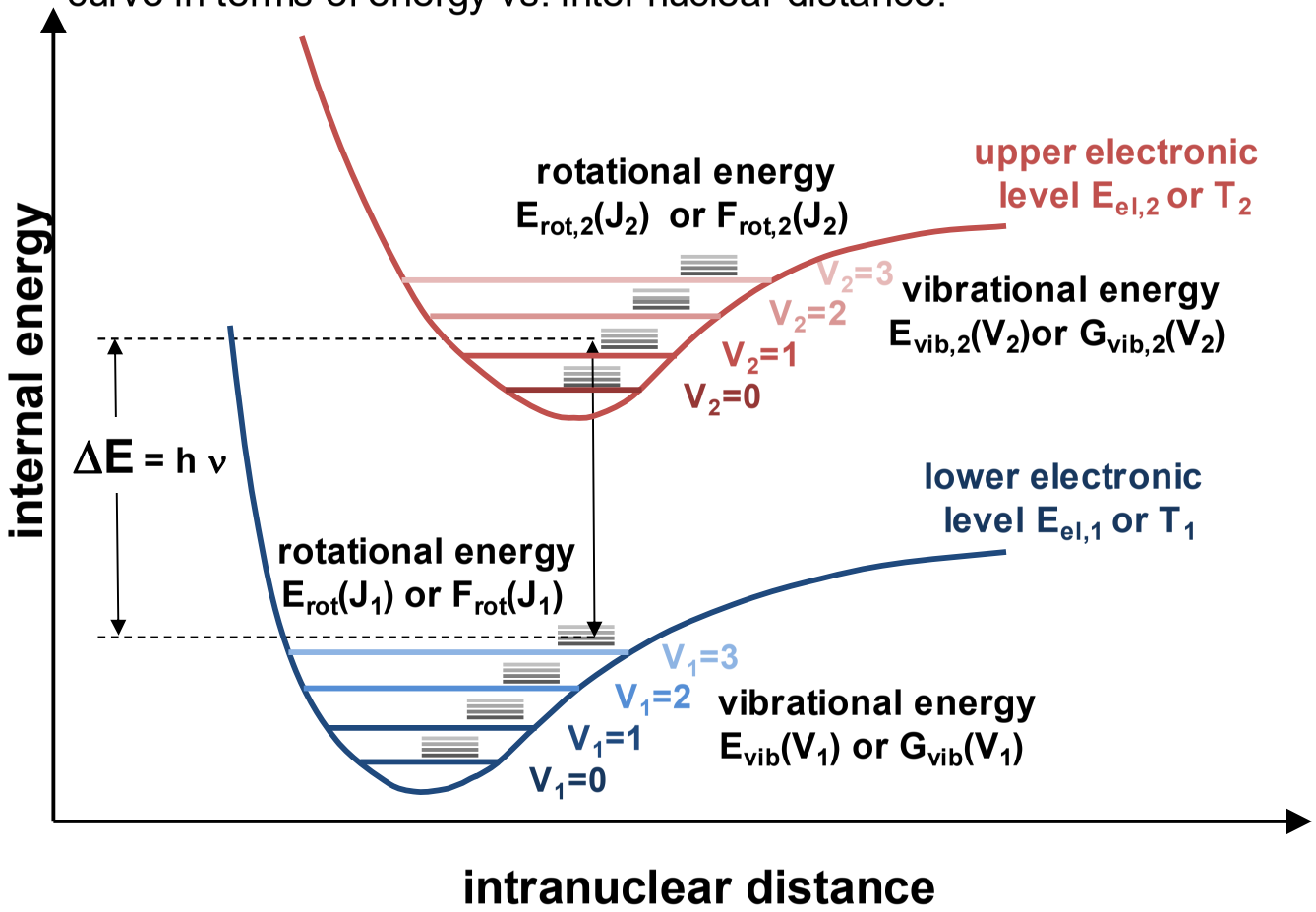

• Excitation of the levels can happen through collisions or absorption of radiation.

• From one upper level, transitions to different lower levels are possible, each one resulting in a different emission line

$$\tilde{\nu} = \frac{1}{hc}\left(\Delta E_{el} + \Delta E_{vib} + \Delta E_{rot}\right)$$

Emission from Molecules

Temperature determination from molecular radiation

- Within one vibrational transition, a large number of rotational lines is present
  → rovibrational lines (may shift to lower or higher wavelengths, depending on B)
- Similar to the atoms, a Boltzmann plot can be performed to determine T_{rot}.

$$Q_{rot}^{e'v'J'} = (2J'+1)\,exp\left(-\frac{E_{rot}^{e'v'J'}}{kT_{rot}}\right)$$

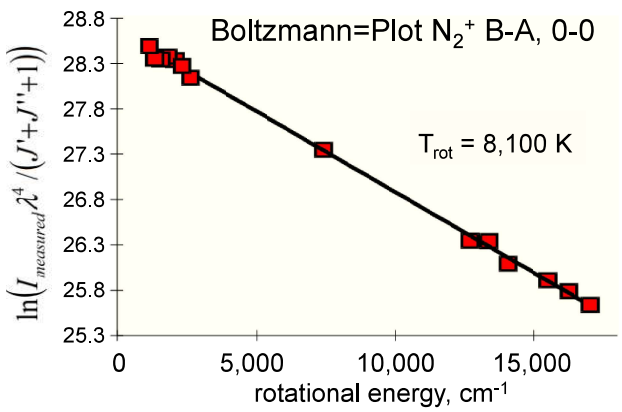

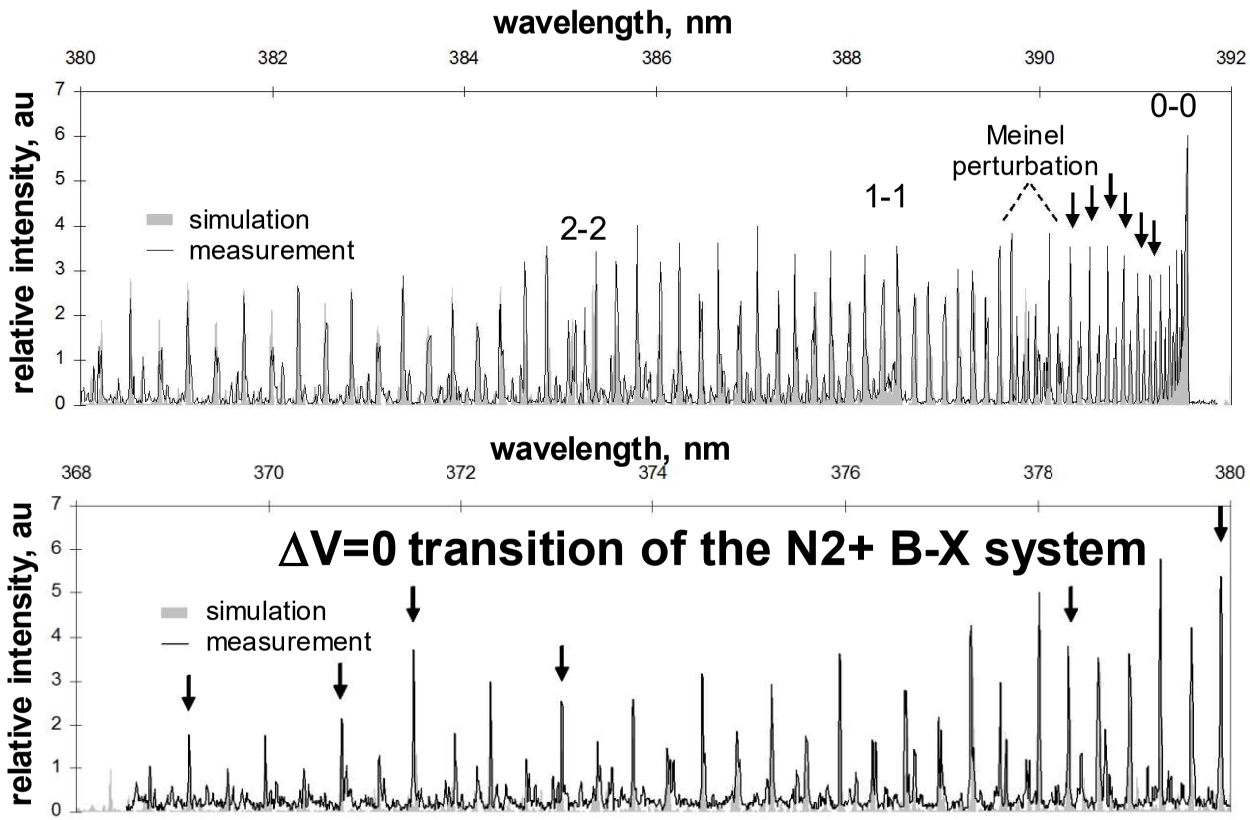

Winter, M., Auweter-Kurtz, M., Kurtz, H.L. and Park, C., "Investigation of an Equilibrium Condition Boundary Layer in front of a Material Probe in a Subsonic Plasma Flow," 31st AIAA Thermophysics Conference, New Orleans, LA, June 17-20, 1996.

Application example: Quantify Radiance

Quantify radiation loads to spacecraft during atmospheric entry in impulse facilities

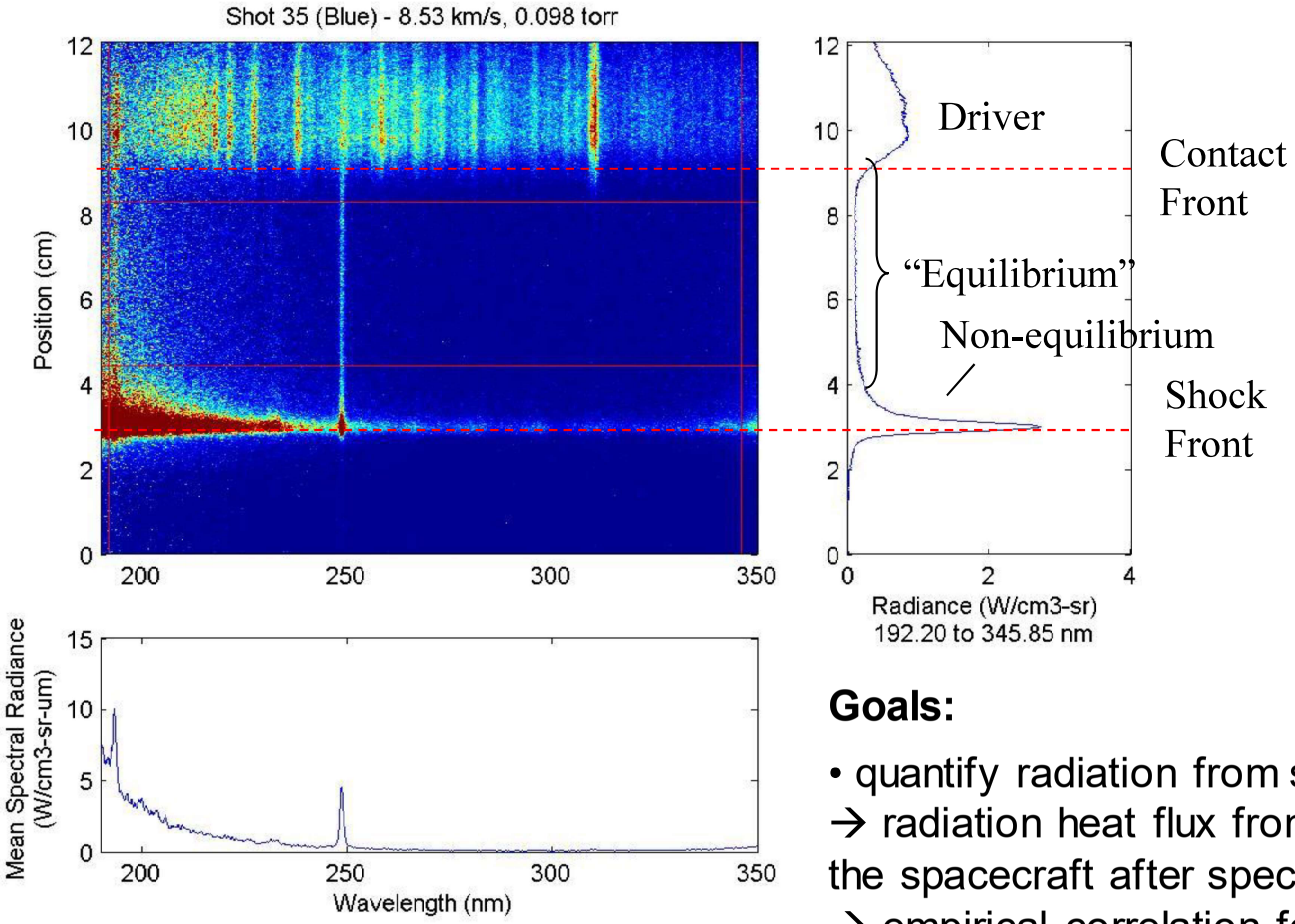

EAST shock tube (NASA Ames):

- reproduction of flight conditions
- no model testing
- 130nm – 8μm in various intervals
- simultaneous measurements with 4 spectrometers possible
- one dimension resolves spectrally, the other spatially → shock and post-shock region are covered in one image

Goals:

- quantify radiation from shock and post shock → radiation heat flux from the plasma upstream of the spacecraft after spectral integration → empirical correlation for radiation heat flux

- Cruden, B., Martinez, R., Grinstead, J. H., Olejniczak, J., "Simultaneous Vacuum Ultraviolet through Near IR Absolute Radiation Measurement with Spatiotemporal Resolution in an Electric Arc Shock Tube," AIAA 2009-4240, 41st AIAA Thermophysics Conference, 22 - 25 June 2009, San Antonio, Texas.
- Aaron Brandis, Christopher Johnston, Marco Panesi, Brett Cruden, Dinesh Prabhu, Deepak Bose, "Investigation of Nonequilibrium Radiation for Mars Entry," AIAA 2013-1055, 51st AIAA Aerospace Sciences Meeting including the New Horizons Forum and Aerospace Exposition, 2013.

Emission Spectroscopy Summary

- Useful tool to access information on energy and composition of a plasma, often occuring in high enthalpy hypersonic flows.
  - identification of species;
  - total radiation flux
  - quantities from line broadening
    - Doppler temperature, electron density
  - identification of thermal non-equilibrium.
  - measurement of excitation temperatures
    - line ratios / Boltzmann plot / simulations.

Advantages

- Simplicity: no laser required
- One instrument can measure many different things

Disadvantages

- Only works in luminous flows;
- Only probes excited states
- Proper calibration is imperative
- Path averaged (but can use tomography).

Conclusion

- Variety of different molecular-based measurement technologies are available for measuring hypersonic freestream flows.
  - Can measure temperature, density, velocity, species concentrations, etc.
  - Which is best? Which technique to use?
- Must start measurement campaign with an interview of "customer" to determine the requirements
  - How do different measurement technique capabilities satisfy the requirements?

Measurement Examples

Measurand	Technique	Facility Type	Mach #	Seeding	Species Probed	Accuracy	Precision	Mean meas.	Spatial Resolution	Sample Time	Meas. Rate	Ref.
Concentration	Absorption	BD	N/A	None	CO, CO_2		5%	0.05-0.06	Path-integrated	0.17 ms	up to 6 kHz	67
Concentration	ns CARS	BD	2	None	N_2, O_2, C_2H_4, CO_2, CO, H_2	--	--	500-1300 K	0.075 mm x 1 mm	10 ns	20 Hz	281
Density	PLIF	BD	10	I_2	I_2	--	1%	3e17 mol/cm^3	0.3 mm	200 ns	30 Hz	105
Density	PLIF	BD	2.07	I_2	I_2	--	--	0.34 kg/m^3	0.1 mm	--	--	106
Density	PLIF	UJ	4.5	Kr	Kr	7%	--	0.02 kg/m^3	0.047 mm	--	--	107
Density (Dr)	FLDI	FPST		None	air		0.5%		10 mm	10 ns	100 MHz	178
Electron Number Density	Emission	ST	30	0-2% H_2	H, N, O	20%	--	1e16 cm^{-3}	1 cm	1 us	single pulse	368
Flow Visualiz.	PLIF	AJ	5	None	NO, O	--	3%, 10%	--	1 mm	--	10 Hz	83
Flow Visualiz.	PLIF	FPST	7.9	None	NO	--	15.0%	--	0.25 mm	100 ns	10 Hz	92
Flow Visualiz.	PLIF	AJ	5	None	NO	--	--	--	0.1 mm	1 us	10 Hz	94
Mole Fraction	PLIF	ST	2.7	None	NO	--	10%	0.5	0.28 mm	400 ns	10 Hz	102
Mole Fraction	PLIF	ET	2.3	CH_3	CH_3	--	--	0.5	0.096 mm	400 ns	--	103
Mole Fraction	PLIF	BD	8.2	NO	NO	--	25%	0.07	0.1 mm	75 s	10 Hz	104
Number Density	Absorption	ST	30	None	CO, CO_2	30%	--	5.00E+16	5 mm	0.5 us	2 MHz	392
Number Density	LIF	AJ	2	None	None	20%	--	8.00E+15	--	180s	--	
Number Density	Emission	AJ	4	None	N	10%	--	1e16 cm^{-3}	2 cm	--	--	350
Pressure	fs/ps CARS	gas cell	--	None	air	<7.5%	2%	0.4-3 atm	0.1 x 1 mm	<1 ns	1-10 kHz	255
Pressure	FRS	BD	2	None	air	4-5%	--	yes	0.285 mm	--	--	205
Pressure	PLIF	BD	3	NO	NO	10-30%	--	2.25 kPa	0.25 mm	217 ns	10 Hz	108
Pressure	PLIF	UJ	--	I_2	I_2	4%	5%	100 kPa	0.23 mm	60 s	3 Hz	109
Pressure	PLIF	UJ	1.5	I_2	I_2	--	8%	135 Torr	0.16 mm	250 ms	4 Hz	110
Pressure	Absorption	FPST	--	None	CO_2	--	14%	350 Pa	Integrated	20 ms	600 Hz	

Velocity Measurements

Measurand	Technique	Facility Type	Mach #	Seeding	Species Probed	Accuracy	Precision	Mean meas.	Spatial Resolution	Sample Time	Meas. Rate	Ref.
Velocity	MTV	BD	10	NO_2	NO_2	2.80%	1%	1400 m/s	0.1 x 2 mm	2 us	10 Hz	
Velocity	MTV	BD	5	NO_2	NO_2	--	1.6-2.5%	719 m/s	0.1 x 2 mm	2 us	500 kHz	152
Velocity	MTV (HTV)	BD, Vitiated	2	H_2O	H_2O	1.20%	1-2.2%	680 m/s	0.1 x 2 mm	10-100us	10 Hz	141
Velocity	MTV (KTV)	BD	14	Krypton	Krypton	2-3%	0.2-1.25%	1920 m/s	0.1 x 5 mm	4 us	10 Hz	168
Velocity	MTV (FLEET)	BD	14	None	air	1%	<0.5%	1920 m/s	0.1 x 10 mm	7 us	1 kHz	169
Velocity	PIV	BD	2.01	TiO_2	--	2%	--	500 m/s	3 mm	1 us	25 Hz	305, 306
Velocity	PIV	BD	5	TiO_2	--	0.50%	2%	700 m/s	1 mm	1 us	10 Hz	332
Velocity	PIV	ST	4.5 - 6	TiO_2	--	--	2%	1600 m/s	6 mm	1.5 us	10 Hz	293
Velocity	PIV	BD	7	TiO_2	--	1%	2%	1040 m/s	1 mm	1 us	10 Hz	293
Velocity	Tomo-PIV	Jet	1.4	Al_2O_3	--	--	1%-4%	750 m/s	2 mm	--	2 Hz	304
Velocity	TR-PIV	SJTCF	1.4	Oil	--	--	2%	300 m/s	0.7 mm	--	50 kHz	308
Velocity	FRS	BD	2	None	air	2-3%	--	--	0.285 mm	--	--	205
Velocity	CC-DGV	BD	1.65	alumina	--	3%	--	600 m/s	0.05 mm	2 min	--	196
Velocity	IRS	BD	--	None	air	--	3%	--	0.1 mm	30 ns	10 Hz	
Velocity	PLIF	AJ	5	None	NO	--	13%	500 m/s	0.1 mm	72 s	10 Hz	94
Velocity	PLIF	FPST	7	None	NO	--	5%	1300 m/s	0.17 mm	50 ns	N/A	111
Velocity	PLIF	FPST	10	None	NO	--	10%	500 m/s	0.5 mm	200 ns	N/A	112
Velocity	LIF	AJ	4.8	None	O	--	11%	3600 m/s	0.09 mm	--	--	101
Velocity	LIF	AJ	N/A	None	N, O	--	10%	5000 m/s	0.5 mm	--	--	113
Velocity	LIF	UJ	5	I_2	I_2	--	2%	718 m/s	--	15 min	N/A	114
Velocity	LIF	AJ	2	None	None	5%	--	4000 m/s	0.5-3 mm	100 ns	180 sec	395
Velocity	Absorption	ST	N/A	None	K	--	4.5%	4450 m/s	Integrated	100 us	10 kHz	26

Temperature Measurements

Measurand	Technique	Facility Type	Mach #	Seeding	Species Probed	Accuracy	Precision	Mean meas.	Spatial Resolution	Sample Time	Meas. Rate	Ref.
Temperature	ns CARS	BD, Vitiated	2	None	air	2-5%	3-5%	300-2500 K	0.1 x 1 mm	10 ns	10-30 Hz	272
Temperature	ns CARS	BD	2	None	air	--	--	500-1300 K	0.1 x 1 mm	10 ns	20 Hz	266
Temperature	fs/ps CARS	flames	--	None	air	1-5%	1-1.5%	500-2500 K	0.1 x 1 mm	10-100 ps	1 kHz	243
Temperature	fs/ps CARS	Plasma, detonation	--	None	air	--	2%	300-2500 K (5000 K T_{vib})	0.1 x 1 mm	10-100 ps	1 kHz	259
Temperature	fs/ps CARS	flames	--	None	air	--	--	300-2000 K	0.035 x 1 mm	100 ps	10 Hz	246
Temperature	FRS	BD	2	None	air	2%	--	yes	0.285 mm	--	--	205
Temperature	Absorption	ST	30	None	None	10%	--	7000 K	5 mm	0.5 us	2 MHz	392
Temperature	Emission	AJ	2	None	None	10%	--	800 K	0.5 mm	30 s	--	341
Temperature	LIF	AJ	2	None	--	25%	--	1600 K	--	180s	--	393
Temperature	LIF	AJ	2	None	None	15%	--	1200 K	0.5-3 mm	100 ns	20 Hz	
Temperature	Absorption	AJ	N/A	None	O*	--	4%	7260 K	Integrated	1 s	100 Hz	78
Temperature	Absorption	ST	N/A	None	CO	--	4%	7400 K	Integrated	20 us	50 kHz	37
Temp. (Elec.)	Emission	ST	30	None	CO	3%	--	7000 K	2 mm	.1-1 us	single pulse	352
Temp. (Rot)	PLIF	FPST	--	None	NO	--	--	700 K	--	--	--	95
Temp. (Rot)	PLIF	BD	8.2	NO	NO	3%	4%	300 K	0.1 mm	75 s	10 Hz	98
Temp. (Rot)	PLIF	BD	4.7	NO_2	NO_2	--	5%	56 K	0.028 mm	3 us	10 Hz	96
Temp. (Rot)	PLIF	UJ	12	I_2	I_2	--	--	11.5 K	0.1 mm	60 s	--	97
Temp. (Rot)	PLIF	FPST	7	None	NO	--	4%	450 K	0.11 mm	650 ns	--	99
Temp. (Rot/Vib.)	Emission	ST	30	None	None	10%	--	7000 K	2 mm	0.1-1 us	--	352

Compare with Facility Needs

Facility	Type	Mach Number	Enthalpy (MJ/kg)	Velocity (m/s)	P_{static} (kPa)	T_{static} (K)	Density (kg/m3)
VKI Mach 6 H3	Blowdown Air	6	--	939	1.28	61.0	0.073
AEDC Tunnel 9	Blowdown N2	13.2	1.9	1920	0.5	51	0.003
Purdue Boeing Mach 6 Quiet Tunnel	Ludwig Tube	5.93	--	872.7	0.37	53.9	0.024
EAST	Shock Tube	4	94	9400	30	10000	0.005
T5	Free Piston Shock Tunnel	5.1	11.9	4320	34	1800	0.062
Lens XX	Expansion Tunnel	7.3	20.7	6086	3.68	1881	0.0068
NASA Ames IHF	Arc Jet	4	20	4000	3	1500	0.004

- Community has techniques which have been demonstrated at these conditions to measure key parameters (P, T, ρ, u, v, w, χ_i) over wide range of conditions.
  - Have been used in wide range of facilities, applications, incl. inflow.
- But some techniques and measurements are:
  - 'demonstrations' and not validated
  - not accurate or precise enough to be useful
  - too complicated and need to be simplified or refined

Is precision high enough?

Facility	Type	U'/U	T'/T	m'/m (rho'/rho)	P'/P
VKI Mach 6 H3	Blowdown Air	0.6%	0.8%	5.2%	1.0%
Purdue Boeing Mach 6 Quiet Tunnel	Ludwig Tube	--	--	0.2%	0.01%
T5	Free Piston Shock Tunnel	--	--	<1% @ high frequency	--

- One glaring lack of instrumentation is in the ability to measure the RMS fluctuations in the freestream of hypersonic flows.
  - Need <1% or better <<1% precision.
  - Very few techniques show this level of precision
    - FLDI; MTV and CARS are close
    - We have work to do!

Conclusion

- Variety of different molecular-based measurement technologies are available for measuring hypersonic nonequilibrium flows.
  - Can measure temperature, density, velocity, species concentrations, etc.
  - Which is best? Which technique to use?
- Must start measurement campaign with an interview of "customer" to determine the requirements
  - How do different measurement technique capabilities satisfy the requirements?
  - Also consider practical issues:
    - Experience of the research team
    - Available equipment / budget
    - Schedule, difficulty of method, etc.
  - Rarely a perfect match, but a match can provide the data needed to advance or validate theory or computations

End

AIAA Progress Series Book, May, 2015

HYPERSONIC NONEQUILIBRIUM FLOWS: FUNDAMENTALS AND RECENT ADVANCES

Most Recent Book
Available Books

PRICES

PDF
Member: $79.95
List: $116.95
Add to Cart

Hardback
Member: $89.95
List: $129.95
Add to Cart

Progress in Astronautics and Aeronautics

Hypersonic Nonequilibrium Flows: Fundamentals and Recent Advances

Eswar Josyula, U.S. Air Force Research Laboratory, Wright-Patterson Air Force Base, Ohio
eISBN: 978-1-62410-329-2
print ISBN: 978-1-62410-328-5
DOI: 10.2514/4.103292

© 2015 American Institute of Aeronautics and Astronautics
Download the Full PDF

About the Book

The high-temperature environment poses an unusual challenge in understanding the basic physics of hypersonic flight. A lack of such understanding can lead to risks and uncertainties in the design of aerospace vehicles. *Hypersonic Nonequilibrium Flows* documents recent, unprecedented scientific advances in the field of nonequilibrium processes for aerospace applications. These advances have been driven primarily by interest in space access and exploration, or in developing military technologies involving hypersonic flight regimes.

In the modeling of hypersonic flows, the last decade has witnessed a reexamination of fundamental principles of kinetic theory and quantum chemistry to describe the kinetic and thermal states, respectively, of the individual gas particles. Modern aerospace programs where nonequilibrium energy transfer processes play a major role may broadly be categorized as exo- and endo-atmospheric. The exo-atmospheric flight programs consist of Earth and planetary reentry programs, as well as access to space programs for applications that include space exploration, flight experiments and demonstrations, missile defense, and the nascent space tourism industry. The endo-atmospheric flight programs are primarily motivated by hypersonic military applications requiring high-precision engagement for tactical, theater and strategic defense, as well as applications involving intelligence, surveillance, and reconnaissance.

The nonequilibrium processes considered in this volume are generally associated with flight Mach numbers between 7 and 25, where the shock-layer temperatures range from 3000 to 25,000 K.

Hypersonic Nonequilibrium Flows includes fundamental governing equations of nonequilibrium fluid transport and computational approach to calculation of rates and cross-sections in quantized energy states; DSMC approach; radiative heat transfer; a CFD perspective; surface chemistry, with additional chapters on high enthalpy facilities and the associated diagnostic techniques.

Hypersonic Nonequilibrium Flows: Fundamentals and Recent Advances

Edited by Eswar Josyula

Table of Contents:

1. *Fundamental Fluid Transport Equations for Hypersonic Nonequilibrium Flows*, **Eswar Josyula, Prakash Vedula**
2. *Computation of Hypersonic Nonequilibrium Flows using the Direct Simulation Monte Carlo Method*, **Iain D. Boyd**
3. *First Principles Calculation of Heavy Particle Rate Coefficients*, **Richard L. Jaffe, David W. Schwenke, Marco Panesi**
4. *Radiation from Hypersonic Bodies—A Window on Non-Equilibrium Processes*, **Deborah A. Levin**
5. *CFD Methods for Hypersonic Flows and Aerothermodynamics*, **Graham V. Candler, Pramod K. Subbareddy, Ioannis Nompelis**
6. *Surface Chemistry in Non-Equilibrium Flows,* **Jochen Marschall , Matthew MacLean, Paul E. Norman, Thomas E. Schwartzentruber**
7. *High-Enthalpy Facilities and Plasma Wind Tunnels for Aerothermodynamics Ground Testing*, **Olivier Chazot, Francesco Panerai**
8. *Molecular-Based Optical Diagnostics for Hypersonic Nonequilibrium Flows*, **Paul M. Danehy, Brett F. Bathel, Craig T. Johansen, Michael Winter, Sean O'Byrne, Andrew D. Cutler**

Temperature and Equilibrium

- Temperature
  - Classical thermodynamics
    - Heat flowing from object A to B → $T_A > T_B$
  - Statistical thermodynamics
    - Describe by Boltzmann distribution
    - e.g. Maxwellian Velocity Distribution

      width ~ $\sqrt{T}$

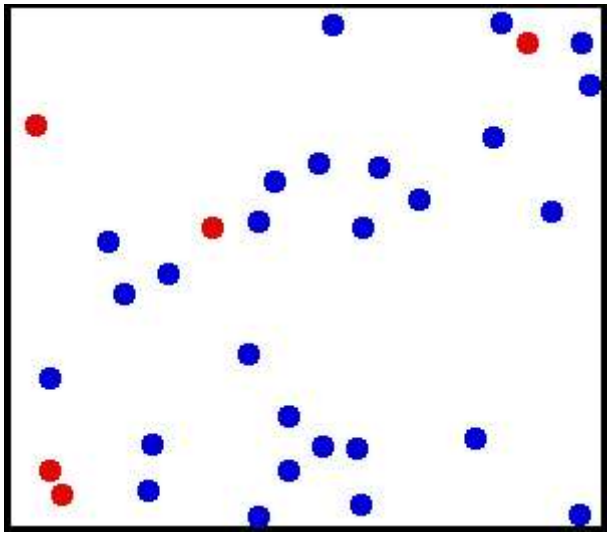

http://en.wikipedia.org/wiki/Temperature
Greg L at the English language Wikipedia

- Equilibrium
  - Classical thermodynamics
    - Thermal equilibrium: $T_A = T_B$
  - Statistical thermodynamics
    - One temperature can describe all the different energy modes (via Boltzmann)
  - Chemical equilibrium:
    - Reactants and product concentrations don't further change with time

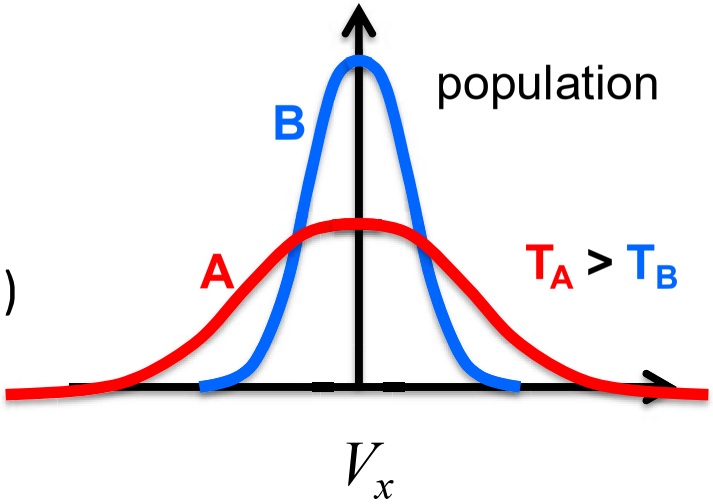

Some Hypersonic Nonequilibrium Flows

- Shock wave:

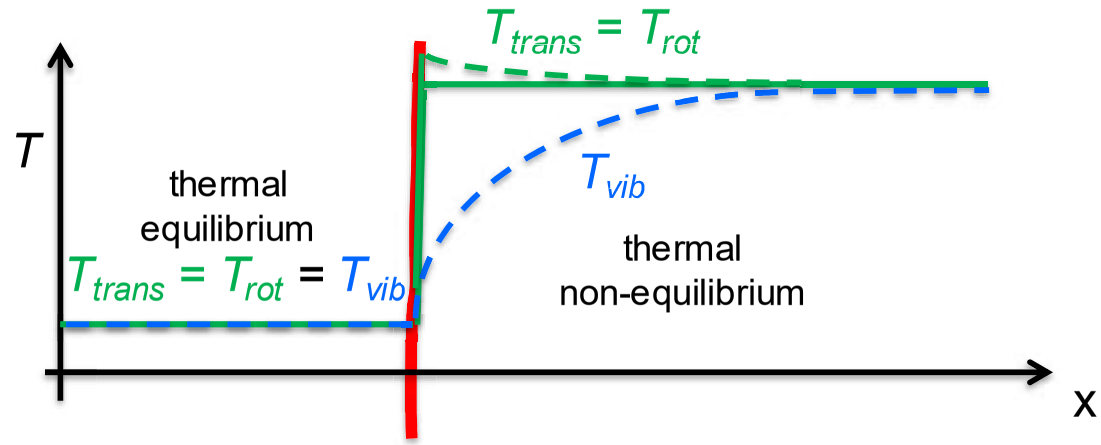

- Expansion:

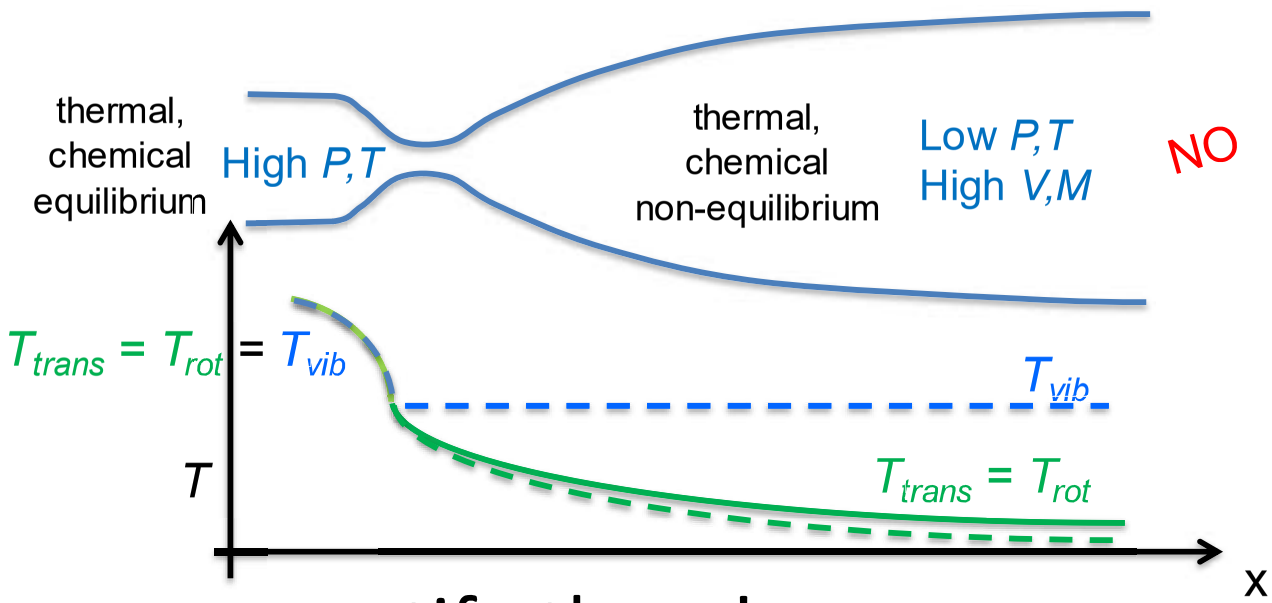

- We can measure, quantify these!

Species Concentrations

- Problem: How to deal with unknown Q_{21}?
- Solutions:
  - Saturated LIF: $(W_{12} + W_{21}) \gg (Q_{21} + A_{21})$
    - Q_{21} is negligible compared to W's
    - Hard to achieve
  - Predissociation
    - $Q_{pre} >> Q_{21}$
  - Measure τ_{LIF}
    - Determine Q_{21} from τ_{LIF}
  - Measure other species present and predict τ_{LIF}
    - Raman/Rayleigh/LIF (Sandia and DLR)
  - Counter-propagating beams, take ratio (Versluis, 1997)
- Potential problems: absorption, rad. trapping

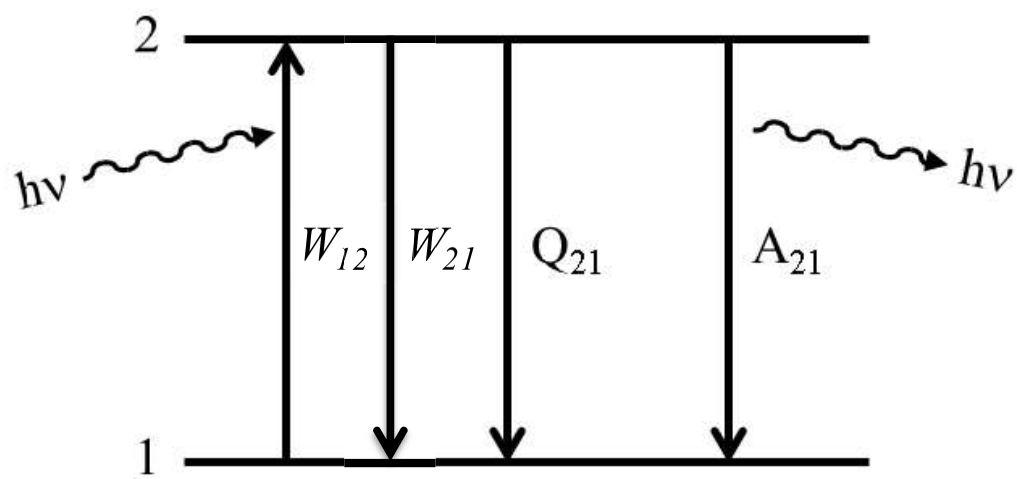

Rayleigh and Raman Theory 1

- Scattered intensity, I, is proportional to the square of the induced dipole moment, $\vec{p}$:

$$\vec{p} = \varepsilon_0 \alpha \vec{E}$$

where ε_0 is the permittivity of free space, α is the molecular polarizability and $\vec{E}$ is the incident electric field given by:

$$\vec{E} = \overrightarrow{E_0} \cos(\omega_0 t)$$

where $\overrightarrow{E_0}$ is the amplitude of the electric field, ω_0 is the frequency of the laser light and t is time.

Rayleigh and Raman Theory 2

- Polarizability, α, depends on internal structure
  - varies with time during vibrational oscillations at the natural frequency of the molecule, ω_v

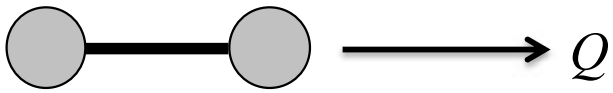

  - α varies with spatial coordinate, Q
    - More loosely held electrons → more polarizable
    - Taylor Series Expansion:

$$\alpha = \alpha_0 + \left(\frac{\partial \alpha}{\partial Q}\right)_0 dQ$$

where dQ is small displacement about equilibrium positions which occurs during normal vibration

$$dQ = Q_0 \cos(\omega_v t)$$

Rayleigh and Raman Theory 3

- Substituting previous equations into $\vec{p} = \varepsilon_0 \alpha \vec{E}$:

$$\vec{p} = \left[\alpha_0 + \left(\frac{\partial \alpha}{\partial Q}\right)_0 Q_0 \cos(\omega_v t)\right] \varepsilon_0 \overrightarrow{E_0} \cos(\omega_0 t)$$

- Expanding and using trig identity:

$$\vec{p} = \alpha_0 \varepsilon_0 \overrightarrow{E_0} \cos(\omega_0 t) + \tfrac{1}{2}\left(\frac{\partial \alpha}{\partial Q}\right)_0 \varepsilon_0 Q_0 \overrightarrow{E_0} [\cos(\omega_0 - \omega_v)t + \cos(\omega_0 + \omega_v)t]$$

Rayleigh Scattering — Stokes Raman — anti-Stokes Raman

- Resulting induced dipole moment (and scattering) is at three frequencies
- Amplitude is usually determined empirically:

$$\left(\frac{\partial \sigma}{\partial \Omega}\right)_{zz} \equiv \frac{I_{zz}^{\Omega}}{NI}$$

Differential Cross Section
(varies by molecule and with I but not with P, T)
(zz indicates polarization of laser and detection)

$$I_{zz}^{\Omega} = \left(\frac{\partial \sigma}{\partial \Omega}\right)_{zz} NI$$

scattered power per solid angle — diff. cross section — number density — laser irradiance

Rayleigh and Raman Theory 4

- Selection Rules: Raman Activity
  - Not every molecule or vibrational mode produces Raman

$$\vec{p} = \alpha_0 \varepsilon_0 \overrightarrow{E_0} \cos(\omega_0 t) + \frac{1}{2}\left(\frac{\partial \alpha}{\partial Q}\right)_0 \varepsilon_0 Q_0 \overrightarrow{E_0}[\cos(\omega_0 - \omega_v)t + \cos(\omega_0 + \omega_v)t]$$

  - Amplitude of Raman is proportional to the magnitude of: $\left(\frac{\partial \alpha}{\partial Q}\right)_0$
  - Polarizability, α, must *change* during vibrations to be Raman active
  - Raman active:
  - Raman inactive:

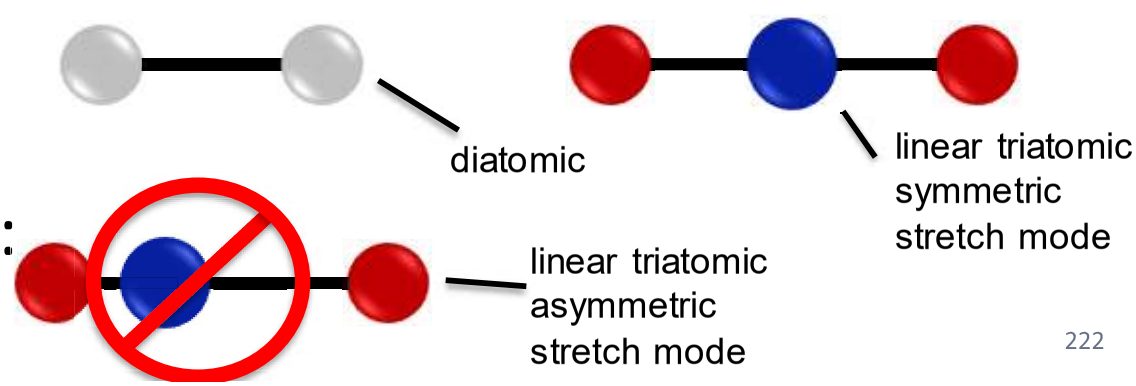

Rayleigh Scattering: ρ

- When precise measurements are required, high S/N is needed
  - Use high powered lasers, focused to a point
    - If too high: laser-induced breakdown
- Sandia, Livermore, Calif.:
  - Raman/Rayleigh/LIF line imaging at P = 1 atm
  - 4 double-pulse Nd:YAG lasers: 1.8 J/pulse
  - Camera images Rayleigh along line
    - ~10 pix / mm along 6-mm-long probe volume
  - N_2, O_2, CH_4, CO_2, H_2O and H_2 from Raman
  - CO from 2 photon LIF
  - Temperature from Rayleigh density, ρ,
    - Need composition to determine $\left(\frac{\partial \alpha}{\partial Q}\right)_0$
    - If known P, idea gas law give T
    - T precision reported: ~0.75%
    - (ρ precision is probably same)
  - Cutting edge MHz laser: 40x lower energy (Jiang, 2011)

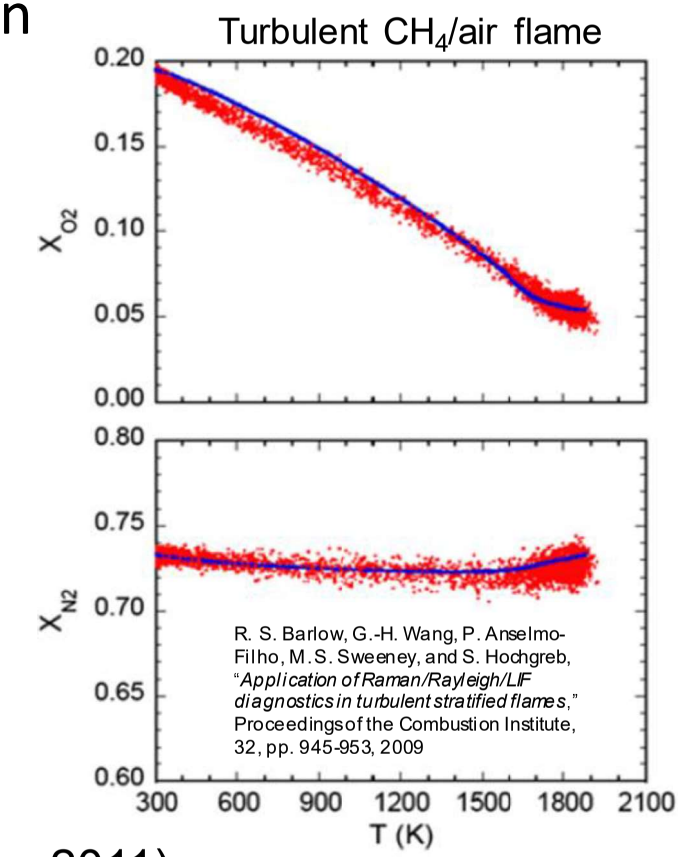

R. S. Barlow, G.-H. Wang, P. Anselmo-Filho, M. S. Sweeney, and S. Hochgreb, "*Application of Raman/Rayleigh/LIF diagnostics in turbulent stratified flames*," Proceedings of the Combustion Institute, 32, pp. 945-953, 2009

Emission from Molecules

- Rigid Rotator and Harmonic Oscillator
  - simple model, mainly to be used to account for rotational and vibrational energies in CFD codes → energy conservation
  - not suitable (at least the harmonic oscillator for spectral simulation)
  - The harmonic oscillator, however, does not describe real molecules:
    - for r ~ inf. → E = dissociation energy
    - for r ~ 0 → E ~ inf.

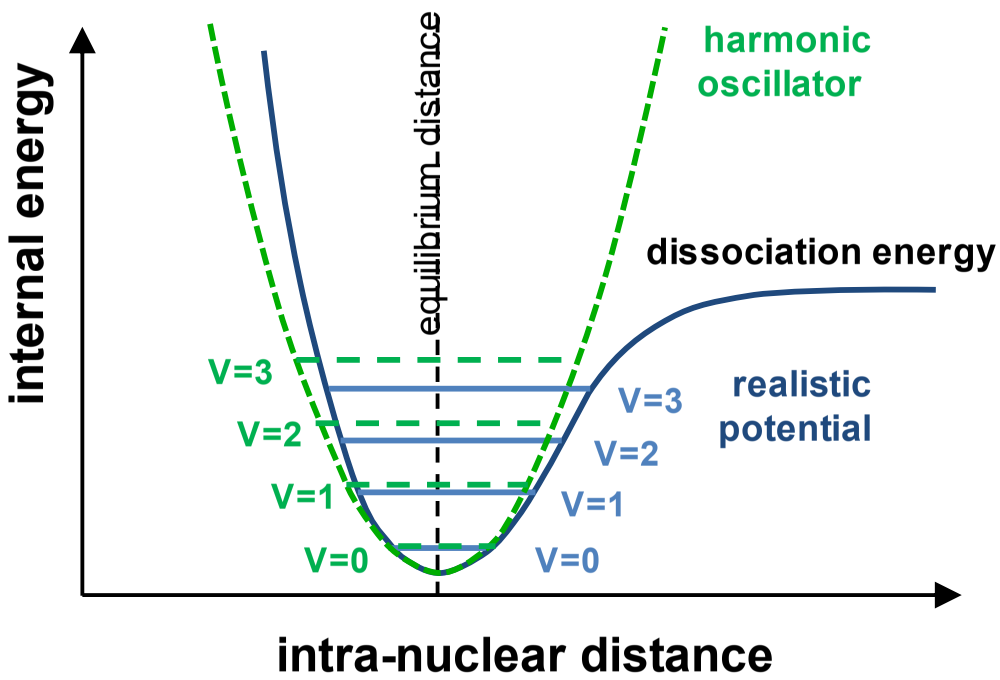

Morse Potential

$$U(x) = D_e\left(1 - e^{-\beta x}\right)^2$$

- x: distance to r_e (re: equilibrium distance between the nuclei)
- D_e: Well depth of the potential (dissociation energy- energy at minimum)

$$\beta = 1{,}2177 \cdot 10^{-7}\, \omega_e \sqrt{\frac{\mu_A}{D_e}}$$

- μ_A: reduced mass of the molecule

vibrational energy increment from V to V+1 now decreases with V:

$$G(V) = \omega_e\left(V + \frac{1}{2}\right) - \omega_e x_e\left(V + \frac{1}{2}\right)^2$$

Abel-Inversion

- emission spectroscopy is a line of sight method
  → only integrated data, no spatial resolution

  Abel integral equation:

$$I(z) = 2\int_{r=z}^{R} \frac{r}{\sqrt{r^2 - z^2}} \; \varepsilon(r) \; dr$$

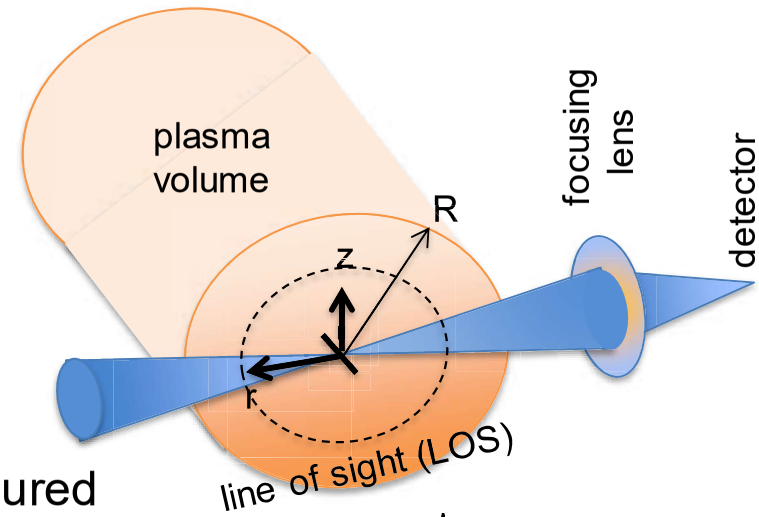

  Typically, integrals along the line of sight are measured
  → the local emission is desired.

$$\varepsilon(r) = -\frac{1}{\pi}\int_{z=r}^{\infty} \frac{\left(dI/dz\right)}{\sqrt{z^2 - r^2}} \; dz$$

  Solving this equation is usually only possible in special cases (e.g. a constant local distribution $\varepsilon(r)$=const. yields and elliptical profile in I(z))

  Under the assumptions of rotational symmetry and optically thin medium, local emission values can be obtained from an Abel-Inversion.

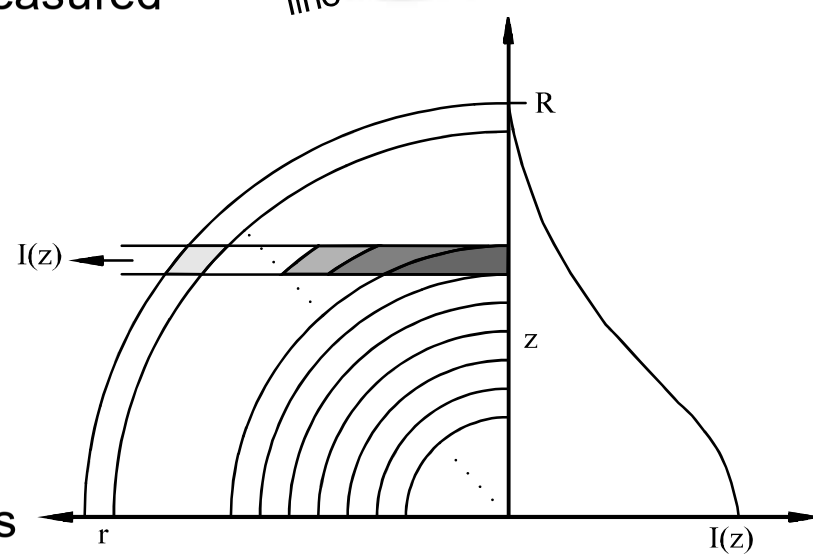

Example: Arc Jet Emission

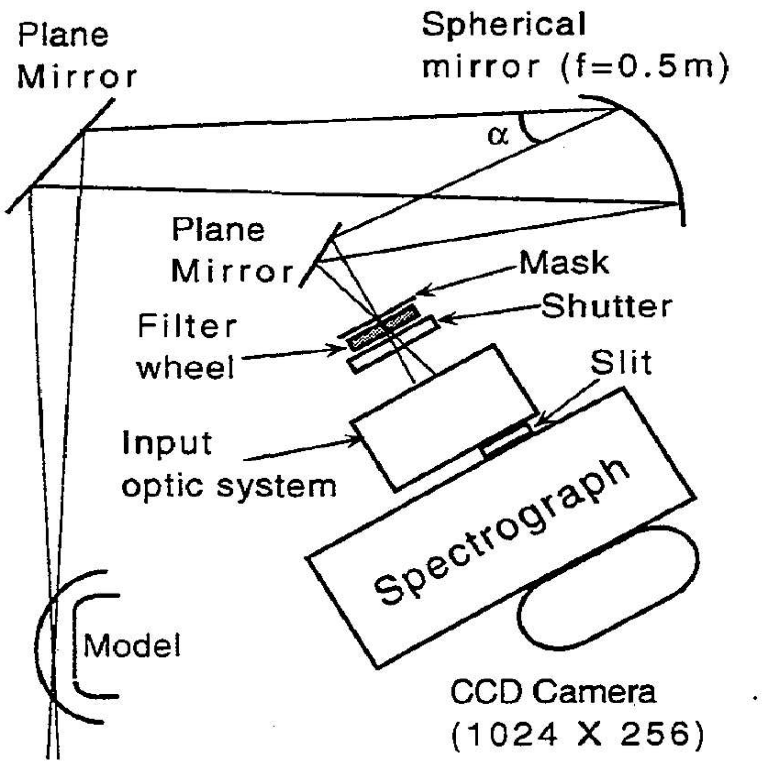

Park, C. S., Newfield, M. E., Fletcher, D. G., and Gokcen, T., "Spectroscopic Measurement of the Flows in an Arc-Jet Facility," AIAA Paper 1998-0893.

- Park, et al. (1998) performed emission spectroscopy in the NASA Ames Aerodynamic Heating Facility (AHF) arc jet
- Mirrors re-focus the image onto a mask pattern
  - At 4:1 magnification, 2.5cm axial length imaged onto 6.3mm mask
- The masked image is then refocused onto the spectrometer
  - Openings in the mask define 3mm sections measured independently
- The model is rotated out of the flow to characterize the freestream

Freestream Temperature

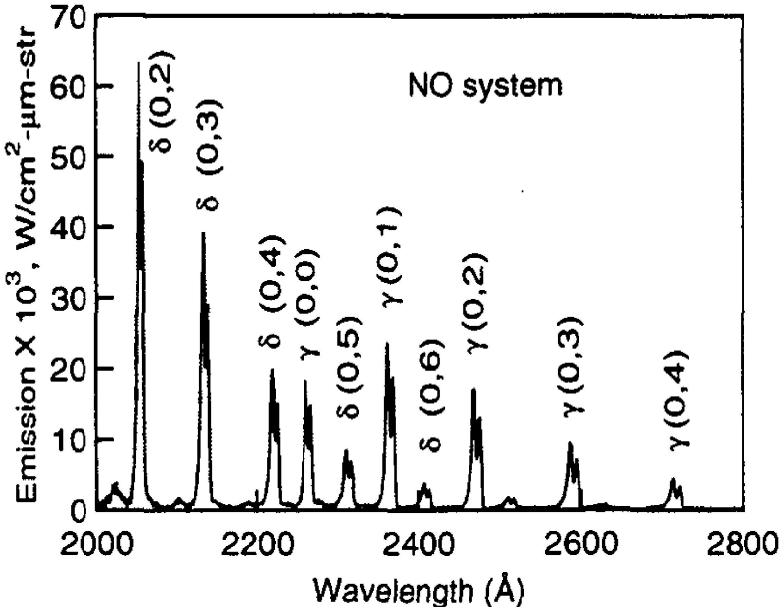

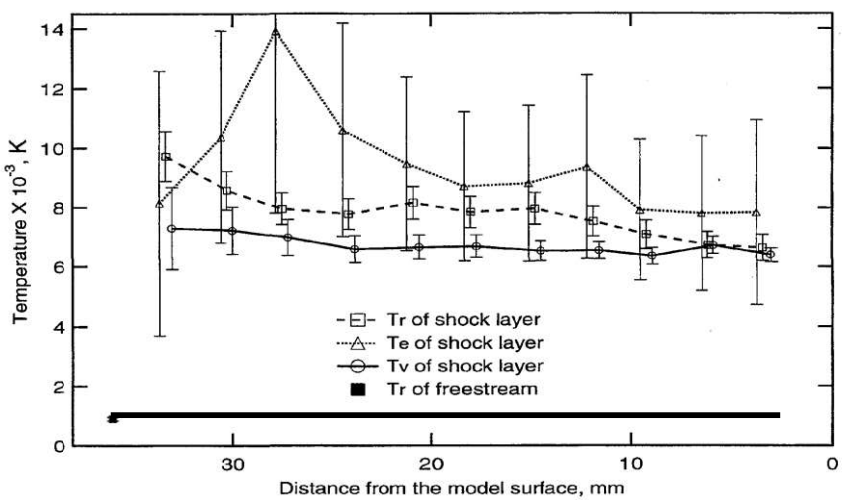

- Emission from NO γ and δ bands observed
- Individual vibrational transitions measured
  - All originating from $\nu'=0$
    - Vibrational Temperature could not be determined
  - Width of vibrational line depends on rotational temperature
    - Dependence determined with NEQAIR code
- Freestream Rotational Temperature
  - Analysis results are slightly different for each band
  - Not a function of position (over 2.5 cm)
  - 860-990 ± 100K (High Condition)
  - 570-630 ± 55K (Low Condition)
- With model inserted, also possible to determine vibrational and electronic temperature

Park, C. S., Newfield, M. E., Fletcher, D. G., and Gokcen, T., "Spectroscopic Measurement of the Flows in an Arc-Jet Facility," AIAA Paper 1998-0893.

Electron Density : Shock Tubes

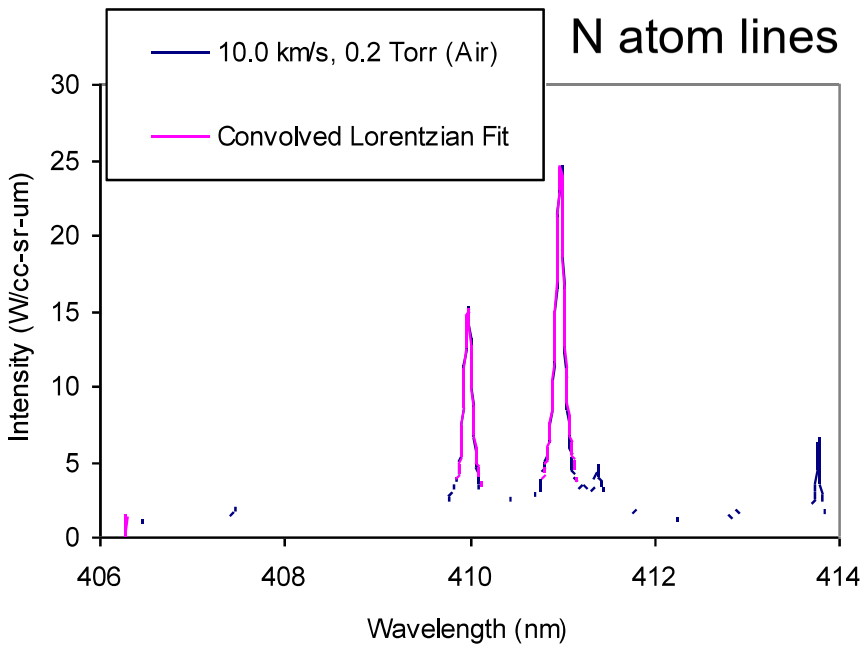

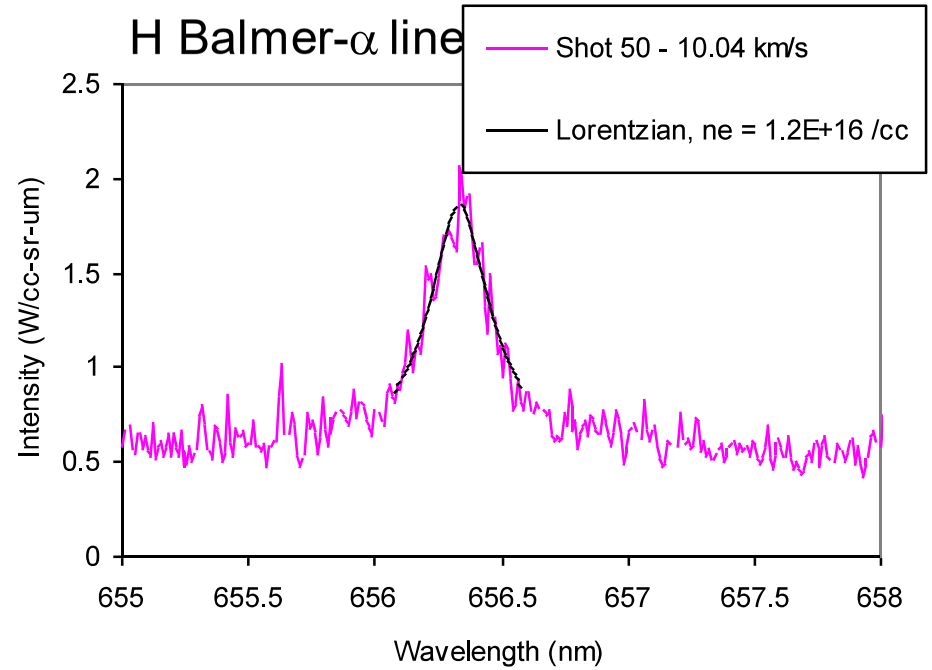

(Cruden et al)

- Individual atomic lines may be fit with Lorentzian function when broadening dominated by Stark Effect
- Linewidth is proportional to electron density
- Typical detection limit ~5 x 10^{15} cm^{-3}

Electron Density vs. Conditions

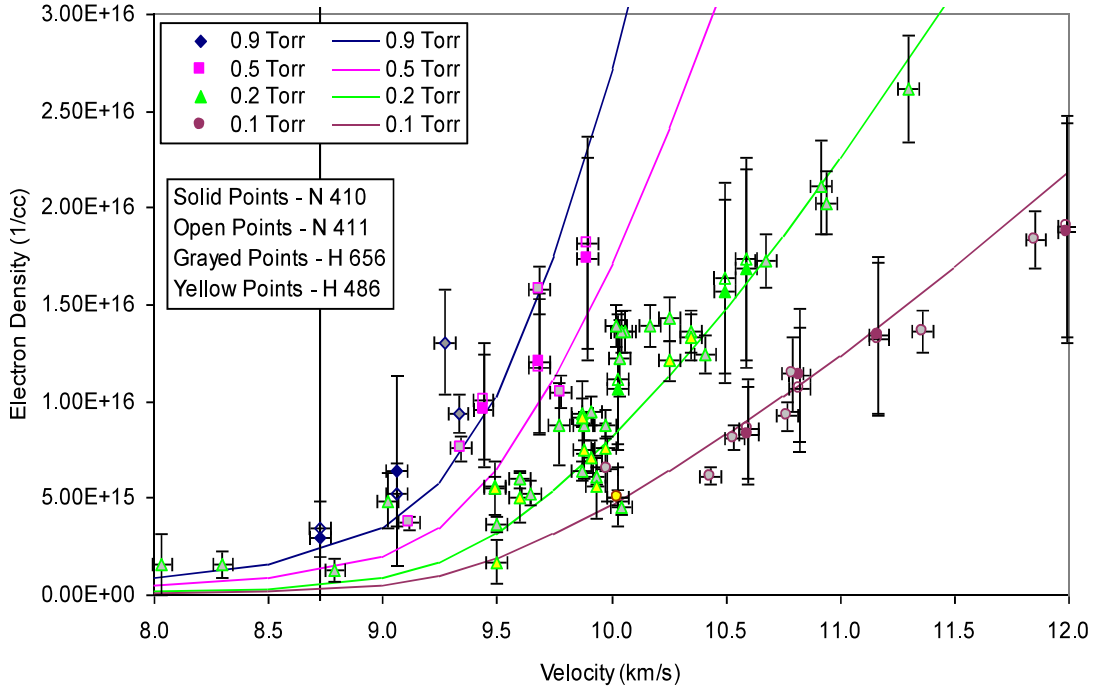

- Electron Density was measured over a range of velocity and pressure for air shocks from 8-12 km/s
- Solid lines are comparison to Rankine Hugoniot equilibrium

Cruden, B. A., "Electron Density Measurement in Reentry Shocks for Lunar Return," *Journal of Thermophysics and Heat Transfer*, Vol. 26, No. 2, 2012, pp. 222-230.

Temperature Measurement : Shock Tubes

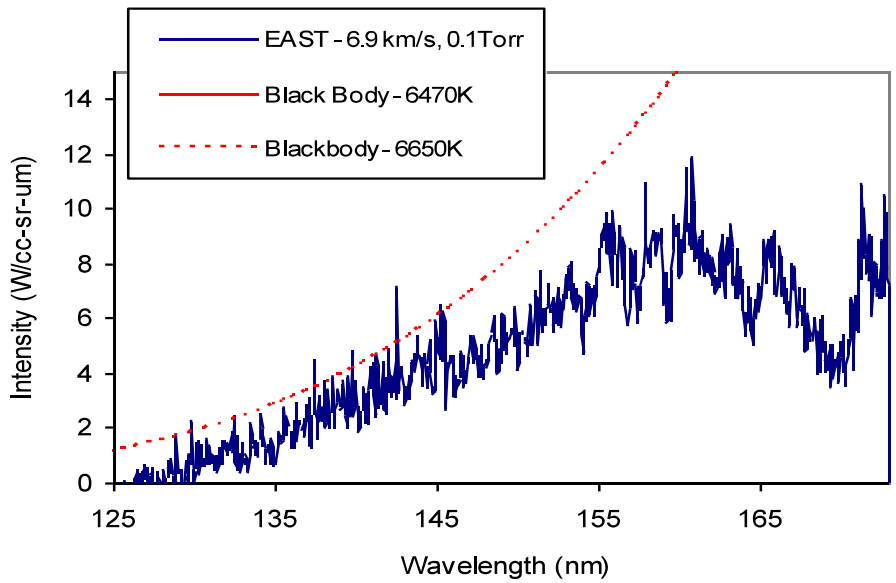

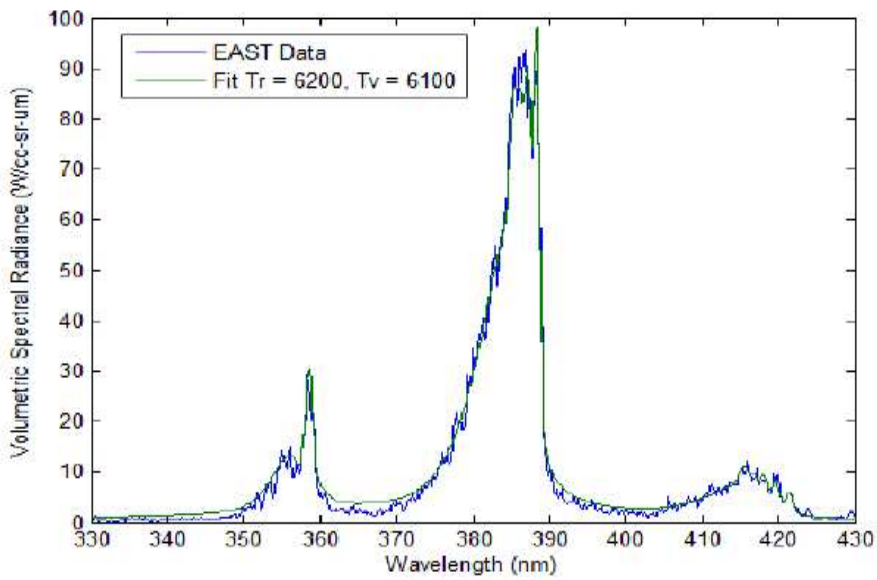

(Cruden et al)

- Temperature inferred from emission data by two methods
- BlackBody limited radiation may be fit by Planck curve
  - Typical accuracy ~100K
- Molecular spectra may be fit (modeled) to different values of *rotational* and *vibrational* temperature
  - Accuracy generally ~10%
  - Spectra used includes C_2, CN, NO, N_2, N_2^+

Temperature vs Position

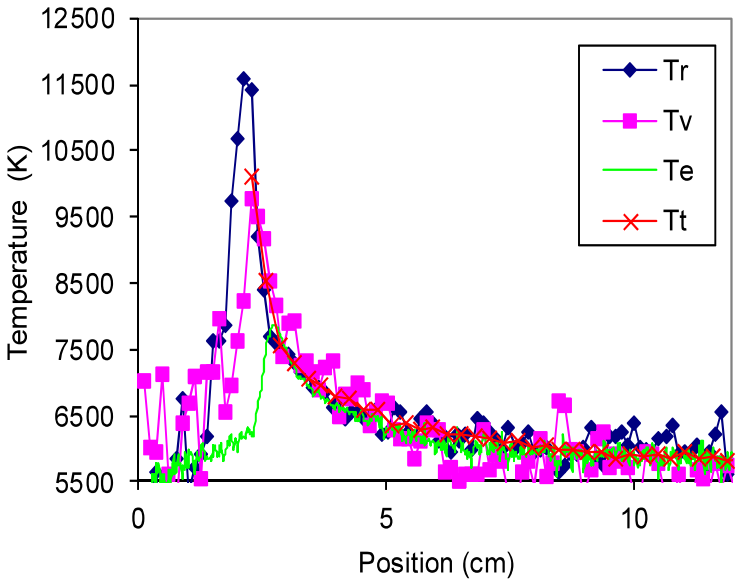

(Cruden et al)

- Four temperatures determined behind incident shock:
  - T_e from Planck Limited Emission
  - T_r, T_v from C2 molecular emission
  - T_t from TDLAS

Molecular Band Structure

- Transition energies with the same difference in vibrational quantum number $\Delta\nu$ are similar
→ The different vibrational transitions tend to group for the same $\Delta\nu$.
- $\Delta V = 0$: 0-0, 1-1, 2-2, 3-3, ...

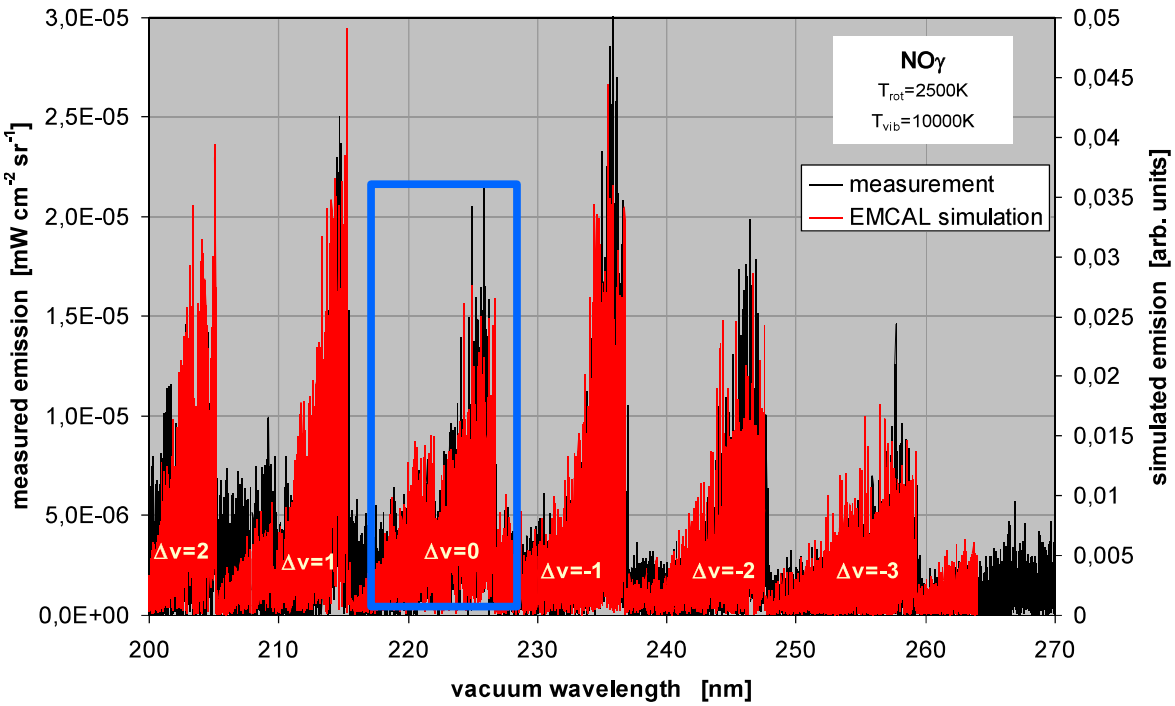

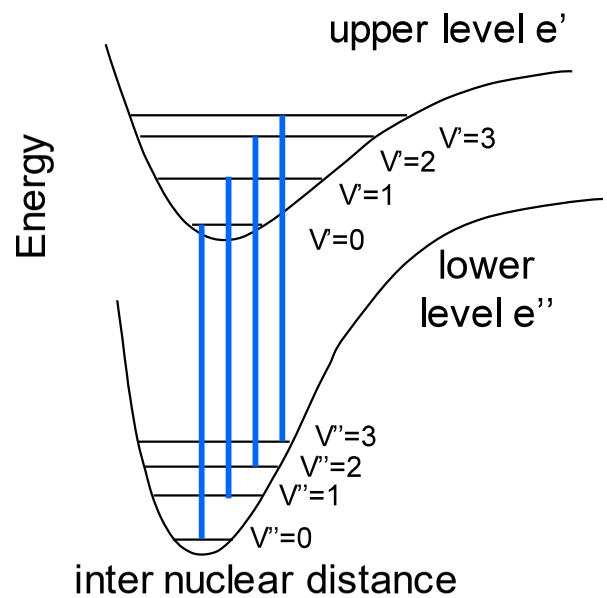

Nitric Oxide

Michael W. Winter and Monika Auweter-Kurtz: *Status on Molecular Simulation Capabilities of PARADE and EMCAL and Comparison with Experimental Data in High Spectral Resolution*, 5th European Symposium on Aerothermodynamics for Space Vehicles, Köln, Deutschland, 8–11.11.2004.

Molecular Band Structure

- Transition energies with the same difference in vibrational quantum number $\Delta\nu$ are similar
→ The different vibrational transitions tend to group for the same $\Delta\nu$.
- $\Delta V = 1$: 1-0, 2-1, 3-2, 4-3, ... → higher ΔE → lower λ

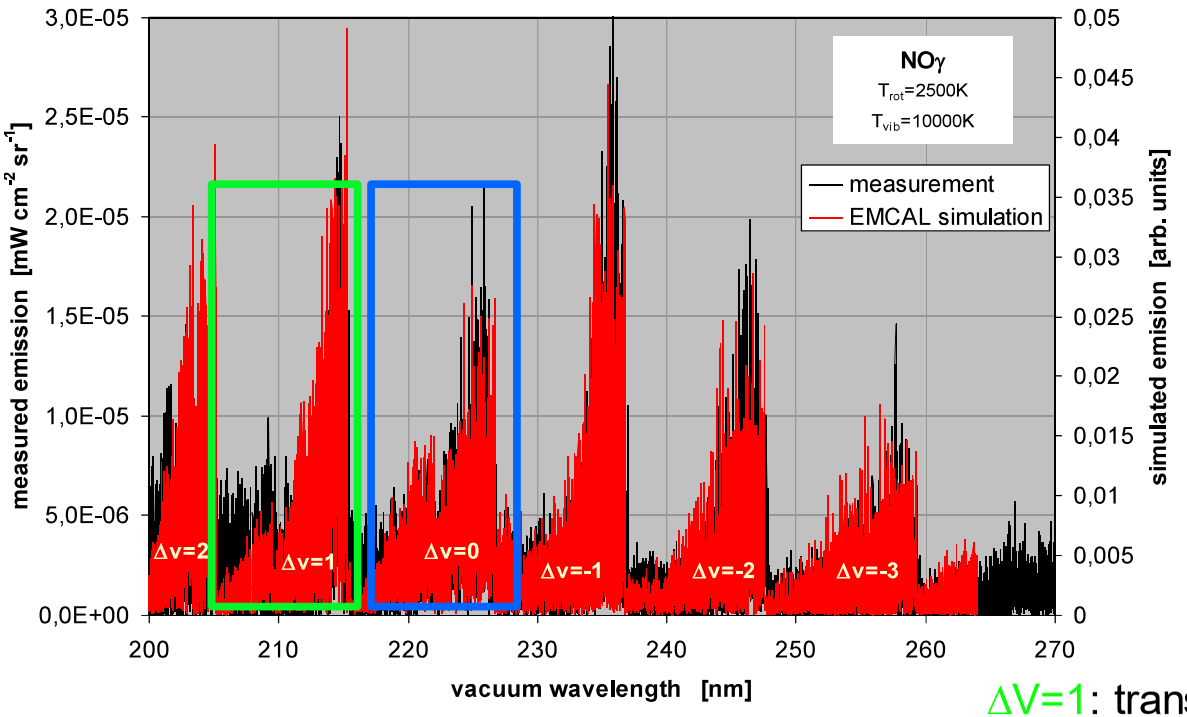

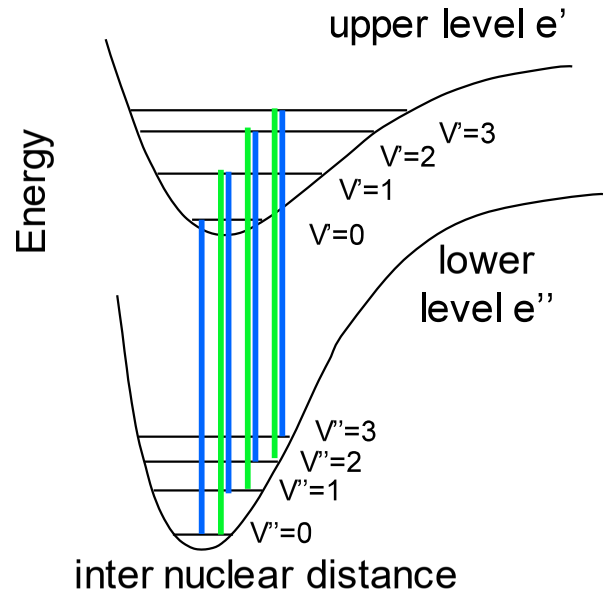

$\Delta V=1$: transition energy higher than $\Delta V=0$

Michael W. Winter and Monika Auweter-Kurtz: *Status on Molecular Simulation Capabilities of PARADE and EMCAL and Comparison with Experimental Data in High Spectral Resolution*, 5th European Symposium on Aerothermodynamics for Space Vehicles, Köln, Deutschland, 8–11.11.2004.

Doppler-based LIF Velocimetry

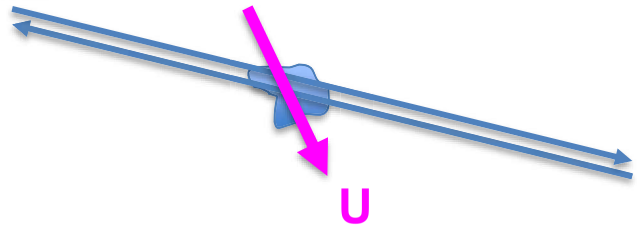

- Self-referenced tuning Doppler velocimetry
  - O-atom LIF velocimetry
  - Laser passed through measurement volume, followed by a delay line that returns beam along original path
  - Requires high-speed measurement device (e.g. photomultiplier tube) to resolve forward and return signals
  - Does not require reference cell measurement
  - $\nu_0 = \frac{\nu_f + \nu_r}{2} \rightarrow U = \frac{c}{\cos\theta} \cdot \frac{(\Delta\nu/2)}{([\nu_f + \nu_r]/2)}$

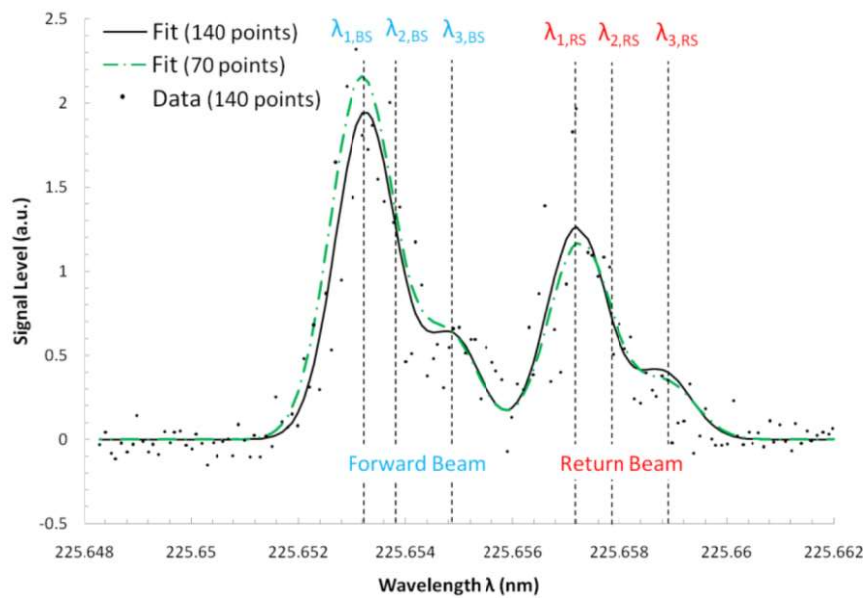

B. Bathel, C. Johansen, J. Inman, S. Jones, and P. Danehy, "*Review of Fluorescence-Based Velocimetry Techniques to Study High-Speed Compressible Flows*," AIAA Paper 2013-339, 51st AIAA Aerospace Sciences Meeting, Grapevine, TX, January 7-10, 2013.